

**Development of Selective Nitrile Inhibitors and ‘Activity-Based’
Probes For Human Cathepsins K and S**

Dissertation

zur

Erlangung des Doktorgrades (Dr. rer. nat.)

der

Mathematisch-Naturwissenschaftlichen Fakultät

der

Rheinischen Friedrich-Wilhelms-Universität Bonn

vorgelegt von

Maxim Frizler

aus

Kamyschnoje, Kasachstan

Bonn 2012

Angefertigt mit Genehmigung der Mathematisch-Naturwissenschaftlichen
Fakultät der Rheinischen Friedrich-Wilhelms-Universität Bonn.

1. Referent: Herr Professor Dr. Michael Gütschow
2. Referent: Frau Professor Dr. Christa E. Müller

Tag der Promotion: 14.05.2012

Erscheinungsjahr: 2012

Meiner Familie und Friederike
in Dankbarkeit

TABLE OF CONTENTS

1. INTRODUCTION.....	1
1.1. GENERAL REMARKS.....	2
1.2. FUNCTIONS OF CATHEPSINS B, K, S, L, AND C.....	6
1.3. INVOLVEMENT OF CATHEPSINS IN DISEASES.....	8
1.4. BONE REMODELING AND OSTEOPOROSIS.....	11
1.5. ANTIGEN PRESENTATION AND AUTOIMMUNE DISEASES.....	13
1.6. NITRILE-BASED INHIBITORS OF CYSTEINE CATHEPSINS.....	15
1.6.1. EARLY STUDIES.....	15
1.6.2. CONVERSIONS OF THIOIMIDATE ADDUCTS.....	18
1.6.3. SELECTIVE NITRILE-BASED INHIBITORS OF CATHEPSINS K AND S.....	20
1.6.4. AZADIPEPTIDE NITRILES AS INHIBITORS OF CYSTEINE PROTEASES...	22
1.7. ACTIVITY-BASED PROBES.....	24
1.8. AIM.....	26
2. RESULTS AND DISCUSSION.....	27
2.1. AZADIPEPTIDE NITRILES AS CATHEPSIN K INHIBITORS.....	28
2.1.1. SYSTEMATIC SCAN FOR P2 SUBSTITUENTS.....	28
2.1.2. KINETIC PLOTS (SLOW-BINDING INHIBITION) AND EQUATIONS.....	30
2.1.3. STRUCTURE-ACTIVITY RELATIONSHIPS OF 33–38, 42, 45 AND 46.....	36
2.1.4. L-LEUCINE-DERIVED AZADIPEPTIDE NITRILES.....	39
2.1.5. KINETIC PLOTS (FAST-BINDING INHIBITION).....	44
2.1.6. STRUCTURE-ACTIVITY RELATIONSHIPS OF 50, 51 62–66, 67, 68, 79, 80....	45
2.1.7. CONCLUSIONS I.....	51
2.1.8. HOMOCYCLCOLEUCINE-BASED AZADIPEPTIDE NITRILES.....	52
2.1.9. KINETIC CHARACTERISATION OF 43, 111 AND 92.....	62
2.1.10. FLUORESCENT AZADIPEPTIDE NITRILES.....	65
2.1.11. KINETIC CHARACTERISATION OF 119, 120 AND 122.....	67

2.1.12. SPECTRAL PROPERTIES OF 122.....	69
2.1.13. CONCLUSIONS II.....	70
2.2. CATHEPSIN S-SELECTIVE NITRILE INHIBITORS.....	71
2.2.1. KINETIC CHARACTERISATION OF 129–138 AND 144, 148.....	76
2.2.2. CONCLUSIONS III.....	79
2.3. DEVELOPMENT OF ‘ACTIVITY-BASED’ PROBES.....	80
2.3.1. KINETIC CHARACTERISATION OF 158 AND 160, 161.....	83
2.3.2. SPECTRAL PROPERTIES OF 158 AND IMAGING EXPERIMENT.....	86
2.3.3. CONCLUSIONS IV.....	88
3. EXPERIMENTAL SECTION.....	89
3.1. INHIBITION ASSAYS AND EQUATIONS.....	90
3.1.1. CATHEPSIN L INHIBITION ASSAY (I).....	90
3.1.2. CATHEPSIN L INHIBITION ASSAY (II).....	91
3.1.3. CATHEPSIN S INHIBITION ASSAY (I).....	92
3.1.4. CATHEPSIN S INHIBITION ASSAY (II).....	93
3.1.5. CATHEPSIN K INHIBITION ASSAY (I).....	94
3.1.6. CATHEPSIN K INHIBITION ASSAY (II).....	95
3.1.7. CATHEPSIN B INHIBITION ASSAY.....	96
3.1.8. EQUATIONS.....	97
3.2. SPECTRAL PROPERTIES AND IMAGING EXPERIMENT.....	98
3.3. PREPARATION OF COMPOUNDS.....	99
3.4. NMR SPECTRA.....	189
4. REFERENCES.....	221
ZUSAMMENFASSUNG.....	242

ABBREVIATIONS

ABP	'activity-based' probe
Ac	acetyl
AMC	7-amino-4-methylcoumarin
APP	amyloid precursor protein
BACE1	β -site APP-cleaving enzyme
Bn	benzyl
Boc	<i>tert</i> -butyloxycarbonyl
BODIPY	boron dipyrromethene (difluoride)
Cath	cathepsin
Cbz (Z)	carboxybenzyl
CD	cluster of differentiation
CDI	1,1'-carbonyldiimidazole
CHAPS	3-[(3-cholamidopropyl)dimethylammonio]-1-propanesulfonate
CHMP	committee for medicinal products for human use
CLIP	class II-associated invariant chain peptide
compd	compound
d	doublet
DAD	diode array detector
dd	double doublet
DIPEA	<i>N,N</i> -diisopropylethylamine
DMAP	dimethylaminopyridine
DMF	dimethylformamide
DMSO	dimethyl sulfoxide
DPP-IV	dipeptidyl peptidase IV
dt	double triplet
DTT	dithiothreitol
EDC	1-ethyl-3-(3-dimethylaminopropyl)carbodiimide
EDTA	ethylenediaminetetraacetic acid
EI	electron ionization (electron impact)
ESI	electrospray ionization
Et	ethyl
GFP	green fluorescent protein

GLP	glucagon-like peptide
HBTU	2-(1 <i>H</i> -benzotriazole-1-yl)-1,1,3,3-tetramethylammonium hexafluorophosphate
HOBt	1-hydroxybenzotriazole
HPLC	high performance liquid chromatography
HSAB	hard and soft acids and bases
<i>i</i> -Bu	isobutyl
IFN	interferon
IL	interleukin
<i>i</i> -Pr	isopropyl
IR	infrared spectroscopy
m	multiplet
MCPBA	<i>meta</i> -chloroperoxybenzoic acid
Me	methyl
MHC	major histocompatibility complex
MS	mass spectrometry
NMM	<i>N</i> -methylmorpholine
NMR	nuclear magnetic resonance
pNA	<i>para</i> -nitroaniline/ <i>para</i> -nitroanilide
RANK	receptor activator of nuclear factor- κ B
rt	room temperature
s	singlet
SARs	structure-activity relationships
SDS-PAGE	sodium dodecyl sulfate polyacrylamide gel electrophoresis
sept	septet
SERM	selective oestrogen receptor modulator
t	triplet
<i>t</i> -Bu	<i>tert</i> -butyl
TEA	triethylamine
TFA	trifluoroacetic acid
THF	tetrahydrofuran
TNF	tumor necrosis factor
<i>tert</i>	tertiary
UV	ultraviolet
VIS	visible

1. INTRODUCTION

1.1. GENERAL REMARKS

The human genome encodes more than 500 proteases (for a review, see [1]). Among them, a heterogeneous group is referred to as cathepsins, regardless of the catalytic mechanism. Cathepsins were described initially as lysosomal proteolytic enzymes due to their localization in the lysosomes. Whereas cathepsins A and G are serine proteases, and cathepsins D and E are aspartic proteases, cathepsins B, C, F, H, K, L, O, S, V, W and X are cysteine proteases of the papain-like subfamily C1A and represent the largest and best characterized group of cathepsins. Cysteine proteases of the C1A subfamily are ubiquitous among living organisms including bacteria, viruses, plants, lower and higher animals. Most of the cysteine cathepsins are endopeptidases, with the exception of the true exopeptidases cathepsins C and X. The main function of the eleven papain-like lysosomal cysteine proteases listed above is the degradation of proteins that have entered the lysosomal system. The cleavage of the peptide bond, catalyzed by cysteine cathepsins, is initiated by the nucleophilic attack of the active site cysteine to form an acyl enzyme and to release the first product. In the second step of the acyl transfer, the hydrolysis of the thiol ester bond leads to the release of the second product and to the formation of the free enzyme. The proteolytic activity is mediated by a catalytic triad composed of the cysteine residue located at the centre of the catalytic site, a histidine residue, and an asparagine residue for keeping the imidazole ring of histidine in a favourable orientation to the thiol group of the catalytic cysteine [2].

Cysteine cathepsins are synthesized as inactive proenzymes and processed to active enzymes during maturation. Synthesis of cathepsins starts on membrane ribosomes with an amino-terminal signal peptide mediating the nascent polypeptide chain into the rough endoplasmic reticulum (for a review, see [3]). Following cotranslational cleavage of the presequence, the proenzymes are then transported to the Golgi complex for modification of the oligosaccharides to high-mannose carbohydrates and phosphorylation of the mannose residues. This modification allows the binding of procathepsins to membrane-bound mannose-6-phosphate receptors directing them into transport vesicles targeted to late endosomes (for reviews, see [4] and [5]). Within the acidic environment of late endosomes, the prodomain is cleaved converting the inactive zymogens into the mature active enzymes [6], [7]. Activation can occur either autocatalytically [8], [9], as exemplified, or through cleavage catalyzed by cathepsin D [6], [10], L or S [11] or other typical lysosomal proteases (for a review, see [5]).

Cathepsins are monomeric enzymes with molecular weights between 22 and 28 kDa with one exception; cathepsin C forms a tetrameric complex, which has a molecular weight of 200 kDa [12], [13]. They all have a papain-like fold revealed in the early days of crystallography [14]. However, structural characterization of cathepsins began in the early 1990s with the structure of cathepsin B [15]. Crystal structures of all human lysosomal cysteine cathepsins or their mammalian orthologs with the exception of cathepsins O and W are now available. In contrast to the structure of the processed form of cathepsins, only a few zymogen structures are available ([15–28]; for a review, see [29]). The papain-like fold consists of two domains, L and R, folded together displaying a V-shaped configuration. The active site lies at the interface between these two domains. The L-domain is mainly composed of three α -helices whereas the R-domain is based on a β -barrel motif. The crystal structure of the zymogen already revealed the configuration of the activated mature enzyme. The prodomain forms an α -helical domain and is folded in such a way that it blocks access to the active site cleft [30–33]. Propeptides are in fact inhibitors of their cognate enzymes, as shown for cathepsin K, L and S by kinetic analyses [34].

Substrates bind along the active site cleft of the mature enzyme in an extend conformation [35]. According to the Schechter and Berger [36] nomenclature, the subsites on the protease are called S (for subsites), and the substrate amino acid residues are called P (for peptide). The amino acid residues of the amino-terminal side of the scissile bond are named P1, P2, P3, P..., and those residues of the carboxy-terminal side are numbered P1', P2', P3' P...'. By definition, the scissile bond is located between P1 and P1' residues (Fig. 1).

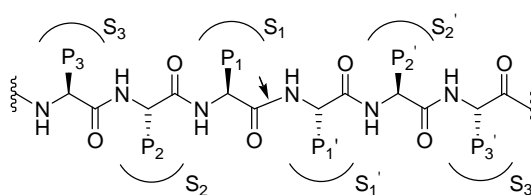


Figure 1. Schematic depiction to illustrate the Schechter and Berger nomenclature.

Predominantly three substrate binding sites of cysteine cathepsins, S2, S1 and S1', mediate main as well as side chain contacts between substrates and enzymes (for a review, see [37]). Whereas the S2 binding site is a deep pocket, *e.g.* in the case of cathepsins K, S, and L, the S1 and S1' sites provide a binding surface [23], [25], [26], [31]. The S1' pocket of cathepsins X and B is relatively deep and well-defined [28], [38] compared to the endopeptidases cathepsin K, S, and L. In addition, cathepsin B possesses a shallow S2' subsite. The carboxydiptidase

activity is attributed to the presence of an occluding loop, an extra peptide segment, which provides an appropriately spaced acceptor (His-110 and His-111) for the negatively charged C-terminal carboxylate of the substrate at the P2' position [15]. Generally, interactions between the endopeptidases and the P3 and P2' residues of the substrate are solely based on side chains. Thus, the papain-like cysteine proteases represent a special group of peptidases with a small number of substrate-binding sites compared to serine proteases and aspartic proteases.

Most of the enzymes are endopeptidases (cathepsins F, K, L, O, S, V, and W) in which the active-site cleft extends along the whole length of the two-domain interface. However, the papain-like cysteine peptidase subfamily also comprises exopeptidases (cathepsins B, C, H and X) (for reviews, see [29], [39]). Cathepsin B is a carboxydipeptidase, cathepsin C an aminodipeptidase, cathepsin H an aminomonopeptidase, and cathepsin X primarily possesses a carboxymonopeptidase activity. Among these exopeptidases, access to the substrate binding sites is restricted by additional features preventing the binding of longer peptidyl substrates and providing interaction with charged N or C chain termini of substrates; loops in the case of cathepsin B [15] and X [40–42], or propeptide parts in the case of cathepsin H [19] and C [17]. Beside their exopeptidase activity, cathepsins B and H also exhibit endopeptidase activity by conformational flexibility (for reviews, see [4], [39]).

Apart from determinants of gene expression, activity of papain-like cysteine cathepsins is regulated by a number of factors, with pH being the most important. The majority of cysteine proteases are unstable and weakly active at neutral pH and thus are optimized to function in acidic intracellular vesicles. Cathepsin precursors are inactive until they reach their appropriate localization, where activation generally requires an acidic environment, thus preventing indiscriminate activation following mislocalization (for reviews, see [33], [43]). Furthermore, the active site cysteine is readily oxidized preventing thiol-dependent proteolysis, therefore these enzymes need a reducing environment that is provided in the lysosomal compartments by a cysteine-specific lysosomal transport system [44]. Activity is also dependent on the balance between the amount of active enzyme and the amount of endogenous inhibitors. Numerous inhibitors of papain-like cysteine cathepsins have been described. The most abundant is the superfamily of cystatins, which bind tightly and essentially irreversibly to the corresponding cysteine proteases [45].

As soluble enzymes with a clear preference for slightly acidic pH conditions and reducing environments, cysteine cathepsin activity is mainly localized within the compartments of the endosomal-lysosomal system and traditionally believed to be responsible for bulk protein

turnover. By the use of cathepsin gene knockouts, functional redundancy of cathepsins regarding unspecific protein degradation was shown ([46–51]; for a review, see [52]). However, beside their role in non-selective protein turnover, gene knockouts also revealed specific and individual functions which are very important for normal cell processes (for a review, see [3]). These specific functions are often associated with restricted tissue localization of the cathepsins, as demonstrated for cathepsin S being predominantly expressed in spleen [53], the thymus and testis-specific cathepsin V [54] also known as cathepsin L2, and cathepsin K which is highly expressed in ovaries and osteoclasts [55]. Although cathepsins B, C, F, H, L, O, and X are ubiquitously or widely expressed (for a review, see [3]), this does not preclude them from being involved in more specialized processes because subcellular localization of cathepsins in different organelles and even at the cell surface under specific physiological circumstances must be considered ([56]; for a review, see [57]). An enormous amount of data describing the function of cathepsins has been achieved through the generation of gene-targeted knockout animal models (for a review, see [58]). A few remarks about the more specific functions of the five most extensively characterized cathepsins B, K, S, L and C are given in the following paragraphs.

1.2. FUNCTIONS OF CATHEPSINS B, K, S, L, AND C

Cathepsin B is involved in physiological processes, such as remodeling of the extracellular matrix, promoting cell migration during wound healing ([59]; for a review, see [60]), and apoptosis ([61], [62]; for reviews, see [63], [64]). In addition, cathepsin B-deficient mice show alterations in pancreas and thyroid physiology [65], [66], but do not display any severe phenotype suggesting that cathepsin B is not essential in normal development [65]. This is probably due to a functional redundancy of cathepsins B and L because combined deficiency in mice is lethal [67], which was not observed for single-deficient mice [51].

Cathepsin K was shown to be crucial for bone matrix degradation (for a review, see [43]). This enzyme was initially detected in osteoclasts, multinucleated cells mediating normal bone remodeling [55], [68], [69]. Later, cathepsin K mRNA was detected in a variety of tissues [70–72]. Cathepsin K is secreted by osteoclasts and degrades several components of the bone matrix including type I collagen, the main constituent of the organic matrix of bones, as well as osteopontin and osteonectin. The degradation of collagen mediated by cathepsin K occurs not only outside osteoclasts but also in lysosomes within the osteoclasts [73] because inhibition of cathepsin K by specific inhibitors or by cathepsin K antisense oligonucleotides results in the accumulation of undigested collagen fibrils in lysosomes within the osteoclasts (for a review, see [74]). Recently, beside its collagen degrading activity, a regulatory function in bone resorption was identified for cathepsin K [75].

Cathepsin S has been demonstrated to play an essential role in the MHC class II antigen presentation pathway. It is the major processing enzyme of the MHC class II invariant chain necessary for subsequent peptide loading ([49], [76–78]; for reviews, see [79], [80]), which was investigated by the use of a specific cathepsin S inhibitor [81]. Cathepsin S activity was quantified mainly in endosomes of antigen presenting cells using a novel specific substrate [82]. In addition, the repertoire of antigenic peptides in cathepsin S-deficient mice was changed providing an involvement of cathepsin S in the generation of antigenic peptides [78].

Also, cathepsin L (and F) seems to participate in processing of the MHC class II invariant chain, primarily in cells or tissues not expressing cathepsin S [47], [83]. Furthermore, cathepsin L is involved in epidermal homeostasis and regular hair-follicle morphogenesis and recycling; cathepsin L-deficient mice developed periodic hair loss and epidermal hyperplasia [51] similar to the phenotype of the *furless* mouse mutant [84]. Within secretory vesicles, cathepsin L is responsible for the generation of several peptide neurotransmitters and

hormones (for a review, see [85]). Recently, it was shown that cathepsin L participates in the turnover of the extracellular matrix by conversion of proheparanase into its active form which is able to degrade heparan sulfate in the extracellular matrix and on the cell surface [86].

Cathepsin C (also referred to as dipeptidyl peptidase I) appears to be important for the processing and activation of serine proteases in immune cells. For instance, cathepsin C is involved in the conversion of pro-granzymes into proteolytically active enzymes. It was reported that granzymes A and B from cytotoxic T-lymphocytes of cathepsin C-deficient mice are mostly inactive ([50]; for a review, see [87]). Granzymes are serine proteases which are required for cytotoxic lymphocyte granule-mediated apoptosis of target cells. Cathepsin C also activates pro-inflammatory serine proteases, *e.g.* cathepsin G, neutrophil elastase and proteinase-3, expressed in mature neutrophils involved in inflammation [88], [89].

1.3. INVOLVEMENT OF CATHEPSINS IN DISEASES

Imbalance of normal cathepsin activity is associated with a number of pathological events, including rheumatoid arthritis and osteoarthritis, inflammation, cancer, neurological disorders, multiple sclerosis, pancreatitis, diabetes, osteoporosis and lysosomal storage diseases. Cysteine cathepsins are important processing enzymes participating in proteolytic cascades, their altered expression and/or activity is involved in a high number of diseases (for reviews, see [43], [74], [90–99]). Furthermore, many of the diseases mentioned above correlate with subcellular mislocalization of these enzymes, for example outside lysosomes in the cytosol or in the extracellular environment (for a review, see [3]).

As mentioned before, cathepsin K is the major enzyme responsible for the degradation of the protein matrix of bone. The important role of cathepsin K for the function of osteoclasts was first suggested by the finding that cathepsin K activity deficiency induces pycnodysostosis, a disorder with an increase in bone mineral density (for reviews, see [29], [33], [43], [74]). This emerging evidence has made cathepsin K an important pharmacological target for the treatment of osteoporosis (for reviews, see [97], [98], [100]).

Cathepsin S has been discussed to be involved in autoimmune diseases such as rheumatoid arthritis because it mediates the degradation of the MHC class II invariant chain Ii, which is afterwards competent for binding antigenic peptides. Additionally, cathepsin S has been implicated in the degradation of endosomal/lysosomal proteins to generate the peptide fragments that are loaded into the MHC class II peptide-binding groove in human antigen-presenting cells ([49]; for reviews, see [43], [76–80]). Therefore, selective inhibition of cathepsin S is a potential mechanism for modulating the immune response. It has been shown that inhibition of cathepsin S alters autoantigen presentation and the development of organ specific autoimmunity in a murine model exhibiting an autoimmune disorder [101].

Cytosolic forms of cathepsin B, one of the most stable proteases at neutral pH, and cathepsins D and L, leaking out of the lysosomes, were shown to participate in apoptosis ([61], [62], [102]; for reviews, see [63], [64]). For instance, it was published recently that granulysin, a lipid-binding protein exhibiting antimicrobial activity, can target lysosomes of tumor cells and induce partial release of lysosomal contents into the cytosol, triggering programmed cell death [103]. Because a variety of different models confirm the biological importance of cathepsins in the regulation of apoptosis under physiological conditions, it is hence not surprising that altered activity or subcellular localization of cathepsins leads to

defects in the apoptotic mechanism closely related to the development of various diseases, in which the life span of cells is reduced (for a review, see [64]).

Several cysteine cathepsins were identified to be involved in cancer progression on the basis of their increased expression and/or activity in various human and mouse tumors ([104]; for reviews, see [91–96]). During cancer progression, cathepsins are often translocated to the cell surface or secreted into the extracellular milieu. They can still function outside tumor cells because the extracellular microenvironment of tumors is generally acidic (for a review, see [105]). In the extracellular milieu, cysteine cathepsins can promote tumor invasion either through uncontrolled cleavage of components of the extracellular matrix and basement membrane, through activation of growth factors or other proteases such as matrix metalloproteinases and urokinase plasminogen activator, which in turn promote invasion, or through cleavage of cell adhesion proteins (for a review, see [93]).

Several genetic disorders have been attributed to mutations in genes of cysteine cathepsins. For example, pycnodysostosis, characterized by severe bone abnormalities, is a rare, autosomal recessive skeletal disease caused by a mutation located within the *cathepsin K* gene [106]. On the other hand, loss-of-function mutation in the gene encoding cathepsin C leads to Papillon-Lefèvre syndrome, an autosomal recessive disorder, characterized by palmoplantar keratosis and severe early-onset periodontitis [107]. Similarly, disorders can also be based on down-regulation of the endogenous inhibitors of cysteine cathepsins which is the case for the hereditary form of monogenic epilepsy caused by a mutation in the gene encoding stefin B (cystatin B) ([108]; for reviews, see [17], [29]).

In addition, cathepsins were reported to be implicated in neurodegenerative diseases, such as Morbus Alzheimer. The formation of the amyloid β peptide ($A\beta$), deposited in the brain as amyloid plaques playing the major role in the pathogenesis of Alzheimer's disease, is initiated by processing the amyloid precursor protein (APP) through cleavage by the two proteases β -secretase and γ -secretase. It is widely accepted that the major neuronal β -secretase is a transmembrane aspartyl protease termed BACE1 (β -site APP-cleaving enzyme 1) (for reviews, see [109], [110]). It has been proposed that cathepsin B may function as β -secretase [111]. However, an $A\beta_{42}$ reducing activity of cathepsin B was demonstrated in a study with transgenic cathepsin B deficient mice, expressing human APP containing the Swedish and Indiana mutations at the β -secretase and γ -secretase sites. The authors proposed anti-amyloidogenic and neuroprotective functions of cathepsin B [112]. On the other hand, it was reported that cysteine protease inhibitors reduced levels of brain $A\beta_{40}$ and $A\beta_{42}$ in a guinea pig model of human $A\beta$ production [113]. Moreover, the β -secretase activity to cleave

the wild-type APP in regulated secretory vesicles, represented by cathepsin B, was suppressed by cysteine protease inhibitors. *In vivo* treatment of London APP mice with the inhibitors resulted in an improvement in memory deficit, a reduced amyloid plaque load and decreased A β 40 and A β 42 [114]. A recently published article showed that lowering A β levels in brain of cathepsin B-deficient mice depends on the type of APP expressed in these transgenic knockout mice. Whereas cathepsin B knockout in mice expressing human APP containing the rare Swedish and Indiana mutations had no effect on A β , the use of cathepsin B-deficient mice expressing human wild-type APP resulted in substantial decreases in brain A β . It was therefore concluded that cathepsin B is a target for inhibitors to lower A β in Alzheimer's disease [115]. An epoxide inhibitor of cathepsin B as well as small interfering RNA produced decreases in A β 42 release. It was discussed by the authors that cathepsin B acts as a secondary neuronal β -secretase, or indirectly modulates β -secretase activity [116]. Another cysteine cathepsin, cathepsin L, might also be involved in APP processing, even though this enzyme is responsible for the opposing effect, the reduction of A β 42 levels [116].

It is now becoming clear that cysteine cathepsins should be seriously considered as potential drug targets in several diseases, most notably in a wide range of cancers, osteoporosis and autoimmune diseases. Small-molecule inhibitors directed against cathepsin K or cathepsin S are currently under clinical trials for the treatment of osteoporosis and bone metastasis, or for the treatment of autoimmune diseases ([137]; for reviews, see [74], [90], [92], [96], [100]).

1.4. BONE REMODELING AND OSTEOPOROSIS

The human skeleton is metabolically active organ that undergoes continuous remodeling processes throughout the lifespan. Approximately 10% of human bone is replaced each year whereas the full renewal is completed every 10 years. The bone remodeling cycle involves a complex series of sequential steps with three main phases: (1) resorption of mineralized bone by osteoclasts; (2) appearance of mononuclear cells on the bone surface; and (3) formation of bone matrix by osteoblasts that subsequently become mineralized (Fig. 2) (for reviews, see [117], [118]).

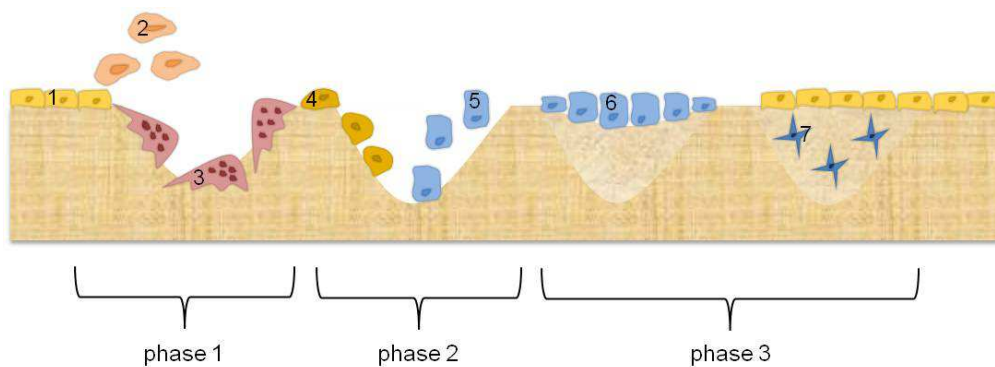


Figure 2. Bone remodeling cycle [119].

(1) Resting bone surface; (2) Preosteoclasts; (3) Active osteoclasts; (4) Mononuclear cells; (5) Preosteoblasts; (6) Osteoblasts; (7) Osteocytes.

In turn, the osteoclastic bone resorption requires two processes: (1) demineralization of the inorganic bone components; and (2) degradation of the organic bone matrix. The first phase involves acid secretion by the osteoclast into the resorption lacunae, and the second phase is the proteolytic degradation of the organic bone matrix. The major proteolytic activity in osteoclasts is represented by cathepsin K with 98% of the total cysteine protease activity in these cells. Osteoclast-expressed cathepsin K is able to degrade several organic bone components including type I collagen, which constitutes approximately 90% of the organic bone matrix, as well as osteopontin and osteonectin (for reviews, see [97], [119]).

An imbalance between bone resorption and bone formation (also known as abnormal bone remodeling) can result in different diseases such as pycnodysostosis and osteoporosis. Osteoporosis is a skeletal disorder characterized by reduced bone density and micro-architectural deterioration leading to enhanced bone fragility and high risk for spontaneous fractures. Osteoporosis can be classified as primary type I (postmenopausal osteoporosis),

primary type II (senile osteoporosis) and secondary (with traceable aetiology) (for a review, see [120]). Aside from its human cost, osteoporosis is a considerable public health problem with enormous economic impact. For example, 3.79 million osteoporotic fractures were estimated in Europe in the year 2000 causing the total direct costs of 31.7 billion € [121].

Current treatment options of osteoporosis are mainly four classes of drugs: (1) calcitonins; (2) bone calcium regulators; (3) selective oestrogen receptor modulators (SERMs); and (4) parathyroid hormones (PTHs). Bisphosphonates, belonging to the bone calcium regulators, dominate the osteoporosis market as a gold standard for osteoporosis treatment. The most promising innovative antiosteoporotic drug is denosumab. Denosumab is a humanized monoclonal antibody that inhibits RANK-L (the ligand of receptor activator of nuclear factor- κ B) preventing differentiation of osteoclast precursors into bone resorbing osteoclasts (for a review, see [122]). The Committee for Medicinal Products for Human Use (CHMP) adopted a positive opinion for denosumab on December 17, 2009. The approved indication for this drug is: (1) treatment of osteoporosis in postmenopausal women at increased risk of fractures; and (2) treatment of bone loss associated with hormone ablation in men with prostate cancer at increased risk of fractures [123]. A further interesting new drug candidate for osteoporosis treatment is odanacatib (**13**, Fig. 10). Odanacatib is a potent and selective nitrile-containing cathepsin K inhibitor which is currently in the clinical development. Two studies have been carried out to evaluate the efficacy and safety of odanacatib. In a randomized, placebo controlled, double-blind phase I study in post-menopausal women, the optimal dose of odanacatib was determined. Reductions in resorption markers were greatest for doses > 50 mg weekly and doses ≥ 2.5 mg daily. In a further double-blind, randomized, placebo-controlled trial including 399 post-menopausal women, the efficacy and safety of odanacatib was evaluated. In this phase II study, statistically significant reductions of resorption markers were observed in patients receiving 50 mg odanacatib weekly. Furthermore, bone biopsies were carried out in 28 patients and showed no adverse histologic effects. To clarify the efficacy of odanacatib in term of fracture reductions, a phase III study is ongoing, with results expected in 2012. This is a clinical, randomized, double-blind trial with 16,000 patients [124].

1.5. ANTIGEN PRESENTATION AND AUTOIMMUNE DISEASES

Major histocompatibility complex class II molecules (MHC-II) are expressed by only few specialized antigen-presenting cell types including macrophages as well as dendritic and B cells. MHC-II molecules are involved in the presentation of antigenic fragments required in the endocytic pathway for the activation of CD4 positive T cells. MHC class II molecules are $\alpha\beta$ heterodimers that are synthesized and assembled in the endoplasmic reticulum. The heterodimerisation is assisted by the invariant chain (Ii) chaperon molecule that additionally blocks the MHC-II peptide-binding groove preventing premature peptide loading. Furthermore, the invariant chain is important for the transport of assembled MHC class II molecules through the Golgi apparatus ([125]; for a review, see [126]). In general, two main proteolytic events occur during MHC-II-mediated antigen presentation: (1) cleavage of the antigens to small antigenic peptides for the binding in the binding groove of MHC-II molecules; and (2) degradation of the invariant chain (Fig. 3).

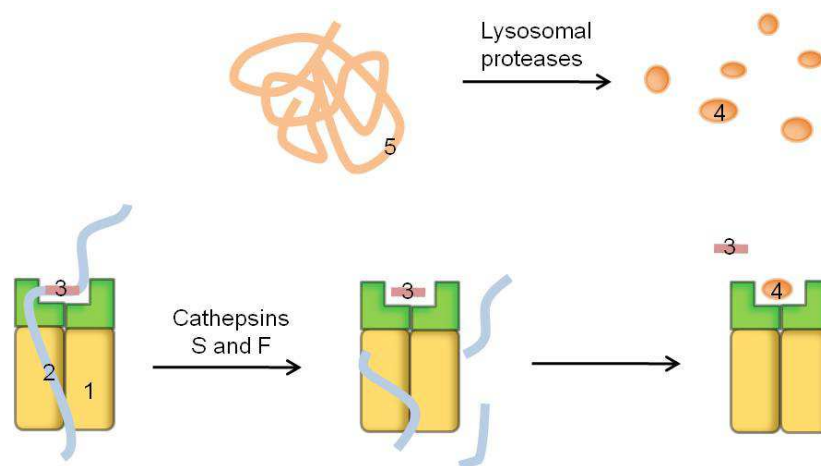


Figure 3. MHC-II-mediated antigen presentation and the role of cathepsin S [119].

(1) MHC class II molecule (MHC-II); (2) Invariant chain (Ii); (3) CLIP; (4) Antigenic peptide; (5) Antigen.

Antigen processing seems to be a multienzyme-catalyzed process involving several cysteine and aspartic proteases. It was not possible until now to identify single proteases playing a crucial role in the cellular antigen degradation. In contrast, cathepsin S was described as the major processing enzyme of the invariant chain in the MHC-II-mediated antigen presentation confirmed by the delayed Ii processing in the cells isolated from cathepsin S deficient mice. Cathepsin S is capable to cleave the invariant chain leaving an approximately 15 amino acid

long class II associated invariant chain peptide (CLIP), which can be replaced by antigenic peptides (Fig. 3). It was further reported that the role of cathepsin S in the Ii degradation process in the cells from cathepsin S-deficient mice can be adopted by cathepsin F, which is expressed at high levels in macrophages, but not in dendritic and B cells. The proteolytic synergism of cathepsins S and F in the Ii degradation process could be used for the modulation of the immune response using selective inhibitors of these enzymes ([83]; for reviews, see [119], [126]).

Autoimmunity is understood as a failure of self tolerance. Because it is not possible to explain all autoimmune diseases by a single theory, it was suggested to consider the ‘mosaic’ of autoimmunity [127] involving genetic, hormonal, immunological, and environmental factors. Autoimmune diseases can be divided in systemic (*e.g.* systemic lupus erythematosus) and organ-specific (*e.g.* type I diabetes mellitus). It is further distinguished between diseases, in which the selection and regulation of T and B cells is generally altered, and diseases responsible for a particular antigen (for reviews, see [128], [129], [130]). The most important drugs currently used for the treatment of autoimmune diseases are immunosuppressive agents such as corticosteroids, cytotoxic compounds (azathioprine and 6-mercaptopurine), antimetabolites (methotrexate), and calcineurin inhibitors (cyclosporin A) (for a review, see [131]). The innovative therapeutic strategies for the treatment of autoimmune disorders includes follow therapeutic possibilities: (1) anti-CD4, anti-CD3 and anti-CD28 antibody treatment that could potentially be used to regulate T cell population; (2) lytic anti-CD20 therapy to regulate B cell population (rituximab for the treatment of rheumatoid arthritis and systemic lupus erythematosus [132]); and (3) therapies directed against cytokines important for the T cell growth (IL-2, IL-4, IL-7, IL-15, IL-21) and inflammation (TNF, IL-1, IL-6, IFN- γ). TNF monoclonal antibodies (infliximab [133]) and the TNF-receptor (TNFR) fusion protein (etanercept [134]) are already in clinical use (for a review, see [135]). Furthermore, cathepsin S is currently considered to be an interesting new target for the therapy of autoimmune disorders, since it was found that cathepsin S inhibitors prevents autoimmunity in murine models of Sjögren syndrome and myasthenia gravis [136], [137].

1.6. NITRILE-BASED INHIBITORS OF CYSTEINE CATHEPSINS

1.6.1. EARLY STUDIES

Inhibitors of cysteine cathepsins are mainly peptidic or peptidomimetic structures containing electrophilic groups prone to covalent interactions with the active-site cysteine. Among them, nitrile inhibitors receive the most attention in current drug discovery (for a review, see [178]). The first nitrile compounds, for which inhibition of a cysteine protease has been described, were acetamidoacetonitrile **1** and benzamidoacetonitrile **2** shown in Figure 4. These acylated glycine nitriles inhibited the plant protease papain at pH 7 with K_i values of 31 mM and 390 μ M, respectively [138]. Compound **4**, *N*-acetyl-L-phenylalanyl-glycine-nitrile, represents a dipeptide nitrile with a decreased K_i value (0.73 μ M) towards papain [139], [140].

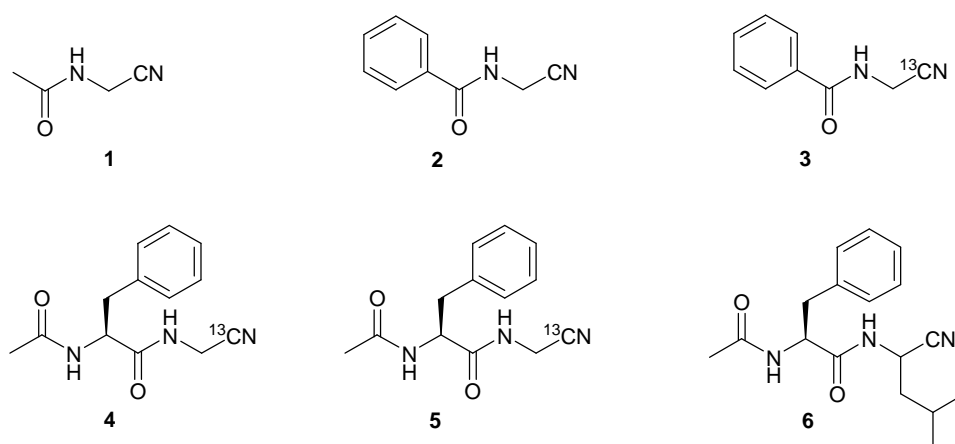


Figure 4. Nitrile-based inhibitors of papain.

The reaction of nitrile-based inhibitors with cysteine proteases involves the reversible formation of thioimide adducts (Fig. 5) as it has been initially discovered for papain. This process can be considered as Pinner-type reaction. The Pinner reaction is an organic reaction of a nitrile with an alcohol under acid catalysis. The conversion results in an imide which can be transformed to either an ester or an amidine. NMR experiments provided the first evidence for the formation of a covalent thioimide link between nitrile inhibitors and papain, and also for the regeneration of the nitrile function when the adduct dissociates. It was reported in 1986 that the ¹³C-labeled dipeptide nitrile **5**, upon interaction with papain, yielded a ¹³C NMR signal of the thioimide at 182 ppm, which disappeared, when the

inhibitor was displaced from the active site cysteine [141]. In a similar study, a model thioimide was prepared from **4** and *N*-acetyl-L-cysteine and used to assign the signal for the protein-bound thioimide [142]. Complementary NMR results have also been reported with the ^{13}C -labeled benzamidoacetonitrile **3** [143]. Compound **6**, a dipeptide nitrile with L-Phe in P2 and DL-Leu in P1 position inhibited papain with $K_i = 5.8 \mu\text{M}$ [142].

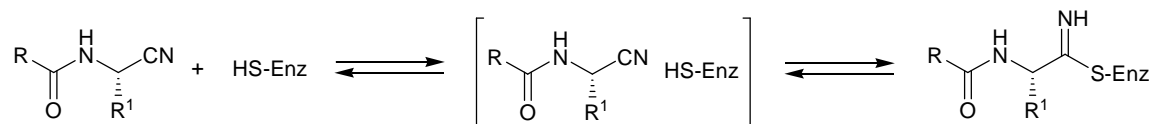


Figure 5. Interaction of cysteine proteases with nitrile-based inhibitors.

A linear free energy correlation for binding of pairs of peptide aldehydes and peptide nitriles was found, indicating an overall similarity in the way in which these two groups of ligands bind to papain, regardless of the difference in geometry at the reacting carbon, *i.e.* sp^2 versus sp for aldehyde versus nitrile ligands; sp^3 versus sp^2 for their adducts [144]. The carbon atom of the thioimide adopts a trigonal geometry, different from that of tetrahedral hemithioacetals formed between cysteine proteases and aldehydes. Thus, the thioimide structure resembles more closely the acyl-enzyme than the tetrahedral intermediate of the enzyme-catalyzed substrate hydrolysis (Fig. 6).

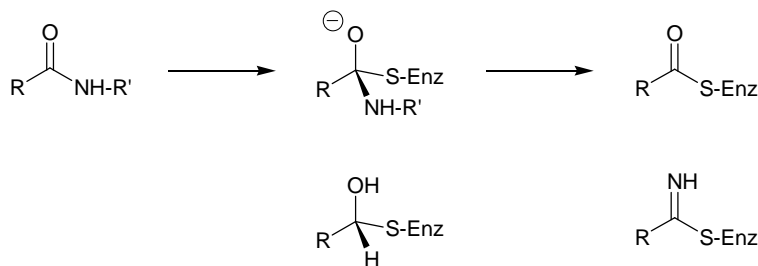


Figure 6. The overall mechanism of cysteine protease-catalyzed substrate hydrolysis is considered to consist of a number of steps involving a covalent acyl-enzyme and transient anionic tetrahedral intermediates and transition states. The formation of the acyl-enzyme complex *via* the tetrahedral intermediate is shown (*top*). The oxyanion is stabilized by interaction with hydrogen bond donors. Comparison of the geometries of hemithioacetal (*left*) and thioimide (*right*) adducts with intermediates in the reaction pathway for substrate hydrolysis. Aldehyde inhibitors form hemithioacetals with the active site cysteine, nitrile inhibitors form thioimides.

The oxyanion hole of cysteine proteases contributes to catalysis by stabilizing inherently unstable transition states. This region in papain is defined by two hydrogen bond donors on

the backbone amide nitrogen of Cys25 and the side chain amide nitrogen of Gln19. Mutants of papain (Gln19Ala, Gln19Glu) have been used to determine the kinetic parameters for inhibition by Phe-Gly-derived aldehyde and nitrile inhibitors. Mutation of Gln19 caused an important loss of inhibition by the peptide nitrile inhibitor, and thioimide adducts with the papain mutants were less stable. However, despite the structural similarity of the hemithioacetals to the tetrahedral intermediate, the affinity of the peptide aldehyde inhibitor was almost unaffected by Gln19 mutations [145].

As a further notable result of these early studies, it was found that amino acid or peptide-derived nitriles did show some selectivity for cysteine over serine proteases [140], [142], and the cyano group was not considered a typical 'warhead' for serine protease [146]. For nitrile inhibitors, the addition of the soft sulfur nucleophile of the cysteine proteases or the hard oxygen nucleophile of the serine proteases can be considered according to the principle of hard and soft acids and bases (HSAB), but has not been investigated so far [147], [148]. Noteworthy, the inhibition of the serine protease dipeptidyl peptidase IV (DPP-IV) by nitrile compounds has received much attention during the last years. Glucagon-like peptide 1 (GLP-1) receptor agonism has emerged as a validated approach for the treatment of type 2 diabetes [149]. Cyanopyrrolidines such as vildagliptin (**7**) and saxagliptin (**8**) are dipeptide nitriles with a basic amino group (Fig. 7). Vildagliptin and saxagliptin were characterized as reversible, slow-binding inhibitors of DPP-IV [146], [150]. The X-ray crystal structure of the DPP-IV: saxagliptin complex revealed the covalent attachment between the active site serine and the inhibitor nitrile carbon [151]. Thus, the so formed imidate corresponds to the thioimide adduct of cysteine protease inhibition by nitriles.

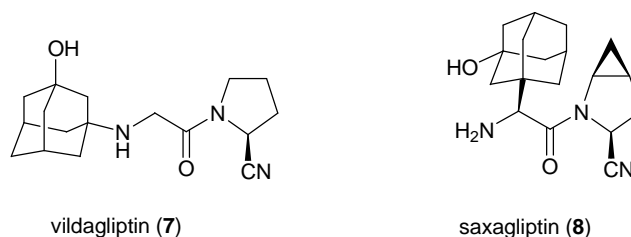


Figure 7. Inhibitors of the serine protease DPP-IV for the treatment of type 2 diabetes.

1.6.2. CONVERSIONS OF THIOIMIDATE ADDUCTS

Chemical transformations of nitriles require strong acid/base conditions or the use of peroxides. Nitrile-hydrolyzing enzymes from microorganisms are known and the question raised whether cysteine proteases exhibit such an activity. In the case of papain [141], [142], [152], the thioimide adduct was found to revert to nitrile, instead of hydrolyzing to form an amide (Fig. 8). However, a peptide nitrile hydratase activity was engineered by a single selected mutation Gln19Glu at the active site of papain. A k_{cat} value, increased by a factor of at least 4×10^5 , was observed at pH 5 for this papain variant compared to the wild type enzyme. The role of the glutamic acid residue is to participate in the acid-catalyzed hydrolysis of the thioimide to the carboxamide by the provision of a proton. The more reactive protonated thioimide readily undergoes nucleophilic attack by water [153]. Because of the well-known amidase activity of papain, the carboxamide is then transformed to the corresponding carboxylic acid (Fig. 8). The enzymatic hydrolysis of nitriles by papain mutant Gln19Glu was also studied in aqueous-organic media [154]. The proposed mechanism of nitrile hydratase activity of the papain mutant was supported by molecular dynamic studies [155].

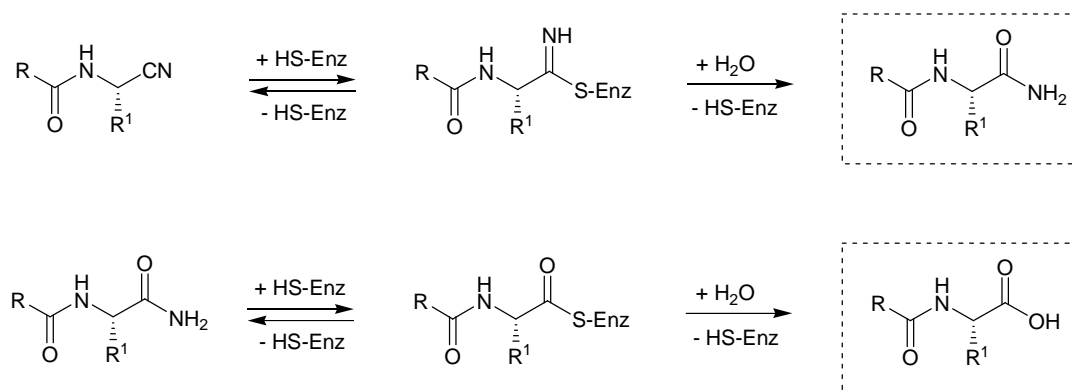


Figure 8. Mechanism for the nitrile hydratase (*top*) and amidase (*bottom*) activities of papain. The wild type enzyme displays very weak nitrile hydratase activity. The resulting carboxamide is hydrolyzed to the acid by the natural amidase activity of the enzyme.

However, the papain-catalyzed conversion of benzamidoacetonitrile **2** or *N*-acetyl-L-phenylalanyl-glycine-nitrile **4** to carboxylic acids *via* corresponding amides could be accomplished with high enzyme concentration in the presence of an external thiol as monitored with NMR and HPLC. An attack of β -mercaptoethanol or *N*-acetylcysteamine at

the thioimide adduct produces a non-enzyme bound thioimide, which is readily hydrolyzable. Once the amide is formed, papain catalyzes its conversion to the acid [156]. This pathway was later considered in an investigation with **9**, a biaryl inhibitor of cathepsin K (Fig. 9). However, no detectable amounts of the corresponding amide **10** or acid **11** were observed in the HPLC profiles of the incubation mixture of **9**, cathepsin K, and external thiols [157].

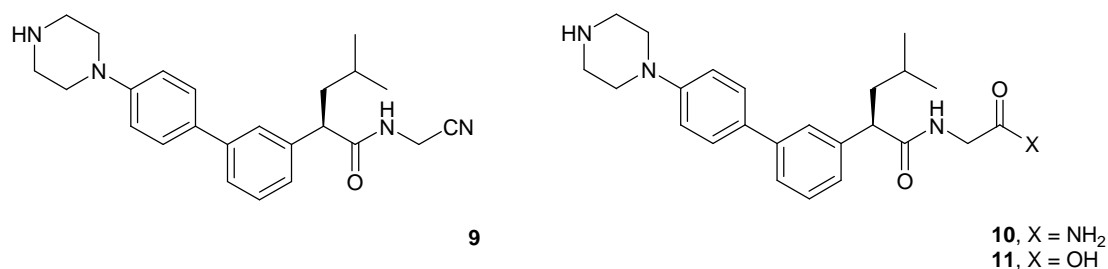


Figure 9. Structure of **9**, a non-peptidic biaryl inhibitor of human cathepsin K, and its amide and acid analogues **10** and **11**. Compound **9** (500 nM, *i.e.* 100-fold K_i) was a poor substrate for nitrilase activity of cathepsin K (enzyme concentration 1 μ M, β -mercaptoethanol 1 mM, DTT 2.5 mM, pH 5.5, room temperature, 30 min). The amide **10** was readily converted to **11** by cathepsin K, and this amidase activity was blocked by the irreversible cysteine protease inhibitor E64.

1.6.3. SELECTIVE NITRILE-BASED INHIBITORS OF CATHEPSINS K AND S

Considerable scientific attempts have been made to develop highly potent and selective cathepsin K inhibitors, as it became obvious from a number of recent publications (for a review, see [178]). These efforts resulted in the discovery of balicatib (**12**) and odanacatib (**13**) for which several clinical trials have already been conducted (Fig. 10) [97], [124], [158]. The 1-amino-1-cyclohexanecarboxylic acid (homocycloleucine), contributing to the cathepsin K selectivity in balicatib (**12**), was discovered by the introduction of various substituents into the P2 position of Cbz-protected dipeptide nitriles. The following optimization of the P3 substituent led to the identification of balicatib as highly potent and selective cathepsin K inhibitor [159]. Unfortunately, a small number of patients during a phase II study in women with postmenopausal osteoporosis developed morphea-like skin changes under treatment with balicatib [160]. The lysosomal accumulation of balicatib due to its basic piperazine moiety was reported as a possible reason for the observed skin pathology [161]. Regarding this potential toxic effect, further clinical development of balicatib is on hold. In contrast, odanacatib is a non-basic selective cathepsin K inhibitor obtained by the combination of a relatively large biaryl substituent at the P3 position and a fluorinated P2 leucine moiety [162]. As it is shown in Figure 10, odanacatib (**13**) has a peptidomimetic structure in which the P3-P2 amide linker is replaced by a trifluoroethylamine group for the enhancement of the binding affinity [163]. Moreover, the unnatural cyclopropane moiety was introduced into the P1 position to stabilize the inhibitor molecule toward proteolytic degradation ([162]; for a review, see [164]). Odanacatib is currently in the phase III clinical development [124].

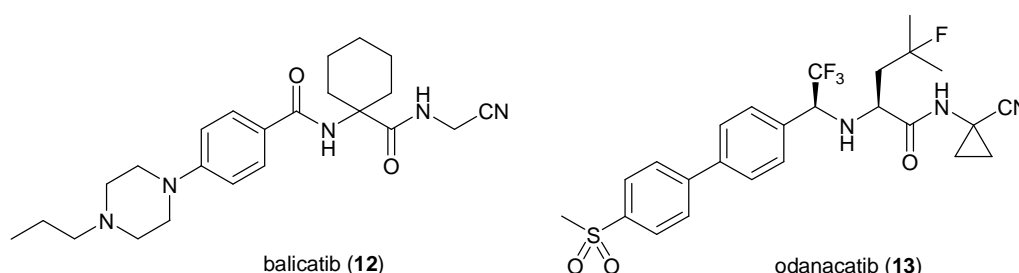


Figure 10. Structures of the cathepsin K inhibitors balicatib (**12**) [159] and odanacatib (**13**) [162].

Selective cathepsin S inhibitors were obtained by the combination of a sulfone moiety, attached to a large group at the P2 position, and a small aromatic P3 substituent (*e.g.* **14** and **15**, Fig. 11). While cathepsin S accommodates the isobutylcysteinesulfone moiety of **14**,

unfavorable interactions with the S2 pocket of cathepsin K provided a rationale for the selectivity of this inhibitor: IC_{50} values of 0.4 nM (cathepsin S), 3058 nM (cathepsin K), 337 nM (cathepsin B), and 132 nM (cathepsin L) were reported for compound **14**. Furthermore, the 2,6-dichlorobenzyl analogue **15** ($IC_{50} = 0.7$ nM) was completely inactive against cathepsins K and B, while being 350-fold selective for cathepsin S over cathepsin L ([165]; for a review, see [178]). Furthermore, it was recently reported on the development of highly potent and selective cathepsin S inhibitors, containing electrophilic α -ketoamide moiety (*e.g.* **16**, Fig. 11) as a ‘warhead’, for which a patent application was carried out (for a patent evaluation, see [166]). These compounds bear *gem*-dialkyl substituted cycloaliphatic rings at the P2 position in combination with small aromatic or saturated heterocyclic/cycloaliphatic P3 substituents.

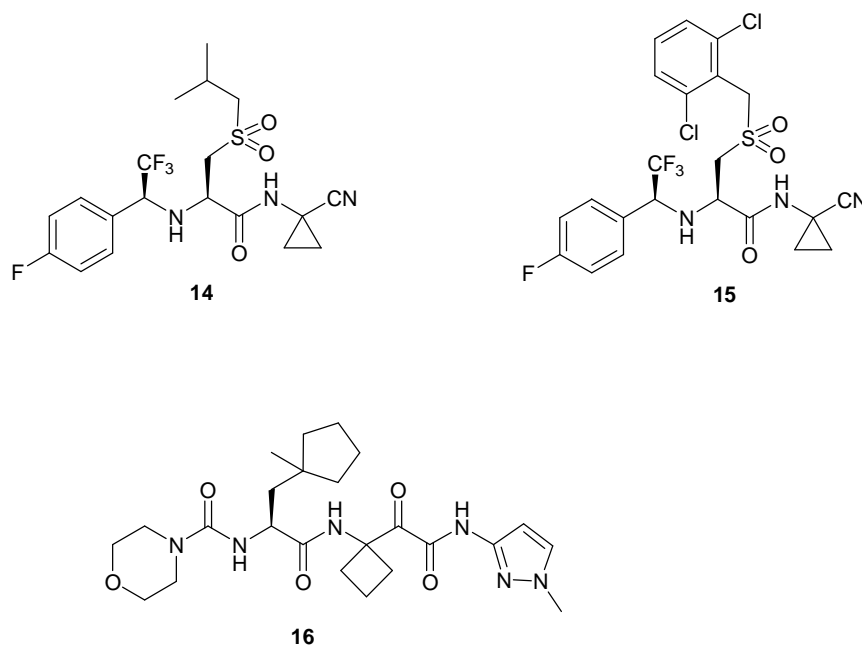


Figure 11. Structures of selective cathepsin S inhibitors **14–16**.

Cathepsin S-selective inhibitors RWJ-445380 and CRA-028129 are already in the clinical development for rheumatoid arthritis and psoriasis, respectively. Unfortunately, neither the results of clinical trials nor the structures of compounds RWJ-445380 and CRA-028129 are available until now (for reviews, see [96], [167]).

1.6.4. AZADIPEPTIDE NITRILES AS INHIBITORS OF CYSTEINE PROTEASES

The isoelectronic replacement of the C α H group by a nitrogen atom to give azapeptides is a common structural modification in the chemistry of peptides. Azapeptides have attracted much interest due to their unique properties and applications as peptidomimetics in a variety of biological systems. Recently, it was reported on proteolytically stable azadipeptide nitriles as a novel class of cysteine protease inhibitors with picomolar K_i values towards therapeutically relevant cathepsins K, S and L. These azadipeptide nitriles were composed of a Cbz-protected P2 amino acid and a P1 aza-amino nitrile whose nitrogens are essentially alkylated for reasons of the synthetic access (Fig. 12) [168]. Furthermore, the azadipeptide nitriles proved to be strong inhibitors of falcipains 1 and 2 from *Plasmodium falciparum* parasite and showed further antimalarial activity [169].

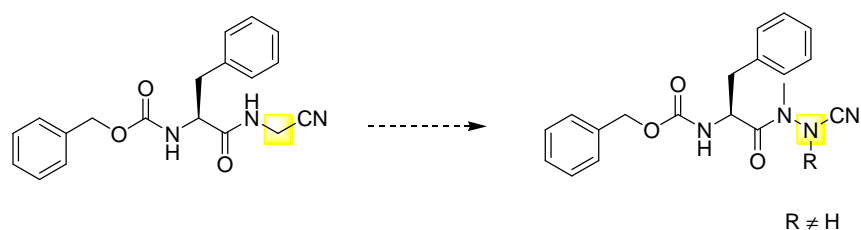


Figure 12. C α /N-exchange leading to an azadipeptide nitrile.

Azadipeptide nitriles exhibited dramatically improved activities toward tested cysteine proteases in contrast to the corresponding carba-analogues. The improved potency of azadipeptide nitriles can be explained by the formation of a resonance-stabilized isothiosemicarbazide adducts with the active-site cysteine of target enzymes (Fig. 13). Furthermore, it has been shown that the covalent isothiosemicarbazide adduct has a reversible nature ([168]; for a review, see [178]).

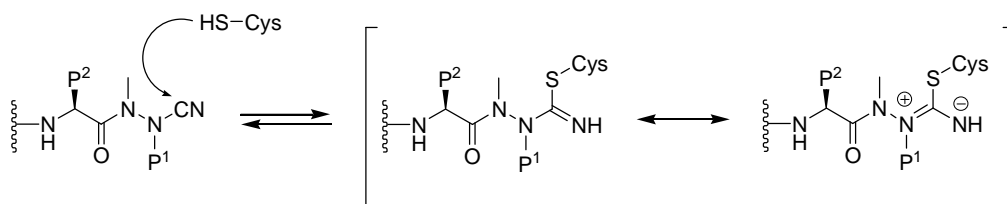


Figure 13. Reversible formation of an isothiosemicarbazide adduct.

In a recent publication, Yao and coworkers reported on the development of organelle-specific drug delivery systems to selectively transport azadipeptide nitriles into the lysosomes [170]. The reported delivery system consists of a Tat peptide derived from the human immunodeficiency virus transactivator protein covalently attached to a non-selective azadipeptide nitrile [168] using the ‘click’ chemistry (compound **17**, Fig. 14). Biological testing showed that the Tat peptide was capable to promote delivery of the attached azadipeptide nitrile to the lysosomes of HepG2 cells.

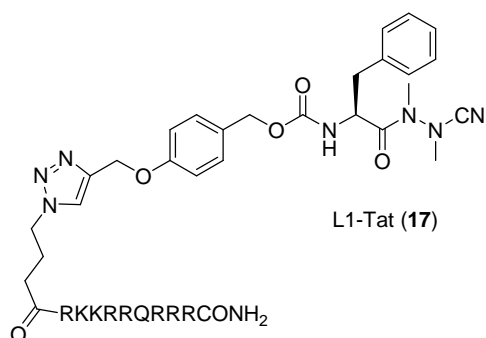


Figure 14. Inhibitor-Tag conjugate L1-Tat.

Despite their excellent inhibitory activity, the reported azadipeptide nitriles were nonselective and it remained unclear whether the selectivity for a single target cathepsin can be achieved at all with this class of inhibitors.

1.7. 'ACTIVITY-BASED' PROBES

Chemical probes that bind into the catalytic site and allow for direct detection of the active enzyme form are termed 'activity-based' probes (ABPs), or 'mechanism-based' probes. ABPs consist mainly of three parts: (1) specific inhibitor; (2) linker; and (3) fluorescent or radioactive reporter. In contrast to chromogenic/fluorogenic substrates and reversible inhibitors, ABPs bind covalently to the active site in an irreversible manner. The applications for ABPs include *de novo* enzyme discovery, high-throughput screening, *in vivo* imaging, and diagnostic of certain diseases (for a review, see [171]).

Recently, it was reported on the development of specific fluorescent ABPs (*e.g.* **18**, Fig. 15) that covalently label active caspases *in vivo* [172]. Caspases are proteolytic enzymes which belong to the C14D subfamily of cysteine proteases. Among them, caspase-3 has been identified as a key mediator of apoptosis in mammalian cells [173]. The monitoring of caspase-3 using specific ABPs allow therefore direct quantification of apoptosis to assess, *e.g.*, chemotherapeutic response in cancer patients.

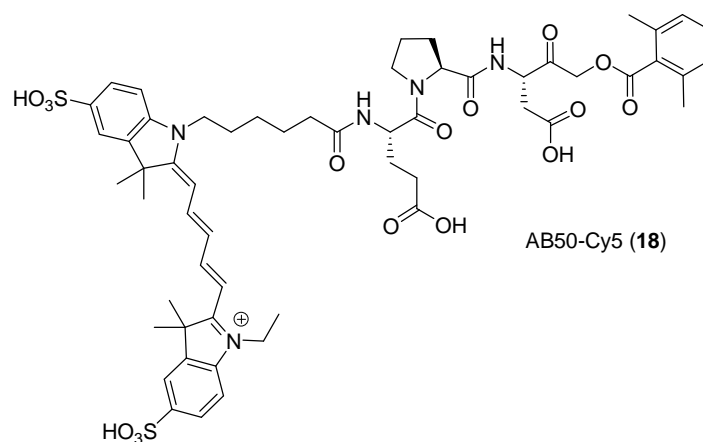


Figure 15. Structure of the caspase probe AB50-Cy5 (**18**) [172].

Furthermore, a cell-permeable, radioiodinated, 'activity-based' probe [125 I]BIL-DMK (Fig. 16) was developed for the determination of cysteine cathepsin activity in whole-cell enzyme occupancy assays [174]. Non-selective activity-based probe [125 I]BIL-DMK contains a diazomethylketone moiety that covalently interacts as a 'warhead' with the active-site of cysteine cathepsins in an irreversible manner. [125 I]BIL-DMK is highly reactive toward the pharmaceutically important cathepsins L, S, K and B. Recently, it was reported that [125 I]BIL-

DMK was used to probe cathepsin S activity in the leukocyte fraction of the whole blood to study distribution and diurnal modulation of this enzyme [175].

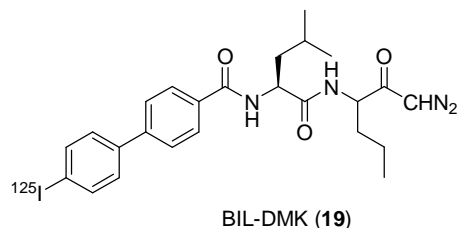


Figure 16. Structure of the radioiodinated cathepsin probe [^{125}I]BIL-DMK (19) [175].

A further interesting activity based probe was developed for ultrasensitive *in situ* visualization of active glucocerebrosidase molecules. Deficiency of glucocerebrosidase causes a lysosomal storage disorder called Gaucher disease. For the diagnostic and treatment of Gaucher disease, it is very important to know the amounts of the active form of glucocerebrosidase in affected cells. The activity-based probe MDW941 (compound 20, Fig. 17) consist of an epoxide-containing cyclophellitol derivative covalently attached to a BODIPY fluorophore. Using MDW941, it was possible to determine the glucocerebrosidase activity by SDS-PAGE in cell lysates of normal individuals and in Gaucher material [176].

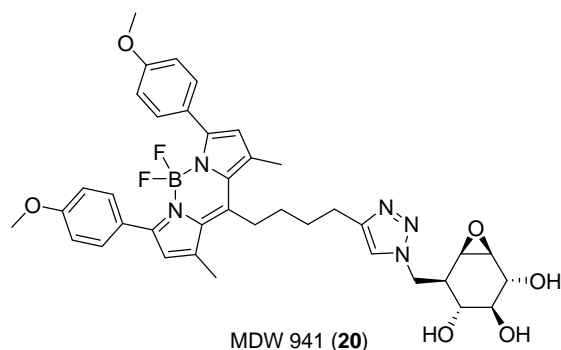


Figure 17. Structure of the glucocerebrosidase probe MDW941 (20) [176].

Although the development of fluorescent ‘activity-based’ probes for cathepsin X was recently published [177], no such ABPs are known for selective probing of cathepsins K and S until now. Therefore, the development of potent ‘activity-based’ probes for these enzymes, *e.g.* for diagnostic and monitoring of osteoporosis and autoimmune disorders, represents an interesting new topic in the field of Medicinal Chemistry.

Parts of the ‘Introduction’ of this work are congruent with the recently published review on nitrile inhibitors of cysteine cathepsins by Frizler *et al.* [178].

1.8. AIM

The aim of this work was the development of potent and selective nitrile-based peptidomimetic inhibitors for human cathepsins K and S, containing a proteolytically stable azadipeptide scaffold, as well as the preparation and characterization of ‘activity-based’ probes for these enzymes.

To obtain highly potent and selective cathepsin K inhibitors, the stepwise optimization of the inhibitor structure was planned (Fig. 18). In the phase **I** of the development process, various substituents had to be introduced into the P2 position of the Cbz-protected azadipeptide nitrile scaffold to obtain a lead structure for further optimization. In the phase **II**, the modification of the P3 moiety as well as of the P3-P2 linker was to be performed.

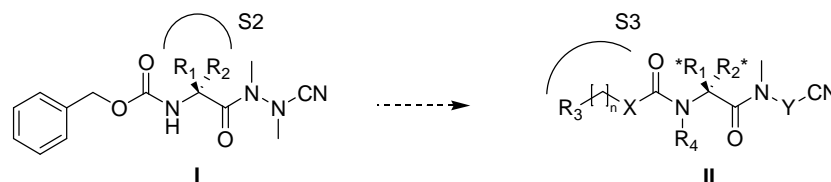


Figure 18. An overview of the planned diversity points for the stepwise optimization of inhibitor molecules to achieve the selectivity for cathepsin K. R_1 , R_2 , R_3 = various substituents; $*R_1$, R_2^* = optimized substituents; R_4 = Me or H; X = N, O or 0; Y = NMe or CH_2 , n = 0 or 1.

In a second project of this work, the systematic scan for P3 substituents of the dipeptide nitrile scaffold, containing isobutylcysteinesulfone moiety [165] at the P2 position, had to be performed to explore the S3 binding pocket of cathepsin S (Fig. 19, *left*).

Finally, irreversible, fluorescent ‘activity-based’ probes for cathepsins K and S, bearing a vinyl sulfone ‘warhead’, were to be prepared and evaluated *in vitro* (Fig. 19, *right*).

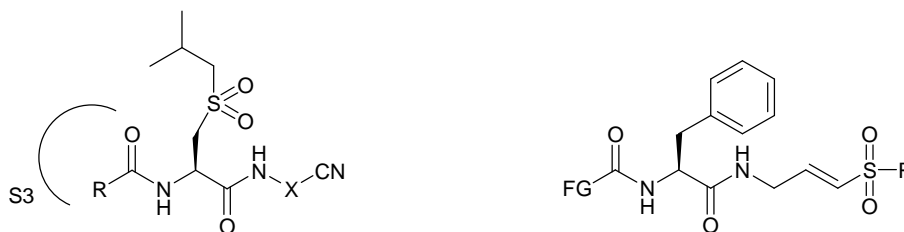


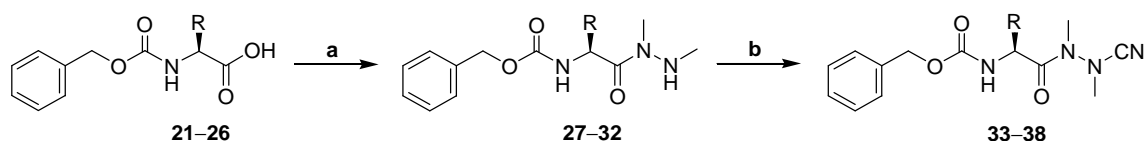
Figure 19. Systematic scan for P3 substituents (*left*) and fluorescent ‘activity-based’ probes (*right*). R = various substituents; Y = NMe or CH_2 ; FG = fluorescent group.

2. RESULTS AND DISCUSSION

2.1. AZADIPEPTIDE NITRILES AS CATHEPSIN K INHIBITORS

2.1.1. SYSTEMATIC SCAN FOR P2 SUBSTITUENTS

To develop potent and selective nitrile inhibitors of cathepsin K, a systematic scan for P2 substituents of the azadipeptide nitrile scaffold was performed. For this purpose, various Cbz-protected L-amino acids **21–26** were converted into the corresponding mixed anhydrides [179–181] by the reaction with isobutyl chloroformate in the presence of *N*-methylmorpholine. The following addition of an aqueous solution of 1,2-dimethylhydrazine, which was previously displaced with sodium hydroxide from its dihydrochloride salt, provided the formation of 1,2-dimethylhydrazides **27–32**. The crude products **27–32** were purified on silica gel by column chromatography and subjected to the final reaction with cyanogen bromide leading to the target compounds **33–38** (Scheme 1).

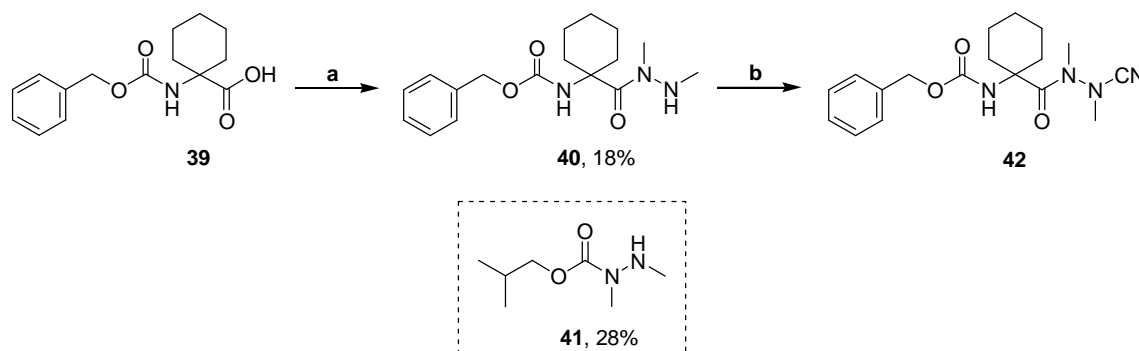


Scheme 1. Synthesis of carbamate-based azadipeptide nitriles **33–38**.

a) 1. $\text{ClCO}_2i\text{-Bu}$, NMM, THF, $-25\text{ }^\circ\text{C}$; 2. $(\text{MeNH})_2 \times 2\text{HCl}$, NaOH, H_2O , THF, $-25\text{ }^\circ\text{C}$ to rt; b) BrCN, NaOAc, MeOH, rt; **21**, **27**, **33**, R = H; **22**, **28**, **34**, R = Me; **23**, **29**, **35**, R = *i*-Pr; **24**, **30**, **36**, R = (*S*)-1-methylpropyl; **25**, **31**, **37**, R = cyclohexylmethyl; **26**, **32**, **38**, R = 4-hydroxybenzyl.

While 1,2-dimethylhydrazides **27–32**, containing α -monosubstituted amino acids, were easily obtained in moderate yields, the reaction of Cbz-protected 1-amino-1-cyclohexanecarboxylic acid (homocycloleucine) **39** with 1,2-dimethylhydrazine was more complicated, although the same reaction conditions were used as in the case of **27–32**. The 1,2-dimethylhydrazide **40** was formed in a very low yield, and it was further not possible to isolate the desired product from the obtained reaction mixture in a pure form. Therefore, the synthetic route to azadipeptide nitrile **42** had to be optimized. Different from the procedure noted in Scheme 1, compound **39** was activated *via* a mixed anhydride and reacted with 1,2-dimethylhydrazine dihydrochloride in the presence of triethylamine under water-free conditions. The new synthetic route was associated with a slight improved yield of compound **40** and allowed for isolation of this product in a pure form. Finally, the 1,2-dimethylhydrazide **40** was converted into the corresponding azadipeptide nitrile **42** by the reaction with cyanogen bromide.

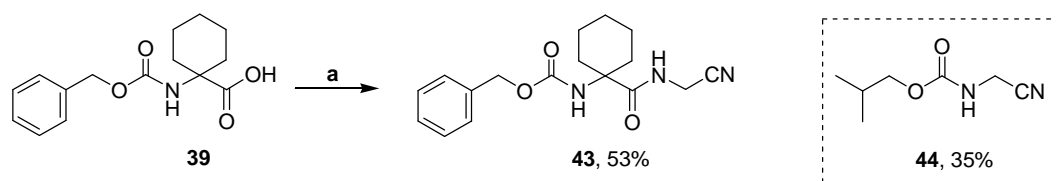
The carbamate **41** was isolated as the major byproduct resulting from the nucleophilic attack of 1,2-dimethylhydrazine at the carbonate carbon of the mixed anhydride (Scheme 2).



Scheme 2. Synthesis of the homocycloleucine-derived azadipeptide nitrile **42**.

a) 1. $\text{ClCO}_2i\text{-Bu}$, TEA, THF, $-25\text{ }^\circ\text{C}$; 2. $(\text{MeNH})_2 \times 2\text{HCl}$, THF, $-25\text{ }^\circ\text{C}$ to rt; b) BrCN , NaOAc , MeOH, rt.

For comparative investigations, the homocycloleucine-derived dipeptide nitrile **43** [159] was synthesized (Scheme 3). When compound **39** was reacted with aminoacetonitrile monosulfate in the presence of triethylamine, the dipeptide nitrile **43** was formed in a moderate yield of 53%. The carbamate **44** was identified as a main byproduct of the reaction.



Scheme 3. Synthesis of the homocycloleucine-derived dipeptide nitrile **43**.

a) 1. $\text{ClCO}_2i\text{-Bu}$, TEA, THF, $-25\text{ }^\circ\text{C}$; 2. $\text{H}_2\text{NCH}_2\text{CN} \times \text{H}_2\text{SO}_4$, THF, $-25\text{ }^\circ\text{C}$ to rt.

Obviously, the presence of the *gem*-disubstituted carbon in the Cbz-protected homocycloleucine-derived mixed anhydride was responsible for low yields of the desired coupling products. This effect was particularly strong when 1,2-dimethylhydrazine, a rather weak, but steric demanding nucleophile was used. For comparison, the mixed anhydride coupling of protected $\text{C}\alpha$ -monosubstituted amino acids with aminoacetonitrile or 1,2-dimethylhydrazine occurred with less pronounced formation of carbamate or carbamate byproducts, respectively [168], [182]. Compounds **33–38** were synthesized by Friederike Lohr in the course of her diploma thesis under my supervision.

2.1.2. KINETIC PLOTS (SLOW-BINDING INHIBITION) AND EQUATIONS

The inhibitory activity of compounds, interacting with their target enzymes in a competitive manner, is mainly characterized by the K_i values. In contrast to IC_{50} values, the true inhibition constant K_i is independent from the substrate concentration and assay conditions and is therefore advantageous to evaluate competitive inhibitors. For example, K_i values obtained under different assay conditions are directly comparable. The calculation of the K_i value requires the knowledge of the Michaelis constant (K_m) defined as the substrate concentration for which the velocity of an enzyme reaction is half of its maximal value.

For the following kinetic investigations, the Michaelis constants were therefore determined. The target cathepsins L, S and B were assayed photospectrometrically in the presence of increasing concentrations of the chromogenic substrates Z-Phe-Arg-pNa, Z-Phe-Val-Arg-pNa and Z-Arg-Arg-pNa, respectively. The formation of *p*-nitroaniline was measured at 405 nm. Cathepsin K was assayed fluorometrically in the presence of the fluorogenic substrate Z-Leu-Arg-AMC. In the cathepsin K assay, the excitation wavelength was 360 nm and the corresponding wavelength for emission was 440 nm. The enzymes were assayed with at least seven different concentrations of the particular chromogenic or fluorogenic substrate in duplicate experiments. The steady-state reaction rates (v_s) were calculated as slopes of the progression lines by linear regression (Fig. 21a). To obtain the K_m values, the steady-state velocities were further plotted against increasing substrate concentrations and analyzed by non-linear regression (Fig. 21b) using the Michaelis-Menten equation (Fig. 20a). The Lineweaver-Burk (Fig. 22a) and Hanes-Woolf (Fig. 22b) plots were performed to review possible systematic errors. The corresponding equations for Lineweaver-Burk and Hanes-Woolf plots are shown in Figure 20b and 20c, respectively.

$$(a) \quad v_s = \frac{V_{\max} \times [S]}{K_m + [S]} \qquad (b) \quad \frac{1}{v_s} = \frac{1}{V_{\max}} + \frac{K_m}{V_{\max}} \times \frac{1}{[S]}$$

$$(c) \quad \frac{[S]}{v_s} = \frac{[S]}{V_{\max}} + \frac{K_m}{V_{\max}}$$

Figure 20. Michaelis-Menten (a), Lineweaver-Burk (b) and Hanes-Woolf (c) equations.

v_s – steady-state velocity ($M s^{-1}$); V_{\max} – maximum reaction rate ($M s^{-1}$); $[S]$ – substrate concentration (M); K_m – Michaelis constant (M). In Figures 21 and 22, dimensionless units instead of concentrations are used at the ordinates.

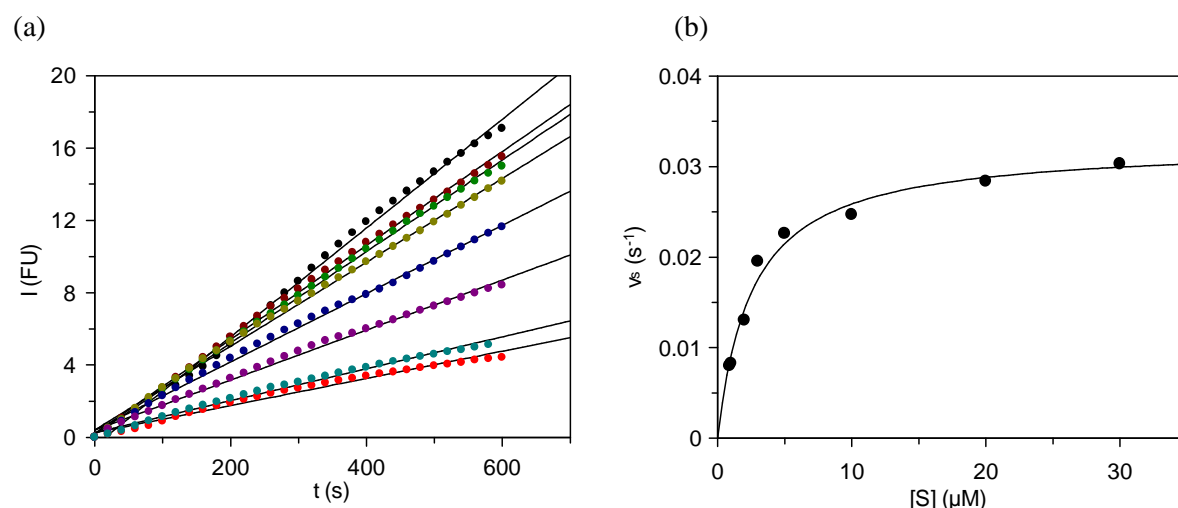


Figure 21. (a) Cathepsin K-catalyzed hydrolysis of Z-Leu-Arg-AMC (100 mM sodium citrate pH 5.0, 100 mM NaCl, 1 mM EDTA, 0.01% CHAPS, 2% DMSO, 50 μM DTT, 25 °C) (•) [S] = 30 μM; (●) [S] = 20 μM; (●) [S] = 10 μM; (●) [S] = 5 μM; (●) [S] = 3 μM; (●) [S] = 2 μM; (●) [S] = 1 μM; (●) [S] = 0.9 μM. (b) Plot of steady-state reaction rates (v_s) versus increasing concentration of Z-Leu-Arg-AMC. The non-linear regression of the data pairs (v_s , [S]) gave a K_m value of 2.6 ± 0.3 μM.

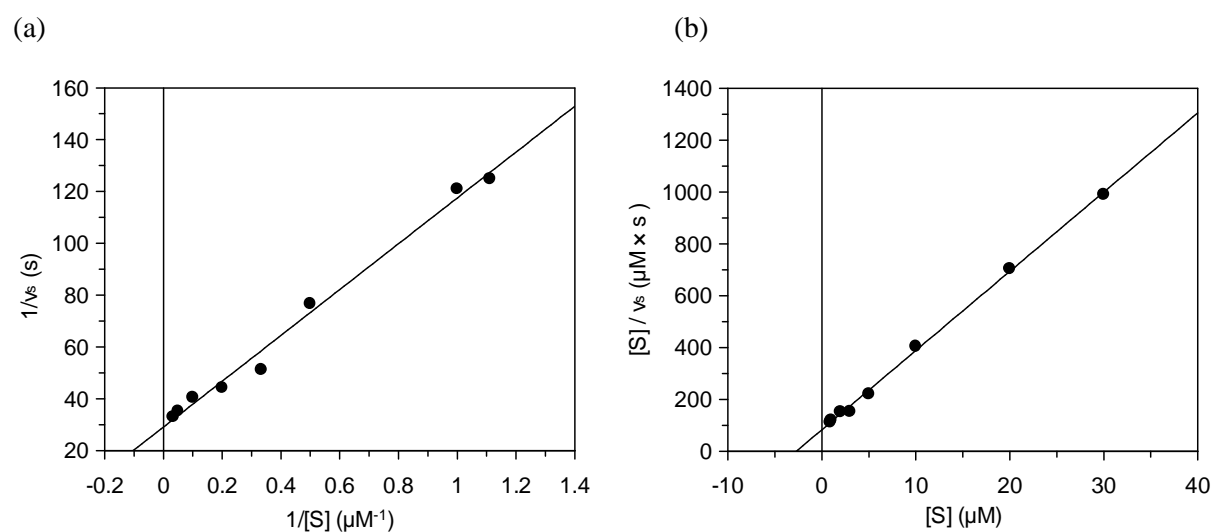


Figure 22. (a) Lineweaver-Burk plot of $1/v_s$ versus $1/[S]$. $K_m = 3.0 \pm 0.1$ μM. (b) Hanes-Woolf of $[S]/v_s$ versus [S]. Linear regression gave a K_m value of 2.7 ± 0.1 μM.

The K_m values and the corresponding standard errors, obtained by non-linear regression using the Michaelis-Menten equation (Fig 20a), are listed in Table 1. The final substrate concentrations in the inhibition assays were follows: (1) cathepsin L assay (human recombinant cathepsin L from Calbiochem) – 100 μM (= 10.0 K_m) Z-Phe-Arg-pNa; (2) cathepsin L assay (human isolated cathepsin L from Enzo Life Sciences) – 100 μM

(= 5.88 K_m) Z-Phe-Arg-pNa; (3) cathepsin S assay (human recombinant cathepsin S from Calbiochem) – 100 μM (= 1.49 K_m) Z-Phe-Val-Arg-pNa or 100 μM (= 0.85 K_m) Z-Phe-Arg-pNa; (4) cathepsin K assay (human recombinant procathepsin K from Calbiochem) – 40 μM (= 15.4 K_m) Z-Leu-Arg-AMC; (5) cathepsin K assay (recombinant cathepsin K from Enzo Life Sciences) – 40 μM (= 13.3 K_m) Z-Leu-Arg-AMC; (6) cathepsin B assay (human isolated cathepsin B from Calbiochem) – 500 μM (= 0.45 K_m) Z-Arg-Arg-pNa.

Table 1. K_m values (μM).

	Z-Phe-Arg-pNa ^a	Z-Phe-Val-Arg-pNa ^a	Z-Leu-Arg-AMC ^b	Z-Arg-Arg-pNa ^a
cathepsin L	10 ± 1 ^c 17 ± 2 ^d	n.d. ^e	n.d.	n.d.
cathepsin S	117 ± 9	67 ± 5	n.d.	n.d.
cathepsin K	n.d.	n.d.	2.6 ± 0.3 ^f 3.0 ± 0.6 ^g	n.d.
cathepsin B	n.d.	n.d.	n.d.	1100 ± 100

^aAssays were carried out with a total DMSO amount of 2% and at 37 °C. ^bAssay was performed with a total DMSO amount of 2% and at 25 °C. ^cHuman recombinant cathepsin L from Calbiochem. ^dHuman isolated cathepsin L from Enzo. ^eNot determined. ^fHuman recombinant procathepsin K from Calbiochem (measurements were performed after activation of the enzyme). ^gHuman recombinant cathepsin K from Enzo.

The inhibitory activities of the target compounds **33–38** and **42**, together with already known inhibitors **45** and **46** [168] (Table 2), were evaluated on therapeutically relevant human cathepsins L, S, K and B as described in ‘Experimental Section’. The tested azadipeptide nitriles all showed slow-binding kinetic behavior resulting in hyperbolic progress curves of enzymatic reactions in the presence of inhibitor (Fig. 24a). For calculation of the steady-state reaction rates (v_s) and the first-order rate constants (k_{obs}), the slow-binding equation was used (Fig. 23a). To obtain the IC_{50} values (apparent inhibition constants K_i'), the steady-state velocities (v_s) were plotted *versus* increasing inhibitor concentrations (Fig. 24b), and the resulting data pairs (v_s , [I]) were analyzed by non-linear regression using the IC_{50} equation (Fig. 23b). Because azadipeptide nitriles were described as reversible inhibitors with a competitive inhibition mode [168], the IC_{50} values were further corrected using the Cheng-Prusoff equation (Fig. 23c) to obtain the corresponding true inhibition constants (K_i). The structure-activity relationships (SARs) of all inhibitors in this study were analyzed on the bases of their K_i values because the true inhibition constants are independent on substrate concentrations and used assay conditions, and allow therefore for a direct comparison.

$$(a) \quad E/I = v_s t + \left(\frac{v_i - v_s}{k_{obs}} \right) \times (1 - e^{-k_{obs}t}) + d \quad (b) \quad IC_{50} = \frac{[I]}{\left(\frac{v_0}{v_s} - 1 \right)}$$

$$(c) \quad K_i = \frac{IC_{50}}{\left(1 + \frac{[S]}{K_m} \right)}$$

Figure 23. Slow-binding (a), IC_{50} (b) and Cheng-Prusoff (c) equations.

(a) E – extinction; I – fluorescence intensity; v_s – steady-state reaction rate ($M s^{-1}$); v_i – initial reaction rate ($M s^{-1}$); k_{obs} – first-order rate constant (s^{-1}); t – time (s); d – offset; (b) IC_{50} – half maximal inhibitory concentration (M); v_0 – steady-state reaction rate in the absence of inhibitor (Ms^{-1}); v_s – steady-state reaction rate in the presence of inhibitor ($M s^{-1}$); [I] – inhibitor concentration (M); (c) K_i – true inhibition constant (M); IC_{50} – half maximal inhibitory concentration (M); [S] – substrate concentration (M); K_m – Michaelis constant (M). In Figure 24, dimensionless units instead of concentrations are used at the ordinates.

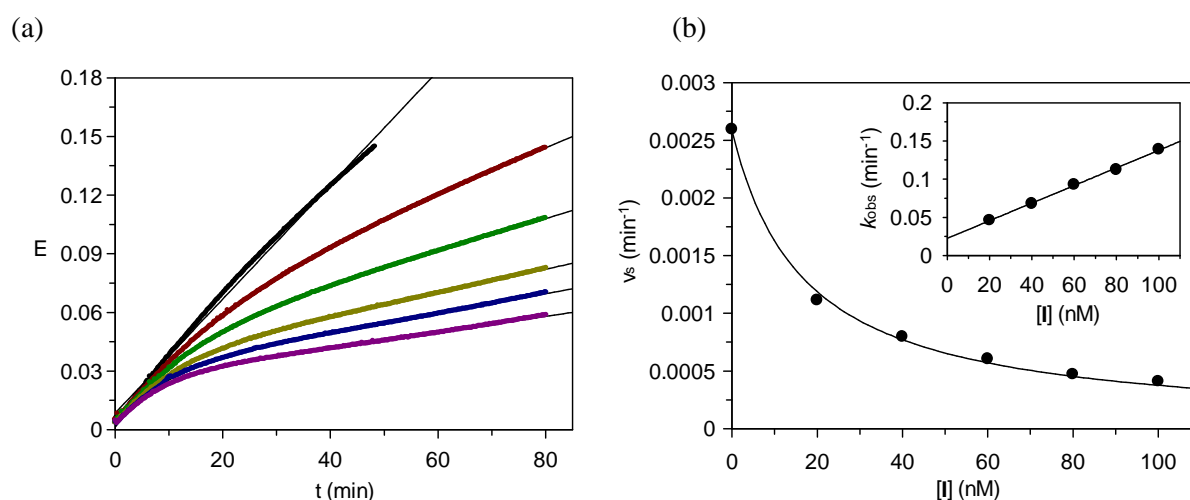


Figure 24. (a) Monitoring of the human cathepsin L-catalyzed hydrolysis of Z-Phe-Arg-pNa ($100 \mu M$) in the presence of increasing concentrations of compound **35** (\bullet , 0; \bullet , 20 nM; \bullet , 40 nM; \bullet , 60 nM; \bullet , 80 nM; \bullet , 100 nM). The reaction (100 mM sodium phosphate buffer pH 6.0, 100 mM NaCl, 5 mM EDTA, 0.01% Brij 35, 2% DMSO, 100 μM DTT, 37 $^{\circ}C$) was initiated by addition of the enzyme. The formation of *p*-nitroaniline was measured at 405 nm. (b) Plot of the rates of hydrolysis of Z-Phe-Arg-pNa versus increasing concentrations of **35**. Non-linear regression gave an apparent inhibition constant $K_i' = (1 + [S]/K_m)K_i = 17 \pm 1$ nM. The inset is a plot of the first-order rate constants k_{obs} versus increasing concentrations of **35**. Linear regression gave a second-order rate constant $k_{on}' = k_{on}/(1 + ([S]/K_m)) = (19 \pm 1) \times 10^3 M^{-1}s^{-1}$.

The slow-binding behavior of azadipeptide nitriles, which inhibited the target cathepsins in a time-dependent manner, approves for the determination of the association rate constants (k_{on}) as a second kinetic parameter to evaluate their biological activity. Slow-binding inhibitors display a slow onset of the inhibition on a time scale of seconds to minutes because the equilibrium between enzyme, inhibitor, and enzyme-inhibitor (EI) complex is established slowly. Two basic mechanisms have been proposed to explain slow enzyme inhibition in the case of reversible, covalent inhibitors. Mechanism A assumes the formation of the covalent complex EI* as a single, slow step whereby the magnitudes of $k_{+3}[I]$ and k_{-3} are small relative to $k_{+1}[S]$, k_{-1} and k_{+2} (Fig. 25a). However, mechanism B assumes rapid formation of a non-covalent EI complex that undergoes a slow isomerization to a covalent EI* complex. In this case, the magnitudes of k_{+4} and k_{-4} are small relative to $k_{+1}[S]$, k_{-1} and k_{+2} , and in particular to $k_{+3}[I]$ and k_{-3} (Fig. 25b) [183], [184].

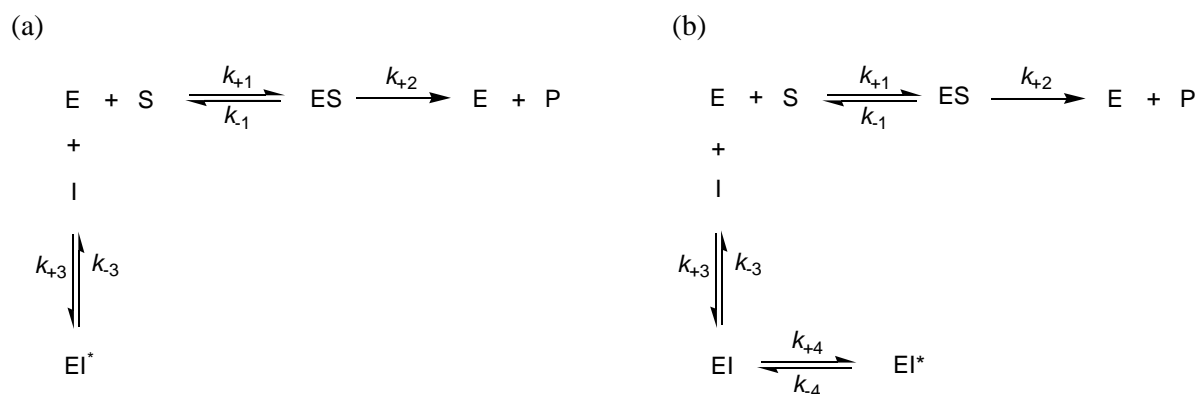


Figure 25. Mechanism A (a) and mechanism B (b) of the slow-binding inhibition.

For the differentiation between two mechanisms, the k_{obs} values (first-order rate constant for the development of the steady-state between free enzyme, inhibitor, and EI* complex), obtained from hyperbolic progress curves, were plotted against increasing inhibitor concentrations. As it exemplarily depicted for compound **35** (Fig. 24b), the k_{obs} values of azadipeptide nitriles **33–38**, **42**, **45** and **46** showed a linear dependence on the increasing inhibitor concentrations. The linear dependence of k_{obs} on $[I]$, which is mathematically described by equation shown in Figure 26a, indicated the one-step mechanism A (Fig. 25a) as the inhibition mode of compounds **33–38**, **42**, **45** and **46** on cathepsins L, S, K and B. The apparent $k_{+3}/(1+[S]/K_m) = k_{on}$ values were therefore easily obtained by linear regression of the data pairs (k_{obs} , $[I]$) using the equation depicted in Figure 26c. In the case of mechanism B, the k_{obs} values exhibit non-linear dependency on $[I]$ described by the equation for two step inhibition (Fig. 26b).

$$(a) \quad k_{\text{obs}} = \frac{k_{+3} \times [\text{I}]}{1 + \frac{[\text{S}]}{K_m}} + k_{-3}$$

$$(b) \quad k_{\text{obs}} = \frac{k_{+4} \times [\text{I}]}{\frac{k_{-3}}{k_{+3}} \times \left(1 + \frac{[\text{S}]}{K_m}\right) + [\text{I}]} + k_{-4}$$

$$(c) \quad k_{\text{obs}} = k_{\text{on}}' \times [\text{I}] + k_{\text{off}}$$

Figure 26. Relationships between k_{obs} and $[\text{I}]$ for mechanism A (a) and mechanism B (b); equation for the determination of the apparent second-order association rate constants (c).

k_{obs} – first-order rate constant of the approach to steady-state (s^{-1}); k_{-3} – dissociation first-order rate constant (s^{-1}); k_{+3} – association second-order rate constant ($\text{M}^{-1}\text{s}^{-1}$); k_{-3}/k_{+3} – dissociation constant (M); k_{-4} – first-order rate constant of the EI* decay (s^{-1}); k_{+4} – first-order rate constant of the EI* formation (s^{-1}); $[\text{I}]$ – inhibitor concentration (M); $[\text{S}]$ – substrate concentration (M); K_m – Michaelis constant (M); k_{on}' – apparent second-order association rate constant ($\text{M}^{-1}\text{s}^{-1}$); k_{off} – first-order dissociation rate constant (s^{-1}).

The calculated apparent second-order association rate constants (k_{on}') were further corrected by multiplication with a factor $(1 + [\text{S}]/K_m)$ to obtain the corresponding true second-order association rate constants (k_{on}). The first-order dissociation rate constants (k_{off}) of compounds **33–38**, **42**, **45** and **46** were calculated as a multiplication product of K_i and k_{on} using the equation in Figure 27a. The standard errors for k_{off} were obtained by multiplication of k_{off} values with their relative overall errors (Fig. 27b) [185–187].

$$(a) \quad K_i = \frac{k_{\text{off}}}{k_{\text{on}}}$$

$$(b) \quad F_{\text{rel}} = \sqrt{(f_{\text{rel}})^2 + (f_{\text{rel}})^2}$$

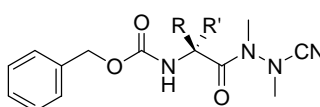
Figure 27. Equations for calculation of k_{off} values (a) and their relative overall errors (b).

(a) k_{obs} – first-order rate constant of the steady-state development (s^{-1}); k_{on} – true second-order association rate constant ($\text{M}^{-1}\text{s}^{-1}$); k_{off} – first-order dissociation rate constant (s^{-1}); (b) F_{rel} – relative overall standard error; f_{rel} – relative standard errors for K_i and k_{on} values.

2.1.3. STRUCTURE-ACTIVITY RELATIONSHIPS OF 33–38, 42, 45 AND 46

Regardless of the substitution pattern, compounds **33–38**, **42**, **45** and **46** displayed all the time-dependent, slow-binding behavior. Analysis of the progress curves over 80 min then allows for the determination of the second-order association rate constants (k_{on}) and the first-order dissociation rate constants (k_{off}). The estimated K_i values of compounds **33–38**, **42**, **45** and **46** as well as the corresponding standard errors are shown in Table 2.

Table 2. K_i values of carbamate-based compounds **33–38**, **42**, **45** and **46**.



cmpd	R	R'	K_i (nM)			
			cath L	cath S	cath K	cath B
33	H	H	860 ± 60 ^a	800 ± 30	260 ± 30	840 ± 70
34	Me	H	480 ± 50	9.1 ± 1	33 ± 2	55 ± 7
35	<i>i</i> -Pr	H	1.5 ± 0.1	1.5 ± 0.2	0.87 ± 0.14	4.3 ± 0.2
36	(<i>S</i>)-1-methylpropyl	H	2.6 ± 0.3	0.83 ± 0.1	0.46 ± 0.06	0.88 ± 0.08
37	cyclohexylmethyl	H	0.40 ± 0.04	0.20 ± 0.03	0.071 ± 0.010	0.48 ± 0.07
38	4-hydroxybenzyl	H	0.36 ± 0.03	0.86 ± 0.02	0.16 ± 0.01	0.38 ± 0.03
42	-(CH ₂) ₅ -		400 ± 60	130 ± 5	1.8 ± 0.3	170 ± 10
45	<i>i</i> -Bu	H	0.90 ± 0.04	0.33 ± 0.02	0.064 ± 0.003	0.43 ± 0.01
46	Bn	H	0.16 ± 0.01 ^a	0.51 ± 0.03 ^a	0.14 ± 0.01	0.68 ± 0.04

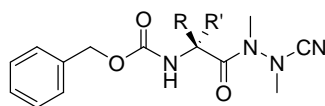
^aThe progress curves were followed over 20 min and analyzed by non-linear regression.

The glycine derivative **33** with unsubstituted P2 position exhibited the weakest inhibitory activity on the studied cathepsins. Furthermore, the simple methylation of the P2 position, resulting in compound **34**, led to a ca. 2–88-fold improvement in the potency towards cathepsins L, S, K and B. The activity improvement was much stronger when larger aliphatic and cycloaliphatic groups such as isopropyl (**35**), (*S*)-1-methylpropyl (**36**), isobutyl (**45**), and cyclohexylmethyl (**37**) substituents were introduced in the P2 position of the azadipeptide nitrile scaffold. Particularly for cathepsin K, the L-leucine-based azadipeptide nitrile **45** was

ca. 4100-fold more active, comparing with the corresponding glycine derivative **33**, and showed also a slight preference for this enzyme. The introduction of aromatic benzyl (**46**) and 4-hydroxybenzyl (**38**) substituents into P2 position did not result in further advantages regarding potency improvement or selective inhibition of cathepsin K. In contrast, the homocycloleucine-based compound **42**, although less potent on cathepsin K compared with the potent inhibitors **45** and **37**, showed already considerable selectivity for this enzyme over cathepsin L, S and B (220-fold, 72-fold and 100-fold, respectively). Azadipeptide nitriles **42** and **45** were selected for further optimization of the P3 substituent, while their P2 residues, interacting with the S2 subsite of cysteine cathepsins, were maintained in all further compounds of this study.

The k_{on} values of compounds **33–38**, **42**, **45** and **46** varied considerably depending on the substitution at the P2 position, while the corresponding k_{off} values were in the same range (Tables 3 and 4). For example, the 17000-fold higher k_{on} value of **45** for cathepsin K, compared to that of the glycine derivative **33**, is reflected by the improved potency of **45** (64 pM *versus* 260 nM, Table 2).

Table 3. k_{on} values of carbamate-based compounds **33–38**, **42**, **45** and **46**.

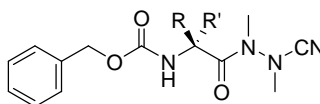


cmpd	R	R'	k_{on} ($10^3 \text{ M}^{-1} \text{ s}^{-1}$)			
			cath L	cath S	cath K	cath B
33	H	H	$0.51 \pm 0.01^{\text{a}}$	1.7 ± 0.1	0.10 ± 0.01	0.11 ± 0.02
34	Me	H	1.3 ± 0.1	67 ± 3	1.4 ± 0.2	0.81 ± 0.31
35	<i>i</i> -Pr	H	210 ± 10	400 ± 100	81 ± 10	7.6 ± 0.7
36	(<i>S</i>)-1-methylpropyl	H	81 ± 3	250 ± 20	160 ± 30	28 ± 4
37	cyclohexylmethyl	H	2900 ± 100	9600 ± 800	410 ± 50	58 ± 11
38	4-hydroxybenzyl	H	4200 ± 100	500 ± 30	320 ± 20	79 ± 22
42	-(CH ₂) ₅ -		1.3 ± 0.1	7.8 ± 1	60 ± 10	1.0 ± 0.1
45	<i>i</i> -Bu	H	620 ± 50	2000 ± 100	1700 ± 200	130 ± 10
46	Bn	H	$4500 \pm 700^{\text{a}}$	$3000 \pm 600^{\text{a}}$	320 ± 60	150 ± 10

^aThe progress curves were followed over 20 min and analyzed by non-linear regression.

The k_{off} values of tested compounds **33–38**, **42**, **45** and **46** were approximately in the same range and seemed to be independent from the substituent at the P2 position of the azadipeptide nitrile scaffold (Table 4). Therefore, it could be assumed that azadipeptide nitriles depart from the catalytic site of cysteine cathepsins without significant interactions with the corresponding binding pockets when the dissociation of the isothiosemicarbazide (Fig. 13) adducts occurs. This finding reflects the difficulty in delivering significant binding energy from non-covalent interactions, as discussed for cysteine cathepsins and concluded from the large and relatively shallow active site of these target enzymes [164]. The cathepsin L measurements of compounds **33–38** were performed by Friederike Lohr in the course of her diploma thesis under my supervision.

Table 4. k_{off} values of carbamate-based compounds **33–38**, **42**, **45** and **46**.



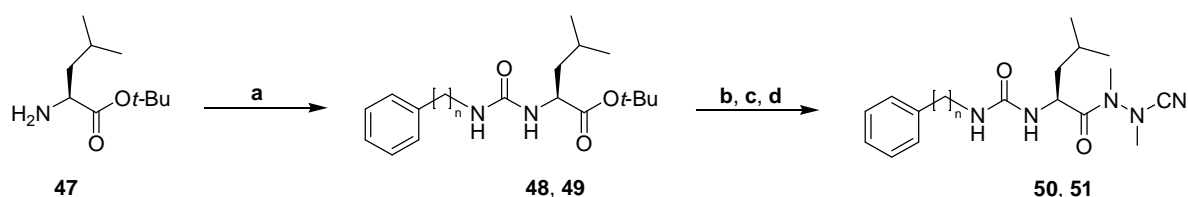
cmpd	R	R'	$k_{\text{off}} (10^{-3} \text{s}^{-1})$			
			cath L	cath S	cath K	cath B
33	H	H	$0.44 \pm 0.03^{\text{a}}$	1.4 ± 0.1	0.026 ± 0.004	0.092 ± 0.018
34	Me	H	0.62 ± 0.08	0.61 ± 0.07	0.046 ± 0.007	0.045 ± 0.018
35	<i>i</i> -Pr	H	0.32 ± 0.03	0.60 ± 0.17	0.070 ± 0.014	0.033 ± 0.003
36	(<i>S</i>)-1-methylpropyl	H	0.21 ± 0.03	0.21 ± 0.03	0.074 ± 0.017	0.025 ± 0.004
37	cyclohexylmethyl	H	1.2 ± 0.1	1.9 ± 0.3	0.029 ± 0.005	0.028 ± 0.007
38	4-hydroxybenzyl	H	1.5 ± 0.1	0.43 ± 0.03	0.051 ± 0.005	0.030 ± 0.009
42	-(CH ₂) ₅ -		0.52 ± 0.09	1.0 ± 0.1	0.11 ± 0.03	0.17 ± 0.02
45	<i>i</i> -Bu	H	0.56 ± 0.05	0.66 ± 0.05	0.11 ± 0.01	0.056 ± 0.005
46	Bn	H	$0.72 \pm 0.12^{\text{a}}$	$1.5 \pm 0.3^{\text{a}}$	0.045 ± 0.009	0.10 ± 0.01

^aThe progress curves were followed over 20 min and analyzed by non-linear regression.

2.1.4. L-LEUCINE-DERIVED AZADIPEPTIDE NITRILES

THE L-leucine-based azadipeptide nitrile **45** was selected for the stepwise structure optimization to develop potent and selective cathepsin K inhibitors. For this purpose, the isobutyl substituent at the P2 position of the azadipeptide nitrile scaffold was maintained, and the P3 moieties as well as the P3-P2 linker were varied.

At first, the carbamate group of **45** was replaced by a urea moiety to permit additional hydrogen bond formation. The corresponding azadipeptide nitriles **50** and **51** (Scheme 4) differ in the length of the P3-P2 linker. The route to the urea-based inhibitors **50** and **51** rests upon the finding that the carbamoyl-protected L-leucine can be converted *via* mixed anhydride method without racemisation [188]. L-Leucine *tert*-butyl ester **47** was reacted with CDI and benzylamine or aniline, respectively. The resulting derivatives **48** and **49** were treated with TFA to cleave the *tert*-butyl ester, transformed into the corresponding 1,2-dimethylhydrazides, and reacted with cyanogen bromide to obtain **50** and **51**.

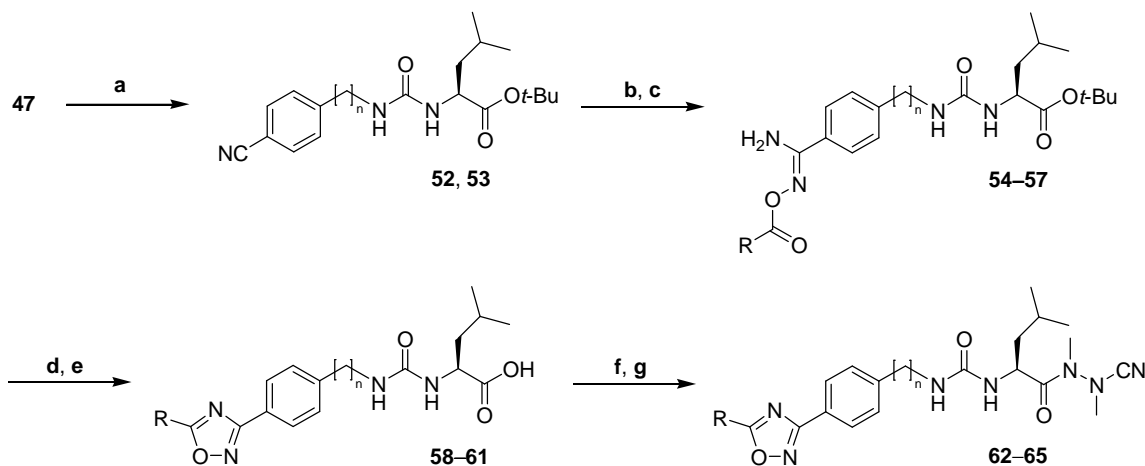


Scheme 4. Synthesis of the urea-based compounds **50** and **51**.

a) (n = 1) 1. CDI, THF, Δ ; 2. benzylamine, THF, Δ ; (n = 0) 1. CDI, THF, Δ ; 2. aniline, DIPEA, MeCN, Δ ; b) TFA, CH₂Cl₂, rt; c) 1. ClCO₂*i*-Bu, NMM, THF, -25 °C; 2. (MeNH)₂ × 2HCl, NaOH, H₂O, THF, -25 °C to rt; d) BrCN, NaOAc, MeOH, rt; **48**, **50**, n = 1; **49**, **51**, n = 0.

On the basis of recent results on cathepsin K-selective dipeptide nitriles with large biaryl P3 substituents [164], the P3 moiety of compounds **50** and **51** was next extended to improve the potency and selectivity for cathepsin K over cathepsins L, S and B. A 1,2,4-oxadiazole heterocycle as a common bioisoster of amide and ester groups [189] was chosen for the extension. Two benzylurea derivatives bearing a methyl group (**62**) and a 2-thienyl substituent (**63**) in position 5 of the 1,2,4-oxadiazole ring, as well as their phenylurea counterparts **64** and **65** were synthesized (Scheme 5). The synthetic route includes the conversion of aromatic nitriles **52** and **53** to acyloxyamidines **54–57**, and the oxadiazole ring closure carried out in acetic acid at 80 °C [190], followed by deprotection with TFA to obtain compounds **58–61**. The free acids **58–61** were activated *via* a mixed anhydride and reacted with 1,2-dimethyl-

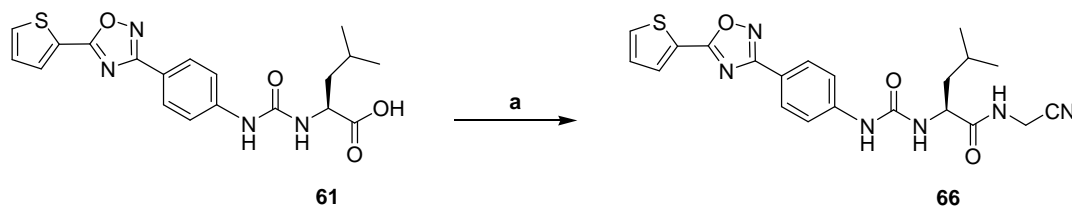
hydrazine to obtain the corresponding 1,2-dimethylhydrazides, which were finally converted to azadipeptide nitriles **62–65** with cyanogen bromide.



Schemes 5. Synthesis of the urea-based compounds **62–65**.

a) ($n = 1$) 1. CDI, THF, Δ , 2. 4-(aminomethyl)benzocyanide \times HCl, DIPEA, THF, Δ ; ($n = 0$) 4-cyanophenyl isocyanate, THF, rt; b) $NH_2OH \times HCl$, DIPEA, EtOH, Δ ; c) ($R = Me$) Ac_2O , MeCN, rt; ($R = 2$ -thienyl) 2-thenoyl chloride, DIPEA, MeCN, rt; d) AcOH, $80^\circ C$; e) TFA, CH_2Cl_2 , rt; f) 1. $ClCO_2i-Bu$, NMM, THF, $-25^\circ C$, 2. $(MeNH)_2 \times 2HCl$, NaOH, H_2O , THF, $-25^\circ C$ to rt; g) BrCN, NaOAc, MeOH, rt; **52**, $n = 1$; **53**, $n = 0$; **54, 58, 62**, $n = 1$, $R = Me$; **55, 59, 63**, $n = 1$, $R = 2$ -thienyl; **56, 60, 64**, $n = 0$, $R = Me$; **57, 61, 65**, $n = 0$, $R = 2$ -thienyl.

For a direct comparison of kinetic properties, compound **66** was further synthesized as a carba-analogue of the azadipeptide nitrile **65**. The synthetic route to **66** includes the activation of the free acid **61** via a mixed anhydride and the following reaction with aminoacetonitrile monosulfate (Scheme 6).



Scheme 6. Synthesis of the urea-based dipeptide nitrile **66**.

a) 1. $ClCO_2i-Bu$, NMM, THF, $-25^\circ C$, 2. $H_2NCH_2CN \times H_2SO_4$, NaOH, H_2O , THF, $-25^\circ C$ to rt.

As it became obvious with inhibitor **65**, the combination of the extended P3 triaryl motif with a short P3-P2 linker was advantageous, it was decided to further reduce the linker leading to the design of amide-based azadipeptide nitriles **67** and **68** (Scheme 11). Because of the racemisation of *N*-acylamino acids known to occur during the activation of their

carboxylic groups, a convergent synthesis for the amide-based compounds was developed. To realize the planned synthetic route, the desired compounds **67** and **68** were retrosynthetically divided into the synthetic equivalents **69**, **70**, **71** and cyanogens bromide (Fig. 28) which should be assembled to target molecules. While cyanogen bromide was commercially available, the building blocks **69** and **70**, **71** had to be prepared.

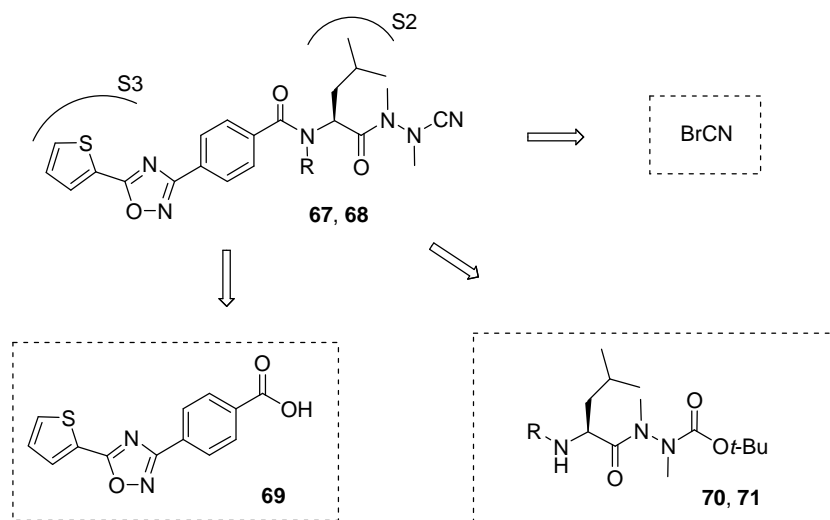
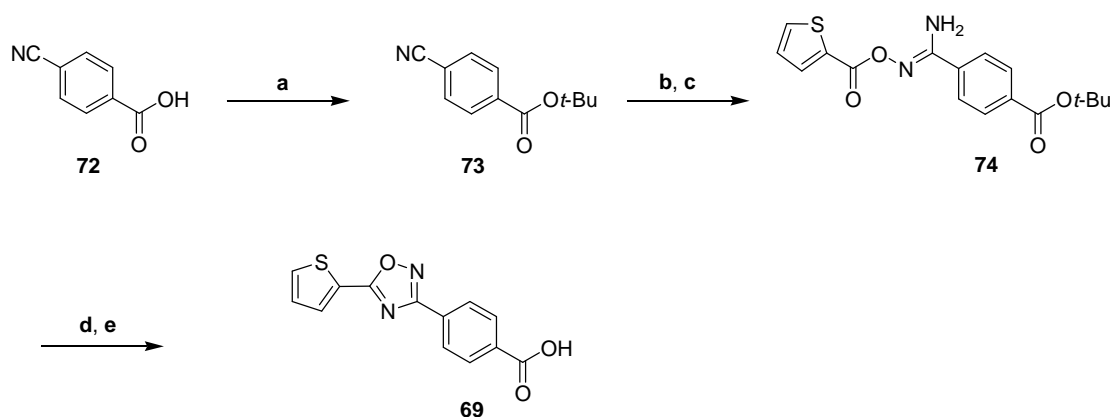


Figure 28. The planned synthetic route to compounds **67** and **68**.

67, **70**, R = H; **68**, **71**, R = Me.

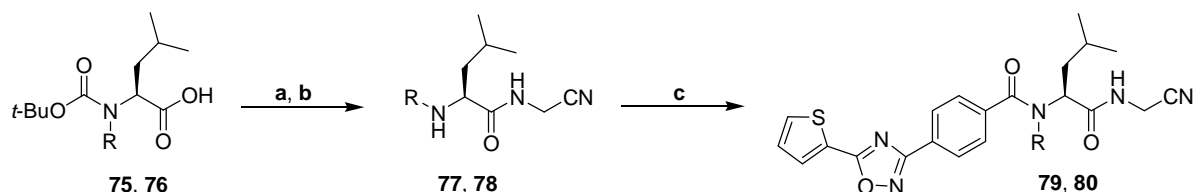
The convergent synthetic route was first employed in a modified form for the carba-analogues **79** and **80** (Scheme 8). At first, the P3 building block **69** was prepared in five steps with an overall yield of 49% (Scheme 7). The crucial step to compound **69** was the formation of the acyloxyamidine **74**, followed by the formation of 1,3,4-oxadiazole ring and the ester cleavage.



Scheme 7. Synthesis of compound **69** as the P3 building block.

a) 1. (COCl)₂, CH₂Cl₂, DMF, rt; 2. *tert*-butanol, pyridine, rt; b) NH₂OH × HCl, DIPEA, EtOH, Δ; c) 2-thenoyl chloride, DIPEA, MeCN, rt; d) AcOH, 80 °C; e) TFA, CH₂Cl₂, rt.

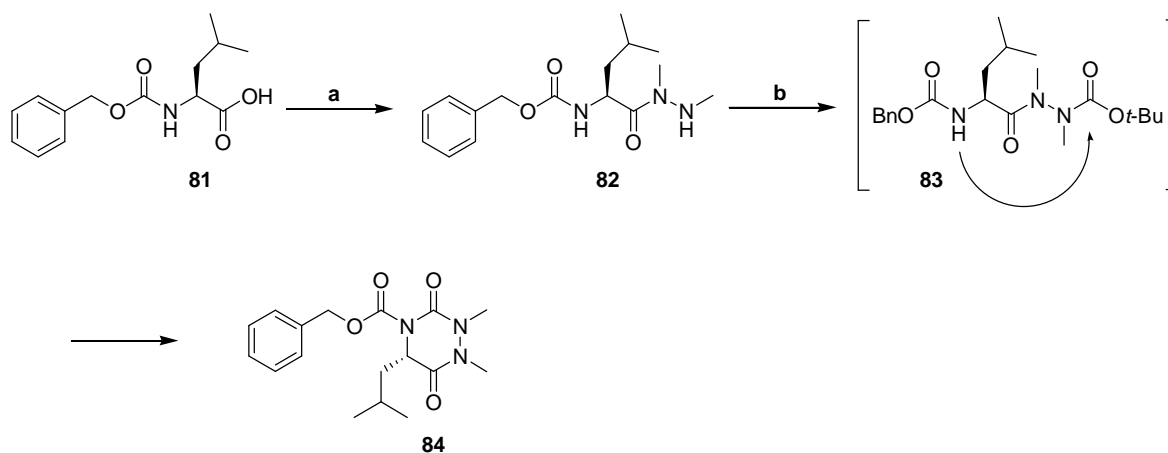
Next, Boc-protected L-leucine **75** and *N*-methyl-L-leucine **76** were reacted with aminoacetonitrile, followed by removal of the protecting group using methanesulfonic acid and basic extraction to produce **77** and **78**. In the final step, the building block **69** was activated and coupled with **77** and **78** to obtain dipeptide nitriles **79** and **80** (Scheme 8).



Scheme 8. Synthesis of amide-based dipeptide nitriles **79** and **80**.

a) 1. $\text{ClCO}_2i\text{-Bu}$, NMM, THF, $-25\text{ }^\circ\text{C}$, 2. $\text{H}_2\text{NCH}_2\text{CN} \times \text{H}_2\text{SO}_4$, NaOH, H_2O , THF, $-25\text{ }^\circ\text{C}$ to rt; b) MeSO_3H , THF, rt, basic extraction; c) (R = H) **69**, $\text{ClCO}_2i\text{-Bu}$, NMM, THF, $-25\text{ }^\circ\text{C}$ to rt; (R = Me) **69**, EDC, DMAP, CH_2Cl_2 , rt; **75**, **77**, **79**, R = H; **76**, **78**, **80**, R = Me.

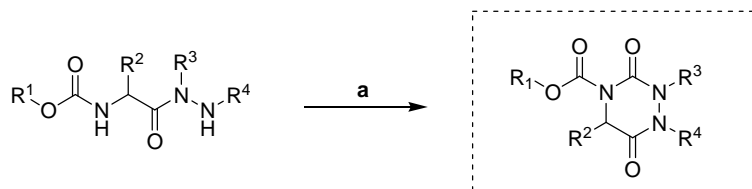
To produce the synthetic equivalents **70** and **71** (Fig. 28) for the synthesis of the desired amide-based azadipeptide nitriles **67** and **68**, it was intended to first protect the terminal hydrazide nitrogen of **82**, followed by the deprotection of the α -amino group. However, after treatment of **82** with $(\text{Boc})_2\text{O}$ in acetonitrile and in the presence of DMAP, the 1,2,4-triazinane-3,6-dione **84** was obtained, instead of the orthogonal protected azadipeptide ester **83** (Scheme 9). The attack of the NH nitrogen at the carbamate carbon operates in this ring closure. Although the sodium hydride-promoted formation of the 1,2,4-triazinane-3,6-dione scaffold has been described [191], the reaction to compound **84** represents the first example of a direct 1,2,4-triazinane-3,6-dione cyclization of a Cbz-protected azadipeptide *tert*-butyl ester.



Scheme 9. Formation of 1,2,4-triazinane-3,6-dione derivative **84**.

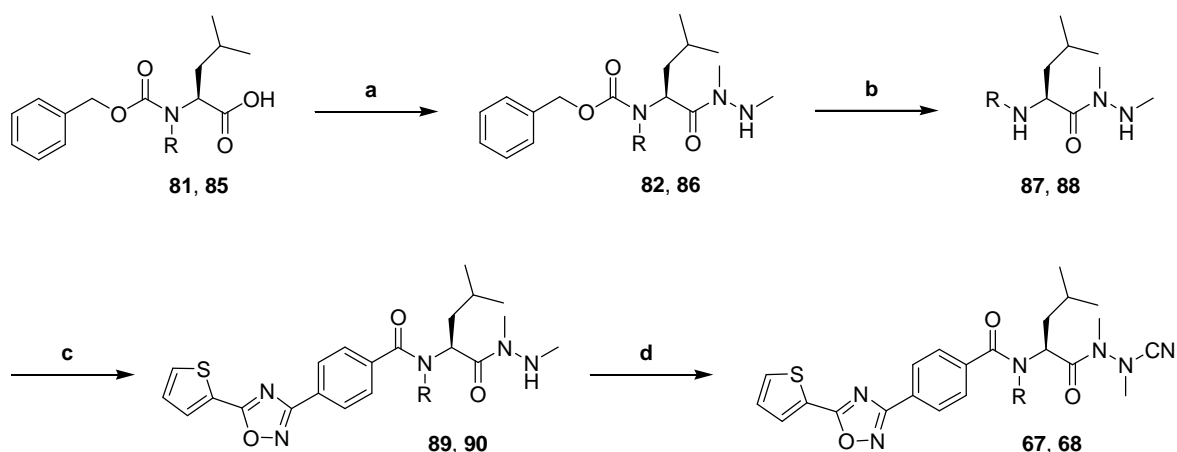
a) 1. $\text{ClCO}_2i\text{-Bu}$, NMM, THF, $-25\text{ }^\circ\text{C}$, 2. $(\text{MeNH})_2 \times 2\text{HCl}$, NaOH, H_2O , THF, $-25\text{ }^\circ\text{C}$ to rt; b) $(\text{Boc})_2\text{O}$, DMAP, MeCN, rt.

The cyclisation reaction of Cbz-protected 1,2-dimethylhydrazides to 1,2,4-triazinane-3,6-diones by the reaction with $(\text{Boc})_2\text{O}$ in the presence of DMAP, as described in this work, represents an easy synthetic access to new potential peptidomimetic structures with at least four diversity points (Scheme 10).



Scheme 10. Synthetic access to potential peptidomimetic 1,2,4-triazinane-3,6-diones. $(\text{Boc})_2\text{O}$, DMAP, MeCN, rt.

The finally successful synthesis of amide-based dipeptide nitriles **67** and **68**, the aza-analogues of **79** and **80**, is outlined in Scheme 11. The Cbz protecting group of the 1,2-dimethylhydrazides **82** and **86** was hydrogenolytically removed to obtain derivatives **87** and **88**. The synthetic equivalent **69** (Fig. 28) was activated with EDC in the presence of DMAP and reacted with **87** and **88** leading to the formation of compounds **89** and **90**. In the final reaction step with cyanogen bromide, the amide-based azadipeptide nitriles **67** and **68**, bearing a large P3 substituent, were obtained.



Scheme 11. Synthesis of amide-based azadipeptide nitriles **67** and **68**.

a) 1. $\text{ClCO}_2i\text{-Bu}$, NMM, THF, $-25\text{ }^\circ\text{C}$, 2. $(\text{MeNH})_2 \times 2\text{HCl}$, NaOH, H_2O , THF, $-25\text{ }^\circ\text{C}$ to rt; b) H_2 , Pd/C, 2 bar, MeOH, rt; c) **69**, EDC, DMAP, CH_2Cl_2 , rt; d) BrCN, NaOAc, MeOH, rt; **81**, **82**, **87**, **89**, **67**, R = H; **85**, **86**, **88**, **90**, **68**, R = Me.

2.1.5. KINETIC PLOTS II (FAST-BINDING INHIBITION)

Urea-based and amide-based azadipeptide nitriles were tested on human cathepsins L, S, K and B as described in ‘Experimental Section’. Azadipeptide nitriles **50**, **51**, **62–65**, **67** and **68** showed a time-dependent slow-binding inhibition type similar to their carbamate-derived counterparts, while the carba-analogues **66**, **79** and **80** appeared as fast-binding inhibitors.

The kinetic parameters K_i , k_{on} , and k_{off} of slow-binding inhibitors **50**, **51**, **62–65**, **67** and **68** were calculated as described in chapter 2.1.2. Before the IC_{50} and k_{on} were corrected to zero-substrate concentration, the reversibility of the isothiosemicarbazide formation (Fig. 13) was shown in a reactivation experiment with compound **68** [192].

In the case of fast-binding inhibitors **66**, **79** and **80**, the progress lines were analyzed by linear regression (Fig. 29a), and the resulting steady-state rates (v_s) were plotted against $[I]$. The corresponding IC_{50} values were obtained by non-linear regression of the data pairs (v_s , $[I]$) as shown in Figure 29b. The IC_{50} values were corrected using the Cheng-Prusoff equation (Fig. 23c) to obtain the true inhibition constants (K_i).

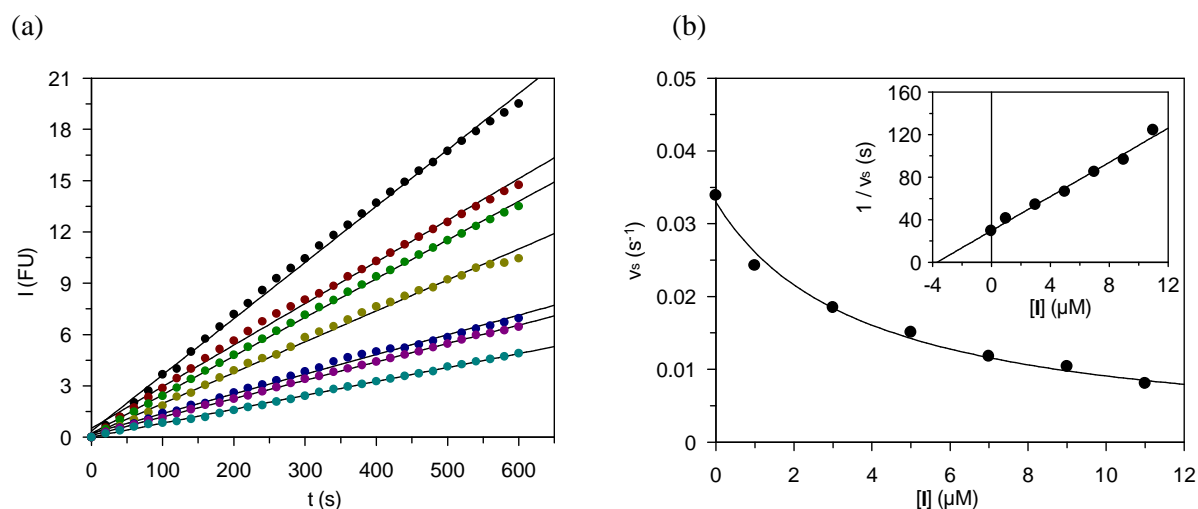


Figure 29. Fast-binding behavior of dipeptide nitrile **80**. (a) Monitoring of the human cathepsin K-catalyzed hydrolysis of Z-Leu-Arg-AMC (40 μM) in the presence of increasing concentrations of compound **80** (\bullet , 0; \bullet , 1 μM ; \bullet , 3 μM ; \bullet , 5 μM ; \bullet , 7 μM ; \bullet , 9 μM ; \bullet , 11 μM). The reaction (100 mM citrate buffer pH 5.0, 100 mM NaCl, 5 mM EDTA, 0.01% CHAPS, 100 μM DTT, 2% DMSO, 25 $^{\circ}C$) was initiated by addition of the enzyme. Fluorescence emission at 440 nm was measured after excitation at 360 nm. Fluorescence units (FU) were corrected for background fluorescence. (b) Plot of the rates of hydrolysis of Z-Leu-Arg-AMC versus concentrations of **80**. Non-linear regression gave an apparent inhibition constant $K_i' = (1+[S]/K_m)K_i = 3.8 \pm 0.3 \mu M$. The inset is a Dixon plot of the data.

2.1.6. STRUCTURE-ACTIVITY RELATIONSHIPS OF 50, 51 62–66, 67, 68, 79, 80

In general, the replacement of the carbamate P3-P2 linker by a urea moiety resulted in an improved inhibitory activity of urea-based azadipeptide nitriles toward cathepsins L, S, K and B. With K_i values of 11 and 17 pM, respectively, compounds **50** and **51** were even more potent for cathepsin K than the corresponding carbamate-based derivative **45** (Tables 2 and 5). This finding could be explained by the fact that urea-derived inhibitors, *e.g.* **50** and **51**, can potentially form an additional hydrogen bond to the target cathepsins, in contrast to the corresponding compounds with a carbamate P3-P2 linker, *e.g.* **45**.

Table 5. K_i values of urea-based compounds **50**, **51** and **62–66** on human cathepsins L, S, K and B.

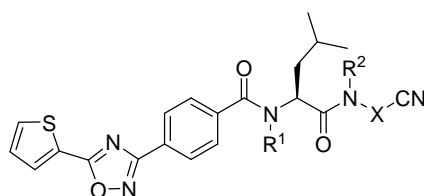
cmpd	R ¹	n	R ²	X	K_i (nM)			
					cath L	cath S	cath K	cath B
50	H	1	Me	NMe	0.39 ± 0.01	0.20 ± 0.01	0.011 ± 0.001	0.65 ± 0.09
51	H	0	Me	NMe	0.045 ± 0.002	0.16 ± 0.01	0.017 ± 0.001	1.3 ± 0.1
62		1	Me	NMe	1.4 ± 0.1	0.17 ± 0.01	0.11 ± 0.01	2.8 ± 0.3
63		1	Me	NMe	1.1 ± 0.1	0.16 ± 0.01	0.072 ± 0.002	1.3 ± 0.1
64		0	Me	NMe	2.0 ± 0.2	0.19 ± 0.03	0.045 ± 0.007	2.4 ± 0.3
65		0	Me	NMe	4.4 ± 0.2	0.32 ± 0.02	0.022 ± 0.001	2.4 ± 0.1
66		0	H	CH ₂	4700 ± 400	180 ± 10	34 ± 1	> 22000

The inhibitors **62–65** containing extended P3 moieties exhibited similar binding affinities on cathepsin K with picomolar K_i values. Triaryl derivatives **63** and **65** were slightly more potent than the methyl substituted biaryl compounds **62** and **64**. Among the six urea-based azadipeptide nitriles, **65** displayed the most promising selectivity profile for cathepsin K over

cathepsins L, S, and B (Table 5). The corresponding carba-analogue **66** showed the same trend to selectively inhibit cathepsin K, but with approximately three orders of magnitude higher K_i value. A fast-binding inhibition behavior was observed for the carba-analogue **66**, in contrast to the azadipeptide nitriles **50**, **51** and **62–65**.

A further shortening of P3-P2 linker of **65** and **66** led to the amide-based dipeptide nitrile **79** and azadipeptide nitrile **67**. While the carba-analogue **79** with a fast-binding behavior exhibited a 300–7600-fold selectivity for cathepsin K over cathepsins L and B and a moderate selectivity over cathepsin S, the corresponding azadipeptide nitrile **67**, a slow-binding inhibitor, was more potent, but much less selective (Table 6). Interestingly, the methylated counterparts of **79** and **67**, compounds **80** and **68**, showed a remarkable selectivity for cathepsin K over cathepsins L, S and B. Moreover, compound **68** represents the first cathepsin K-selective azadipeptide nitrile at all. Azadipeptide nitrile **68** still exhibited a picomolar inhibition constant for cathepsin K in combination with a 200–4300-fold selectivity over antitargets, cathepsins L, B, and S. Probably, the hydrogen-bond donating CONH linker of **67** contributes to the binding to the four cathepsins studied whereas the P2 and P3 moieties are already optimized for cathepsin K. Therefore, the disruption of hydrogen bond formation by the methylation a CONH linker is better tolerated by cathepsin K than by the other cathepsins. This suggestion is confirmed by the experimental data.

Table 6. K_i values of amide-based compounds **79**, **80**, **67** and **68** on human cathepsins L, S, K and B.



cmpd	R ¹	R ²	X	K_i (nM)			
				cath L	cath S	cath K	cath B
79	H	H	CH ₂	940 ± 40	140 ± 10	2.9 ± 0.4	> 22000
80	Me	H	CH ₂	> 22000	> 22000	270 ± 20	> 22000
67	H	Me	NMe	0.22 ± 0.03	0.15 ± 0.01	0.032 ± 0.005	0.36 ± 0.06
68	Me	Me	NMe	2700 ± 300 ^a	140 ± 10 ^a	0.63 ± 0.03	510 ± 40 ^b

^aThe progress curves were analyzed by linear regression in a time interval between 20 and 30 min.

^bThe progress curves were followed over 20 min and analyzed by non-linear regression.

While compounds **50**, **51** and **62–65** clearly showed slow-binding inhibition type, a fast-binding inhibition behavior was observed for the carba-analogue **66**. The k_{on} values of the latter compounds for the four cathepsins reflect the different K_i values (for k_{on} values of **50**, **51** and **62–65**, see Table 7). Except compound **51**, the highest second-order rate constants (k_{on}) were calculated for association processes between urea-based azadipeptide nitriles and cathepsins S and K. These high k_{on} values correlate with the corresponding low K_i values which were obtained for compounds **50** and **62–65** and outline the difficulty to achieve the inhibitor selectivity for cathepsin K over cathepsin S. As a general trend, it was further observed that the introduction of biaryl or triaryl P3 substituents results in decreased k_{on} values (**50** and **51** versus **62–65**). This effect was particularly strong in the case of triaryl derivatives **63** and **65** and cathepsin L. Moreover, the phenylurea-derived inhibitors **51**, **64** and **65** showed slightly higher second-order association rate constants than the corresponding benzylureas **50**, **62** and **63**.

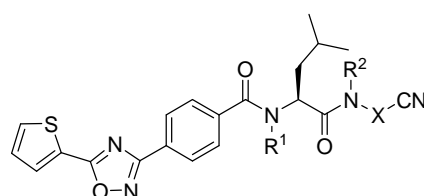
Table 7. k_{on} values of urea-based compounds **50**, **51** and **62–65**.

cmpd	R ¹	n	R ²	X	k_{on} ($10^3 \text{ M}^{-1} \text{ s}^{-1}$)			
					cath L	cath S	cath K	cath B
50	H	1	Me	NMe	710 ± 40	1900 ± 100	3500 ± 100	60 ± 9
51	H	0	Me	NMe	3400 ± 100	2000 ± 200	4000 ± 200	250 ± 10
62		1	Me	NMe	310 ± 20	1300 ± 100	540 ± 90	17 ± 4
63		1	Me	NMe	82 ± 4	1500 ± 200	650 ± 150	55 ± 3
64		0	Me	NMe	250 ± 10	1000 ± 100	1300 ± 200	54 ± 6
65		0	Me	NMe	44 ± 5	1200 ± 100	2400 ± 200	78 ± 2
66		0	H	CH ₂	n.d. ^a	n.d.	n.d.	n.d.

^a Not determined

In the case of the amide-based azadipeptide nitrile **67**, as expected, the highest k_{on} value was calculated for cathepsin K. However, the differences in the second-order rate constants of **67** on cathepsins L, S and B were less pronounced than, *e.g.*, in the case of the urea-derived azadipeptide nitrile **65** containing the same triaryl moiety at the P3 position. Furthermore, the methylation of the P3-P2 linker strongly affected the enzyme-inhibitor association rate (**67** *versus* **68**, Table 8). The *N*-methyl compound **68** showed clearly decreased k_{on} values, reflecting a delayed approach to steady-state. This effect was less pronounced at cathepsin K, for which the optimized substructures, common in **67** and **68**, attenuate the lack of a hydrogen bond formation to the backbone amide of Gly66 [164] in the case of **68**. The methylation of the P2-P3 amide linker in compound **67**, which was applied for the development of cathepsin K inhibitor **68**, represents an important new approach to achieve the selectivity of azadipeptide nitriles toward particular cysteine proteases. This approach was first used in the presented work and requires a two step modification of the azadipeptide nitrile scaffold. In the first step, the substitution pattern of the inhibitor molecule had to be optimized for a target cysteine protease. In the second step, the hydrogen bond to the P3-P2 linker was to be disrupted, *e.g.*, by *N*-alkylation to achieve the selectivity.

Table 8. k_{on} values of amide-based compounds **67** and **68**.



cmpd	R ¹	R ²	X	k_{on} ($10^3 \text{ M}^{-1}\text{s}^{-1}$)			
				cath L	cath S	cath K	cath B
79	H	H	CH ₂	n.d. ^a	n.d.	n.d.	n.d.
80	Me	H	CH ₂	n.d.	n.d.	n.d.	n.d.
67	H	Me	NMe	800 ± 80	800 ± 70	3300 ± 400	1600 ± 200
68	Me	Me	NMe	n.d. ^{a,b}	n.d. ^{a,c}	63 ± 6	0.62 ± 0.01 ^d

^aNot determined

^bFor [**68**] = 20 μM, a k_{obs} value could not be obtained by non-linear regression of the progress curves. A limit $k_{obs}(1+[S]/K_m)/[I] < 1.0 \times 10^3 \text{ M}^{-1}\text{s}^{-1}$ was therefore estimated.

^cFor [**68**] = 350 nM, a k_{obs} value could not be obtained by non-linear regression. A limit $k_{obs}(1+[S]/K_m)/[I] < 20 \times 10^3 \text{ M}^{-1}\text{s}^{-1}$ was therefore estimated.

^dThe progress curves were followed over 20 min and analyzed by non-linear regression.

In contrast to k_{on} values, the corresponding k_{off} values of the urea- and amide-based azadipeptide nitriles were independent from the substitution pattern and the nature of the P3-P2 linker. As shown in Table 9, the first-order rate constants of compounds **50**, **51** and **62–65** were approximately in the same range for each enzyme. Furthermore, it could not be observed that the k_{off} values of azadipeptide nitriles **50**, **51** and **62–65** significantly differed between cathepsins L, S, K and B. However, the first-order dissociation rate constants of urea-based azadipeptide nitriles and cathepsin K were slightly lower than the corresponding k_{off} values on cathepsins L and S.

Table 9. k_{off} values of urea-based compounds **50**, **51** and **62–65**.

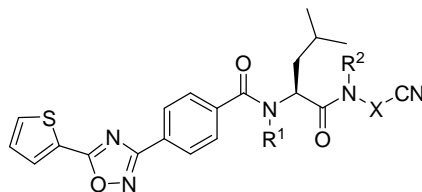
cmpd	R ¹	n	R ²	X	k_{off} (10^{-3} s^{-1})			
					cath L	cath S	cath K	cath B
50	H	1	Me	NMe	0.28 ± 0.02	0.38 ± 0.03	0.039 ± 0.004	0.039 ± 0.008
51	H	0	Me	NMe	0.15 ± 0.01	0.32 ± 0.04	0.068 ± 0.005	0.33 ± 0.03
62		1	Me	NMe	0.43 ± 0.04	0.22 ± 0.02	0.059 ± 0.011	0.048 ± 0.012
63		1	Me	NMe	0.090 ± 0.009	0.24 ± 0.04	0.047 ± 0.011	0.072 ± 0.007
64		0	Me	NMe	0.50 ± 0.05	0.19 ± 0.04	0.059 ± 0.013	0.13 ± 0.02
65		0	Me	NMe	0.19 ± 0.02	0.38 ± 0.04	0.053 ± 0.005	0.19 ± 0.01
66		0	H	CH ₂	n.d. ^a	n.d.	n.d.	n.d.

^aNot determined

While the first-order rate constants of the amide-derived compound **67** were obtained for the four tested cathepsins and showed no significant differences to those of amide-based azadipeptide nitriles, the k_{off} values of *N*-methyl derivative **68** could be calculated only for cathepsins K and B (Table 10). Because the association of compound **68** with cathepsins

L and S was very slow, it was not possible to determine the second-order rate constants from the hyperbolic progress curves for these two enzymes. For this reason, the first-order rate constants of **68** for cathepsins L and S could not be calculated because of $k_{\text{off}} = K_i \times k_{\text{on}}$.

Table 10. k_{off} values of amide-based compounds **67** and **68**.



cmpd	R ¹	R ²	X	k_{off} (10^{-3} s^{-1})			
				cath L	cath S	cath K	cath B
79	H	H	CH ₂	n.d. ^a	n.d.	n.d.	n.d.
80	Me	H	CH ₂	n.d.	n.d.	n.d.	n.d.
67	H	Me	NMe	0.18 ± 0.03	0.12 ± 0.01	0.11 ± 0.02	0.58 ± 0.12
68	Me	Me	NMe	n.d.	n.d.	0.040 ± 0.004	0.32 ± 0.03 ^b

^aNot determined

^bThe progress curves were analyzed by non-linear regression in a time interval of 20 min.

2.1.7. CONCLUSIONS I

In this study, using the example of cathepsin K, an approach to design of highly potent and selective azadipeptide nitrile inhibitors was demonstrated. Whereas the carba-analogous dipeptide nitriles typically show fast-binding kinetics, a different, slow-binding behavior was observed for azadipeptide nitriles. Thus, it was possible to determine the influence of structural features on association and dissociation rate constants for the presented series of peptidomimetic nitrile inhibitors. A strong impact of structural variations in azadipeptide nitriles on the enzyme-inhibitor association rate was demonstrated. Although reversibly [192] forming isothiosemicarbazide adducts, these compounds gain their inhibitory activity not only from the covalent attraction, but also from specific non-covalent interactions to the active site. The dissociation rate, however, was not affected by the compounds' structure. This finding reflects the difficulty in delivering significant binding energy from non-covalent interactions, as concluded from the large and relatively shallow active site of cysteine cathepsins.

Furthermore, synthetic routes to urea- and amide-based azadipeptide nitriles were established in the presented study. Compound **68** was identified as the first cathepsin K-selective azadipeptide nitrile with a picomolar K_i value. The selectivity for cathepsin K was achieved by the stepwise optimization of the inhibitor scaffold combined with the methylation of the P3-P2 amide linker. To explain the remarkable selectivity profile of **68** (200–4300-fold) toward cathepsin K, it was suggested that the P3 and P2 substituents in compound **68**, which were optimized for cathepsin K, can compensate the negative effect of the hydrogen bond disruption by *N*-methylation. Therefore, the CONMe linker was better tolerated by cathepsin K than by the other cathepsins. The described approach represents a new method to develop selective azadipeptide nitriles and can eventually be applied for the other cysteine cathepsins.

Moreover, the first example for direct cyclization of a Cbz-protected azadipeptide *tert*-butyl ester to the corresponding 1,2,4-triazinane-3,6-dione was described. This cyclization reaction represents an easy synthetic access to 1,2,4-triazinane-3,6-dione scaffolds for the preparation of new potential peptidomimetic structure with at least four possible diversity points.

Parts of this study are described in a recently published manuscript by Frizler *et al.* [192].

2.1.8. HOMOCYCLCOLEUCINE-BASED AZADIPEPTIDE NITRILES

As described in chapter 2.1.1, the homocycloleucine-derived azadipeptide nitrile **42** with a P3-P2 carbamate linker was identified as potent cathepsin K inhibitor ($K_i = 1.8$ nM). Furthermore, this compound was already 72–220-fold selective for cathepsin K over cathepsins L, S and B (Table 2). To improve the potency and selectivity of the azadipeptide nitrile **42** toward cathepsin K, it was decided to combine its P2 substituent with the already for cathepsin K optimized triaryl P3 substituent and the P3-P2 linkers of **65** and **67** (Fig. 30).

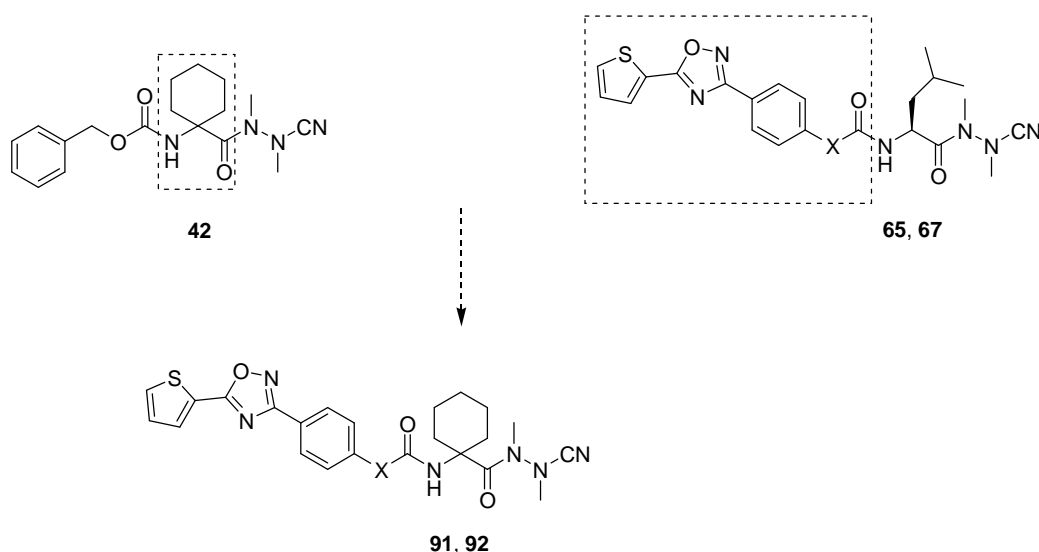
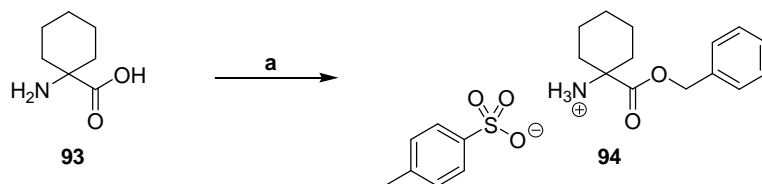


Figure 30. Combination of the P2 residue of compound **42** with the P3 substituents of **65** and **67**. **65, 91**, X = NH; **67, 92**, X = O.

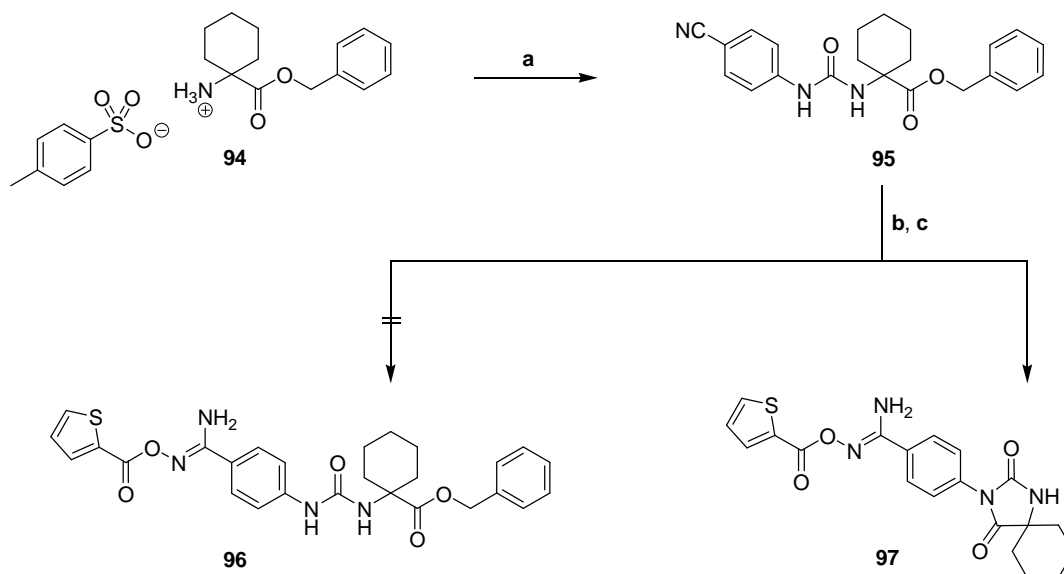
In the first attempt to prepare compound **91** (Fig. 30), the following synthetic route was applied. Commercially available homocycloleucine **93** was first converted into the corresponding benzyl ester **94** by the reaction with benzyl alcohol in toluene under Dean-Stark conditions and in the presence of *p*-toluenesulfonic acid (Scheme 12).



Scheme 12. Synthesis of compound **94**.

a) benzyl alcohol, *p*-toluenesulfonic acid, toluene, Δ .

Next, compound **94** was reacted with 4-cyanophenyl isocyanate in dry THF to obtain the urea derivative **95** in high yield and purity. To transform the nitrile compound **95** to the corresponding *N*-(thiophene-2-carboxyloxy)benzimidamide **96**, it was heated with hydroxylamine hydrochloride in the presence of DIPEA, followed by the reaction with 2-thiophenecarbonyl chloride in the presence of DIPEA. Surprisingly, the desired compound **96** was not formed. The isolated product was characterized as the hydantoin derivative **97** (Scheme 13).

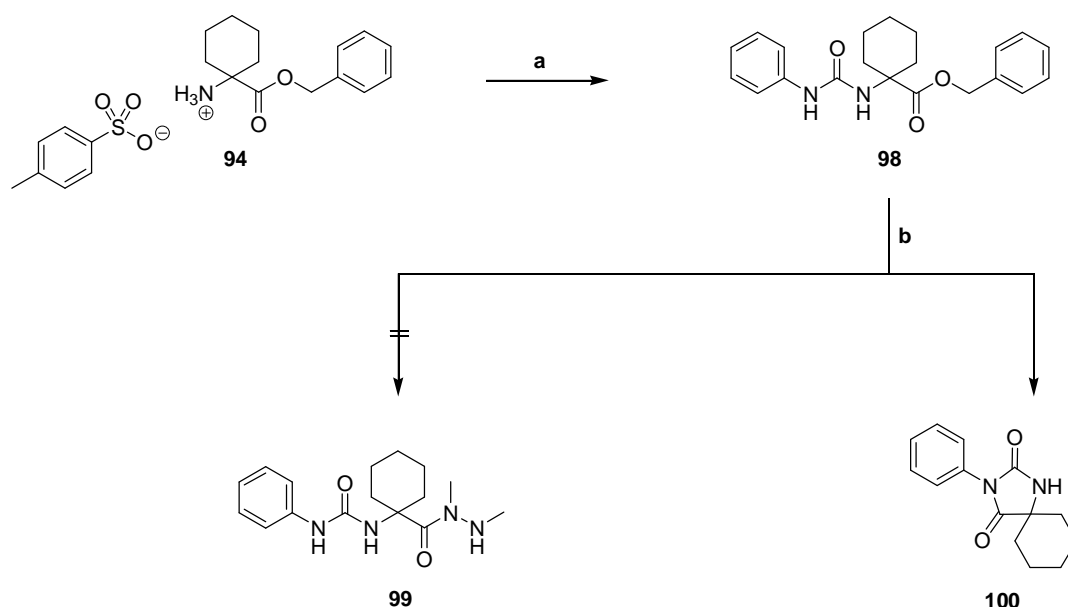


Scheme 13. Unexpected formation of the hydantoin derivative **97** under basic conditions.

a) 4-cyanophenyl isocyanate, TEA, THF, rt; b) $\text{NH}_2\text{OH} \times \text{HCl}$, DIPEA, EtOH, Δ ;
c) 2-thiophenecarbonyl chloride, DIPEA, MeCN, rt.

It was supposed that the polarization of the N-H-bond of the aryl-substituted urea nitrogen by a strong organic base (DIPEA) caused the nucleophilic attack on the carbonyl carbon of the benzyl ester moiety. The hydantoin ring was formed by the following elimination of the benzyl alcohol. The supposed mechanism was confirmed by the reaction of compound **98** with 1,2-dimethylhydrazine dihydrochloride in the presence of DIPEA (Scheme 14), where the formation of the desired 1,2-dimethylhydrazide **99** could not be annotated. Instead, the hydantoin derivative **100** was isolated as a main product. Interestingly, the formation of a hydantoin was not observed for the transformation of **53** into the corresponding L-leucine-derived *N*-(thiophene-2-carboxyloxy)benzimidamide **57** (Scheme 5). The high cyclisation tendency of homocysteine-derived compounds could be explained by the *gem*-dialkyl effect which was first described in 1915 by Beesley, Thorpe and Ingold as part of a study on the formation and stability of spiro compounds [193]. These authors showed that the

increasing size of two substituents on a tetrahedral center leads to enhanced reactivity between parts of the other two residues for intramolecular reactions. The first explanation for the *gem*-dialkyl effect was the internal angle reduction and is commonly referred to as the ‘Thorpe-Ingold effect’ or the ‘theory of valency deviation’. Because the theory of valency deviation is not generally valid, it was later extended by further theories. For example, the ‘reactive-rotamer hypothesis’ expects the *gem*-disubstitution to promote the formation of reactive *gauche* conformers, in which the functionalities are located syn-periplanar to each other, as a possible reason for the enhanced cyclisation tendency (for reviews, see [194], [195]).



Scheme 14. Reaction of **98** with $(\text{NHMe})_2 \times 2\text{HCl}$ in the presence of DIPEA.

a) 4-cyanophenyl isocyanate, DIPEA, THF, rt; b) $(\text{NHMe})_2 \times 2\text{HCl}$, DIPEA, THF, rt;

In contrast to the L-leucine-based compounds, the linear synthesis of the homocycloleucine-derived azadipeptide ntrile **91** (Fig. 30) was not successful due to the cyclisation reaction described in Scheme 13. Therefore, a convergent synthetic route was developed. As shown in Figure 31, compound **91** was retrosynthetically divided into the synthetic equivalents **101**, **94** and **102**. The synthetic equivalents **101** and **102** had to be synthesized, while the P2 building block **94** was already prepared (Scheme 12). In the first step of the envisaged synthetic route, the P3 building block **101** was to be coupled with the P2 building block **94** using the Lossen rearrangement leading to the corresponding urea-derived intermediate. In the second step, the benzyl ester of the obtained intermediate was to be cleaved *via* a catalytic hydrogenation on Pd/C, followed by the coupling of the resulting acid with **102** using the mixed anhydride

procedure. The mixed anhydride protocol allows gentle coupling in the absence of strong bases, which is important to avoid the possible intramolecular cyclisation.

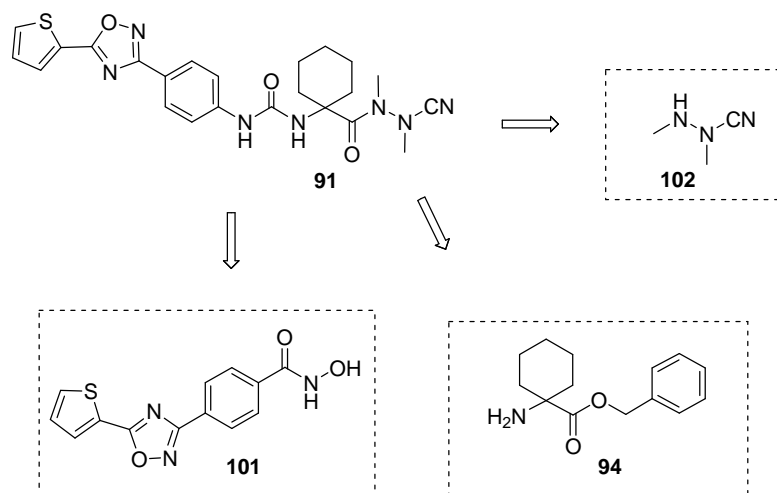
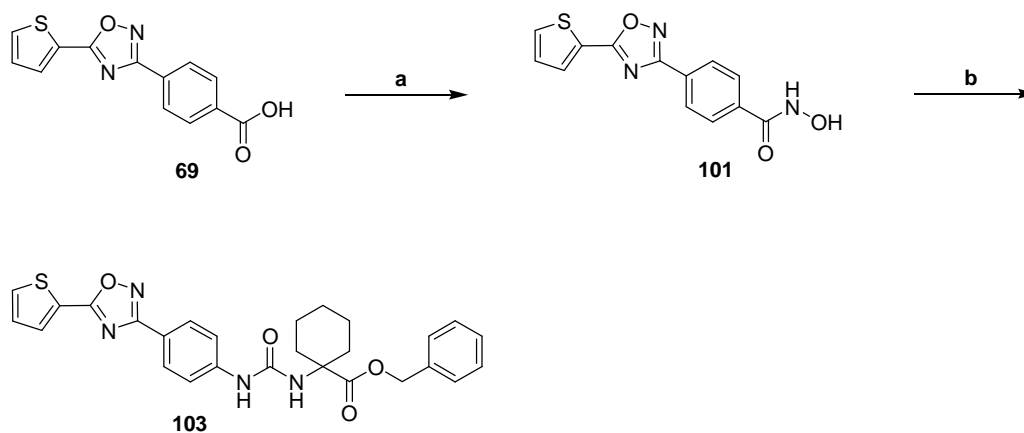


Figure 31. Retrosynthetic route to compound **91**.

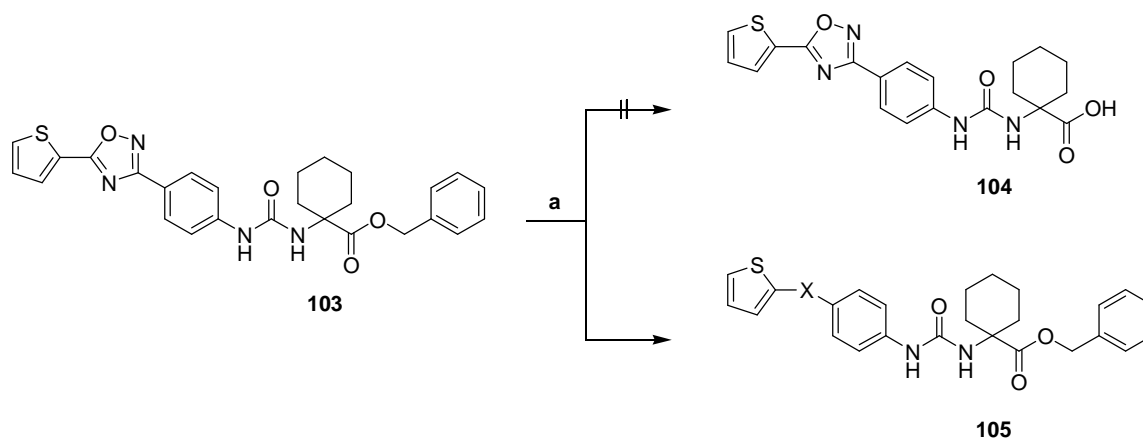
The hydroxamic acid **101** was synthesized as the P3 building block as shown in Scheme 15. The carboxylic group of the triaryl derivative **69** (Scheme 7) was activated with isobutyl chloroformate to a mixed anhydride and reacted with hydroxylamine [196] to obtain compound **101**. The crude product could be easily purified by a simple recrystallization from ethanol/ethyl acetate. Next, the hydroxamic acid **101** was converted into the corresponding isocyanate by the reaction with EDC in the presence of DMAP *via* Lossen rearrangement [197] and reacted *in situ* with the P2 building block **94** to obtain the urea-based intermediate **103** in high yield and purity.



Scheme 15. Synthesis of compound **101** as the P3 building block and its coupling to intermediate **103**.

a) 1. $\text{ClCO}_2i\text{-Bu}$, NMM, THF, $-25\text{ }^\circ\text{C}$, 2. $\text{NH}_2\text{OH} \times \text{HCl}$, NaOH, MeOH, THF, $-25\text{ }^\circ\text{C}$ to rt;
b) 1. EDC, DMAP, THF, rt; 2. **94** after basic extraction, THF, rt.

In the next step, it was tried to cleave the benzyl ester of **103** *via* catalytic hydrogenation on Pd/C to obtain the free acid **104** for the further coupling with 1,2-dimethylhydrazinecarbonitrile **102**. Unfortunately, the hydrogenolytic cleavage of the benzyl ester of **103** was not successful. The isolated product, which was purified by column chromatography, showed a mass-to-charge ratio value (m/z) of 505.3 ($[M + H]^+$) in the recorded MS(ESI) spectrum. In combination with NMR spectra, this finding indicated the catalytic hydrogenation of the 1,2,4-oxadiazole ring to the corresponding dihydro-1,2,4-oxadiazole derivative **105** instead of deprotection of the carboxylic group (Scheme 16). However, the location of the double bond within the formed dihydro-1,2,4-oxadiazole heterocycle was not clearly resolved and has to be clarified by further experiments.



Scheme 16. Formation of the hydrogenated product **105**.

a) H_2 , Pd/C, MeOH, rt, atmospheric pressure; X = dihydro-1,2,4-oxadiazole ring.

To realize a new synthetic strategy, the desired compound **91** was again retrosynthetically divided into three synthetic equivalents (compounds **101**, **106**, and BrCN, Fig. 32).

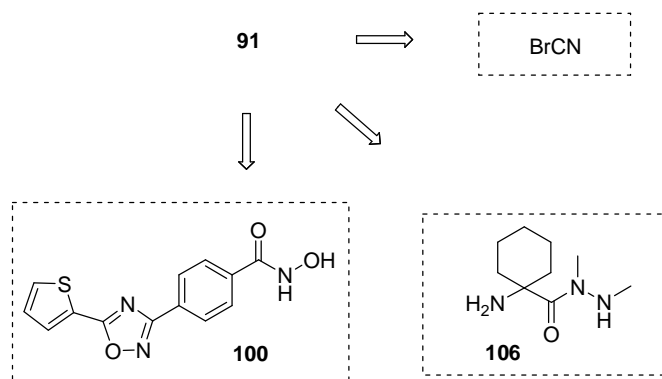
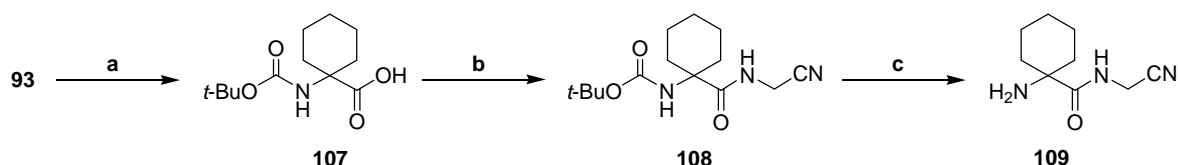


Figure 32. New retrosynthetic route to compound **91**.

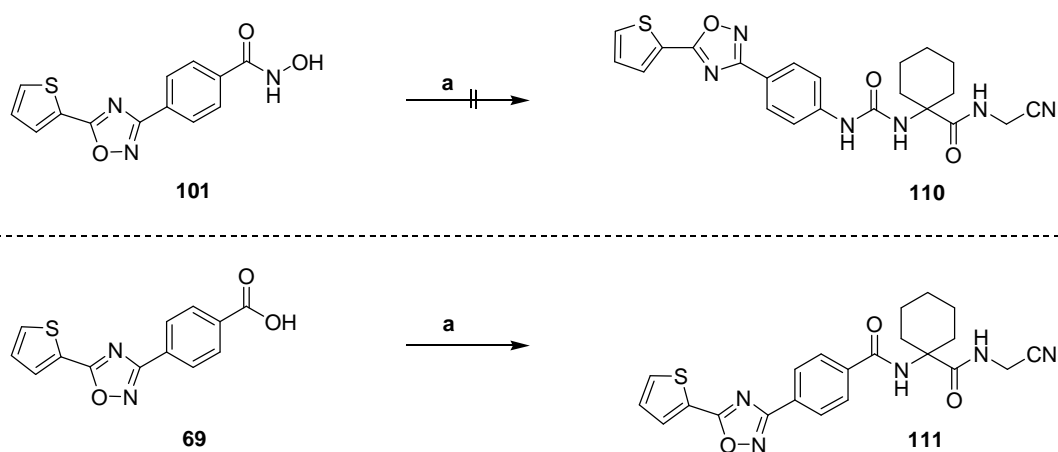
This synthetic route was first applied in a modified form to the carba-analogues **110** and **111** (Scheme 18). Boc-protected homocycloleucine **107** was activated with isobutyl chloroformate to a mixed anhydride followed by the reaction with aminoacetonitrile monosulfate in the presence of TEA. The obtained dipeptide nitrile **108** was treated with methanesulfonic acid to cleave the Boc protecting group. The basic extraction of the resulting methanesulfonate salt led to compound **109** as the P2 building block (Scheme 17).



Scheme 17. Synthesis of the P2 building block **109**.

a) $(\text{Boc})_2\text{O}$, NaOH, dioxane, rt; b) 1. $\text{ClCO}_2i\text{-Bu}$, NMM, THF, $-25\text{ }^\circ\text{C}$, 2. $\text{H}_2\text{NCH}_2\text{CN} \times \text{H}_2\text{SO}_4$, TEA, THF, $-25\text{ }^\circ\text{C}$ to rt; c) MeSO_3H , THF, rt, basic extraction.

Next, the obtained P2 building block **109** was reacted *via* Lossen rearrangement with the P3 building block **101**. Unfortunately, this reaction was not successful, and the formation of the desired compound **110** could not be observed. However, the reaction of compound **109** with the P3 building block **69** led to the formation of the corresponding dipeptide nitrile **111** containing a P3-P2 amide linker (Scheme 18).



Scheme 18. Planned synthetic route to compound **110** (above) and synthesis of dipeptide nitrile **111**.

a) EDC, DMAP, **109**, THF, rt.

Due to the comparable kinetic profiles of urea- and amide-derived azadipeptide nitriles (**65** *versus* **67**), it was decided not to further attempt preparing urea-based cathepsin inhibitors containing homocycloleucine at the P2 position. For reasons of synthetic access, the P3-P2

amide linker was maintained in all compounds of this study. In Figure 33, the final retrosynthetic route to the amide-based azadipeptide nitrile **92** is shown. While cyanogen bromide was commercially available and compound **69** was already obtained (Scheme 7), the P2 building block **106**, containing a *gem*-disubstituted amino acid (homocycloleucine), had to be synthesized.

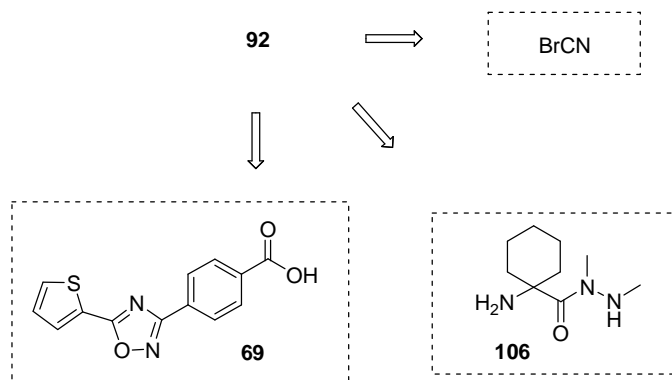
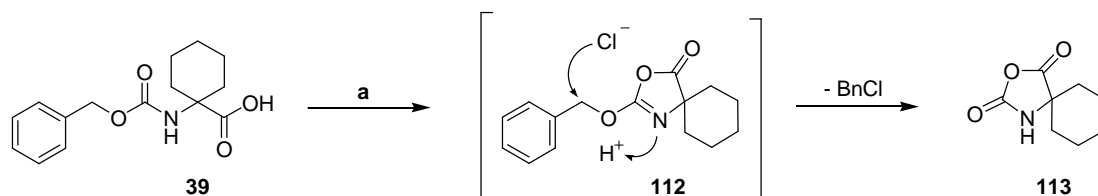


Figure 33. Retrosynthetic route to the amide-based azadipeptide nitrile **92**.

To prepare the P2 building block **106**, it was first tried to improve the coupling of Cbz-protected homocycloleucine **39** (Scheme 2) with 1,2-dimethylhydrazine. When compound **39** was reacted with oxalyl chloride for activation, the *N*-carboxyanhydride (NCA) **113** was obtained in a yield of 83% (Scheme 19). Its formation was envisaged to occur *via* nucleophilic attack of the carbamate oxygen at the activated carboxylic group to produce the 5(4*H*)-oxazolone **112**. Under the used conditions in the absence of a base [198], a chloride-promoted displacement of the benzyl group was operative [199].

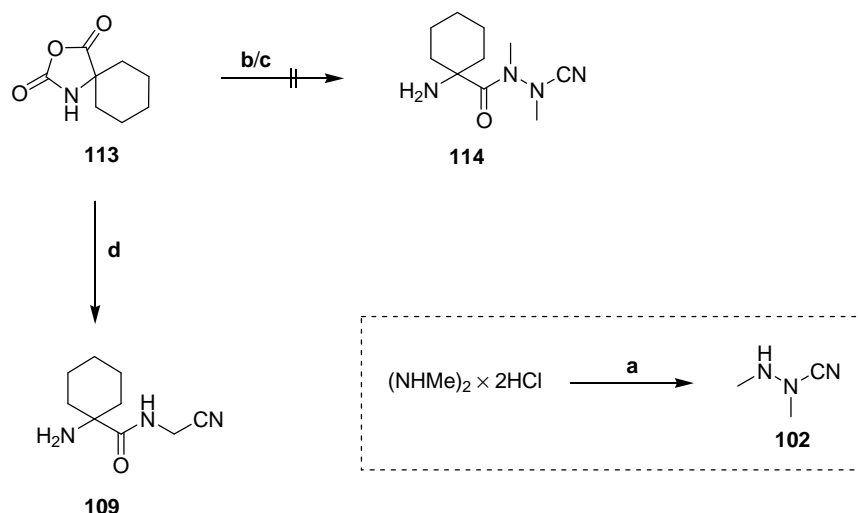


Scheme 19. Synthesis of the homocycloleucine-NCA **113**.

a) $(\text{COCl})_2$, CH_2Cl_2 , DMF, rt.

The obtained Leuchs anhydride **113** was reacted with 1,2-dimethylhydrazinecarbonitrile **102** (Fig. 31) in order to obtain the azadipeptide nitrile **114** as a building block (Scheme 20) which could have been directly coupled with compound **69** leading to the desired product **92** in only one further step. However, the transformation of **113** into **114** was not observed under

different conditions, ranging from a reaction in THF at room temperature to a reaction in DMF at 130 °C in a sealed tube. In contrast, the transformation of **113** with aminoacetonitrile in THF carried out in an autoclave at 100°C, provided homocycloleucyl-glycine-nitrile **109** in 72%. Thus, two alternative routes from homocycloleucine **93** to the P2 building block **109** (via **107** and **108**, or via **39** and **113**) were employed.



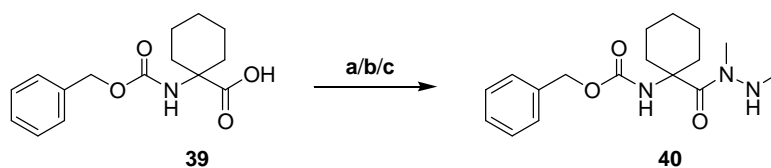
Scheme 20. Reaction of **113** with different nucleophiles. *Box.* Synthesis of **102**.

a) BrCN , H_2O , NaOH , rt; b) **102**, THF, rt; c) **102**, DMF, 130 °C; d) $\text{N}_2\text{NCH}_2\text{CN} \times \text{H}_2\text{SO}_4$, THF, DIPEA, 100 °C.

The unexpectedly [200] low reactivity of the homocycloleucine-derived NCA **113** was considered to result from the *gem*-dialkyl effect. It has been well established that this effect promotes cyclisation reactions due to an increased number of *gauche* interactions in the open chain substrates and/or a relief of steric strain in the cyclic products (for reviews, see [194], [195]). However, the *gem*-dialkyl effect also leads to an enhanced stability of the corresponding cyclic compounds, and it was therefore assumed that it accounts for the protection of **113** against hydrazinolytic cleavage. As noted above, the mixed anhydride coupling of Cbz-protected homocycloleucine **39** took place with low yields for reasons of steric interference (Scheme 2). Additionally, these reactions might be impaired by the *gem*-dialkyl effect leading to the formation of heterocyclized compound(s).

In further attempts to improve the yield of the dimethylhydrazide **40**, the EDC/DMAP and HBTU/HOBt coupling protocols were used (see also the ‘Experimental Section’). In the first experiment, the Cbz-protected homocycloleucine **39** was activated with EDC in the presence of DMAP, treated with triethylamine and 1,2-dimethylhydrazine dihydrochloride and stirred at room temperature for 24 h to obtain **40** in yield of 36% (18% in the case of the mixed

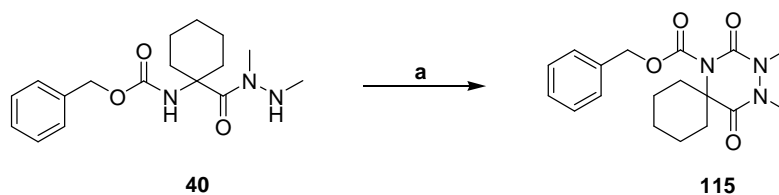
anhydride method, see also Scheme 2). When the reaction mixture was alternatively heated to reflux for 24 h, the yield of **40** was slightly improved to 39%. The HBTU/HOBt protocol offered no further synthetic advantages. Compound **40** was isolated only in a yield of 29% when **39** was activated with HBTU in the presence of HOBt, treated with triethylamine and 1,2-dimethylhydrazine dihydrochloride, and stirred for 3 d at room temperature. In general, it was not possible to significantly improve the yield of 1,2-dimethylhydrazide derivative **40** due to the already discussed *gem*-dialkyl effect. The EDC/DMAP protocol in combination with the heating of the reaction mixture represents the best coupling procedure to prepare the 1,2-dimethylhydrazide **40** (Scheme 21).



Scheme 21. Synthesis of **40** using different coupling procedures.

a) 1. EDC, DMAP, THF, rt; 2. (NHMe)₂ × 2HCl, TEA, rt, 24 h; 36%; b) 1. EDC, DMAP, THF, rt; 2. (NHMe)₂ × 2HCl, TEA, Δ, 24 h; 39%, c) 1. HBTU, HOBt, THF, rt; 2. (NHMe)₂ × 2HCl, TEA, rt, 3 d; 29%.

Before starting the final synthetic sequence to the desired amide-based azadipeptide nitrile **92**, compound **40** was reacted with (Boc)₂O in the presence of DMAP for the confirmation of the supposed mechanism of the 1,2,4-triazinane-3,6-dione formation described in chapter 2.1.4, Scheme 9. The resulting product **115** was characterized as an unique spiro compound with 1,3,4-triazaspiro[5.5]undecan-2,5-dione scaffold (Scheme 22).

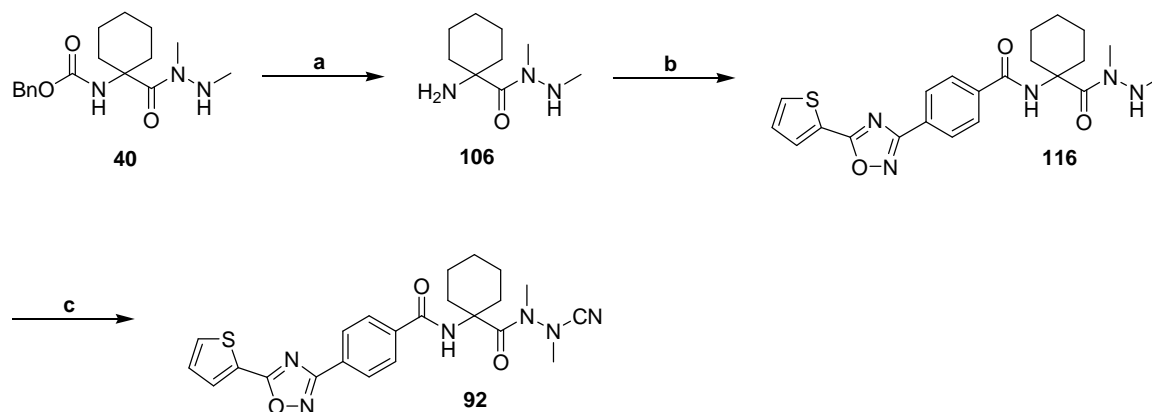


Scheme 22. Formation of **115** by the reaction with (Boc)₂O in the presence of DMAP.

a) (Boc)₂O, DMAP, MeCN, rt.

The finally successful synthesis of compound **92**, the aza-analogue of **111**, is outlined in Scheme 23. The Cbz protecting group of the dimethylhydrazide **40** was hydrogenolytically removed to obtain the building block **106**. The synthetic equivalent **69** (Fig. 33) was activated with EDC in the presence of DMAP and reacted with **106** leading to the formation of

compound **116**. In the final reaction step with cyanogen bromide, the homocycloleucine-based azadipeptide nitrile **92**, bearing a large P3 substituent, was obtained.



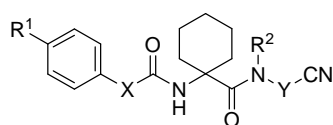
Scheme 23. Synthesis of the amide-based azadipeptide nitrile **92**.

a) Pd/C, H₂, MeOH, rt; b) **69**, EDC, DMAP, CH₂Cl₂, rt; c) BrCN, NaOAc, MeOH, rt.

2.1.9. KINETIC CHARACTERISATION OF 43, 111 AND 92

The product **92**, as well as its carba-analogue **111**, were tested on the human cathepsins L, S, K and B (Table 11). Again, the azadipeptide nitrile **92** showed a slow-binding behavior and a lower K_i value than the carba-analogue **111**, a fast-binding inhibitor. A comparison of the two aza derivatives **92** and **42** revealed that the introduction of a large substituent in the P3 position as well as the replacement of the P3-P2-linker was advantageous and led to an improved potency and selectivity for cathepsin K. The same trend was also observed for the corresponding dipeptide nitriles **43** and **111**. The improved inhibitory activity of the triaryl derivatives **111** and **92**, compared with their monoaryl counterparts **42** and **43**, could be explained by enhanced hydrophobic interactions between **111** and **92** and the tested cathepsins (particularly cathepsin K) due to the increased molecular weight and lipophilicity. Interestingly, the homocycloleucine moiety at the P3 position alone seems to be a sufficient structural feature to develop cathepsin K-selective azadipeptide nitriles, while the L-leucine-derived azadipeptide nitriles requires the methylation of the P3-P2 amide linker to achieve the selectivity for cathepsin K over cathepsins L, S and B (**68** versus **92**). Furthermore, compound **92** was slightly more potent on cathepsin K ($K_i = 0.35$ nM) than the corresponding *N*-methylated counterpart **68** ($K_i = 0.63$ nM) and less potent but much more selective than the non-methylated L-leucine-derived azadipeptide nitrile **67** ($K_i = 0.032$ nM).

Table 11. K_i values of compounds **42**, **43**, **111** and **92** on human cathepsins L, S, K and B.



compd	R ¹	X	R ²	Y	K_i (nM)			
					cath L	cath S	cath K	cath B
42 ^a	H	CH ₂ O	Me	NMe	400 ± 50	130 ± 5	1.8 ± 0.3	170 ± 10
43	H	CH ₂ O	H	CH ₂	> 5000	> 5000	55 ± 6	> 5000
111		0	H	CH ₂	> 5000	> 5000	13 ± 1	> 5000
92		0	Me	NMe	280 ± 50 ^b	78 ± 3	0.35 ± 0.04	150 ± 10

^aThe kinetic data of compound **42** are shown here for reasons of better illustration and are also depicted in Table 2. ^bThe enzymatic reaction was started by addition of chromogenic substrate after the enzyme was preincubated with inhibitor for 30 min. The reaction lines were analyzed by linear regression.

Additionally, the analysis of the progress curves in the case of slow-binding inhibitors **42** (see also Table 3) and **92** allowed for the determination of the second-order association rate constants (k_{on}) and the corresponding first-order dissociation rate constants (k_{off}). The results are shown in Tables 12 and 13. Because it was not possible to obtain the first-order rate constant (k_{obs}) for the development of the steady-state equilibrium between compound **92** and cathepsin L by non-linear regression, a limit $k_{obs}(1+[S]/K_m)/[I] < 10 \times 10^3 \text{ M}^{-1}\text{s}^{-1}$ was estimated for $[92] = 5 \mu\text{M}$. In general, the obtained k_{on} values of compounds **42** and **92** correlate with the corresponding K_i values (Tables 11 and 12). Furthermore, the estimated k_{on} values were clearly influenced by homocycloleucine/L-leucine replacement. Except of the *N*-methylated derivative **68**, the L-leucine-containing inhibitors **45**, **50**, **51**, **62–65** and **67** exhibited greater k_{on} values than **42** and **92** on the four tested cathepsins (Tables 3, 7, 8 and 12). The second-order association rate constants of **42** and **92** on cathepsin K were less affected than those on cathepsins L, S and B by the introduction of the homocycloleucine moiety into the azadipeptide nitrile scaffold. These results reflect the selectivity of homocycloleucine-derived azadipeptide nitriles for cathepsin K over the antitargets, cathepsins L, S and B.

Table 12. k_{on} values of compounds **42** and **92** on human cathepsins L, S, K and B.

cmpd	R ¹	X	R ²	Y	$k_{on} (\times 10^3 \text{ M}^{-1}\text{s}^{-1})$			
					cath L	cath S	cath K	cath B
42 ^a	H	CH ₂ O	Me	NMe	1.3 ± 0.1	7.8 ± 1	60 ± 10	1.0 ± 0.1
43	H	CH ₂ O	H	CH ₂	n.d. ^b	n.d.	n.d.	n.d.
111		0	H	CH ₂	n.d.	n.d.	n.d.	n.d.
92		0	Me	NMe	n.d. ^{b,c}	4.8 ± 0.3	180 ± 20	0.70 ± 0.01

^aThe kinetic data of compound **42** are shown herein for reasons of better illustration and also depicted in Table 3.

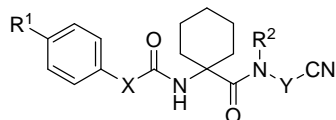
^bNot determined.

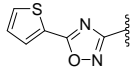
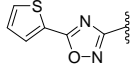
^cFor $[92] = 5 \mu\text{M}$, a k_{obs} value could not be obtained by non-linear regression. Therefore, a limit $k_{obs}(1+[S]/K_m)/[I] < 10 \times 10^3 \text{ M}^{-1} \text{ s}^{-1}$ was estimated.

As shown in Table 13, the calculated first-order dissociation rate constants (k_{off}) of **42** and **92** were in the same range, and showed to be independent from the structural modification

of the P3 substituent and the P3-P2 linker. Furthermore, the k_{off} values were not affected by homocysteine/L-leucine replacement (*e.g.* **92** versus **67**).

Table 13. k_{off} values of compounds **42** and **92** on human cathepsins L, S, K and B



cmpd	R ¹	X	R ²	Y	$k_{\text{off}} (\times 10^{-3} \text{ s}^{-1})$			
					cath L	cath S	cath K	cath B
42 ^a	H	CH ₂ O	Me	NMe	0.52 ± 0.08	1.0 ± 0.1	0.11 ± 0.03	0.17 ± 0.02
43	H	CH ₂ O	H	CH ₂	n.d. ^b	n.d.	n.d.	n.d.
111		0	H	CH ₂	n.d.	n.d.	n.d.	n.d.
92		0	Me	NMe	n.d.	0.37 ± 0.03	0.063 ± 0.01	0.11 ± 0.01

^aThe kinetic data of compound **42** are shown here for reasons of better illustration and are also depicted in Table 4.

^bNot determined.

2.1.10. FLUORESCENT AZADIPEPTIDE NITRILES

To study the ability of azadipeptide nitriles to penetrate the cell membrane as well as to investigate their cell distribution and accumulation, it is important to have pharmacological tools which allow for visualization of these compounds. Therefore, it was decided to introduce a fluorescent reporter in the homocycloleucyl-methylazaalanine nitrile scaffold of the cathepsin K-selective inhibitor **92** to obtain a VIS-detectable homocycloleucine-based azadipeptide nitrile.

At first, the fluorescent dipeptide nitriles **119** and **120** were synthesized, as shown in Scheme 24, to study their kinetic profiles on cathepsins L, S, K and B. For the labeling of the P3 position, two different fluorophores, compounds **117** and **118** (Fig. 34), were used. While dansyl chloride **117** was commercially available, the coumarin derivative **118** was synthesized by Matthias Mertens as previously described [202].

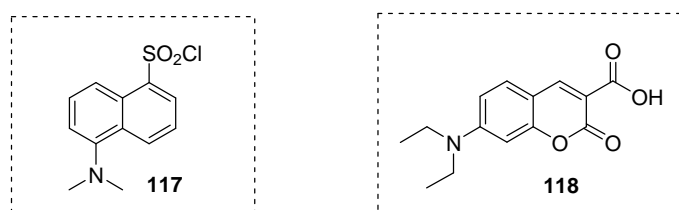
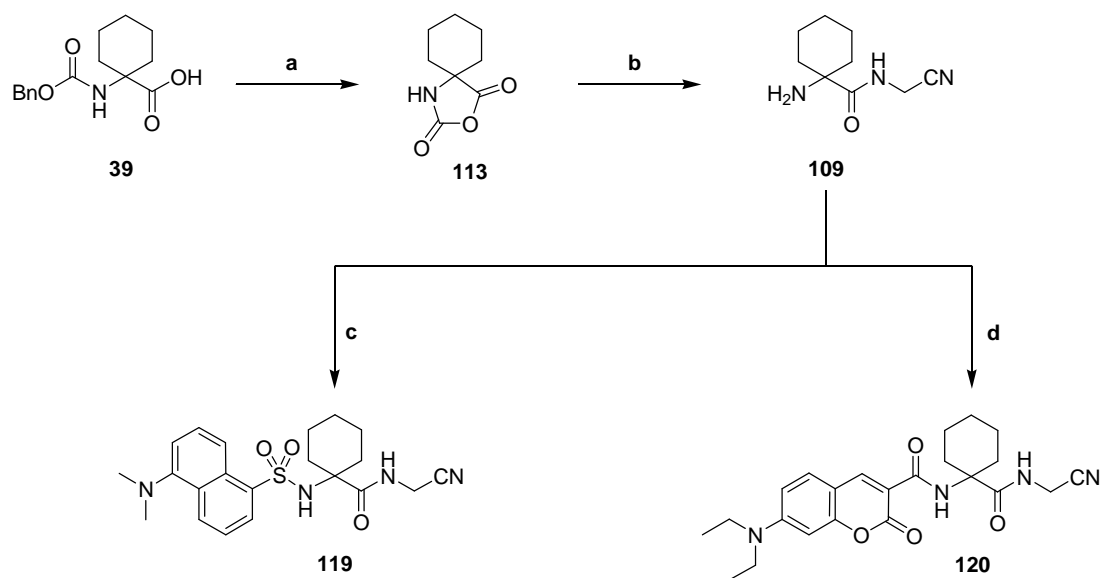


Figure 34. Compounds **117** and **118** as P3 fluorophores.

The Cbz-protected homocycloleucine **39** was reacted with oxalyl chloride in the presence of a catalytic amount of DMF to obtain homocycloleucine-NCA **113** in high yield and purity. Compound **113** was further converted with aminoacetonitrile leading to the dipeptide nitrile **109**. Finally, the free amino group of **109** was reacted with dansyl chloride **117** and the coumarin derivative **118** to obtain the fluorescent labeled dipeptide nitriles **119** and **120**, respectively. As expected, the reactivity of the amino group of **109** was decreased due to the *gem*-disubstitution of the α -carbon of the homocycloleucine at the P2 position (see also chapter 2.1.8). Therefore, the target compounds **119** and **120** were isolated by chromatographic separation only in low yields of 36% and 20%, respectively.

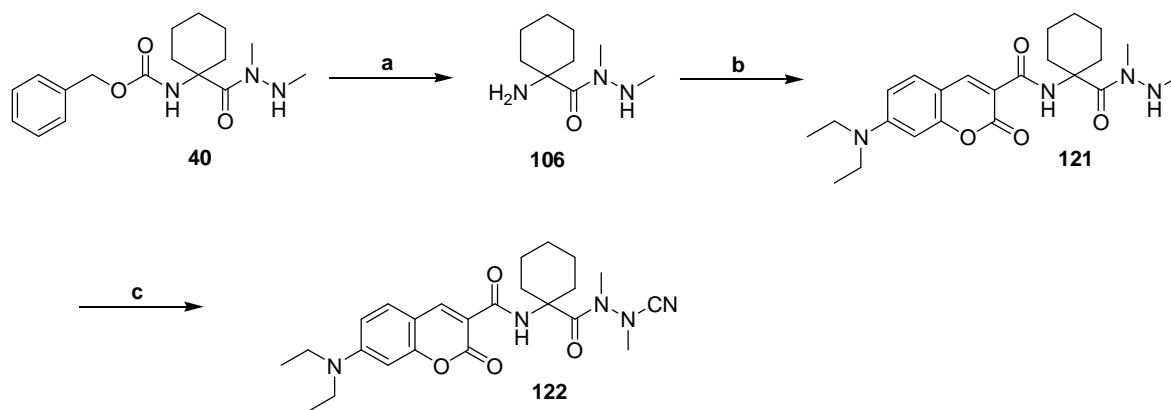
Due to the better kinetic properties of the dipeptide nitrile **120** compared with the corresponding dansyl derivative **119**, it was decided to introduce the coumarin fluorophore **118** into the azadipeptide nitrile scaffold of compound **92**. The synthetic route to the first fluorescent homocycloleucine-based azadipeptide nitrile **122** is shown in Scheme 25.



Scheme 24. Synthesis of the fluorescent labeled dipeptide nitriles **119** and **120**.

a) $(\text{COCl})_2$, CH_2Cl_2 , DMF, rt; b) $\text{N}_2\text{NCH}_2\text{CN} \times \text{H}_2\text{SO}_4$, THF, DIPEA, $100\text{ }^\circ\text{C}$; c) **117**, TEA, THF, rt then Δ ; d) **118**, EDC, DIPEA, THF, rt.

Cbz-protected compound **40** was hydrogenated on Pd/C to obtain **106**. The carboxylic group of the P3 fluorophor **118** was activated with EDC and reacted with the P2 building block **106** leading to the 1,2-dimethylhydrazide derivative **121**. Finally, compound **121** was converted into the corresponding azadipeptide nitrile **122** by the reaction with cyanogen bromide.



Scheme 25. Synthesis of the fluorescent labeled azadipeptide nitrile **122**.

a) Pd/C, H_2 , MeOH, rt; b) **118**, EDC, DMAP, THF, rt; c) BrCN, NaOAc, MeOH, rt.

2.1.11. KINETIC CHARACTERISATION OF 119, 120 AND 122

The obtained fluorescent compounds **119**, **120** and **122** were tested on cathepsins L, S, K and B. While the dipeptide nitriles **119** and **120** showed a fast-binding behavior, the aza-analogous counterpart **122** was, as expected, a slow-binding inhibitor. The fluorescent probe **120** with the *N*-(7-diethylamino)-2-oxo-2*H*-chromene-3-carbonyl moiety at the P3 position was a better cathepsin K inhibitor than the corresponding dansyl derivative **119** (Table 14). Furthermore, the replacement of the α -carbon in compound **120** by a nitrogen atom, leading to the azadipeptide nitrile **122**, resulted in an improvement of the inhibitory activity. However, compared with compound **92**, the introduction of the P3 building block **118** into the homocycloleucyl-methylazaalanine nitrile scaffold led to an approximately 50-fold weaker cathepsin K inhibitor **122** (0.35 nM *versus* 19 nM). The fluorescent probe **122** showed a moderate selectivity for cathepsin K over cathepsins L and S (approximately 40-fold), and was only 7-fold selective for cathepsin K over cathepsin B.

Table 14. K_i values of compounds **119**, **120**, and **122** on human cathepsins L, S, K and B.

cmpd	R ¹	R ²	Y	K_i (μ M)			
				cath L	cath S	cath K	cath B
119		H	CH ₂	> 40	6.6 \pm 1	0.88 \pm 0.18	> 40
120		H	CH ₂	> 40	8.4 \pm 1.5	0.23 \pm 0.02	> 40
122		Me	NMe	0.76 \pm 0.08 ^a	0.75 \pm 0.03	0.019 \pm 0.002	0.14 \pm 0.01

^aThe enzymatic reaction was started by addition of chromogenic substrate after the enzyme was preincubated with inhibitor for 30 min. The reaction lines were plotted by linear regression.

The k_{on} values of compound **122** were different reflecting the corresponding K_i values (Table 15). The highest second-order association rate constant of **122** was calculated for cathepsin K.

Table 15. k_{on} values of compound **122** on human cathepsins L, S, K and B.

cmpd	R ¹	R ²	Y	$k_{\text{on}} (\times 10^3 \text{ M}^{-1} \text{ s}^{-1})$			
				cath L	cath S	cath K	cath B
119		H	CH ₂	n.d. ^a	n.d.	n.d.	n.d.
120		H	CH ₂	n.d.	n.d.	n.d.	n.d.
122		Me	NMe	n.d. ^{a,b}	0.49 ± 0.09	9.3 ± 1.7	0.32 ± 0.03

^aNot determined.^bFor [**122**] = 30 μM, a k_{obs} value could not be obtained by non-linear regression. Therefore, a limit $k_{\text{obs}}(1+[S]/K_m)/[I] < 1.0 \times 10^3 \text{ M}^{-1} \text{ s}^{-1}$ was estimated.

In contrast to k_{on} values, the first-order rate constants (k_{off}) of **122** were, as expected, approximately in the same range (Table 16).

Table 16. k_{off} values of compound **122** on human cathepsins L, S, K and B.

cmpd	R ¹	R ²	Y	$k_{\text{off}} (\times 10^{-3} \text{ s}^{-1})$			
				cath L	cath S	cath K	cath B
119		H	CH ₂	n.d. ^a	n.d.	n.d.	n.d.
120		H	CH ₂	n.d.	n.d.	n.d.	n.d.
122		Me	NMe	n.d.	0.37 ± 0.07	0.18 ± 0.04	0.045 ± 0.005

^aNot determined.

2.1.12. SPECTRAL PROPERTIES OF **122**

The absorption and emission spectra of the fluorescence-labeled azadipeptide nitrile **122** were recorded in different solvents to study its spectral properties. The absorption maxima of **122** in dichloromethane, methanol, and water were 422, 424, and 434 nm, respectively. The corresponding emission spectra were 460 nm (dichloromethane), 472 nm (methanol), and 486 nm (water). In general, a slight bathochromic shift of absorption and emission maxima was observed in polar media such as methanol and water. The Stokes shift of **122** in dichloromethane was 38 nm (Fig. 35a). Furthermore, the fluorescence of compound **122** was clearly quenched by methanol and water (Fig. 35b).

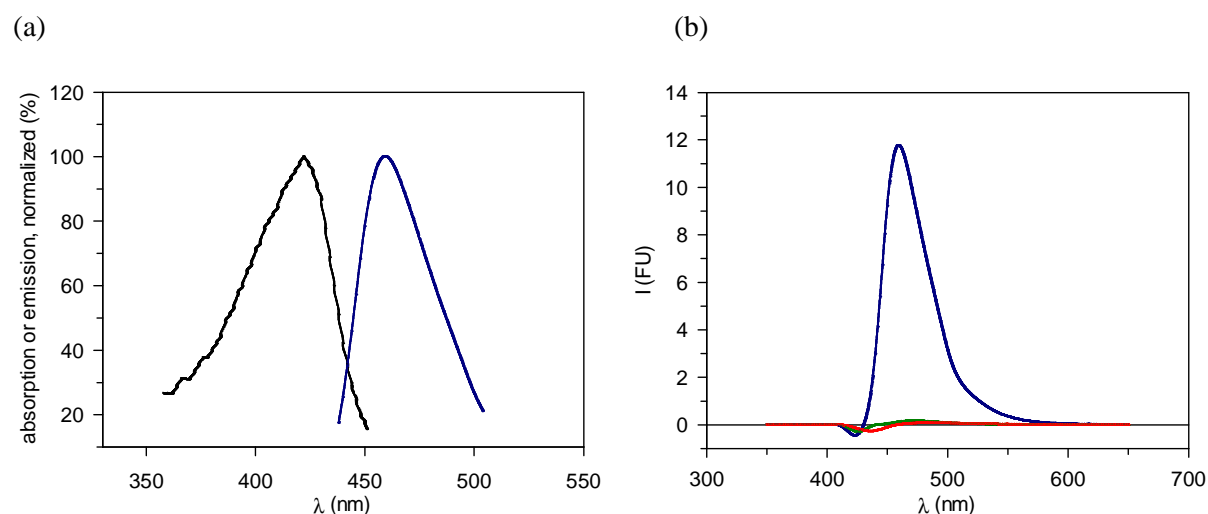


Figure 35. Spectral properties of the azadipeptide nitrile **122** in different solvents. (a) Excitation (•) and emission (•) spectrum of **122** in CH_2Cl_2 ; (b) Emission spectra of **122** in CH_2Cl_2 (•), MeOH (•), and H_2O (•).

Table 17. Absorption and emission maxima of compound **122**.

	CH_2Cl_2	EtOH	H_2O
λ_{ex} (nm)	422	424	434
λ_{em} (nm)	460	472	486

2.1.13. CONCLUSIONS II

In this study, a synthetic route to homocycloleucine-derived azadipeptide nitriles was described for the first time. In contrast to azadipeptide nitriles containing a P2 leucine residue, the synthesis of the corresponding homocycloleucine-based inhibitors was considerably more complicated. Herein, the *gem*-dialkyl effect was discussed as a possible reason for the decreased reactivity of homocycloleucine derivatives for the intramolecular reaction as well as their improved tendency for cyclisation reactions. This effect was particularly strong when 1,2-dimethylhydrazine, a rather weak, but steric demanding nucleophile was used to obtain the desired aza-analogous nitrile inhibitors.

Furthermore, homocycloleucine was confirmed to be a particularly suitable building block for the design of cathepsin K inhibitors. The incorporation of this amino acid into the azadipeptide nitrile scaffold afforded remarkable selectivity and, when combined with the triaryl motif at the P3 position, excellent inhibitory potency. In contrast to the amide-based L-leucine-derived azadipeptide nitriles, the methylation of the P3-P2 amide linker was not necessary to achieve cathepsin K selectivity.

The possible determination of association and dissociation rate constants in the azadipeptide nitrile series enabled us to estimate the influence of a homocycloleucine/L-leucine replacement on these parameters. Whereas k_{off} values were not affected, the L-leucine-containing inhibitors exhibited greater k_{on} values than their homocycloleucine-derived counterparts. Moreover, the second-order association rate constants for cathepsin K were less affected by the homocycloleucine/L-leucine replacement than those for cathepsins L, S and B reflecting the cathepsin K-selectivity of homocycloleucine-derived azadipeptide nitriles.

Moreover, a fluorescence-labeled cathepsin K inhibitor with an azadipeptide scaffold was synthesized, and its kinetic and spectral properties were studied. A coumarin fluorophore was introduced in the homocycloleucine-methylazaalanine-nitrile scaffold, and the fluorescent azadipeptide nitrile **122** was obtained.

Parts of this study are described in a recently published manuscript by Frizler *et al.* [201].

2.2. CATHEPSIN S-SELECTIVE NITRILE INHIBITORS

In previous studies, it was described that the combination of a large group at the P2 position with a small P3 substituent is advantageous for the selective inhibition of cathepsin S (for a review, see [178]). Furthermore, a sulfone within the P2 substituent was proved to be a suitable moiety [165] (Fig. 11). However, it remained unclear, whether cathepsin S can accept larger biaryl and fused aromatic substituents at the P3 position. To clarify this question, it was decided to synthesize a small library of dipeptide nitriles, in which the isobutylsulfone moiety was to be maintained at the P2 position, and various aromatic substituents had to be introduced in the P3 position. It was further envisaged to evaluate the synthesized compounds on cysteine cathepsins L, S, K and B. Moreover, a dipeptide nitrile, exhibiting the best activity/selectivity profiles for cathepsin S, had to be transformed into the corresponding azadipeptide nitrile by C α /N replacement (Fig. 36).

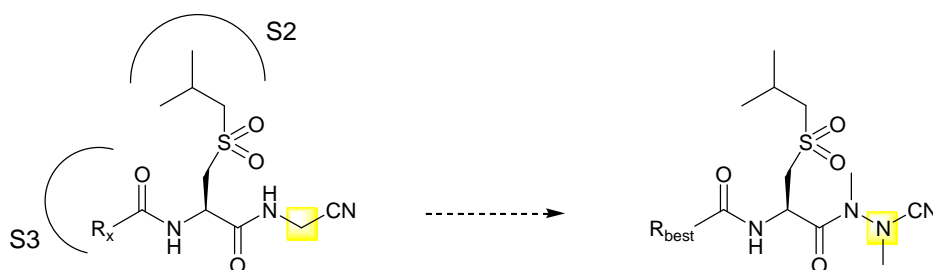
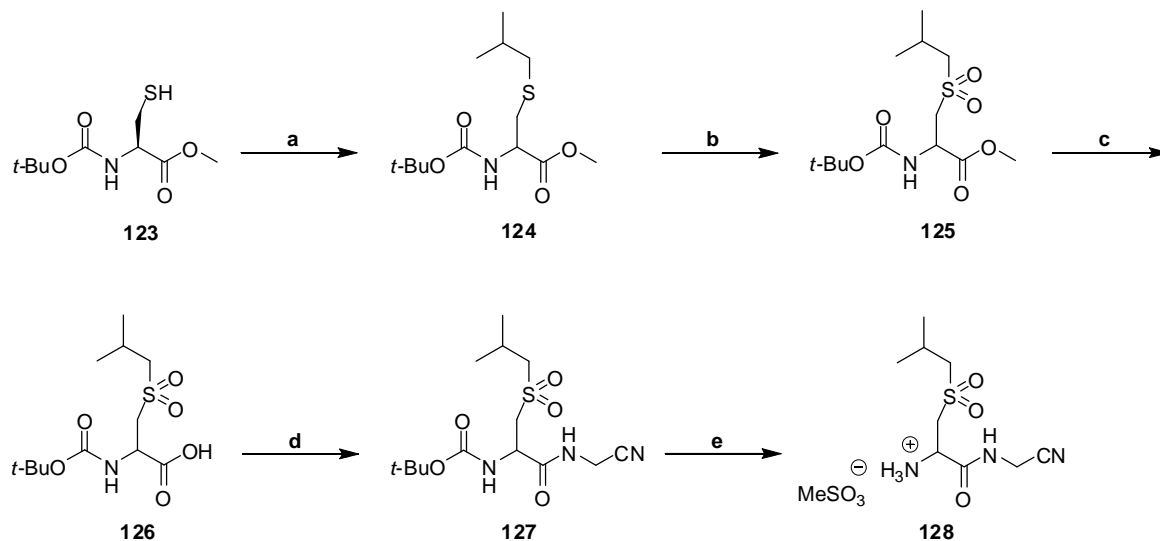


Figure 36. Optimization of the P3 substituent and the transformation into an azadipeptide nitrile.

R_x = various aryl, biaryl and fused aromatic P3 substituents; R_{best} = a P3 substituent, whose introduction into the dipeptide nitrile scaffold improves the activity against cathepsin S and enhances the selectivity for this enzyme over antitargets, cathepsins L, K and B.

To obtain dipeptide nitriles with different P3 substituents, the P2 building block **128** was synthesized as shown in Scheme 26. The thiol group of the commercially available Boc-protected cysteine methyl ester **123** was alkylated with isobutyl bromide in the presence of sodium methanolate to obtain the thioether derivative **124**. The thioether group of **124** was further oxidized with MCPBA leading to the corresponding sulfone **125**. The methyl ester was cleaved under basic conditions, and compound **126** was obtained as a free acid. In the next step, the carboxylic group of **126** was coupled with aminoacetonitrile *via* a mixed anhydride leading to the Boc-protected dipeptide nitrile **127**. Finally, the Boc protecting group of **127** was cleaved with methanesulfonic acid to obtain compound **128** as the

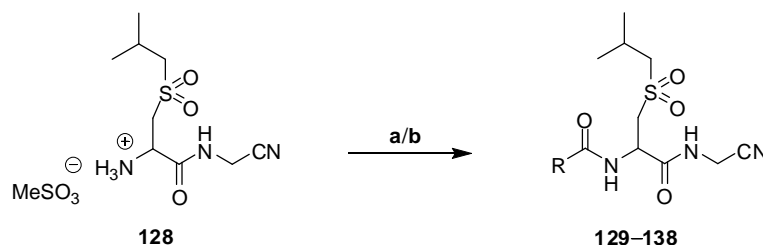
P2 building block. The amino group of **128** was further coupled with various P3 substituents to obtain target dipeptide nitriles **129–138** (Scheme 27). The compounds **129–138** were synthesized by Janina Schmitz in the course of her master thesis under my supervision.



Scheme 26. Synthesis of compound **128** as the P2 building block.

(a) isobutyl bromide, NaOMe, MeOH, Δ ; (b) MCPBA, CH_2Cl_2 , rt; (c) LiOH, THF/ H_2O , rt; (d) 1. TEA, $\text{ClCO}_2i\text{-Bu}$, THF, $-25\text{ }^\circ\text{C}$; 2. $\text{H}_2\text{NCH}_2\text{CN} \times \text{H}_2\text{SO}_4$, THF, rt; (e) MeSO_3H , THF, rt.

Compounds **129** and **130** were obtained by the reaction of the P2 building block **128** in the presence of TEA with benzoyl chloride and thiophene-2-carbonyl chloride, respectively. In contrast, dipeptide nitriles **131–138** were synthesized by the coupling of **128** with the corresponding P3 building blocks using EDC/DMAP protocol (Scheme 27). While the P3 building blocks in compounds **129–134** were commercially available, those of **135–138** were synthesized by Janina Schmitz under my supervision.



Scheme 27 Synthesis of dipeptide nitriles **129–138**.

a) RCOCl , TEA, THF, rt, **129**, R = phenyl, **130**, R = 2-thienyl; b) RCOOH , EDC, DMAP, TEA, THF, rt; **131**, R = 4-(2-thienyl)phenyl; **132**, R = 5-(2-thienyl)-2-thienyl; **133**, R = benzo[*b*]thiophen-2-yl; **134**, thieno[2,3-*b*]thiophen-2-yl; **135**, R = 5-(phenyl)-2-thienyl; **136**, R = 4-(phenyl)-2-thienyl, **137**, R = 5-(3-thienyl)-2-thienyl, **138**, R = 5-(1*H*-tetrazole-5-yl)-2-thienyl.

Although Perrey *et al.* [206] described the alkylation of the *N*-acyl-cysteine in the presence of sodium methanolate without racemisation, dipeptide nitriles **129–138** were obtained in a racemic form, as it was exemplary shown for compound **129** using chiral HPLC (Fig. 37).

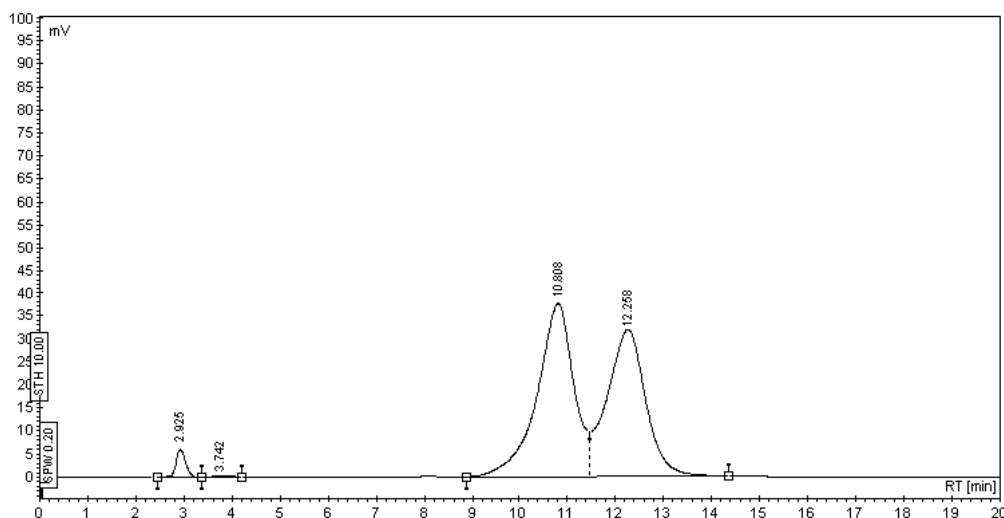


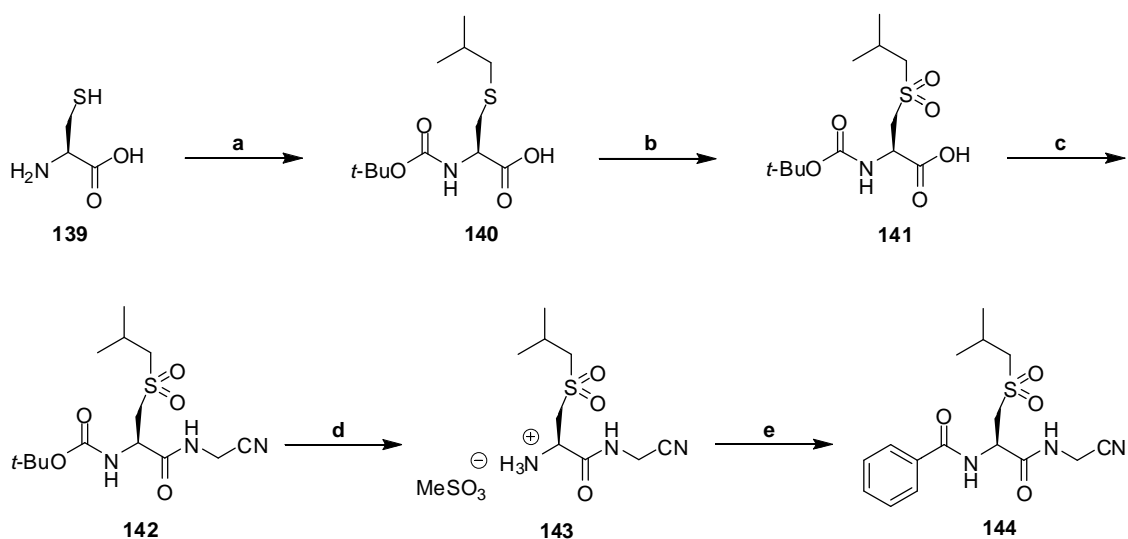
Figure 37. The chiral chromatogram of compound **129**.

Column: LiChroCART[®] 250-4 ChiraDex[®] (5 μ m); *Conditions:* 95% H₂O/5% MeOH, run time – 20 min, flow – 1 mL/min, UV detector – 214 nm, temperature – 30 °C; *Enantiomeric ratio* = 53:47.

Generally, the presented synthetic route to the P2 building block **128** (Scheme 26) contains two steps with a high risk for racemisation: (1) alkylation of the thiol group of the cysteine derivative **123** in the presence of sodium methanolate, and (2) the cleavage of the methyl ester of **125** with lithium hydroxide.

To prevent the racemisation, a changed synthetic route was applied (Scheme 28) [207]. In this route, the thiol group of L-cysteine **139** was alkylated in the presence of a weaker base, sodium hydroxide, followed by the protection of the amino group using (Boc)₂O to obtain compound **140**. To avoid the complicated purification, the thioether derivative **140** was oxidized with KMnO₄ instead of MCPBA (Scheme 26) leading to the corresponding sulfone **141** in high yield and purity. The sulfone derivative **141** was further coupled with aminoacetonitrile *via* a mixed anhydride to form the Boc-protected dipeptide nitrile **142**. Finally, the Boc protecting group of **142** was cleaved with methanesulfonic acid, and the P2 building block **143** was obtained. Because the racemic benzoyl derivative **129** (Scheme 27) showed the best potency and selectivity profiles for cathepsin S, it was decided to introduce the benzoyl substituent into the synthesized P2 building block **143** to obtain the dipeptide nitrile **144** predominantly as R-enantiomer. The enantiopurity of **144** was shown by chiral HPLC on LiChroCART[®] 250-4 ChiraDex[®] (5 μ m) column using the isocratic elution with

H₂O/MeOH (95:5) and a flow of 1 mL/min (Fig. 38). A 1 mM solution of compound **144** in MeCN was injected into the HPLC. The resulting chromatogram showed only one peak (10.7 min) indicating the full enantiomeric purity of **144**.



Scheme 28. Synthesis of compound **144** without racemisation.

(a) 1. isobutyl bromide, NaOH, EtOH, rt; 2. (Boc)₂O, NaOH, EtOH, rt; (b) KMnO₄, AcOH, H₂O, rt; (c) 1. TEA, ClCO₂*i*-Bu, THF, -25 °C; 2. H₂NCH₂CN × H₂SO₄, THF, rt; (d) MeSO₃H, THF, rt; (e) benzoyl chloride, DIPEA, THF, rt.

The peak of the enantiopure compound **144** at 10.7 min (Fig. 38) corresponds to the first peak of the racemic dipeptide nitrile **129** (10.8 min, Fig. 37) under used chromatographic conditions and represents the R-enantiomers in both chiral chromatograms.

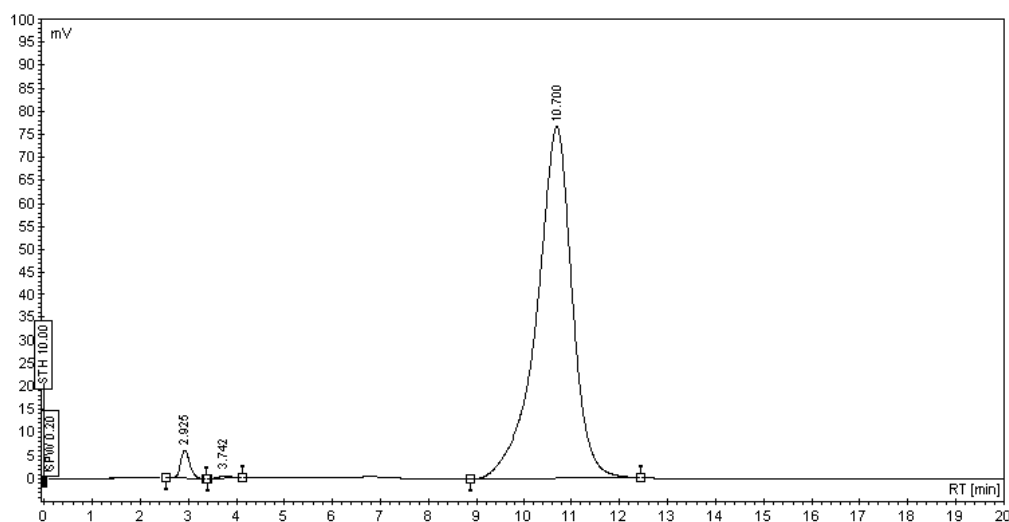


Figure 38. The chiral chromatogram of compound **144**.

Column: LiChroCART[®] 250-4 ChiraDex[®] (5 μm); Conditions: 95% H₂O/5% MeOH, run time – 20 min, flow – 1 mL/min, UV detector – 214 nm, temperature – 30 °C; Enantiomeric ratio = 100.

In a further experiment (Fig. 39), the 1 mM solutions of **129** and **144** in MeCN were mixed (1:1), and the resulting mixture was injected into the HPLC. Compared with the chiral chromatogram of **129** (Fig. 37), a 25% increase of the AUC was observed for the R-enantiomer peak (10.7 min). The corresponding peak of the S-enantiomer (12.2 min) decreases for the same amount of 25%.

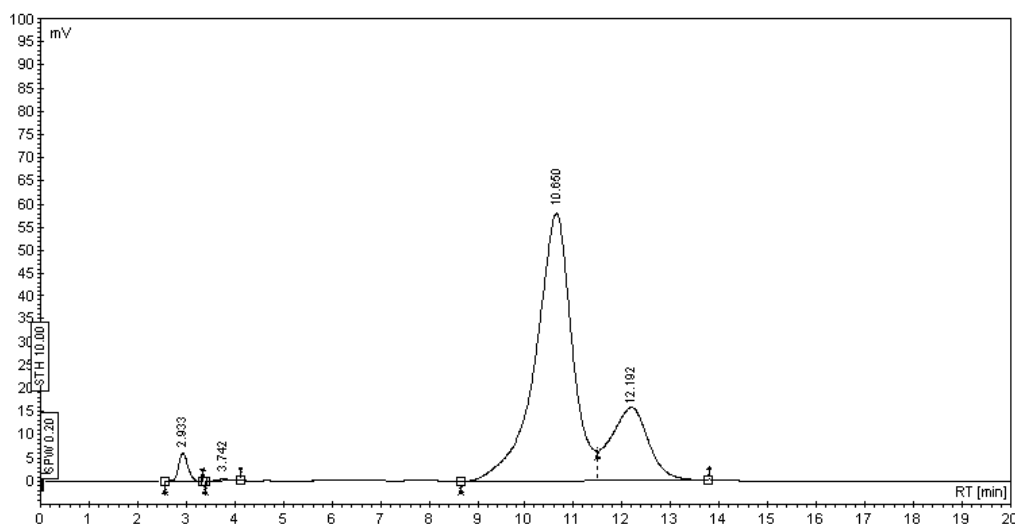
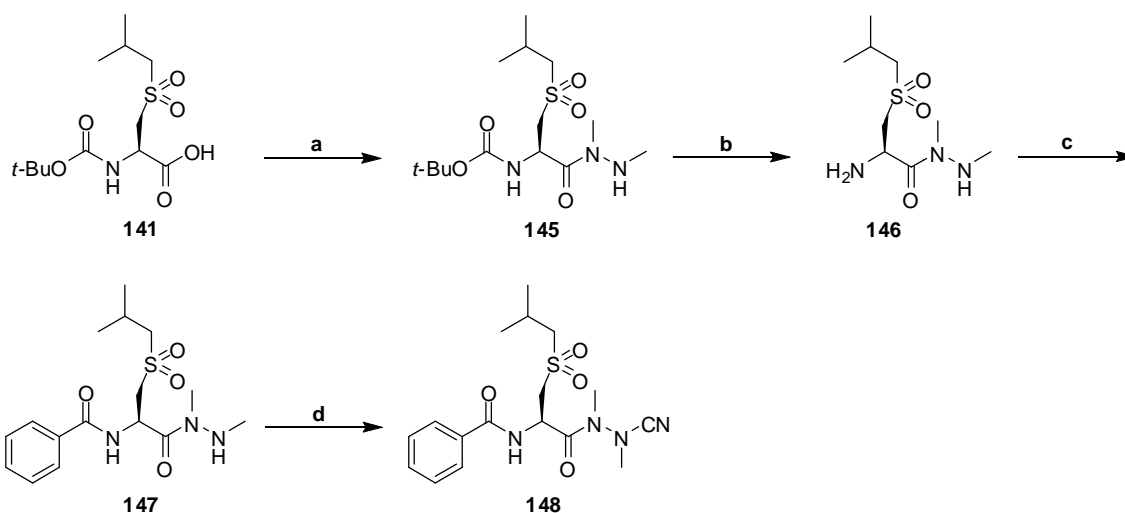


Figure 39. The chiral chromatogram of a 1:1 mixture of compounds **129** and **144**.

Column: LiChroCART[®] 250-4 ChiraDex[®] (5 μ m); *Conditions:* 95% H₂O/5% MeOH, run time – 20 min, flow – 1 mL/min, UV detector – 214 nm, temperature – 30 °C; *Enantiomeric ratio* = 78:22.

To synthesize the azadipeptide nitrile **148** (Scheme 29), compound **141** was converted in the 1,2-dimethylhydrazide **145** which was further deprotected to obtain **146**. Compound **146** was reacted with benzoyl chloride and cyanogen bromide leading to the azadipeptide nitrile **148**.



Scheme 29. Synthesis of azadipeptide nitrile **148**.

(a) 1. NMM, ClCO₂*i*-Bu, THF, -25 °C; 2. (NHMe)₂ × 2HCl, NaOH, H₂O, to rt; (b) AcCl, EtOH, MeCO₂Et, rt, basic extraction; (c) benzoyl chloride, DIPEA, THF, rt; (d) BrCN, NaOAc, MeOH, rt.

2.2.1. KINETIC CHARACTERISATION OF 129–138 AND 144, 148

The racemic dipeptide nitriles **129–138** and the enantiopure benzoyl derivative **144** as well as the azadipeptide nitrile **148** were tested on human cathepsins L, S, K and B (Table 18 and 19). The kinetic investigations of compounds **129–138** were partially carried out by Janina Schmitz in her master thesis under my supervision.

Table 18. K_i values of target compounds **129–138**.

cmpd	R	K_i (μM) ^a			
		cath L	cath S	cath K	cath B
129		> 40 ^b	0.040 ± 0.004	> 40	40 ± 2
130		> 40	0.045 ± 0.002	> 40	24 ± 2
131		> 4 ^c	0.20 ± 0.01	> 4	3.9 ± 0.7
132		> 4	0.094 ± 0.010	1.1 ± 0.1	3.4 ± 0.1
133		> 4	0.089 ± 0.012	> 4	6.8 ± 0.1
134		> 4	0.10 ± 0.01	> 4	7.2 ± 0.2
135		> 4	0.061 ± 0.005	> 4	5.1 ± 0.2
136		> 4	0.060 ± 0.008	> 4	6.4 ± 0.1
137		> 4	0.061 ± 0.005	> 4	5.4 ± 0.2
138		> 40	0.076 ± 0.009	> 4	34 ± 2

^aData were calculated from duplicate experiments by using at least five different inhibitor concentrations.

^bFor cathepsins L and K, all limits > 40 μM relate to IC_{50} values > 45 μM .

^cFor cathepsins L and K, all limits > 4 μM relate to IC_{50} values > 5 μM .

In general, the racemic dipeptide nitriles **129–138** showed all fast-binding kinetic behavior and remarkable inhibitory activities toward cathepsin S (40–200 nM). Among them, compounds **129** and **130**, containing short aromatic P3 substituents (phenyl and 2-thienyl, respectively), were the most potent cathepsin S inhibitors. The K_i value of the benzoyl substituted dipeptide nitrile **129** on cathepsin S was 40 nM, the corresponding 2-thienyl counterpart exhibited a K_i value of 45 nM. The inhibitory activities of the biaryl derivatives **132** and **135–138** were approximately in the same range ($K_i = 60–94$ nM). However, the K_i value of the 4-(phenyl)-2-thienyl substituted dipeptide nitrile **131** was slightly higher than the K_i values of the biaryl counterparts **132** and **135–138**. The fused benzo[*b*]thiophene-2-yl (**133**) and thieno[2,3-*b*]thiophene-2-yl (**134**) derivatives showed inhibitory activities toward cathepsin S with K_i values of 89 and 100 nM, respectively.

Furthermore, compounds **129** and **130** exhibited an excellent selectivity for cathepsin S over the antitargets, cathepsins L, K and B. The introduction of larger biaryl or fused aromatic P3 substituents impaired the selectivity of the resulting dipeptide nitriles **131–137**. The selectivity of the 5-(1*H*-tetrazole-5-yl)-2-thienyl substituted derivative **138** for cathepsin S over cathepsins L and B was comparable with the selectivities of **129** and **130**.

Table 19.^a Kinetic parameters of compounds **144**^b and **148**^c.

cmpd	cathepsin L			cathepsin S		
	k_{on} ($10^3\text{M}^{-1}\text{s}^{-1}$)	k_{off} (10^{-3}s^{-1})	K_i (nM)	k_{on} ($10^3\text{M}^{-1}\text{s}^{-1}$)	k_{off} (10^{-3}s^{-1})	K_i (nM)
144	n.d. ^d	n.d.	37000 ± 1000	n.d.	n.d.	33 ± 5
148	n.d. ^{d,e}	n.d.	15 ± 1^f	2600 ± 400	1.4 ± 0.2	0.55 ± 0.03^g

cmpd	cathepsin K			cathepsin B		
	k_{on} ($10^3\text{M}^{-1}\text{s}^{-1}$)	k_{off} (10^{-3}s^{-1})	K_i (nM)	k_{on} ($10^3\text{M}^{-1}\text{s}^{-1}$)	k_{off} (10^{-3}s^{-1})	K_i (nM)
144	n.d.	n.d.	$> 40000^h$	n.d.	n.d.	24000 ± 1000
148	59 ± 2	0.039 ± 0.004	0.66 ± 0.06	130 ± 20	0.75 ± 0.12	5.8 ± 0.2^g

^aData were calculated from duplicate experiments by using at least five different inhibitor concentrations. ^bLinear regression over 20 min. ^cNon-linear regression over 80 min. ^dNot determined. ^eFor [**148**] = 700 nM, a k_{obs} value could not be obtained by non-linear regression. Therefore, a limit $k_{\text{obs}}(1+[S]/K_m)/[I] < 30 \times 10^3 \text{M}^{-1}\text{s}^{-1}$ was estimated. ^fThe progress curves were analyzed by linear regression in a time interval between 8 and 16 min. ^gThe progress curves were analyzed by non-linear regression in a time interval of 20 min. ^hThe limit $> 40 \mu\text{M}$ relates to the IC_{50} value $> 45 \mu\text{M}$.

The enantiopure dipeptide nitrile **144** showed approximately the same selectivity profile as the corresponding racemic compound **129**. Hence, it was slightly more potent on cathepsin S (33 *versus* 44 nM). The azadipeptide nitrile **148** was 60-fold more active on cathepsin S than its carba counterpart **144** (0.55 *versus* 33 nM), but less selective for cathepsin S over antitargets, cathepsins L, K and B.

While compound **144** was a fast-binding inhibitor, azadipeptide nitrile **148** showed a slow-binding inhibition behavior. Therefore, it was possible to determine k_{on} and k_{off} values for the azadipeptide nitrile **148** and cathepsins S, K and B. For cathepsin L, a limit $k_{\text{obs}}(1+[S]/K_m)/[I] < 30 \times 10^3 \text{ M}^{-1}\text{s}^{-1}$ was estimated. The highest second-order rate constant (k_{on}) was obtained for compound **148** and cathepsin S.

2.2.2. CONCLUSIONS III

The aim of the study was the exploration of the S3 binding pocket of cathepsin S and the development of selective nitrile inhibitors for this enzyme. A series of dipeptide nitriles was synthesized, in which a large isobutylsulfone moiety was maintained at the P2 position, and a systematic scan for P3 substituents was performed.

For the preparation of inhibitors, a convergent synthetic route was applied in which the P2 building block was separately prepared. Small aromatic, biaryl and annulated aromatic P3 substituents were introduced, and the kinetic properties of the obtained racemic dipeptide nitriles were studied on human cathepsins L, S, K and B. Besides the activity of all tested compounds against cathepsin S, dipeptide nitriles with small aromatic substituents (such as phenyl or 2-thienyl) at the P3 position showed a remarkable selectivity for cathepsin S over cathepsins L, K and B.

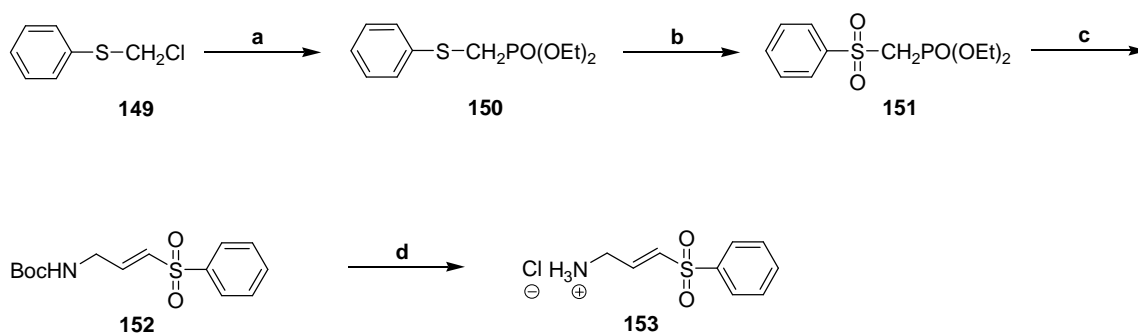
Furthermore, the synthetic route to the P2 building block was changed to prevent the racemisation, and the enantiopure benzoyl substituted dipeptide nitrile **144** was obtained as potent and selective cathepsin S inhibitor. The enantiopurity of **144** was shown by chiral HPLC. The aza-analogous counterpart of **144**, compound **148**, was 60-fold more active on cathepsin S, but less selective for this enzyme over cathepsins L, K and B.

To summarize, the S3 binding pocket of cathepsin S can be addressed with small aromatic as well as with larger biaryl and fused aromatic P3 substituents without significant activity lost of the corresponding inhibitors. However, the introduction of larger biaryl or fused aromatic substituents into the P3 position negatively affected the selectivity of the obtained dipeptide nitriles for cathepsin S. Therefore, the best selectivity profiles were observed for compounds with small aromatic P3 moieties. The enantiopure benzoyl substituted dipeptide nitrile was slightly more active on cathepsin S than its racemic counterpart. The C α /N replacement resulted in a clearly more potent, but less selective cathepsin S inhibitor.

2.3. DEVELOPMENT OF ‘ACTIVITY-BASED’ PROBES

The knowledge of the cellular and/or plasma activities of cathepsins K and S may be important for the diagnostic of enhanced bone turnover and immune response and could be used for monitoring of the therapeutic success during the treatment of osteoporosis and autoimmune disorders [136], [137], [208], [209]. Furthermore, several cysteine cathepsins, particularly cathepsins L and B, are involved in the tumor pathogenesis and represent possible prognostic marker [210], [211]. In the presented study, it was decided to develop an irreversible, fluorescent ‘activity-based’ probe (ABP) for imaging and quantification particularly of cathepsins K and S, but also cathepsins L and B, by *in gel* scanning using SDS-PAGE technique. Furthermore, in collaboration with Dr. Reik Löser from the Institute of Radiopharmacy, Helmholtz-Zentrum Dresden-Rossendorf, the tyrosine-derived nitrile inhibitors of cysteine cathepsins were to be fluoroalkylated to prepare ‘cold’ reference compounds of fluorine-18 radiolabeled ‘activity-based’ probes whose kinetic properties had to be studied on cathepsins L, S, K and B.

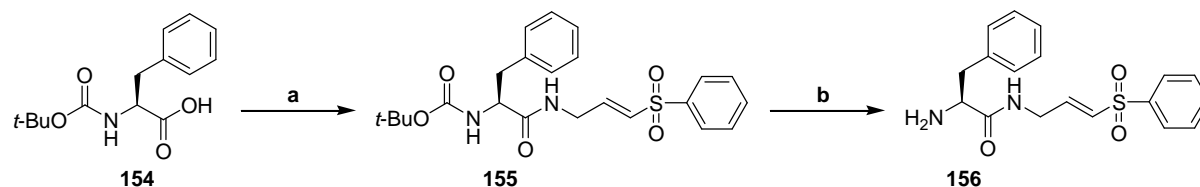
A convergent synthetic route was chosen for the preparation of the fluorescent ‘activity-based’ probe. First, the vinyl sulfone ‘warhead’ **153** was synthesized as shown in Scheme 30 [212]. Commercially available chloromethyl phenyl sulfide **149** was transformed to the alkyl phosphonate **150** via Arbuzov reaction by heating with triethyl phosphite at 130 °C in a sealed tube. The thioether group of **150** was oxidized with KMnO_4 to obtain the sulfone **151**. For preparation of the (*E*)-vinyl sulfone group, Horner-Wadsworth-Emmons reaction was used. In this reaction, compound **151** was coupled with Boc-Gly-H in the presence of NaH to obtain **152**. Finally, the Boc protecting group was removed leading to the vinyl sulfone **153**.



Scheme 30. Synthesis of the vinyl sulfone **153** as an irreversible, covalent ‘warhead’.

(a) 1. $\text{P}(\text{OEt})_3$, 130 °C, sealed tube; (b) KMnO_4 , AcOH, H_2O , rt; (c) Boc-Gly-H, NaH, THF, rt; (d) AcCl, EtOH, AcOEt, rt.

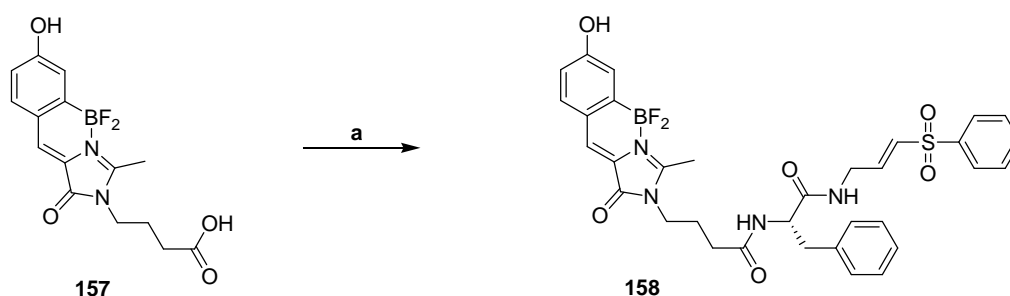
With compound **153** in hands, the building block **156** was synthesized as shown in Scheme 31. Boc-protected phenylalanine **154** was coupled *via* a mixed anhydride with **153** to obtain the vinyl sulfone derivative **155**. The Boc protecting group of **155** was cleaved under acidic conditions leading to the building block **156**.



Scheme 31. Synthesis of the building block **156**.

(a) 1. $\text{ClCO}_2i\text{-Bu}$, NMM, THF, $-25\text{ }^\circ\text{C}$, 2. **153**, NaOH, H_2O , $-25\text{ }^\circ\text{C}$ to rt; (b) AcCl, EtOH, AcCO_2Et , rt, basic extraction.

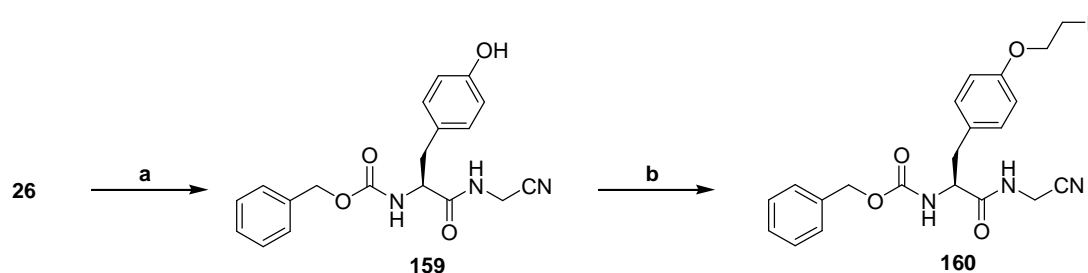
The pH-dependent GFP-like [213], [214] fluorophore **157** was provided by Ilia V. Yampolsky from the Institute of Bioorganic Chemistry, Russian Academy of Sciences, Moscow. It was coupled with the building block **156** *via* a mixed anhydride to obtain the desired ‘activity-based’ probe **168** as shown in Scheme 32.



Scheme 32. Synthesis of the activity-based probe **158**.

(a) 1. $\text{ClCO}_2i\text{-Bu}$, NMM, THF, $-25\text{ }^\circ\text{C}$, 2. **156**, $-25\text{ }^\circ\text{C}$ to rt.

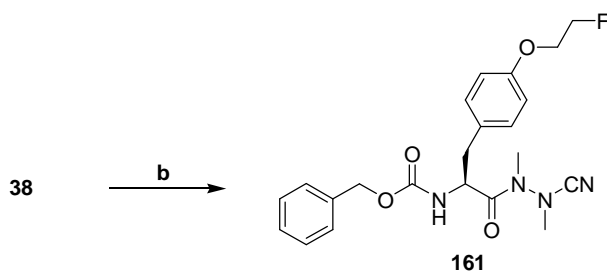
The fluoroethylated azadipeptide nitrile **159** was synthesized as depicted in Scheme 33.



Scheme 33. Synthesis of the fluorine-containing dipeptide nitrile **160**.

(a) 1. $\text{ClCO}_2i\text{-Bu}$, NMM, THF, $-25\text{ }^\circ\text{C}$, 2. $\text{NH}_2\text{CH}_2\text{CN} \times \text{H}_2\text{SO}_4$, NaOH, H_2O , $-25\text{ }^\circ\text{C}$ to rt; (b) NaH, 1-bromo-2-fluoroethane, DMF, rt

Cbz-protected tyrosine **26** was reacted *via* a mixed anhydride with aminoacetonitrile to obtain the dipeptide nitrile **159**. The hydroxyl group of **159** was alkylated with 1-bromo-1-fluoroethane in the presence of sodium hydride leading to compound **160**. Additionally, the azadipeptide nitrile **38** was fluoroethylated using the same synthetic procedure to obtain the azadipeptide derivative **161** (Scheme 33).



Scheme 33. Synthesis of the fluorine-containing dipeptide nitrile **161**.

(a) NaH, 1-bromo-2-fluoroethane, DMF, rt.

2.3.1. KINETIC CHARACTERISATION OF 158 AND 160, 161

The fluorescent ‘activity-based’ probe **158** was tested on human cathepsins L, S, K and B and showed the time-dependent inhibition behavior. In contrast to azadipeptide nitriles, vinyl/allyl sulfones/ketones were described as irreversible, covalent inhibitors of cysteine cathepsins [212], [215], [216]. To determine first-order rate constants (k_{obs}) for the irreversible time-dependent inhibition of cathepsins by **158**, the progress curves were analyzed by non-linear regression using the equation shown in Figure 41a [216], [217], which is derived from the slow-binding equation (Fig. 23a) for the case, if v_s tends to zero. Furthermore, the plots of the calculated k_{obs} values *versus* increasing concentrations of **158** showed to be hyperbolic (Fig. 40b) suggesting the enzyme-inhibitor interaction according to the mechanism B (Fig. 25b). Therefore, k_{inac} and K_i' constants could be obtained by non-linear regression of the data pairs (k_{obs} , [I]) using the equation in Figure 41b. The true inhibition constants (K_i) were calculated as described before (Cheng-Prusoff equation, Fig. 23c). The second order rate constants ($k_{2\text{nd}}$) were calculated as quotient of k_{inac} divided by K_i (Fig. 41c). Compounds **160** and **161** were kinetically characterized as described in 2.1.2.

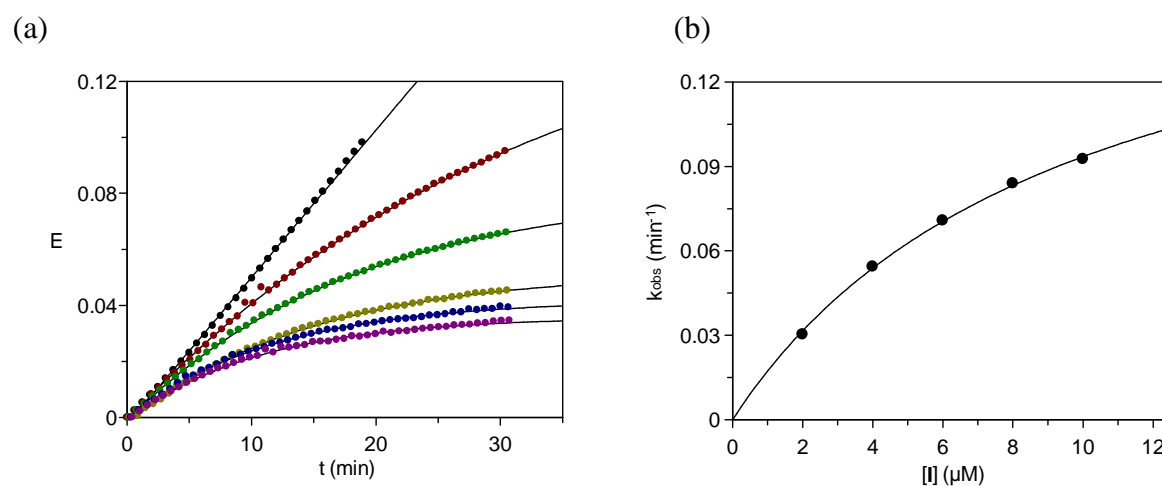


Figure 40. (a) Monitoring of the human cathepsin L-catalyzed hydrolysis of Z-Phe-Arg-pNa (100 μM) in the presence of increasing concentrations of **158** (•, 0 μM; •, 2 μM; •, 4 μM; •, 6 μM; •, 8 μM; •, 10 μM) in duplicate experiments. The reaction (100 mM sodium phosphate buffer pH 6.0, 100 mM NaCl, 5 mM EDTA, 0.01% Brij 35, 100 μM DTT, 2% DMSO, 37 °C) was initiated by addition of the enzyme. The formation of 4-nitroaniline was detected at 405 nm. (b) Plot of the k_{obs} values *versus* [I]. Non-linear regression of the resulting data pairs (k_{obs} , [I]) using equation $k_{\text{obs}} = k_{\text{inac}}[\text{I}]/(K_i' + [\text{I}])$ gave an apparent inhibition constant $K_i' = (1 + [\text{S}]/K_m)K_i = 9.6 \pm 0.7 \mu\text{M}$. The corresponding k_{inac} value was calculated to $0.18 \pm 0.01 \text{ min}^{-1}$.

$$(a) \quad E/I = A \times (1 - e^{-k_{\text{obs}} t}) + d \quad (b) \quad k_{\text{obs}} = k_{\text{inac}} [I] / (K_i' + [I])$$

$$(c) \quad k_{2\text{nd}} = k_{\text{inac}} / K_i$$

Figure 41. Slow-binding equation for irreversible inhibition type (a), equation for calculation of k_{inac} and K_i' values (b), and the second-order rate constant equation (c).

(a) E – extinction; I – fluorescence intensity; $A = v_i/k_{\text{obs}}$ where v_i – initial reaction rate (M s^{-1}); k_{obs} – first-order rate constant (s^{-1}); t – time (s); d – offset; (b) k_{obs} – first-order rate constant (s^{-1}); $k_{\text{inac}} = k_{+4}$ – first-order inactivation rate constant (s^{-1}); $K_i' = k_{-3}/k_{+3}(1 + [S]/K_m)$ – apparent inhibition constant (M); $[I]$ – inhibitor concentration (M); (c) K_i – true inhibition constant (M); $k_{2\text{nd}}$ – second-order rate constant ($\text{M}^{-1}\text{s}^{-1}$).

The calculated kinetic parameters are depicted in Table 20. In general, the APBs **158** was active against all tested cathepsins, but it showed a slight preference for cathepsin S ($k_{2\text{nd}} = 18000 \text{ M}^{-1}\text{s}^{-1}$) and for cathepsin K ($k_{2\text{nd}} = 4600 \text{ M}^{-1}\text{s}^{-1}$). The K_i values, describing the dissoziation of the non-covalent enzyme-inhibitor complex in the case of the irreversible, covalent inhibition type, were particularly low for cathepsins S ($0.11 \mu\text{M}$) and K ($0.24 \mu\text{M}$). The first-order inactivation rate constants were approximately in the same range for the four tested cathepsins (0.0011 – 0.0031 s^{-1}).

Table 20. Kinetic parameters of compound **158**.^a

cmpd	cathepsin L			cathepsin S		
	$k_{2\text{nd}} (\text{M}^{-1}\text{s}^{-1})$	$k_{\text{inac}} (\text{s}^{-1})$	$K_i (\mu\text{M})$	$k_{2\text{nd}} (\text{M}^{-1}\text{s}^{-1})$	$k_{\text{inac}} (\text{s}^{-1})$	$K_i (\mu\text{M})$
158	2200 ± 180	0.0031 ± 0.0001	1.4 ± 0.7	18000 ± 2000	0.0020 ± 0.0001	0.11 ± 0.01

cmpd	cathepsin K			cathepsin B		
	$k_{2\text{nd}} (\text{M}^{-1}\text{s}^{-1})$	$k_{\text{inac}} (\text{s}^{-1})$	$K_i (\mu\text{M})$	$k_{2\text{nd}} (\text{M}^{-1}\text{s}^{-1})$	$k_{\text{inac}} (\text{s}^{-1})$	$K_i (\mu\text{M})$
158	4600 ± 900	0.0011 ± 0.0001	0.24 ± 0.04	290 ± 70	0.0029 ± 0.0003	10 ± 2

^aThe progress curves were analyzed by non-linear regression in a time interval of 30 min.

The fluoroethylated dipeptide nitrile **160** (Table 21), a fast-binding inhibitor, showed only moderate inhibitory activity on cathepsins L, S and K ($K_i = 390, 1200, \text{ and } 2100 \text{ nM}$, respectively). The K_i value of **160** on the carboxydipeptidase, cathepsin B, was $23 \mu\text{M}$. In

contrast to **160**, the corresponding azadipeptide nitrile **161** exhibited a very strong inhibitory activity toward cathepsins L, S, K and B with K_i values in picomolar range (excepted cathepsin B). In general, the calculated second-order rate constants (k_{on}) reflected the low K_i values of **161** on tested cathepsins. The k_{off} values were, as expected, in the same range.

Table 21. Kinetic parameters of compound **160**^a and **161**^b.

cmpd	cathepsin L			cathepsin S		
	k_{on} ($10^3 M^{-1} s^{-1}$)	k_{off} ($10^{-3} s^{-1}$)	K_i (nM)	k_{on} ($10^3 M^{-1} s^{-1}$)	k_{off} ($10^{-3} s^{-1}$)	K_i (nM)
160	n.d. ^c	n.d.	390 ± 30	n.d.	n.d.	1200 ± 80
161	930 ± 100^d	0.68 ± 0.09	0.73 ± 0.06	560 ± 100^d	0.44 ± 0.09	0.79 ± 0.06^b

cmpd	cathepsin K			cathepsin B		
	k_{on} ($10^3 M^{-1} s^{-1}$)	k_{off} ($10^{-3} s^{-1}$)	K_i (nM)	k_{on} ($10^3 M^{-1} s^{-1}$)	k_{off} ($10^{-3} s^{-1}$)	K_i (nM)
160	n.d.	n.d.	2100 ± 200	n.d.	n.d.	23000 ± 3000
161	210 ± 50	0.036 ± 0.009	0.17 ± 0.01	190 ± 10	0.46 ± 0.03	2.4 ± 0.1

^aLinear regression over 20 min. ^bNon-linear regression over 80 min. ^cNot determined. ^dNon-linear regression over 20 min.

2.3.2. SPECTRAL PROPERTIES OF 158 AND IMAGING EXPERIMENT

The absorption and emission spectra of the fluorescent ‘activity-based’ probe **158** were recorded in different solvents to study the spectral properties of this fluorescent compound. The absorption maxima of **158** were approximately in the same range in methanol, water and different aqueous buffer systems, but a slight bathochromic shift was observed in the apolar dichloromethane medium. In contrast to the emission spectra of **158** in the organic solvents such as methanol and dichloromethane, the corresponding emission spectra in water and aqueous buffer systems showed two emission maxima (Fig. 42, Table 22).

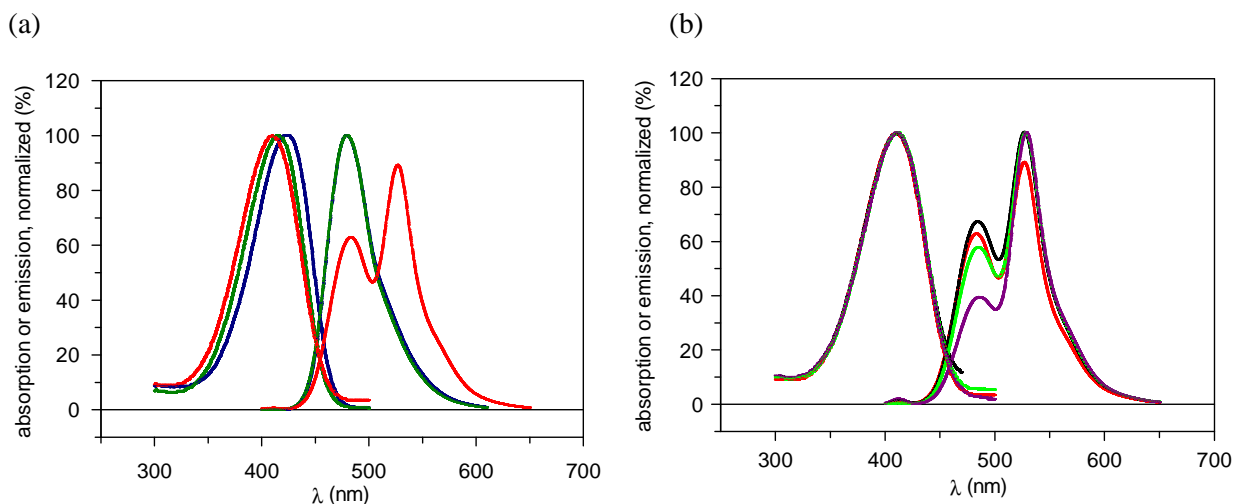


Figure 42. Spectral properties of **158** in different solvents.

(a) Normalized absorption and emission spectra of compound **158** in different solvents. The compound **158** was used in a concentration of 10 μM . (•) CH₂Cl₂; (•) EtOH; (•) H₂O. (b) Normalized absorption and emission spectra of compound **158** at different pH. (•) H₂O; (•) 50 mM sodium phosphate buffer pH 6.5; (•) 100 mM sodium phosphate buffer pH 6.0; (•) 50 mM sodium acetate buffer pH 5.0.

Table 22. Absorption and emission maxima of compound **158**.

	CH ₂ Cl ₂	EtOH	H ₂ O	buffer pH 6.5 ^a	buffer pH 6.0	buffer pH 5.0
λ_{ex} (nm)	423	415	410	411	411	410
λ_{em} (nm)	480	480	486/528	484/526	484/528	486/528

^aFor exact buffer composition, see the ‘Experimental Section’.

To prove the concept, compound **158** was incubated with activated cathepsin K. The final concentrations in the incubation medium were 10 μM **158** and 9.2 $\mu\text{g/mL}$ cathepsin K (for details, see the ‘Experimental Section’). The different volumes of the incubation medium as well as two control samples were separated by SDS-PAGE, and the resulting protein bands were analyzed using fluorescence imaging and Coomassie staining (Fig. 43).

The fluorescence analysis showed fluorescent bands of the labeled cathepsin K in the lines III–VI. The fluorescence intensity was dependent on the loaded amounts of the labeled protein and decreased from III to VI. In control experiments (lines I and II) no fluorescence was measured. The fluorescence was excited at 312 nm and imaged with a super sensitive ‘scientific grade’ CCD-camera (equipped with an ethidium bromide filter) from Intas. Although the excitation was not performed in the absorption maximum of **158**, it was possible to detect 23 ng of the labeled cathepsin K (VI, Fig 43a). Probably, it will be feasible to image smaller amounts of cysteine cathepsins, if a transilluminator with an excitation wavelength of ~ 400 nm will be used.

For comparative investigations, the same SDS-PAGE was stained with Coomassie brilliant blue. The cathepsin K bands were detected in the lines II–V, but, as expected, not in the control line I. Due to the small amount of cathepsin K, no stained band could be observed in the line VI (Fig. 43b).

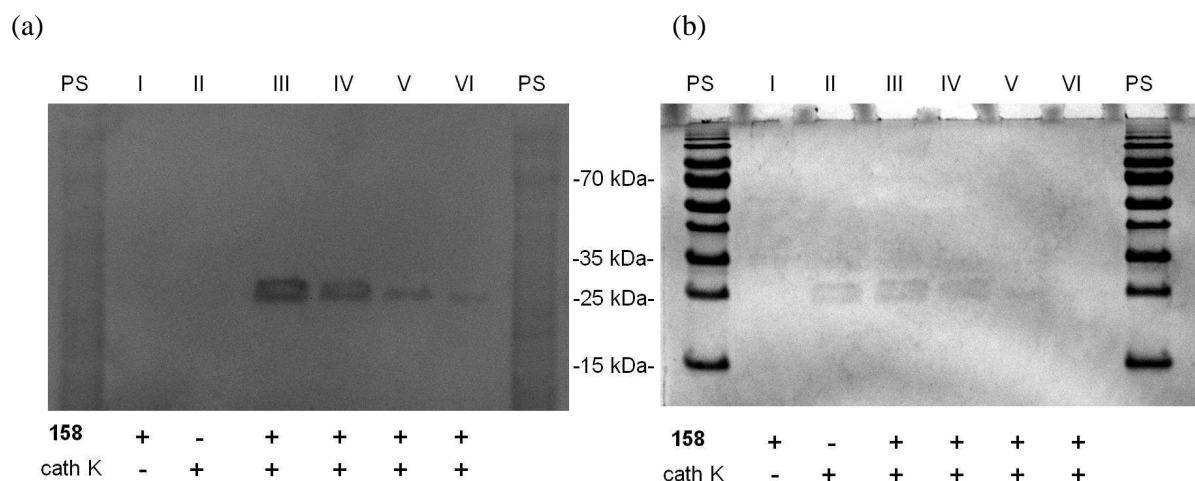


Figure 43. SDS-PAGE images. (a) Fluorescence analysis of the with compound **158** labeled cathepsin K ($\lambda_{\text{ex}} = 312$ nm, ethidium bromide filter, invert image: white to black); (b) Analysis of cathepsin K bands using Coomassie staining. (I) 130 ng of **158**; (II) 184 ng cathepsin K; (III) 184 ng labeled cathepsin K; (IV) 92 ng labelled cathepsin K; (V) 46 ng labelled cathepsin K; (VI) 23 ng labelled cathepsin K; PS – protein standard. The unbound amounts of **158** are not shown.

2.3.3. CONCLUSIONS IV

In the presented study, the fluorescent ‘activity-based’ probe **158**, containing a new GFP-like reporter, was synthesized, and its spectral and kinetic properties were studied.

The vinyl sulfone derivative **158** exhibited the time-dependent irreversible kinetic type on cathepsins L, S, K and B according to the two step mechanism of inhibition. In the main, the irreversible, covalent inhibitor **158** was active on all tested cathepsins, but it showed a slight preference for cathepsins S and K.

The absorption maxima of **158** were approximately in the same VIS range in organic solvents and aqueous media. Only a slight bathochromic shift was observed in dichloromethane. In contrast, the emission spectra of **158** were different depending on the solvent, and showed in water and aqueous buffers two emission maxima.

Furthermore, the possibility to image the cysteine cathepsins on SDS-PAGE by compound **158** was proved on example of cathepsin K. The fluorescence analysis of the resulting gel allowed the imaging of fluorescence-labeled cathepsin K. No fluorescence was measured in the control experiments.

In the second project of this study, the fluoroethylated tyrosine-derived dipeptide nitrile **160** as well as its aza-analogue **161** were synthesized as ‘cold’ reference compounds of fluorine-18 radiolabeled ‘activity-based’ probes to study their kinetic properties on cathepsins L, S, K and B. While the fluoroethylated dipeptide nitrile **160**, a fast-binding inhibitor, was moderate active toward tested cathepsins, the corresponding azadipeptide nitrile **161** with the slow-binding kinetic behavior was clearly more active.

The preliminary results of the described projects could be used to develop fluorescent and radioactive imaging instruments for cysteine cathepsins in the areas of the Cell and Molecular Biology. Furthermore, the fluorescent ‘activity-based’ probe **158** represents a potential tool for quantification of cathepsins S and K in human (*e.g.* in blood plasma) to diagnose and monitor osteoporosis and autoimmune disorders.

3. EXPERIMENTAL SECTION

3.1. INHIBITION ASSAYS AND EQUATIONS

3.1.1. CATHEPSIN L INHIBITION ASSAY (I)

Human recombinant cathepsin L (Calbiochem, Darmstadt, Germany) was assayed spectrophotometrically (Cary 50 Bio, Varian) at 405 nm and at 37 °C. The reactions were followed over 10 min for fast-binding inhibitors and over 80 min for compounds displaying slow-binding behavior, respectively. Assay buffer was 100 mM sodium phosphate buffer pH 6.0, 100 mM NaCl, 5 mM EDTA, and 0.01% Brij 35. An enzyme stock solution of 50 µg/mL in 20 mM sodium acetate buffer pH 5.0, 100 mM NaCl, 10 mM trehalose, 1 mM EDTA, and 50% glycerol was diluted 1:100 with assay buffer containing 5 mM DTT and incubated for 30 min at 37 °C. This enzyme solution was diluted 1:5 with assay buffer containing 5 mM DTT. Inhibitor stock solutions were prepared in DMSO. A 10 mM stock solution of the chromogenic substrate Z-Phe-Arg-pNa was prepared with DMSO. The final concentration of DMSO was 2%, and the final concentration of the substrate was 100 µM (= 10.0 K_m). Assays were performed with a final concentration of 4 ng/mL of cathepsin L. Into a cuvette containing 940 µL assay buffer, inhibitor solution and DMSO in a total volume of 10 µL, and 10 µL of the substrate solution were added and thoroughly mixed. The reaction was initiated by adding 40 µL of the cathepsin L solution. Experiments were performed in duplicate with at least five different inhibitor concentrations.

3.1.2. CATHEPSIN L INHIBITION ASSAY (II)

Human isolated cathepsin L (Enzo Life Sciences, Lörrach, Germany) was assayed spectrophotometrically (Cary 50 Bio, Varian) at 405 nm and at 37 °C. The reactions were followed over 10 min for fast-binding inhibitors and over 80 min for compounds displaying slow-binding behavior, respectively. Assay buffer was 100 mM sodium phosphate buffer pH 6.0, 100 mM NaCl, 5 mM EDTA, and 0.01% Brij 35. An enzyme stock solution of 135 µg/mL in 20 mM malonate buffer pH 5.5, 400 mM NaCl, and 1 mM EDTA was diluted 1:100 with assay buffer containing 5 mM DTT and incubated for 30 min at 37 °C. Inhibitor stock solutions were prepared in DMSO. A 10 mM stock solution of the chromogenic substrate Z-Phe-Arg-pNA was prepared with DMSO. The final concentration of DMSO was 2%, and the final concentration of the substrate was 100 µM (= 5.88 K_m). Assays were performed with a final concentration of 54 ng/mL of cathepsin L. Into a cuvette containing 940 µL assay buffer, inhibitor solution and DMSO in a total volume of 10 µL, and 10 µL of the substrate solution were added and thoroughly mixed. The reaction was initiated by adding 40 µL of the cathepsin L solution. Experiments were performed in duplicate with at least five different inhibitor concentrations.

3.1.3. CATHEPSIN S INHIBITION ASSAY (I)

Cathepsin S (Calbiochem, Darmstadt, Germany) was assayed spectrophotometrically (Cary 50 Bio, Varian) at 405 nm and at 37 °C. The reactions were followed over 10 min for fast-binding inhibitors and over 80 min for compounds displaying slow-binding behavior, respectively. Assay buffer was 50 mM sodium phosphate buffer pH 6.5, 50 mM NaCl, 2 mM EDTA, and 0.01% Triton X-100. An enzyme stock solution of 375 µg/mL in 35 mM potassium phosphate, 35 mM sodium acetate pH 6.5, 2 mM DTT, 2 mM EDTA, and 50% ethylene glycol was diluted 1:100 with assay buffer containing 5 mM DTT and incubated for 30 min at 37 °C. Inhibitor stock solutions were prepared in DMSO. A 10 mM stock solution of the chromogenic substrate Z-Phe-Val-Arg-pNA was prepared with DMSO. The final concentration of DMSO was 2%, and the final concentration of the substrate was 100 µM (= 1.49 K_m). Assays were performed with a final concentration of 75 ng/mL of cathepsin S. Into a cuvette containing 960 µL assay buffer, inhibitor solution and DMSO in a total volume of 10 µL, and 10 µL of the substrate solution were added and thoroughly mixed. The reaction was initiated by adding 20 µL of the cathepsin S solution. Experiments were performed in duplicate with at least five different inhibitor concentrations.

3.1.4. CATHEPSIN S INHIBITION ASSAY (II)

Cathepsin S (Calbiochem, Darmstadt, Germany) was assayed spectrophotometrically (Cary 50 Bio, Varian) at 405 nm and at 37 °C. The reactions were followed over 10 min for fast-binding inhibitors and over 80 min for compounds displaying slow-binding behavior, respectively. Assay buffer was 50 mM sodium phosphate buffer pH 6.5, 50 mM NaCl, 2 mM EDTA, and 0.01% Triton X-100. An enzyme stock solution of 375 µg/mL in 35 mM potassium phosphate, 35 mM sodium acetate pH 6.5, 2 mM DTT, 2 mM EDTA, and 50% ethylene glycol was diluted 1:100 with assay buffer containing 5 mM DTT and incubated for 30 min at 37 °C. Inhibitor stock solutions were prepared in DMSO. A 10 mM stock solution of the chromogenic substrate Z-Phe-Arg-pNa was used in a final concentration of 100 µM (= 0.85 K_m). Assays were performed with a final concentration of 75 ng/mL of cathepsin S. Into a cuvette containing 960 µL assay buffer, inhibitor solution and DMSO in a total volume of 10 µL, and 10 µL of the substrate solution were added and thoroughly mixed. The reaction was initiated by adding 20 µL of the cathepsin S solution. Experiments were performed in duplicate with at least five different inhibitor concentrations.

3.1.5. CATHEPSIN K INHIBITION ASSAY (I)

Cathepsin K was assayed fluorimetrically on Monaco Safas spectrofluorometer flx. The wavelength for excitation was 360 nm and for emission 440 nm. The reactions were followed at 25 °C over 10 min for fast-binding inhibitors and over 80 min for compounds displaying slow-binding behavior, respectively. A human recombinant procathepsin K (Calbiochem, Darmstadt, Germany) stock solution of 150 µg/mL in 25 mM Tris buffer pH 8.0, 500 mM NaCl was diluted 1:3.7 with 32.5 mM sodium acetate buffer pH 3.5 and incubated for 3 h at 25 °C to activate procathepsin K to cathepsin K. After incubation, the solution was aliquoted, frozen in liquid nitrogen, and kept at -70 °C. Assay buffer was 100 mM sodium citrate pH 5.0, 100 mM NaCl, 1 mM EDTA, and 0.01% CHAPS. The enzyme solution was diluted 1:100 with assay buffer containing 5 mM DTT and incubated for 30 min at 37 °C. Inhibitor stock solutions were prepared in DMSO. A 10 mM stock solution of the fluorogenic substrate Z-Leu-Arg-AMC was prepared with DMSO. The final concentration of DMSO was 2%, and the final concentration of the substrate was 40 µM (= 15.4 K_m). Assays were performed with a final concentration of 4 ng/mL of cathepsin K. Into a cuvette containing 970 µL assay buffer, inhibitor solution and DMSO in a total volume of 16 µL, and 4 µL of the substrate solution were added and thoroughly mixed. The reaction was initiated by adding 10 µL of the cathepsin K solution. Experiments were performed in duplicate with at least five different inhibitor concentrations.

3.1.6. CATHEPSIN K INHIBITION ASSAY (II)

Cathepsin K was assayed fluorimetrically on Monaco Safas spektrofluorometer flx. The wavelength for excitation was 360 nm and for emission 440 nm. The reactions were followed at 25 °C over 10 min for fast-binding inhibitors and over 80 min for compounds displaying slow-binding behavior, respectively. A human recombinant cathepsin K (Enzo Life Sciences, Lörrach, Germany) stock solution of 23 µg/mL in 50 mM sodium acetate pH 5.5, 50 mM NaCl, 0.5 mM EDTA, 5 mM DTT was diluted 1:100 with assay buffer (100 mM sodium citrate pH 5.0, 100 mM NaCl, 1 mM EDTA, 0.01% CHAPS) containing 5 mM DTT and incubated for 30 min at 37 °C. Inhibitor stock solutions were prepared in DMSO. A 10 mM stock solution of the fluorogenic substrate Z-Leu-Arg-AMC was prepared with DMSO. The final concentration of DMSO was 2%, and the final concentration of the substrate was 40 µM (= 13.3 K_m). Assays were performed with a final concentration of 2 ng/mL or 5 ng/mL of cathepsin K. Into a cuvette containing 970 µL or 960 µL assay buffer, inhibitor solution and DMSO in a total volume of 16 µL, and 4 µL of the substrate solution were added and thoroughly mixed. The reaction was initiated by adding 10 µL or 20 µL of the cathepsin K solution. Experiments were performed in duplicate with at least five different inhibitor concentrations.

3.1.7. CATHEPSIN B INHIBITION ASSAY

Human isolated cathepsin B (Calbiochem, Darmstadt, Germany) was assayed spectrophotometrically (Cary 50 Bio, Varian) at 405 nm and at 37 °C. The reactions were followed over 10 min for fast-binding inhibitors and over 80 min for compounds displaying slow-binding behavior, respectively. Assay buffer was 100 mM sodium phosphate buffer pH 6.0, 100 mM NaCl, 5 mM EDTA, 0.01% Brij 35. An enzyme stock solution of 1.81 mg/mL in 20 mM sodium acetate buffer pH 5.0, 1 mM EDTA was diluted 1:500 with assay buffer containing 5 mM DTT and incubated for 30 min at 37 °C. Inhibitor stock solutions were prepared in DMSO. A 100 mM stock solution of the chromogenic substrate Z-Arg-ArgpNA was prepared with DMSO. The final concentration of DMSO was 2%, and the final concentration of the substrate was 500 μ M (0.45 K_m). Assays were performed with a final concentration of 72 ng/mL of cathepsin B. Into a cuvette containing 960 μ L assay buffer, inhibitor solution and DMSO in a total volume of 15 μ L, and 5 μ L of the substrate solution were added and thoroughly mixed. The reaction was initiated by adding 20 μ L of the cathepsin B solution. Experiments were performed in duplicate with at least five different inhibitor concentrations.

3.1.8. EQUATIONS

Dipeptide nitriles **43**, **66**, **79**, **80**, **111**, **119**, **120**, **129–138**, **144** and **160** showed a fast-binding inhibition behavior on cathepsins L, S, K and B as reflected by linear progress curves. The apparent inhibition constant K_i' was determined by non-linear regression using equation $v_s = v_0/(1+[I]/K_i')$, where v_s is the steady-state rate, v_0 is the rate in the absence of inhibitor, and $[I]$ is the inhibitor concentration. The true inhibition constant K_i was calculated by correction of K_i' according to $K_i = K_i'/(1+[S]/K_m)$, where $[S]$ is the substrate concentration and K_m is the Michaelis constant.

Progress curves of the reactions of cysteine proteases in the presence of azadipeptide nitriles **33–38**, **42**, **45**, **46**, **50**, **51**, **62–65**, **67**, **68**, **92**, **122**, **148**, **161** were analyzed by nonlinear regression using slow-binding equation $E/I = v_s t + (v_i - v_s)(1 - \exp(-k_{obs}t))/k_{obs} + d$, where E/I is the extinction/fluorescence intensity, v_s is the steady-state rate, v_i is the initial rate, k_{obs} is the observed first-order rate constant, and d is the offset. To obtain K_i' , v_s values as well as the v_0 value were plotted *versus* the inhibitor concentration $[I]$, according to $v_s = v_0/(1+[I]/K_i')$, and K_i was calculated from equation $K_i = K_i'/(1+[S]/K_m)$. The apparent second-order rate constant k_{on}' was obtained by linear regression according to equation $k_{obs} = k_{on}'[I] + k_{off}$. The true rate constant k_{on} was calculated by correction of k_{on}' according to equation $k_{on} = k_{on}'(1+[S]/K_m)$. The first-order rate constant k_{off} for the dissociation of the enzyme-inhibitor complex was calculated according to equation $k_{off} = k_{on}K_i$.

Progress curves of the reactions of cysteine proteases in the presence of the irreversible 'activity-based' probe **158** were analyzed by non-linear regression using the slow-binding equation for the irreversible inhibition type $E/I = A(1 - \exp(-k_{obs}t)) + d$, where E/I is the extinction/fluorescence intensity, $A = v_i/k_{obs}$, v_i is the initial rate, k_{obs} is the observed first-order rate constant, and d is the offset. The apparent inhibition constant K_i' and the inactivation first-order rate constant k_{inac} were determined by non-linear regression using the equation $k_{obs} = k_{inac}[I]/(K_i' + [I])$, where k_{obs} is the observed first-order rate constant, and $[I]$ is the inhibitor concentration. The true second-order rate constant k_{2nd} was calculated according to $k_{2nd} = k_{inac}/K_i$.

3.2. SPECTRAL PROPERTIES AND IMAGING EXPERIMENT

The absorption spectra were performed on Cary 50 Bio device from Varian. Into a cuvette containing 990 μL solvent (dichloromethane, methanol, water), 10 μL of **122** in DMSO (10 mM) were added, and it was thoroughly mixed. In the case of **158**, 10 μL of the compound stock solution in DMSO (1 mM) were added to 990 μL solvent (dichloromethane, methanol, water, cath S buffer pH 6.5, cath L/B buffer pH 6.0, and cath K buffer pH 5.0). The absorption spectra were recorded in a range between 800 and 200 nm after baseline correction. The emission spectra were performed on Monaco Safas spektrofluorometer flx in a range between 800 and 200 nm after baseline correction with the same solutions and in the same concentrations of **152** and **158** as in the case of the absorption measurements.

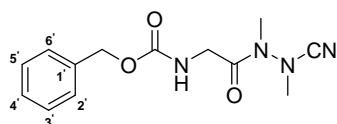
For the imaging experiment, 20 μL of the human recombinant cathepsin K from Enzo 23 $\mu\text{g}/\text{mL}$ in 50 mM sodium acetate pH 5.5, 50 mM NaCl, 0.5 mM EDTA, 5 mM DTT was added to 29 μL of 100 mM sodium citrate buffer pH 5.0, 100 mM NaCl, 1 mM EDTA, 0.01% CHAPS, 5 mM DTT, and it was activated for 40 min at 37 C. 0.5 μL of DMSO and 0.5 μL of **158** in DMSO (1 mM) were added to the activated cathepsin K, and the resulting solution (9.2 $\mu\text{g}/\text{mL}$ cathepsin K, 10 μM ABP **158**) was incubated for 40 min at 37 C. 20 μL , 10 μL , 5 μL , and 2.5 μL of the incubation medium were treated with the reducing (supplemented with 2% (v/v) 2-mercaptoethanol) SDS-loading buffer, heated at 90 °C for 5 min, and separated by SDS/PAGE on the 14% (w/v) polyacrylamide gel. In the control experiment, 20 μL of the activated cathepsin K (9.2 $\mu\text{g}/\text{mL}$) in the absence of **158**, and 20 μL of **158** (10 μM in 100 mM sodium citrate buffer pH 5.0, 100 mM NaCl, 1 mM EDTA, 0.01% CHAPS, 5 mM DTT, 1% DMSO) were used. The fluorescence analysis of the resulting gel was performed with the Gel iX Imager from Intas, equipped with UV-transilluminator (312 nm), super sensitive 'scientific grade' CCD-camera, and an ethidium bromide filter. The Coomassie staining was carried out with Page Blue protein staining solution from Fermentas.

3.3. PREPARATION OF COMPOUNDS

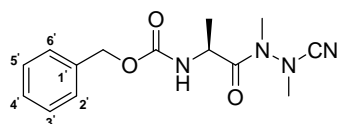
3.3.1. GENERAL METHODS AND MATERIALS

Melting points were determined on a Büchi 510 oil bath apparatus, and are uncorrected. Thin layer chromatography was performed on Merck aluminium sheets. Preparative column chromatography was performed on silica gel 60, 0.060–0.200 mm. ^{13}C NMR (125 MHz) and ^1H NMR (500 MHz) spectra were recorded on a Bruker Avance DRX 500 spectrometer. Elemental analyses were performed with a Vario EL apparatus. LC-DAD chromatograms and ESI-MS spectra were recorded on an Agilent 1100 HPLC system with Applied Biosystems API-2000 mass spectrometer. The (EI) mass spectra were obtained on A.E.I. MS-50 spectrometer. For compound **158**, the MS (ESI) spectra were performed with Bruker Daltonics micrOTOF-Q spectrometer. The chiral analytical HPLC was performed on a Jasco 200 device using LiChroCART[®] 250-4 ChiraDex[®] (5 μm) column. Optical rotation was determined on a Perkin-Elmer 241 polarimeter. IR spectra were recorded on a Bruker Tensor 27 FT-IR spectrometer. Amino acid derivatives were obtained from Bachem (Bubendorf, Switzerland), Acros (Geel, Belgium) and Aldrich (Steinheim, Germany).

3.3.2. PREPARATION OF 33

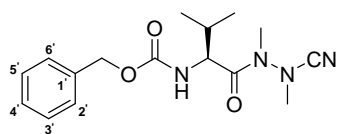


***N*-(Benzyloxycarbonyl)glycyl-methylazaalanine-nitrile.** Compound **21** (1.40 g, 6.69 mmol) was dissolved in dry THF (15 mL) and cooled to $-25\text{ }^{\circ}\text{C}$. To the stirred solution, *N*-methylmorpholine (0.74 mL, 6.73 mmol) and isobutyl chloroformate (0.88 mL, 6.75 mmol) were added consecutively. 1,2-Dimethylhydrazine dihydrochloride (4.44 g, 33.4 mmol) was suspended in H_2O (1 mL), and 5 N NaOH (13.4 mL) was added under ice-cooling. This solution was given to the reaction mixture when the precipitation of *N*-methylmorpholine hydrochloride occurred. It was allowed to warm to room temperature within 30 min, and stirred overnight at rt. After evaporation of the solvent, the resulting aqueous residue was extracted with ethyl acetate (1×40 , 3×10 mL). The combined organic layers were washed with H_2O (15 mL), sat. NaHCO_3 (2×15 mL), H_2O (15 mL), and brine (15 mL). The solvent was dried (Na_2SO_4) and evaporated. The crude product was recrystallized from ethyl acetate/petroleum ether to obtain **27** as a white solid (0.39 g, 23%). Sodium acetate (0.28 g, 3.41 mmol) and cyanogen bromide (0.25 g, 2.36 mmol) were added to a solution of **27** (0.30 g, 1.19 mmol) in MeOH (10 mL). The mixture was stirred at room temperature for 18 h, and the solvent was removed under reduced pressure. The residue was suspended in H_2O (10 mL), a pH of 1–2 was adjusted (10% KHSO_4), and it was extracted with ethyl acetate (3×20 mL). The combined organic layers were washed with H_2O (10 mL), sat. NaHCO_3 (2×10 mL), H_2O (10 mL), and brine (10 mL). The solvent was dried (Na_2SO_4) and removed *in vacuo*. The oily residue was purified by column chromatography on silica gel using ethyl acetate/petroleum ether (1:1) as eluent to obtain **33** as a white solid (0.22 g, 67% from **27**). mp $82\text{--}86\text{ }^{\circ}\text{C}$; ^1H NMR (500 MHz, CDCl_3) δ 3.13, 3.20 ($2 \times \text{s}$, $2 \times 3\text{H}$, $\text{N}(\text{CH}_3)\text{CN}$, CONCH_3), 4.12 (dd, $^2J = 17.8\text{ Hz}$, $^3J = 3.3\text{ Hz}$, 1H, NHCHHCO), 4.23 (dd, $^2J = 18.0\text{ Hz}$, $^3J = 5.7\text{ Hz}$, 1H, NHCHHCO), 5.11 (s, 2H, CH_2O), 5.46 (bs, 1H, NHCH_2CO), 7.28–7.35 (m, 5H, H_{arom}); ^{13}C NMR (125 MHz, CDCl_3) δ 30.39 ($\text{N}(\text{CH}_3)\text{CN}$), 40.85 (CONCH_3), 42.51 (NHCH_2CO), 67.09 (CH_2O), 112.94 (CN), 128.04 (C-2', C-6'), 128.17 (C-4'), 128.50 (C-3', C-5'), 136.14 (C-1'), 156.24 (OCON), 169.98 (NHCH_2CO); FTIR (KBr, cm^{-1}) 2223 ($\text{C}\equiv\text{N}$); Anal. $\text{C}_{13}\text{H}_{16}\text{N}_4\text{O}_3$ (276.29 g/mol) calcd C 56.51, H 5.84, N 20.28; found C 56.41, H 5.81, N 19.03.

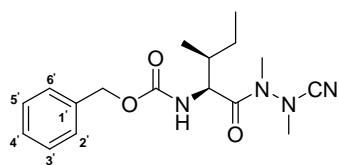
3.3.3. PREPARATION OF 34

***N*-(Benzyloxycarbonyl)alanyl-methylazaalanine-nitrile.** Compound **22** (1.50 g, 6.72 mmol) was dissolved in dry THF (15 mL) and cooled to $-25\text{ }^{\circ}\text{C}$. To the stirred solution, *N*-methylmorpholine (0.74 mL, 6.73 mmol) and isobutyl chloroformate (0.88 mL, 6.75 mmol) were added consecutively. 1,2-Dimethylhydrazine dihydrochloride (4.44 g, 33.4 mmol) was suspended in H_2O (1 mL), and 5 N NaOH (13.4 mL) was added under ice-cooling. This solution was given to the reaction mixture when the precipitation of *N*-methylmorpholine hydrochloride occurred. It was allowed to warm to room temperature within 30 min, and stirred overnight at rt. After evaporation of the solvent, the resulting aqueous residue was extracted with ethyl acetate (1×40 , 3×10 mL). The combined organic layers were washed with H_2O (15 mL), sat. NaHCO_3 (2×15 mL), H_2O (15 mL), and brine (15 mL). The solvent was dried (Na_2SO_4) and evaporated. The crude product was purified using ethyl acetate/petroleum ether (2:1) to obtain **28** as a colourless oil (1.18 g, 66%). Sodium acetate (1.20 g, 14.6 mmol) and cyanogen bromide (0.65 g, 6.14 mmol) were added to a solution of **28** (1.10 g, 4.15 mmol) in MeOH (15 mL). The mixture was stirred at room temperature for 20 h, and the solvent was removed under reduced pressure. The residue was suspended in H_2O (10 mL), a pH of 1–2 was adjusted (10% KHSO_4), and it was extracted with ethyl acetate (3×20 mL). The combined organic layers were washed with H_2O (10 mL), sat. NaHCO_3 (2×10 mL), H_2O (10 mL), and brine (10 mL). The solvent was dried (Na_2SO_4) and removed *in vacuo*. The semisolid residue was purified by column chromatography on silica gel using ethyl acetate/petroleum ether (1:2) as eluent to obtain **34** as a white solid (0.62 g, 51% from **28**). mp $155\text{--}158\text{ }^{\circ}\text{C}$; $[\alpha]_{\text{D}}^{20} = +8.0$ ($c = 0.75$, CHCl_3); ^1H NMR (500 MHz, CDCl_3) mixture rotamers (only the data of the major rotational isomer are noted) δ 1.40 (d, $^3J = 7.3$ Hz, 3H, CHCH_3), 3.19, 3.22 ($2 \times$ s, $2 \times$ 3H, $\text{N}(\text{CH}_3)\text{CN}$, CONCH_3), 4.78–4.83 (m, 1H, NHCHCO), 5.02 (d, $^2J = 12.6$ Hz, 1H, CHHO), 5.10 (d, $^2J = 12.3$ Hz, 1H, CHHO), 5.37 (d, $^3J = 7.3$ Hz, 1H, NHCHCO), 7.28–7.36 (m, 5H, H_{arom}); ^{13}C NMR (125 MHz, CDCl_3) δ 18.24 (CHCH_3), 30.50 ($\text{N}(\text{CH}_3)\text{CN}$), 40.97 (CONCH_3), 46.99 (NHCHCO), 66.97 (CH_2O), 113.55 (CN), 127.97 (C-2', C-6'), 128.20 (C-4'), 128.53 (C-3', C-5'), 136.06 (C-1'), 155.89 (OCON), 174.54 (NHCHCO); FTIR (KBr, cm^{-1}) 2226 ($\text{C}\equiv\text{N}$); Anal. $\text{C}_{14}\text{H}_{18}\text{N}_4\text{O}_3$ (290.32 g/mol) calcd C 57.92, H 6.25, N 19.30; found C 57.51, H 6.24, N 18.97.

3.3.4. PREPARATION OF 35

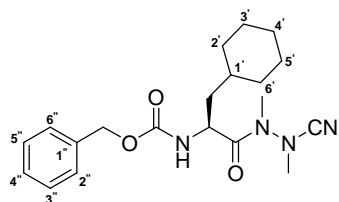


***N*-(Benzyloxycarbonyl)valyl-methylazaalanine-nitrile.** Compound **23** (1.68 g, 6.69 mmol) was dissolved in dry THF (15 mL) and cooled to $-25\text{ }^{\circ}\text{C}$. To the stirred solution, *N*-methylmorpholine (0.74 mL, 6.73 mmol) and isobutyl chloroformate (0.88 mL, 6.75 mmol) were added consecutively. 1,2-Dimethylhydrazine dihydrochloride (4.44 g, 33.4 mmol) was suspended in H_2O (1 mL), and 5 N NaOH (13.4 mL) was added under ice-cooling. This solution was given to the reaction mixture when the precipitation of *N*-methylmorpholine hydrochloride occurred. It was allowed to warm to room temperature within 30 min, and stirred overnight at rt. After evaporation of the solvent, the resulting aqueous residue was extracted with ethyl acetate (1×40 , 3×10 mL). The combined organic layers were washed with H_2O (15 mL), sat. NaHCO_3 (2×15 mL), H_2O (15 mL), and brine (15 mL). The solvent was dried (Na_2SO_4) and evaporated. The crude product was purified by column chromatography using ethyl acetate/petroleum ether (2:1) to obtain **29** as a colourless oil (1.10 g, 56%). Sodium acetate (0.78 g, 9.51 mmol) and cyanogen bromide (0.54 g, 5.10 mmol) were added to a solution of **29** (1.00 g, 3.41 mmol) in MeOH (20 mL). The mixture was stirred at room temperature for 12 h, and the solvent was removed under reduced pressure. The residue was suspended in H_2O (10 mL), a pH of 1–2 was adjusted (10% KHSO_4), and it was extracted with ethyl acetate (3×20 mL). The combined organic layers were washed with H_2O (10 mL), sat. NaHCO_3 (2×10 mL), H_2O (10 mL), and brine (10 mL). The solvent was dried (Na_2SO_4) and removed *in vacuo*. The oily residue was purified by column chromatography on silica gel using ethyl acetate/petroleum ether (2:1) as eluent to obtain **35** as a white solid (0.42 g, 39% from **29**). mp $64\text{--}66\text{ }^{\circ}\text{C}$; $[\alpha]_{\text{D}}^{20} = +20.0$ ($c = 1.10$, CHCl_3); ^1H NMR (500 MHz, CDCl_3) δ 0.94 (d, $^3J = 6.9$ Hz, 1H, CH_3CHCH_3), 1.02 (d, $^3J = 7.0$ Hz, 3H, CH_3CHCH_3), 1.97–2.04 (m, 1H, CH_3CHCH_3), 3.20, 3.23 ($2 \times$ s, $2 \times$ 3H, $\text{N}(\text{CH}_3)\text{CN}$, CONCH_3), 4.65–4.68 (m, 1H, NHCHCO), 5.02 (d, $^2J = 12.3$ Hz, 1H, CHHO), 5.09 (d, $^2J = 12.3$ Hz, 1H, CHHO), 5.26 (d, $^3J = 9.2$ Hz, 1H, NHCHCO), 7.30–7.36 (m, 5H, H_{arom}); ^{13}C NMR (125 MHz, CDCl_3) δ 17.59, 19.56, (CH_3CHCH_3 , CH_3CHCH_3), 30.26, 31.12, 41.21 (CH_3CHCH_3 , $\text{N}(\text{CH}_3)\text{CN}$, CONCH_3), 55.60 (NHCHCO), 67.09 (CH_2O), 113.75 (CN), 128.01 (C-2', C-6'), 128.23 (C-4'), 128.55 (C-3', C-5'), 136.03 (C-1'), 156.49 (OCON), 173.89 (NHCHCO); FTIR (KBr, cm^{-1}) 2224 ($\text{C}\equiv\text{N}$); Anal. $\text{C}_{16}\text{H}_{22}\text{N}_4\text{O}_3$ (318.37 g/mol) calcd C 60.36, H 6.97, N 17.60; found C 60.63, H 7.00, N 16.97.

3.3.5. PREPARATION OF 36

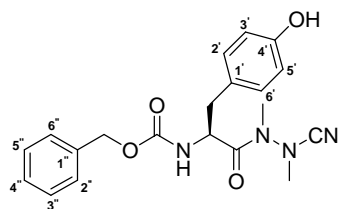
***N*-(Benzyloxycarbonyl)isoleucyl-methylazaalanine-nitrile.** Compound **24** (1.20 g, 4.52 mmol) was dissolved in dry THF (15 mL) and cooled to $-25\text{ }^{\circ}\text{C}$. To the stirred solution, *N*-methylmorpholine (0.50 mL, 4.55 mmol) and isobutyl chloroformate (0.59 mL, 4.53 mmol) were added consecutively. 1,2-Dimethylhydrazine dihydrochloride (2.70 g, 20.3 mmol) was suspended in H_2O (1 mL), and 5 N NaOH (8.20 mL) was added under ice-cooling. This solution was given to the reaction mixture when the precipitation of *N*-methylmorpholine hydrochloride occurred. It was allowed to warm to room temperature within 30 min, and stirred overnight at rt. After evaporation of the solvent, the resulting aqueous residue was extracted with ethyl acetate (1×40 , 3×10 mL). The combined organic layers were washed with H_2O (15 mL), sat. NaHCO_3 (2×15 mL), H_2O (15 mL), and brine (15 mL). The solvent was dried (Na_2SO_4) and evaporated. The crude product was purified using ethyl acetate/petroleum ether (2:1) to obtain **30** as a semisolid product. Sodium acetate (0.48 g, 5.85 mmol) and cyanogen bromide (0.34 g, 3.21 mmol) were added to a solution of **30** (0.65 g, 2.11 mmol) in MeOH (15 mL). The mixture was stirred at room temperature for 20 h, and the solvent was removed. The residue was suspended in H_2O (10 mL), a pH of 1–2 was adjusted (10% KHSO_4), and it was extracted with ethyl acetate (3×20 mL). The combined organic layers were washed with H_2O (10 mL), sat. NaHCO_3 (2×10 mL), H_2O (10 mL), and brine (10 mL). The solvent was dried (Na_2SO_4) and removed *in vacuo*. The semisolid residue was purified by column chromatography on silica gel using ethyl acetate/petroleum ether (1:2) as eluent to obtain **36** as a colorless oil (0.34 g, 23% from **30**). $[\alpha]_{\text{D}}^{20} = +12.7$ ($c = 1.10$, CHCl_3); ^1H NMR (500 MHz, CDCl_3) mixture of rotamers (only the data of the major rotational isomer are noted) δ 0.89 (t, $^3J = 7.4$ Hz, 3H, CH_2CH_3), 0.98 (d, $^3J = 7.0$ Hz, 3H, CHCH_3), 1.10–1.25 (m, 1H, CHCH_3), 1.52–1.77 (m, 2H, CH_2CH_3), 3.20, 3.23 ($2 \times$ s, $2 \times$ 3H, $\text{N}(\text{CH}_3)\text{CN}$, CONCH_3), 4.70 (app. t, $^3J = 8.4$ Hz, 1H, NHCHCO), 5.01 (d, $^2J = 12.0$ Hz, 1H, CHHO), 5.08 (d, $^2J = 12.0$ Hz, 1H, CHHO), 5.24 (d, $^3J = 9.5$ Hz, 1H, NHCHCO), 7.28–7.35 (m, 5H, H_{arom}); ^{13}C NMR (125 MHz, CDCl_3) δ 11.11 (CH_2CH_3), 15.73 (CHCH_3), 24.38 (CH_2CH_3), 30.25, 37.61, 41.22 ($\text{N}(\text{CH}_3)\text{CN}$, CHCH_3 , CONCH_3), 54.77 (NHCHCO) 67.07 (CH_2O), 113.77 (CN), 127.99 (C-2', C-6'), 128.22 (C-4'), 128.53 (C-3', C-5'), 136.02 (C-1'), 156.41 (OCON), 174.08 (NHCHCO); FTIR (KBr, cm^{-1}) 2223 ($\text{C}\equiv\text{N}$); Anal. $\text{C}_{17}\text{H}_{24}\text{N}_4\text{O}_3$ (332.40 g/mol) calcd C 61.43, H 7.28, N 16.86; found C 61.18, H 7.62, N 16.46.

3.3.6. PREPARATION OF 37



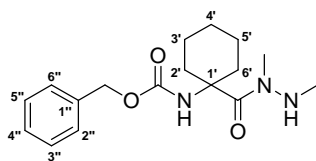
***N*-(Benzyloxycarbonyl)cyclohexylalanyl-methylazaalanine-nitrile.** Compound **25** (1.00 g, 3.27 mmol) was dissolved in dry THF (15 mL) and cooled to $-25\text{ }^{\circ}\text{C}$. To the stirred solution, *N*-methylmorpholine (0.36 mL, 3.27 mmol) and isobutyl chloroformate (0.43 mL, 3.30 mmol) were added consecutively. 1,2-Dimethylhydrazine dihydrochloride (2.20 g, 16.5 mmol) was suspended in H_2O (1 mL), and 5 N NaOH (6.50 mL) was added under ice-cooling. This solution was given to the reaction mixture when the precipitation of *N*-methylmorpholine hydrochloride occurred. It was allowed to warm to room temperature within 30 min, and stirred overnight at rt. After evaporation of the solvent, the resulting aqueous residue was extracted with ethyl acetate (1×40 , 3×10 mL). The combined organic layers were washed with H_2O (15 mL), sat. NaHCO_3 (2×15 mL), H_2O (15 mL), and brine (15 mL). The solvent was dried (Na_2SO_4) and evaporated. The crude product was purified using ethyl acetate/petroleum ether (2:1) to obtain **31** as a colourless oil (0.70 g, 62%). Sodium acetate (0.44 g, 5.36 mmol) and cyanogen bromide (0.30 g, 2.83 mmol) were added to a solution of **31** (0.63 g, 1.81 mmol) in MeOH (50 mL). The mixture was stirred at room temperature for 12 h, and the solvent was removed under reduced pressure. The residue was suspended in H_2O (10 mL), a pH of 1–2 was adjusted (10% KHSO_4), and it was extracted with ethyl acetate (3×20 mL). The combined organic layers were washed with H_2O (10 mL), sat. NaHCO_3 (2×10 mL), H_2O (10 mL), and brine (10 mL). The solvent was dried (Na_2SO_4) and removed *in vacuo*. The oily residue was purified by column chromatography on silica gel using ethyl acetate/petroleum ether (1:2) as eluent to obtain **37** as a colorless oil (0.21 g, 31% from **31**). $[\alpha]_{\text{D}}^{20} = +17.0$ ($c = 1.00$, CHCl_3); ^1H NMR (500 MHz, $\text{DMSO}-d_6$) mixture of rotamers (only the data of the major rotational isomer are noted) δ 0.90–1.79 (m, 13H, $\text{H}_{\text{cyclohexane}}$, CHCH_2), 3.08, 3.20 ($2 \times s$, $2 \times 3\text{H}$, $\text{N}(\text{CH}_3)\text{CN}$, CONCH_3), 4.61 (bs, 1H, NHCHCO), 4.98–5.04 (m, 2H, CH_2O), 7.26–7.37 (m, 5H, H_{arom}), 7.71 (d, $^3J = 7.6$ Hz, 1H, NHCHCO); ^{13}C NMR (125 MHz, $\text{DMSO}-d_6$) δ 25.62, 25.85, 26.13 ($\text{C}_{\text{cyclohexane}}$), 30.49, 31.58, 33.51 ($\text{N}(\text{CH}_3)\text{CN}$, $\text{C}_{\text{cyclohexane}}$), 33.65, 38.18 (CONCH_3 , CHCH_2), 48.92 (NHCHCO) 65.66 (CH_2O), 114.24 (CN), 127.84 (C-2'', C-6''), 127.96 (C-4''), 128.47 (C-3'', C-5''), 137.03 (C-1''), 156.43 (OCON), 174.44 (NHCHCO); FTIR (KBr, cm^{-1}) 2222 ($\text{C}\equiv\text{N}$); Anal. $\text{C}_{20}\text{H}_{28}\text{N}_4\text{O}_3$ (372.46 g/mol) calcd C 64.49, H 7.58, N 15.04; found C 64.81, H 8.14, N 13.94.

3.3.7. PREPARATION OF 38



***N*-(Benzyloxycarbonyl)tyrosyl-methylazaalanine-nitrile.** Compound **26** (10.0 g, 31.7 mmol) was dissolved in dry THF (60 mL) and cooled to $-25\text{ }^{\circ}\text{C}$. To the stirred solution, *N*-methylmorpholine (3.84 mL, 34.9 mmol) and isobutyl chloroformate (4.54 mL, 34.8 mmol) were added consecutively. 1,2-Dimethylhydrazine dihydrochloride (8.43 g, 63.4 mmol) was suspended in H_2O (15 mL), and 10 N NaOH (13.0 mL) was added under ice-cooling. This solution was given to the reaction mixture when the precipitation of *N*-methylmorpholine hydrochloride occurred. It was allowed to warm to room temperature within 30 min, and stirred overnight at rt. After evaporation of the solvent, the resulting aqueous residue was extracted with ethyl acetate ($3 \times 60\text{ mL}$). The combined organic layers were washed with H_2O (30 mL), sat. NaHCO_3 ($2 \times 30\text{ mL}$), H_2O (30 mL), and brine (30 mL). The solvent was dried (Na_2SO_4) and evaporated to obtain **32** as a white solid. Sodium acetate (4.22 g, 51.4 mmol) and cyanogen bromide (4.09 g, 38.6 mmol) were added to a solution of **32** (9.20 g, 25.7 mmol) in MeOH (40 mL). The mixture was stirred at room temperature for 24 h, and the solvent was removed. The residue was suspended in H_2O (30 mL), a pH of ~ 2 was adjusted (10% KHSO_4), and it was extracted with ethyl acetate ($3 \times 60\text{ mL}$). The combined organic layers were washed with H_2O (30 mL), sat. NaHCO_3 (30 mL), H_2O (30 mL), and brine (30 mL). The solvent was dried (Na_2SO_4) and removed *in vacuo*. The oily residue was purified by column chromatography on silica gel using ethyl acetate/petroleum ether (1:1) as eluent to obtain **38** as a white solid (2.82 g, 23% from **26**). mp $158\text{ }^{\circ}\text{C}$; $[\alpha]_{\text{D}}^{20} = +30.0$ ($c = 1.00$, CHCl_3); ^1H NMR (500 MHz, $\text{DMSO}-d_6$) mixture of rotamers (only the data of the major rotational isomer are noted) δ 2.67–2.80 (m, 2H, CHCH_2), 3.11, 3.22 ($2 \times$ s, $2 \times$ 3H, $\text{N}(\text{CH}_3)\text{CN}$, CONCH_3), 4.65 (bs, 1H, NHCHCO), 4.95 (s, 2H, CH_2O), 6.67–7.35 (m, 9H, H_{arom}), 7.82 (d, $^3J = 7.6\text{ Hz}$, 1H, NHCHCO), 9.21 (s, 1H, OH); ^{13}C NMR (125 MHz, $\text{DMSO}-d_6$) mixture of rotamers, w = weak (minor rotational isomer), i = intensive (major rotational isomer) δ 30.17 (w), 30.55 (i), 35.69 (i), 36.23 (w) ($\text{N}(\text{CH}_3)\text{CN}$, CONCH_3), 40.26 (w), 40.45 (i) (CHCH_2), 52.93 (w), 53.46 (i) (NHCHCO), 65.58 (CH_2O), 114.21 (CN), 115.21, 127.69, 127.88, 128.41, 130.11 (i), 130.33, 136.92 (i), 137.04 (w) (C-3', C-5', C-2'', C-6'', C-4'', C-3'', C-5'', C-2', C-6', C-1', C-1''), 156.20 (OCON, C-4'), 173.60 (NHCHCO); Anal. $\text{C}_{20}\text{H}_{22}\text{N}_4\text{O}_4$ (382.41 g/mol) calcd C 62.82, H 5.80, N 14.65; found C 63.11, H 5.86, N 14.20.

3.3.8. PREPARATION OF 40



***N*-(Benzyloxycarbonyl)homocycloleucine 1,2-dimethylhydrazide.** Method A, mixed anhydride coupling protocol: Compound **39** (2.00 g, 7.21 mmol) was dissolved in THF (20 mL) and cooled to -25 °C. Triethylamine (4.38 g, 43.3 mmol) and isobutyl chloroformate (1.08 g, 7.91 mmol) were added, and it was stirred for 3 min at -25 °C. 1,2-dimethylhydrazine dihydrochloride (2.40 g, 18.0 mmol) was added. The resulting reaction mixture was stirred for 19 h at room temperature. THF was evaporated under reduced pressure. The residue was extracted with ethyl acetate (3 × 30 mL), washed with sat. NaHCO₃ (30 mL), H₂O (30 mL), and brine (30 mL). The solvent was dried over Na₂SO₄ and removed under reduced pressure. The oily reaction mixture was separated by column chromatography using ethyl acetate/petroleum ether 9:1 as eluent to obtain **40** as a colorless oil (0.41 g, 18%).

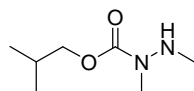
***N*-(Benzyloxycarbonyl)homocycloleucine 1,2-dimethylhydrazide.** Method B, EDC/DMAP coupling protocol, rt: Compound **39** (1.00 g, 3.61 mmol) was dissolved in dry THF (10 mL). DMAP (0.02 g, 0.16 mmol) and EDC (0.62 g, 3.99 mmol) were added, and the solution was stirred for 10 min at room temperature. 1,2-Dimethylhydrazine dihydrochloride (0.96 g, 7.22 mmol) was suspended in dry THF (10 mL) and treated with triethylamine (1.46 g, 14.4 mmol). The resulting reaction mixtures were combined and stirred for 24 h at rt. The solvent was evaporated under reduced pressure. The residue was treated with H₂O and extracted with ethyl acetate (3 × 30 mL). The combined organic layers were washed with sat. NaHCO₃ (2 × 30 mL), H₂O (30 mL), and brine (30 mL). The solvent was dried over Na₂SO₄ and removed under reduced pressure. The crude oily product was purified by column chromatography using CH₂Cl₂/MeOH (19:1) as eluent to obtain **40** as a colorless oil (0.41 g, 36%).

***N*-(Benzyloxycarbonyl)homocycloleucine 1,2-dimethylhydrazide.** Method C, EDC/DMAP coupling protocol, Δ: Compound **39** (1.00 g, 3.61 mmol) was dissolved in dry THF (10 mL). DMAP (0.02 g, 0.16 mmol) and EDC (0.62 g, 3.99 mmol) were added, and the solution was stirred for 10 min at room temperature. 1,2-Dimethylhydrazine dihydrochloride (0.96 g, 7.22 mmol) was suspended in dry THF (10 mL) and treated with triethylamine (1.46 g, 14.4 mmol). The resulting reaction mixtures were combined and heated to reflux for 24 h.

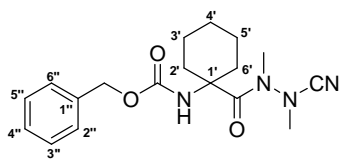
The solvent was evaporated under reduced pressure. The residue was treated with H₂O and extracted with ethyl acetate (3 × 30 mL). The combined organic layers were washed with sat. NaHCO₃ (2 × 30 mL), H₂O (30 mL), and brine (30 mL). The solvent was dried over Na₂SO₄ and removed under reduced pressure. The crude oily product was purified by column chromatography using CH₂Cl₂/MeOH (19:1) as eluent to obtain **40** as a colorless oil (0.45 g, 39%).

***N*-(Benzyloxycarbonyl)homocycloleucine 1,2-dimethylhydrazide.** Method D, HBTU coupling protocol (in the presence of HOBt): Compound **39** (1.00 g, 3.61 mmol) was dissolved in dry THF (10 mL). HOBt × H₂O (0.24 g, 1.78 mmol) and HBTU (1.51 g, 3.98 mmol) were added, and the solution was stirred for 10 min at room temperature. 1,2-Dimethylhydrazine dihydrochloride (0.96 g, 7.22 mmol) was suspended in dry THF (10 mL) and treated with triethylamine (1.46 g, 14.4 mmol). The resulting reaction mixtures were combined and stirred for 3 d at rt. The solvent was evaporated under reduced pressure. The residue was treated with H₂O and extracted with ethyl acetate (3 × 30 mL). The combined organic layers were washed with sat. NaHCO₃ (2 × 30 mL), H₂O (30 mL), and brine (30 mL). The solvent was dried over Na₂SO₄ and removed under reduced pressure. The crude oily product was purified by column chromatography using CH₂Cl₂/MeOH (19:1) and additionally ethyl acetate/petroleum ether (2:1) as eluents to obtain **40** as a colorless oil (0.31 g, 27%).

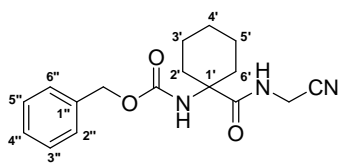
¹H NMR (500 MHz, DMSO-*d*₆) δ 1.13–1.20 (m, 1H, H_{cyclohexane}), 1.41–1.51 (m, 5H, H_{cyclohexane}), 1.66–1.72 (m, 2H, H_{cyclohexane}), 2.11 (bs, 2H, H_{cyclohexane}), 2.30 (d, ³J = 5.7 Hz, 3H, NHCH₃), 2.90 (s, 3H, CONCH₃), 4.97 (s, 2H, CH₂O), 7.27–7.37 (m, 5H, H_{arom}); ¹³C NMR (125 MHz, DMSO-*d*₆) δ 21.28 (C-3', C-5'), 25.21 (C-4'), 31.92 (C-2', C-6'), 34.97 (NHCH₃), 58.63 (C-1'), 65.03 (CH₂O), 127.80 (C-2'', C-6''), 127.86 (C-4''), 128.36 (C-3'', C-5''), 137.36 (C-1'), 154.64 (OCO); MS(ESI) *m/z* = 320.2 ([M + H]⁺).

3.3.9. PREPARATION OF 41

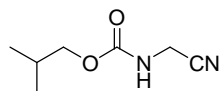
Isobutyl 1,2-dimethylhydrazinecarboxylate. The oily reaction mixture (for reaction conditions, see **3.3.8.**, method A) was separated by column chromatography using ethyl acetate/petroleum ether (9:1) as eluent to obtain a colorless oil (0.50 g) containing compound **41** contaminated with *N*-(Benzyloxycarbonyl)homocycloleucine (compound **40**, see **3.3.8.**). Using ^1H NMR spectrum, the yield of compound **41** was calculated to 0.32 g (28%). ^1H NMR (500 MHz, $\text{DMSO-}d_6$) δ 0.89 (app. d, $^3J = 6.6$ Hz, 6H, $\text{CH}(\text{CH}_3)_2$), 1.86 (sept, $^3J = 6.7$ Hz, 1H, $\text{CH}(\text{CH}_3)_2$), 2.43 (s, 3H, NHCH_3), 2.93 (s, 3H, CONCH_3), 3.78 (d, $^3J = 6.6$ Hz, 2H, CHCH_2); ^{13}C NMR (125 MHz, $\text{DMSO-}d_6$) δ 18.98 ($\text{CH}(\text{CH}_3)_2$), 27.68 ($\text{CH}(\text{CH}_3)_2$), 35.49, 35.59 (NCH_3), 70.93 (CH_2O), 156.16 (OCO); MS(EI) $m/z = 160.1$ ($\text{M}^{\bullet+}$).

3.3.10. PREPARATION OF 42

***N*-(Benzyloxycarbonyl)homocycloleucyl-methylazaalanine-nitrile.** Compound **40** (0.44 g, 1.38 mmol) was dissolved in MeOH (10 mL) and treated with NaOAc (0.31 g, 3.78 mmol) and BrCN (0.30 g, 2.83 mmol). The resulting reaction mixture was stirred for 18 h at room temperature. The solvent was evaporated under reduced pressure. The residue was suspended in H₂O (10 mL), a pH of 1–2 was adjusted (10% KHSO₄), and it was extracted with ethyl acetate (3 × 20 mL). The combined organic layers were washed with H₂O (10 mL), sat. NaHCO₃ (2 × 10 mL), H₂O (10 mL), and brine (10 mL). The solvent was dried (Na₂SO₄) and removed *in vacuo*. The oily residue was purified by column chromatography on silica gel using ethyl acetate/petroleum ether (1:1) as eluent to obtain **42** as a colorless oil (0.24 g, 50%). ¹H NMR (500 MHz, DMSO-*d*₆) δ 1.16–1.25 (m, 1H, H_{cyclohexane}), 1.47 (bs, 5H, H_{cyclohexane}), 1.63–1.69 (m, 2H, H_{cyclohexane}), 1.98–2.01 (m, 2H, H_{cyclohexane}), 2.92 (s, 3H, N(CH₃)CN), 3.07 (s, 3H, CONCH₃), 4.97 (CH₂O), 7.29–7.36 (m, 5H, H_{arom}); ¹³C NMR (125 MHz, DMSO-*d*₆) δ 21.12 (C-3', C-5'), 24.92 (C-4'), 31.64 (C-2', C-6'), 40.41 (CONCH₃), 58.45 (C-1'), 65.69 (CH₂O), 115.02 (CN), 128.08 (C-2'', C-6''), 128.28 (C-4''), 128.48 (C-3'', C-5''), 137.00 (C-1''), 154.68 (OCO), 173.58 (NHCCO); Anal. C₁₈H₂₄N₄O₃ (344.41 g/mol) calcd C 62.77, H 7.02, N 16.27; found C 62.70, H 7.17, N 15.49.

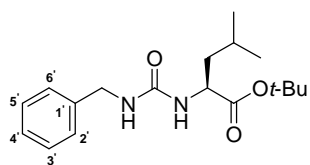
3.3.11. PREPARATION OF 43

***N*-(Benzyloxycarbonyl)homocycloleucyl-glycine-nitrile.** Compound **39** (1.00 g, 3.61 mmol) was dissolved in dry THF (20 mL) and cooled to -25 °C. To the stirred solution, triethylamine (1.09 g, 10.8 mmol) and isobutyl chloroformate (0.54 g, 3.95 mmol) were added consecutively. Aminoacetonitrile monosulfate (1.64 g, 10.6 mmol) was added to the reaction mixture when the precipitation of triethylamine hydrochloride occurred (ca. 5 min). It was allowed to warm to room temperature within 30 min, and stirred for additional overnight. After evaporation of the solvent, the resulting aqueous residue was extracted with ethyl acetate (3 × 60 mL). The combined organic layers were washed with 10% KHSO₄ (30 mL), H₂O (30 mL), sat. NaHCO₃ (30 mL), H₂O (30 mL), and brine (30 mL). The solvent was dried (Na₂SO₄) and evaporated. The product mixture was separated by column chromatography using ethyl acetate/petroleum ether (1:1) as eluent to obtain **43** as a white solid (0.60 g, 53%). mp 110–112 °C; ¹H NMR (500 MHz, DMSO-*d*₆) δ 1.15–1.25 (m, 1H, H_{cyclohexane}), 1.45–1.51 (m, 5H, H_{cyclohexane}), 1.63–1.69 (m, 2H, H_{cyclohexane}), 1.89–1.92 (m, 2H, H_{cyclohexane}), 4.03 (d, ³*J* = 5.1 Hz, 2H, NHCH₂CN), 5.00 (s, 2H, CH₂O), 7.27–7.36 (m, 6H, OCONH/H_{arom}), 8.20 (bs, 1H, NHCH₂CN); ¹³C NMR (125 MHz, DMSO-*d*₆) δ 21.03 (C-3', C-5'), 25.03 (C-4'), 27.76 (NHCH₂CN), 31.81 (C-2', C-6'), 58.90 (C-1'), 65.28 (CH₂O), 117.82 (CN), 127.74 (C-2'', C-6''), 127.84 (C-4''), 128.43 (C-3'', C-5''), 137.20 (C-1''), 154.86 (OCO), 175.20 (NHCCO); Anal. C₁₇H₂₁N₃O₃ (315.37 g/mol) calcd C 64.74, H 6.71, N 13.32; found C 64.76, H 6.72, N 12.81.

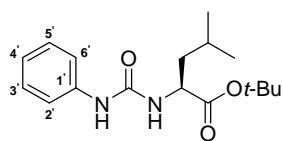
3.3.12. PREPARATION OF 44

***N*-(Isobutyloxycarbonyl)aminoacetonitrile.** The product mixture (for reaction conditions, see **3.3.11.**) was separated by column chromatography using ethyl acetate/petroleum ether (1:1) as eluent to obtain **44** as a colorless oil (0.20 g, 35%). ¹H NMR (500 MHz, DMSO-*d*₆) δ 0.87 (app. d, ³*J* = 6.6 Hz, 6H, CH(CH₃)₂), 1.80–1.88 (m, 1H, CH(CH₃)₂), 3.79 (d, ³*J* = 6.7 Hz, 2H, CH₂O), 4.05 (d, ³*J* = 6.0 Hz, 2H, NHCH₂CN), 7.84 (bs, NHCH₂CN); ¹³C NMR (125 MHz, DMSO-*d*₆) δ 19.64 (CH(CH₃)₂), 28.40 (CH(CH₃)₂), 29.90 (NHCH₂CN), 71.43 (CH₂O), 118.76 (CN), 157.16 (OCO); MS(ESI) *m/z* (neg.) = 155.1 ([M - H]⁻).

3.3.13. PREPARATION OF 48

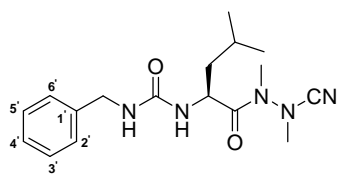


***N*-(Benzylcarbamoyl)leucine *tert*-butyl ester.** The hydrochloride salt of **47** (2.50 g, 11.2 mmol) was dissolved in H₂O (10 mL) and treated with 1 N NaOH solution (13.0 mL). The precipitated free base was extracted with ethyl acetate (3 × 20 mL). The combined organic layers were washed with H₂O (10 mL) and brine (10 mL), and dried over Na₂SO₄. The solvent was removed *in vacuo* to obtain leucine *tert*-butyl ester **47** as a colorless oily residue. This residue was dissolved in dry THF (40 mL) and treated with CDI (2.00 g, 12.3 mmol). The resulting solution was heated to reflux for 2 h. The reaction mixture was further treated with benzylamine (2.01 mL, 18.4 mmol) and heated to reflux for 18 h. After evaporation of the solvent, the residue was suspended in H₂O. The resulting aqueous suspension was adjusted with 10% KHSO₄ to pH ~2 and extracted with ethyl acetate (3 × 20 mL). The combined organic layers were washed with H₂O (20 mL), 10% KHSO₄ (20 mL), H₂O (20 mL), and brine (20 mL). The solvent was dried (Na₂SO₄) and removed *in vacuo*. The solid product was purified by column chromatography using ethyl acetate/petroleum ether (1:1) as eluent to obtain **48** as a white solid (3.25 g, 91%). mp 69 °C; ¹H NMR (500 MHz, DMSO-*d*₆) δ 0.86 (d, ³*J* = 6.3 Hz, 3H, CH₃CHCH₃), 0.89 (d, ³*J* = 7.0 Hz, 3H, CH₃CHCH₃), 1.39 (s, 9H, C(CH₃)₃), 1.41–1.44 (m, 2H, CHCH₂), 1.59–1.68 (m, 1H, CH₃CHCH₃), 4.05–4.09 (m, 1H, NHCHCO), 4.16–4.24 (m, 2H, CH₂NH), 6.15 (d, ³*J* = 8.5 Hz, 1H, NHCHCO), 6.40 (t, ³*J* = 6.0 Hz, 1H, CH₂NH), 7.19–7.31 (m, 5H, H_{arom}); ¹³C NMR (125 MHz, DMSO-*d*₆) δ 21.85, 22.81, 24.49 (CH₃CHCH₃, CH₃CHCH₃, CH₃CHCH₃), 27.78 (C(CH₃)₃), 41.26, 42.94 (CHCH₂, CH₂NH), 51.86 (NHCHCO), 80.27 (C(CH₃)₃), 126.69 (C-4'), 127.06 (C-2', C-6'), 128.29 (C-3', C-5'), 140.83 (C-1'), 157.77 (NHCONH), 173.07 (NHCHCO); Anal. C₁₈H₂₈N₂O₃ (320.43 g/mol) calcd C 67.47, H 8.81, N 8.74; found C 67.59, H 9.12, N 8.54.

3.3.14. PREPARATION OF 49

***N*-(Phenylcarbonyl)leucine *tert*-butyl ester.** The hydrochloride salt of **47** (2.50 g, 11.2 mmol) was dissolved in H₂O (10 mL) and treated with 1 N NaOH solution (13.0 mL). The precipitated free base was extracted with ethyl acetate (3 × 20 mL). The combined organic layers were washed with H₂O (10 mL) and brine (10 mL), and dried over Na₂SO₄. The solvent was removed *in vacuo* to obtain leucine *tert*-butyl ester **47** as a colorless oily residue. This residue was dissolved in dry THF (40 mL) and treated with CDI (2.00 g, 12.3 mmol). The resulting solution was heated to reflux for 2 h. The solvent was removed *in vacuo*, and the obtained residue was treated with dry MeCN (40 mL) and DIPEA (3.05 mL, 17.8 mmol). Aniline (1.67 mL, 18.3 mmol) was further added, and the reaction mixture was heated to reflux for 39 h. After evaporation of the solvent, the residue was suspended in H₂O. The resulting aqueous suspension was adjusted to pH ~2 with 10% KHSO₄ and extracted with ethyl acetate (3 × 20 mL). The combined organic layers were washed with H₂O (20 mL), 10% KHSO₄ (20 mL), H₂O (20 mL), and brine (20 mL). The solvent was dried (Na₂SO₄) and removed *in vacuo*. The oily product was purified by column chromatography using ethyl acetate/petroleum ether (1:2) as eluent to obtain **49** as a white solid (1.29 g, 38%). mp 106–108 °C; ¹H NMR (500 MHz, DMSO-*d*₆) δ 0.89 (d, ³*J* = 6.6 Hz, 3H, CH₃CHCH₃), 0.92 (d, ³*J* = 6.6 Hz, 3H, CH₃CHCH₃), 1.41 (s, 9H, C(CH₃)₃), 1.44–1.50 (m, 2H, CHCH₂), 1.61–1.71 (m, 1H, CH₃CHCH₃), 4.10–4.15 (m, 1H, NHCHCO), 6.35 (d, ³*J* = 8.2 Hz, 1H, NHCHCO), 6.87–7.37 (m, 5H, H_{arom}), 8.51 (s, 1H, C-1'NH); ¹³C NMR (125 MHz, DMSO-*d*₆) δ 21.84, 22.77, 24.53 (CH₃CHCH₃, CH₃CHCH₃, CH₃CHCH₃), 27.77 (C(CH₃)₃), 41.13 (CHCH₂), 51.50 (NHCHCO), 80.62 (C(CH₃)₃), 117.72 (C-2', C-6'), 121.35 (C-4'), 128.78 (C-3', C-5'), 140.25 (C-1'), 154.87 (NHCONH), 172.69 (NHCHCO); Anal. C₁₇H₂₆N₂O₃ (306.40 g/mol) calcd C 66.64, H 8.55, N 9.14; found C 66.23, H 8.91, N 8.78.

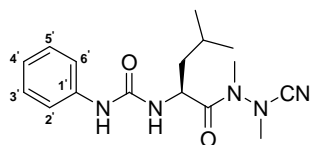
3.3.15. PREPARATION OF 50



***N*-(Benzylcarbamoyl)leucyl-methylazaalanine-nitrile.** Compound **48** (2.00 g, 6.24 mmol) was dissolved in CH₂Cl₂ (40 mL) and treated with TFA (20 mL). The resulting solution was stirred for 3 h at room temperature. After evaporation of the solvent, the oily residue was suspended in H₂O. The resulting aqueous suspension was extracted with ethyl acetate (3 × 20 mL). The combined organic layers were washed with H₂O (2 × 30 mL) and brine (30 mL). The solvent was dried (Na₂SO₄) and removed under reduced pressure. The crude solid product was recrystallized from ethyl acetate/*n*-hexane to obtain *N*-(benzylcarbamoyl)-leucine (0.52 g, 32%). *N*-(Benzylcarbamoyl)leucine (0.48 g, 1.82 mmol) was dissolved in dry THF (20 mL) and cooled to -25 °C. To the stirred solution, *N*-methylmorpholine (0.22 mL, 2.00 mmol) and isobutyl chloroformate (0.26 mL, 1.99 mmol) were added consecutively. 1,2-Dimethylhydrazine dihydrochloride (1.21 g, 9.10 mmol) was suspended in H₂O (1 mL), and 5 N NaOH (4.36 mL) was added under ice-cooling. This solution was given to the reaction mixture when the precipitation of *N*-methylmorpholine hydrochloride occurred. It was allowed to warm to room temperature within 30 min, and stirred for additional 90 min. After evaporation of the solvent, the resulting aqueous residue was extracted with ethyl acetate (3 × 20 mL). The combined organic layers were washed with sat. NaHCO₃ (20 mL), H₂O (20 mL), and brine (20 mL). The solvent was dried (Na₂SO₄) and evaporated. The obtained oily residue was purified by column chromatography on silica gel using ethyl acetate as eluent to obtain *N*-(benzylcarbamoyl)leucine 1,2-dimethylhydrazide. Sodium acetate (0.11 g, 1.34 mmol) and cyanogen bromide (0.07 g, 0.66 mmol) were added to a solution of *N*-(benzylcarbamoyl)leucine 1,2-dimethylhydrazide (0.18 g, 0.59 mmol) in MeOH (30 mL). The mixture was stirred at room temperature for 48 h, and the solvent was removed under reduced pressure. The residue was suspended in H₂O (10 mL), a pH of ~2 was adjusted (10% KHSO₄), and it was extracted with ethyl acetate (3 × 20 mL). The combined organic layers were washed with H₂O (20 mL), sat. NaHCO₃ (2 × 20 mL), H₂O (20 mL), and brine (20 mL). The solvent was dried (Na₂SO₄) and removed *in vacuo*. The oily residue was purified by column chromatography on silica gel using ethyl acetate/petroleum ether (1:1) as eluent to obtain **50** as a white solid (0.15 g, 25% from *N*-(benzylcarbamoyl)leucine). mp 116–118 °C; $[\alpha]_D^{20} = +2.8$ (c = 0.58, CHCl₃); ¹H NMR (500 MHz, DMSO-*d*₆) mixture of rotamers (only the data of the major rotational isomer are noted) δ 0.90–0.93 (m, 6H, CH(CH₃)₂), 1.28–1.43

(m, 2H, CHCH₂), 1.68 (bs, 1H, CH(CH₃)₂), 3.08, 3.22 (2 × s, 2 × 3H, N(CH₃)CN, CONCH₃), 4.19 (d, 2H, ³J = 5.7 Hz, 2H, CH₂NH), 4.74–4.77 (m, 1H, NHCHCO), 6.30 (d, ³J = 8.6 Hz, 1H, NHCHCO), 6.42 (t, ³J = 5.7 Hz, 1H, CH₂NH), 7.19–7.31 (m, 5H, H_{arom}); ¹³C NMR (125 MHz, DMSO-*d*₆) δ 21.44, 23.31, 24.50 (CH₃CHCH₃, CH₃CHCH₃, CH₃CHCH₃), 30.48 (N(CH₃)CN), CONCH₃ obscured by the DMSO signal, 41.00, 42.97 (CHCH₂, CH₂NH), 47.98 (NHCHCO), 114.30 (CN), 126.73 (C-4'), 127.08 (C-2', C-6'), 128.35 (C-3', C-5'), 140.68 (C-1'), 158.01 (NHCONH), 175.32 (NHCHCO); FTIR (KBr, cm⁻¹) 2220 (C≡N); Anal. C₁₇H₂₅N₅O₂ (331.41 g/mol) calcd C 61.61, H 7.60, N 21.13; found C 61.44, H 7.57, N 20.40; LC-MS(ESI) (90% H₂O to 100% MeOH in 20 min, then 100% MeOH to 30 min, DAD 200.0–300.0 nm) t_r = 15.64, 98% purity, *m/z* = 332.2 ([M + H]⁺).

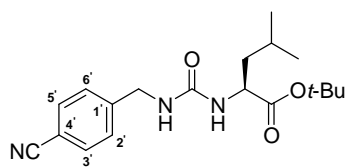
3.3.16. PREPARATION OF 51



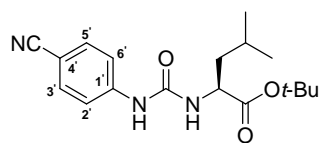
***N*-(Phenylcarbamoyl)leucyl-methylazaalanine-nitrile.** Compound **49** (1.23 g, 4.01 mmol) was dissolved in CH₂Cl₂ (40 mL) and treated with TFA (20 mL). The resulting solution was stirred for 3 h at room temperature. After evaporation of the solvent, the oily residue was suspended in H₂O. The aqueous suspension was extracted with ethyl acetate (3 × 20 mL). The combined organic layers were washed with H₂O (20 mL), 10% KHSO₄ (20 mL), H₂O (20 mL), and brine (20 mL). The solvent was dried (Na₂SO₄) and removed under reduced pressure. The solid product was recrystallized from ethyl acetate/*n*-hexane to obtain *N*-(phenylcarbamoyl)leucine (0.50 g, 50%). *N*-(Phenylcarbamoyl)leucine (0.50 g, 2.00 mmol) was dissolved in dry THF (20 mL) and cooled to -25 °C. To the stirred solution, *N*-methylmorpholine (0.24 mL, 2.18 mmol) and isobutyl chloroformate (0.29 mL, 2.22 mmol) were added consecutively. 1,2-Dimethylhydrazine dihydrochloride (1.47 g, 11.1 mmol) was suspended in H₂O (1 mL), and 5 N NaOH (5.33 mL) was added under ice-cooling. This solution was given to the reaction mixture when the precipitation of *N*-methylmorpholine hydrochloride occurred. It was allowed to warm to room temperature within 30 min, and stirred for additional 90 min. After evaporation of the solvent, the resulting aqueous residue was extracted with ethyl acetate (3 × 20 mL). The combined organic layers were washed with H₂O (20 mL), sat. NaHCO₃ (20 mL), H₂O (20 mL), and brine (20 mL). The solvent was dried (Na₂SO₄) and evaporated. The obtained oily residue was purified by column chromatography on silica gel using ethyl acetate as eluent to obtain *N*-(phenylcarbamoyl)leucine 1,2-dimethylhydrazide. Sodium acetate (0.07 g, 0.85 mmol) and cyanogen bromide (0.04 g, 0.38 mmol) were added to a solution of *N*-(phenylcarbamoyl)leucine 1,2-dimethylhydrazide (0.11 g, 0.38 mmol) in MeOH (30 mL). The mixture was stirred at room temperature for 48 h, and the solvent was removed under reduced pressure. The oily residue was purified by column chromatography on silica gel using ethyl acetate/petroleum ether (1:1) as eluent to obtain **51** as a white solid (0.18 g, 28% from *N*-(phenylcarbamoyl)leucine). mp 103–105 °C; $[\alpha]_D^{20} = +29.5$ ($c = 1.23$, CHCl₃); ¹H NMR (500 MHz, DMSO-*d*₆) mixture of rotamers (only the data of the major rotational isomer are noted) δ 0.93–0.97 (m, 6H, CH(CH₃)₂), 1.35–1.51 (m, 2H, CHCH₂), 1.72 (bs, 1H, CH(CH₃)₂), 3.10, 3.26 (2 × s, 2 × 3H, N(CH₃)CN, CONCH₃), 4.79–4.82 (m, 1H, NHCHCO), 6.48 (d, ³*J* = 7.9 Hz, 1H, NHCHCO), 6.88–7.36 (m, 5H, H_{arom}), 8.53 (s, 1H, C-1'NH); ¹³C NMR (125 MHz, DMSO-*d*₆) δ 21.43, 23.30, 24.55

(CH₃CHCH₃, CH₃CHCH₃, CH₃CHCH₃), 30.53 (N(CH₃)CN), CONCH₃ obscured by the DMSO signal, 41.02 (CHCH₂), 47.78 (NHCHCO), 114.24 (CN), 117.80 (C-2', C-6'), 121.49 (C-4'), 128.81 (C-3', C-5'), 140.09 (C-1'), 155.20 (NHCONH), 174.88 (NHCHCO); FTIR (KBr, cm⁻¹) 2224 (C≡N); Anal. C₁₆H₂₃N₅O₂ (317.39 g/mol) calcd C 60.55, H 7.30, N 22.07; found C 60.11, H 7.36, N 21.15; LC-MS(ESI) (90% H₂O to 100% MeOH in 20 min, then 100% MeOH to 30 min, DAD 220.0–400.0 nm) t_r = 16.24, 94% purity, m/z = 318.3 ([M + H]⁺).

3.3.17. PREPARATION OF 52

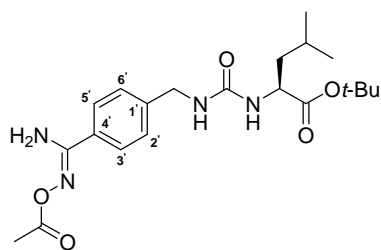


***N*-(4-Cyanobenzylcarbamoyl)leucine *tert*-butyl ester.** The hydrochloride salt of **47** (5.00 g, 22.3 mmol) was dissolved in H₂O (10 mL) and treated with 1 N NaOH solution (24.0 mL). The precipitated free base was extracted with ethyl acetate (3 × 20 mL). The combined organic layers were washed with H₂O (10 mL) and brine (20 mL), and dried over Na₂SO₄. The solvent was removed *in vacuo* to obtain leucine *tert*-butyl ester **47** as a colorless oily residue. This residue was dissolved in dry THF (40 mL) and treated with CDI (3.62 g, 22.3 mmol). The resulting solution was heated to reflux for 2 h. The reaction mixture was further treated with DIPEA (5.73 mL, 33.5 mmol) and 4-(aminomethyl)benzonitrile hydrochloride (5.65 g, 33.5 mmol) and heated to reflux for 18 h. The solvent was evaporated, and the residue was suspended in H₂O. The aqueous suspension was adjusted to pH ~2 with 10% KHSO₄ and extracted with ethyl acetate (3 × 30 mL). The combined organic layers were washed with H₂O (30 mL), 10% KHSO₄ (30 mL), H₂O (30 mL), and brine (30 mL). The solvent was dried (Na₂SO₄) and removed under reduced pressure. The crude product was recrystallized from ethyl acetate to obtain **52** as a white solid (5.72 g, 74%). mp 157 °C; ¹H NMR (500 MHz, DMSO-*d*₆) δ 0.85 (d, ³*J* = 6.6 Hz, 3H, CH₃CHCH₃), 0.89 (d, ³*J* = 6.6 Hz, 3H, CH₃CHCH₃), 1.38 (s, 9H, C(CH₃)₃), 1.41–1.44 (m, 2H, CHCH₂), 1.59–1.67 (m, 1H, CH₃CHCH₃), 4.03–4.07 (m, 1H, NHCHCO), 4.24–4.32 (m, 2H, CH₂NH), 6.28 (d, ³*J* = 8.5 Hz, 1H, NHCHCO), 6.54 (t, ³*J* = 6.2 Hz, 1H, CH₂NH), 7.41 (d, ³*J* = 8.5 Hz, 2H, H-2', H-6'), 7.76 (d, ³*J* = 8.5 Hz, 2H, H-3', H-5'); ¹³C NMR (125 MHz, DMSO-*d*₆) δ 21.82, 22.80, 24.50 (CH₃CHCH₃, CH₃CHCH₃, CH₃CHCH₃), 27.78 (C(CH₃)₃), 41.13, 42.72 (CHCH₂, CH₂NH), 51.92 (NHCHCO), 80.31 (C(CH₃)₃), 109.43 (C-4'), 119.04 (CN), 127.83 (C-2', C-6'), 132.24 (C-3', C-5'), 147.08 (C-1'), 157.79 (NHCONH), 173.00 (NHCHCO); Anal. C₁₉H₂₇N₃O₃ (345.44 g/mol) calcd C 66.06, H 7.88, N 12.16; found C 66.46, H 7.90, N 12.30.

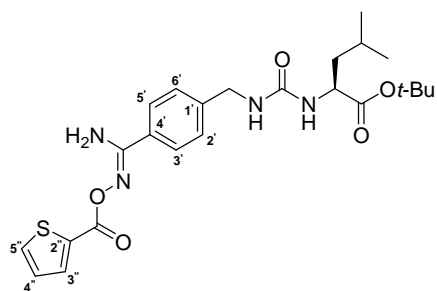
3.3.18. PREPARATION OF 53

***N*-(4-Cyanophenylcarbamoyl)leucine *tert*-butyl ester.** The hydrochloride salt of **47** (5.00 g, 22.3 mmol) was dissolved in dry THF (50 mL) and treated with DIPEA (5.70 mL, 33.3 mmol). The resulting reaction mixture was treated with 4-cyanophenyl isocyanate (3.55 g, 24.6 mmol) and stirred for 4 h at room temperature. After evaporation of the solvent, the residue was suspended in H₂O. The aqueous suspension was adjusted with 10% KHSO₄ to pH ~2 and extracted with ethyl acetate (3 × 30 mL). The combined organic layers were washed with H₂O (20 mL), 10% KHSO₄ (20 mL), H₂O (20 mL), and brine (20 mL). The solvent was dried (Na₂SO₄) and evaporated under reduced pressure. The crude product was recrystallized from ethyl acetate/petroleum ether to obtain **53** as a white solid (6.70 g, 91%). mp 113 °C; ¹H NMR (500 MHz, DMSO-*d*₆) δ 0.88 (d, ³*J* = 6.6 Hz, 3H, CH₃CHCH₃), 0.91 (d, ³*J* = 6.7 Hz, 3H, CH₃CHCH₃), 1.40 (s, 9H, C(CH₃)₃), 1.46–1.54 (m, 2H, CHCH₂), 1.62–1.70 (m, 1H, CH₃CHCH₃), 4.10–4.14 (m, 1H, NHCHCO), 6.61 (d, ³*J* = 8.2 Hz, 1H, NHCHCO), 7.54 (d, ³*J* = 8.9 Hz, 2H, H-3', H-5'), 7.65 (d, ³*J* = 8.8 Hz, 2H, H-2', H-6'), 9.07 (s, 1H, C-1'NH); ¹³C NMR (125 MHz, DMSO-*d*₆) δ 21.82, 22.77, 24.56 (CH₃CHCH₃, CH₃CHCH₃, CH₃CHCH₃), 27.78 (C(CH₃)₃), 40.91 (CHCH₂), 51.64 (NHCHCO), 80.85 (C(CH₃)₃), 102.88 (C-4'), 117.68 (C-2', C-6'), 119.48 (CN), 133.36 (C-3', C-5'), 144.69 (C-1'), 154.40 (NHCONH), 172.36 (NHCHCO); Anal. C₁₈H₂₅N₃O₃ (331.41 g/mol) calcd C 65.23, H 7.60, N 12.68; found C 65.21, H 7.20, N 12.25.

3.3.19. PREPARATION OF 54

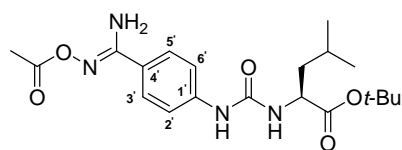


***N*-[(4-Acetoxyamidino)benzylcarbamoyl]leucine *tert*-butyl ester.** Compound **52** (2.00 g, 5.79 mmol) was dissolved in EtOH (50 mL) and treated with DIPEA (1.97 mL, 11.5 mmol) and hydroxylamine hydrochloride (0.81 g, 11.7 mmol). The resulting solution was heated to reflux overnight. EtOH was evaporated, the oily residue was dissolved in dry MeCN (50 mL) and treated with acetic anhydride (1.64 mL, 17.5 mmol). The resulting solution was stirred at room temperature for 5 h. The solvent was removed *in vacuo*, and the oily residue was suspended in H₂O. The aqueous suspension was adjusted to pH ~2 with 10% KHSO₄ and extracted with ethyl acetate (3 × 20 mL). The combined organic layers were washed with 5% KHSO₄ (2 × 20 mL), H₂O (20 mL), sat. NaHCO₃ (2 × 20 mL), H₂O (20 mL), and brine (20 mL). The solvent was dried (Na₂SO₄) and removed under reduced pressure. The solid product was recrystallized from ethyl acetate/*n*-hexane to obtain **54** as a white solid (1.86 g, 76% from **52**). mp 148 °C; ¹H NMR (500 MHz, DMSO-*d*₆) δ 0.86 (d, ³*J* = 6.6 Hz, 3H, CH₃CHCH₃), 0.89 (d, ³*J* = 6.6 Hz, 3H, CH₃CHCH₃), 1.39 (s, 9H, C(CH₃)₃), 1.42–1.44 (m, 2H, CHCH₂), 1.60–1.68 (m, 1H, CH₃CHCH₃), 2.12 (s, 3H, CH₃CO), 4.04–4.09 (m, 1H, NHCHCO), 4.20–4.28 (m, 2H, CH₂NH), 6.21 (d, ³*J* = 8.2 Hz, 1H, NHCHCO), 6.46 (t, ³*J* = 6.2 Hz, 1H, CH₂NH), 6.72 (s, 2H, NH₂), 7.28, 7.64 (d, ³*J* = 8.5 Hz, 2H, d, ³*J* = 8.2 Hz, 2H, H-2', H-6', H-3', H-5'); ¹³C NMR (125 MHz, DMSO-*d*₆) δ 20.00 (CH₃CO), 21.87, 22.85, 24.54 (CH₃CHCH₃, CH₃CHCH₃, CH₃CHCH₃), 27.83 (C(CH₃)₃), 41.23, 42.68 (CHCH₂, CH₂NH), 51.91 (NHCHCO), 80.34 (C(CH₃)₃), 126.70, 126.88 (C-3', C-5', C-2', C-6'), 130.08 (C-4'), 143.49 (C-1'), 156.41 (C=N), 157.83 (NHCONH), 168.64 (CH₃CO), 173.10 (NHCHCO); Anal. C₂₁H₃₂N₄O₅ (420.50 g/mol) calcd C 59.98, H 7.67, N 13.32; found C 59.64, H 7.48, N 13.05.

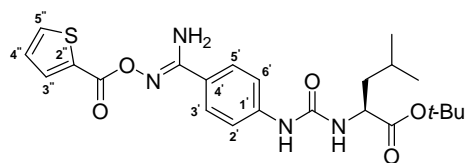
3.3.20. PREPARATION OF 55***N*-{4-[(2-Thiophenecarbonyl)oxyamidino]benzylcarbamoyl}leucine *tert*-butyl ester.**

Compound **52** (3.00 g, 8.68 mmol) was dissolved in EtOH (50 mL), and treated with DIPEA (2.98 mL, 17.4 mmol) and hydroxylamine hydrochloride (1.21 g, 17.4 mmol). The resulting solution was heated to reflux overnight. After evaporation of the solvent, the oily residue was suspended in H₂O. The aqueous suspension was adjusted with 10% KHSO₄ to pH ~2 and extracted with ethyl acetate (3 × 30 mL). The combined organic layers were washed with 10% KHSO₄ (20 mL), H₂O (20 mL), sat. NaHCO₃ (2 × 20 mL), H₂O (20 mL), and brine (20 mL). The solvent was dried (Na₂SO₄) and removed under reduced pressure. The resulting oily residue (2.48 g, 6.55 mmol) was dissolved in dry MeCN (30 mL) and treated with DIPEA (2.24 mL, 13.1 mmol) and 2-thiophenecarbonyl chloride (1.40 mL, 13.1 mmol). The solution was stirred at room temperature for 5 h. The precipitated product was filtrated and washed with 10% KHSO₄ (3 × 20 mL), H₂O (20 mL), sat. NaHCO₃ (3 × 20 mL), H₂O (20 mL), and *n*-hexane (20 mL). The dry product was recrystallised from ethyl acetate/EtOH (10:3) to obtain **55** as a white solid (2.22 g, 52% from **52**). mp 193 °C; ¹H NMR (500 MHz, DMSO-*d*₆) δ 0.87 (d, ³*J* = 6.6 Hz, 3H, CH₃CHCH₃), 0.90 (d, ³*J* = 6.7 Hz, 3H, CH₃CHCH₃), 1.40 (s, 9H, C(CH₃)₃), 1.42–1.45 (m, 2H, CHCH₂), 1.61–1.69 (m, 1H, CH₃CHCH₃), 4.05–4.10 (m, 1H, NHCHCO), 4.22–4.30 (m, 2H, CH₂NH), 6.21 (d, ³*J* = 8.5 Hz, 1H, NHCHCO), 6.48 (t, ³*J* = 6.2 Hz, 1H, CH₂NH), 6.87 (s, 2H, NH₂), 7.24 (dd, ³*J* = 4.9 Hz, ³*J* = 3.6 Hz, 1H, H-4''), 7.32, 7.69 (d, ³*J* = 8.5 Hz, 2H, d, ³*J* = 8.6 Hz, 2H, H-2', H-6', H-3', H-5'), 7.96 (dd, ³*J* = 4.7 Hz, ⁴*J* = 1.3 Hz, 1H, H-5''), 8.12 (dd, ³*J* = 3.8 Hz, ⁴*J* = 1.3 Hz, 1H, H-3''); ¹³C NMR (125 MHz, DMSO-*d*₆) δ 21.85, 22.82, 24.51 (CH₃CHCH₃, CH₃CHCH₃, CH₃CHCH₃), 27.81 (C(CH₃)₃), 41.21, 42.67 (CHCH₂, CH₂NH), 51.88 (NHCHCO), 80.30 (C(CH₃)₃), 126.87, 126.90, 128.35, 129.94, 132.86, 133.76, 133.88, 143.65 (C-3', C-5', C-4', C-2', C-6', C-4'', C-5'', C-3'', C-2'', C-1'), 156.98 (N=C), 157.79 (NHCONH), 159.79 (C-2''CO), 173.07 (NHCHCO); Anal. C₂₄H₃₂N₄O₅S (488.60 g/mol) calcd C 59.00, H 6.60, N 11.47; found C 59.04, H 6.51, N 11.44.

3.3.21. PREPARATION OF 56

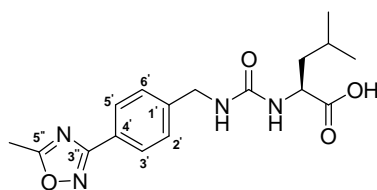


***N*-[(4-Acetoxyamidino)phenylcarbamoyl]leucine *tert*-butyl ester.** Compound **53** (6.30 g, 19.0 mmol) was dissolved in EtOH (50 mL), and treated with DIPEA (6.46 mL, 37.7 mmol) and hydroxylamine hydrochloride (2.64 g, 38.0 mmol). The resulting solution was heated to reflux overnight. After evaporation of the solvent, the oily residue was dissolved in dry MeCN (50 mL) and treated with acetic anhydride (5.39 mL, 57.4 mmol). The solution was stirred at room temperature for 5 h. The solvent was removed *in vacuo*, and the oily residue was suspended in H₂O. The aqueous suspension was adjusted with 10% KHSO₄ to pH ~2 and extracted with ethyl acetate (3 × 30 mL). The combined organic layers were washed with 5% KHSO₄ (2 × 30 mL), H₂O (30 mL), sat. NaHCO₃ (3 × 30 mL), H₂O (30 mL), and brine (30 mL). The solvent was dried (Na₂SO₄) and removed under reduced pressure. The crude product was recrystallized from ethyl acetate to obtain **56** as a white solid (5.40 g, 70% from **53**). mp 95 °C; ¹H NMR (500 MHz, DMSO-*d*₆) δ 0.89 (d, ³*J* = 6.6 Hz, 3H, CH₃CHCH₃), 0.92 (d, ³*J* = 6.6 Hz, 3H, CH₃CHCH₃), 1.41 (s, 9H, C(CH₃)₃), 1.44–1.54 (m, 2H, CHCH₂), 1.63–1.71 (m, 1H, CH₃CHCH₃), 2.11 (s, 3H, CH₃CO), 4.11–4.15 (m, 1H, NHCHCO), 6.45 (d, ³*J* = 8.2 Hz, 1H, NHCHCO), 6.62 (s, 2H, NH₂), 7.42, 7.59 (d, ³*J* = 8.9 Hz, 2H, d, ³*J* = 8.9 Hz, 2H, H-3', H-5', H-2', H-6'), 8.74 (s, 1H, C-1'NH); ¹³C NMR (125 MHz, DMSO-*d*₆) δ 20.00 (CH₃CO), 21.85, 22.77, 24.55 (CH₃CHCH₃, CH₃CHCH₃, CH₃CHCH₃), 27.78 (C(CH₃)₃), 41.07 (CHCH₂), 51.56 (NHCHCO), 80.73 (C(CH₃)₃), 116.98 (C-2', C-6'), 124.26 (C-4'), 127.42 (C-3', C-5'), 142.28 (C-1'), 154.66, 156.24 (N=C, NHCONH), 168.65, 172.56 (CH₃CO, NHCHCO); Anal. C₂₀H₃₀N₄O₅ (406.48 g/mol) calcd C 59.10, H 7.44, N 13.78; found C 58.96, H 7.41, N 13.41.

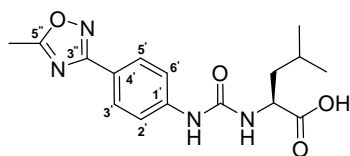
3.3.22. PREPARATION OF 57***N*-{4-[(2-Thiophenecarbonyl)oxyamidino]phenylcarbamoyl}leucine tert-butyl ester.**

Compound **53** (6.10 g, 18.4 mmol) was dissolved in EtOH (50 mL) and treated with DIPEA (6.30 mL, 36.8 mmol) and hydroxylamine hydrochloride (2.56 g, 36.8 mmol). The resulting solution was heated to reflux overnight. After evaporation of the solvent, the oily residue was suspended in H₂O. The aqueous suspension was adjusted to pH ~2 with 10% KHSO₄ and extracted with ethyl acetate (3 × 50 mL). The combined organic layers were washed with 10% KHSO₄ (30 mL), H₂O (30 mL), sat. NaHCO₃ (2 × 30 mL), H₂O (30 mL), and brine (30 mL). The solvent was dried (Na₂SO₄) and removed under reduced pressure. The resulting oily residue (3.96 g, 10.9 mmol) was dissolved in dry MeCN (50 mL), and treated with DIPEA (3.70 mL, 21.6 mmol) and 2-thiophenecarbonyl chloride (1.75 mL, 16.4 mmol). The solution was stirred at room temperature for 5 h. The precipitated product was filtrated and washed with 10% KHSO₄ (3 × 20 mL), H₂O (20 mL), sat. NaHCO₃ (3 × 20 mL), H₂O (20 mL) and *n*-hexane (20 mL). The dry product was recrystallised from ethyl acetate/EtOH (10:3) to obtain **57** as a white solid (3.58 g, 41% from **53**). mp 195–196°C; ¹H NMR (500 Hz, DMSO-*d*₆) δ 0.90 (d, ³*J* = 6.6 Hz, 3H, CH₃CHCH₃), 0.92 (d, ³*J* = 6.7 Hz, 3H, CH₃CHCH₃), 1.41 (s, 9H, C(CH₃)₃), 1.48–1.52 (m, 2H, CHCH₂), 1.64–1.72 (m, 1H, CH₃CHCH₃), 4.12–4.16 (m, 1H, NHCHCO), 6.47 (d, ³*J* = 8.2 Hz, 1H, NHCHCO), 6.77 (s, 2H, NH₂), 7.23 (dd, ³*J* = 4.9 Hz, ³*J* = 3.7 Hz, 1H, H-4''), 7.45, 7.64 (d, ³*J* = 8.8 Hz, 2H, d, ³*J* = 8.8 Hz, 2H, H-3', H-5', H-2', H-6'), 7.95 (dd, ³*J* = 5.1 Hz, ⁴*J* = 1.3 Hz, 1H, H-5''), 8.11 (dd, ³*J* = 3.6 Hz, ⁴*J* = 1.4 Hz, 1H, H-3''), 8.78 (s, 1H, C-1'NH); ¹³C NMR (125 MHz, DMSO-*d*₆) δ 21.87, 22.78, 24.57 (CH₃CHCH₃, CH₃CHCH₃, CH₃CHCH₃), 27.80 (C(CH₃)₃), 41.09 (CHCH₂), 51.58 (NHCHCO), 80.75 (C(CH₃)₃), 117.03 (C-2', C-6'), 124.12 (C-4'), 127.64 (C-3', C-5'), 128.34, 132.97, 133.67, 133.80 (C-4'', C-5'', C-3'', C-2''), 142.45 (C-1'), 154.68 (N=C), 156.86 (NHCONH), 159.83 (C-2''CO), 172.58 (NHCHCO); Anal. C₂₃H₃₀N₄O₅S (474.57 g/mol) calcd C 58.21, H 6.37, N 11.81; found C 58.12, H 6.28, N 11.40.

3.3.23. PREPARATION OF 58

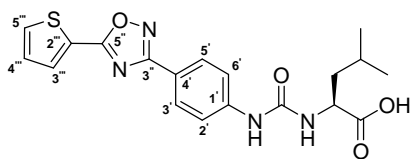


***N*-[4-(5-Methyl-1,2,4-oxadiazol-3-yl)benzylcarbamoyl]leucine.** Compound **54** (1.80 g, 4.28 mmol) was dissolved in concentrated acetic acid (40 mL) and stirred at 80 °C for 5 h. After evaporation of the acetic acid, the oily product was dissolved in CH₂Cl₂ (40 mL) and treated with TFA (20 mL). The resulting solution was stirred for 5 h at room temperature. The solvent was evaporated, and the oily residue was suspended in H₂O. The aqueous suspension was extracted with ethyl acetate (3 × 20 mL). The combined organic layers were washed with H₂O (2 × 30 mL) and brine (30 mL). The solvent was dried (Na₂SO₄) and removed under reduced pressure. The solid product was recrystallized from ethyl acetate/*n*-hexane to obtain **58** as a white solid (0.43 g, 29% from **54**). mp 171 °C; ¹H NMR (500 MHz, DMSO-*d*₆) δ 0.86 (d, ³*J* = 6.6 Hz, 3H, CH₃CHCH₃), 0.89 (d, ³*J* = 6.7 Hz, 3H, CH₃CHCH₃), 1.41–1.51 (m, 2H, CHCH₂), 1.61–1.69 (m, 1H, CH₃CHCH₃), 2.64 (s, 3H, CH₃C-5''), 4.11–4.15 (m, 1H, NHCHCO), 4.23–4.32 (m, 2H, CH₂NH), 6.24 (d, ³*J* = 8.5 Hz, 1H, NHCHCO), 6.51 (t, ³*J* = 6.1 Hz, 1H, CH₂NH), 7.40 (d, ³*J* = 8.5 Hz, 2H, H-2', H-6'), 7.92 (d, ³*J* = 8.5 Hz, 2H, H-3', H-5'), 12.40 (s, 1H, COOH); ¹³C NMR (125 MHz, DMSO-*d*₆) δ 12.13 (CH₃C-5''), 21.75, 22.96, 24.50 (CH₃CHCH₃, CH₃CHCH₃, CH₃CHCH₃), 41.18, 42.76 (CHCH₂, CH₂NH), 51.18 (NHCHCO), 124.76 (C-4'), 127.00, 127.74 (C-3', C-5', C-2', C-6'), 144.67 (C-1'), 157.94 (NHCONH), 167.64, 175.30, 177.46 (C-3'', NHCHCO, C-5''); Anal. C₁₇H₂₂N₄O₄ (346.38 g/mol) calcd C 58.95, H 6.40, N 16.17; found C 59.05, H 6.26, N 16.01.

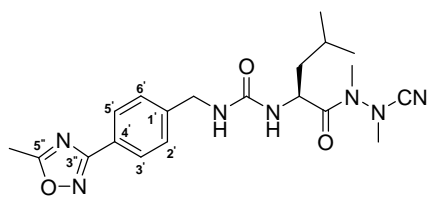
3.3.24. PREPARATION OF 60

N-[4-(5-Methyl-1,2,4-oxadiazol-3-yl)phenyl]leucine. Compound **56** (5.20 g, 12.8 mmol) was dissolved in concentrated acetic acid (40 mL) and stirred at 80 °C for 5 h. After evaporation of the acetic acid, the oily product was dissolved in CH₂Cl₂ (40 mL) and treated with TFA (20 mL). The resulted solution was stirred for 5 h at room temperature. The solvent was evaporated, and the oily residue was suspended in H₂O. The resulting aqueous suspension was extracted with ethyl acetate (3 × 20 mL). The combined organic layers were washed with H₂O (2 × 30 mL) and brine (30 mL). The solvent was dried (Na₂SO₄) and removed under reduced pressure. The solid product was recrystallized from ethyl acetate/*n*-hexane to obtain **60** as a white solid (2.80 g, 66% from **56**). mp 156–158 °C; ¹H NMR (500 MHz, DMSO-*d*₆) δ 0.89–0.92 (m, 6H, CH(CH₃)₂), 1.48–1.58 (m, 2H, CHCH₂), 1.65–1.73 (m, 1H, CH(CH₃)₂), 2.61 (CH₃C-5''), 4.17–4.23 (m, 1H, NHCHCO), 6.52 (d, ³*J* = 8.2 Hz, 1H, NHCHCO), 7.54 (d, ³*J* = 8.8 Hz, 2H, H-2', H-6'), 7.85 (d, ³*J* = 8.8 Hz, 2H, H-3', H-5'), 8.89 (s, 1H, C-1'NH), 12.62 (bs, 1H, COOH); ¹³C NMR (125 MHz, DMSO-*d*₆) δ 12.09 (CH₃C-5''), 21.76, 22.94, 24.55 (CH₃CHCH₃, CH₃CHCH₃, CH₃CHCH₃), 41.05 (CHCH₂), 50.90 (NHCHCO), 117.70 (C-2', C-6'), 119.00 (C-4'), 127.92 (C-3', C-5'), 143.23 (C-1'), 154.70 (NHCONH), 167.53, 174.80, 177.05, (C-3'', NHCHCO, C-5''); Anal. C₁₆H₂₀N₄O₄ (332.35 g/mol) calcd C 57.82, H 6.07, N 16.86; found C 57.75, H 6.38, N 15.75.

3.3.25. PREPARATION OF 61

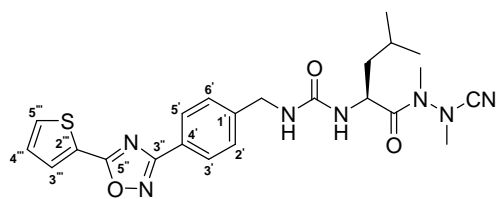


***N*-{4-[5-(2-Thienyl)-1,2,4-oxadiazol-3-yl]phenylcarbonyl}leucine.** Compound **57** (3.00 g, 6.32 mmol) was dissolved in concentrated acetic acid (40 mL) and stirred at 80 °C for 5 h. After evaporation of the acetic acid, the oily product was dissolved in CH₂Cl₂ (40 mL) and treated with TFA (20 mL). The resulting solution was stirred for 3 h at room temperature. After evaporation of the solvent, the oily residue was suspended in H₂O. The aqueous suspension was extracted with ethyl acetate (3 × 30 mL). The combined organic layers were washed with H₂O (2 × 30 mL) and brine (30 mL). The solvent was dried (Na₂SO₄) and removed under reduced pressure. The solid product was recrystallized from ethyl acetate/*n*-hexane to obtain **61** as a white solid (1.29 g, 51% from **57**). mp 146–148 °C; ¹H NMR (500 MHz, DMSO-*d*₆) δ 0.90–0.93 (m, 6H, CH(CH₃)₂), 1.49–1.59 (m, 2H, CHCH₂), 1.65–1.74 (m, 1H, CH(CH₃)₂), 4.19–4.23 (m, 1H, NHCHCO), 6.53 (d, ³*J* = 8.2 Hz, 1H, NHCHCO), 7.35 (dd, ³*J* = 5.1 Hz, ³*J* = 3.8 Hz, 1H, H-4'''), 7.58 (d, ³*J* = 8.8 Hz, 2H, H-2', H-6'), 7.92 (d, ³*J* = 8.5 Hz, 2H, H-3', H-5'), 8.05, 8.09 (dd, ³*J* = 3.8 Hz, ⁴*J* = 1.3 Hz, 1H, dd, ³*J* = 5.1 Hz, ⁴*J* = 1.0 Hz, 1H, H-5''', H-3'''), 8.94 (C-1'NH), 12.63 (s, 1H, COOH); ¹³C NMR (125 MHz, DMSO-*d*₆) δ 21.76, 22.94, 24.56 (CH₃CHCH₃, CH₃CHCH₃, CH₃CHCH₃), 41.02 (CHCH₂), 50.90 (NHCHCO), 117.72 (C-2', C-6'), 118.49 (C-5'''), 124.82 (C-4'), 128.17 (C-3', C-5'), 129.35, 132.77, 134.01, (C-3''', C-4''', C-2'''), 143.52 (C-1'), 154.67 (NHCONH), 168.06, 170.89, 174.78 (C-3'', NHCHCO, C-5''); Anal. C₁₉H₂₀N₄O₄S (400.45 g/mol) calcd C 56.99, H 5.03, N 13.99; found C 56.24, H 5.15, N 13.45.

3.3.26. PREPARATION OF 62***N*-[4-(5-Methyl-1,2,4-oxadiazol-3-yl)benzylcarbamoyl]leucyl-methylazaalanine-nitrile.**

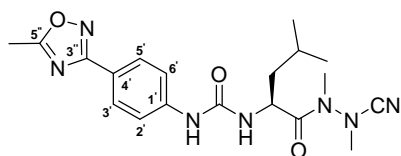
Compound **58** (0.25 g, 0.72 mmol) was dissolved in dry THF (30 mL) and cooled to $-25\text{ }^{\circ}\text{C}$. To the stirred solution, *N*-methylmorpholine (0.09 mL, 0.82 mmol) and isobutyl chloroformate (0.11 mL, 0.84 mmol) were added consecutively. 1,2-Dimethylhydrazine dihydrochloride (0.48 g, 3.61 mmol) was dissolved in H_2O (1 mL), and 5 N NaOH (2.00 mL) was added under ice-cooling. This solution was given to the reaction mixture when the precipitation of *N*-methylmorpholine hydrochloride occurred. It was allowed to warm to room temperature within 30 min, and stirred for additional 90 min. After evaporation of the solvent, the resulting aqueous residue was extracted with ethyl acetate ($3 \times 20\text{ mL}$). The combined organic layers were washed with H_2O (20 mL), sat. NaHCO_3 (20 mL), H_2O (20 mL), and brine (20 mL). The solvent was dried (Na_2SO_4) and evaporated. The crude product was purified by column chromatography on silica gel using $\text{MeOH}/\text{CH}_2\text{Cl}_2$ (1:40) to obtain *N*-[4-(5-methyl-1,2,4-oxadiazol-3-yl)benzylcarbamoyl]leucine 1,2-dimethylhydrazide as a colorless oil. Sodium acetate (0.14 g, 1.71 mmol) and cyanogen bromide (0.07 g, 0.66 mmol) were added to a solution of *N*-[4-(5-methyl-1,2,4-oxadiazol-3-yl)benzylcarbamoyl]leucine 1,2-dimethylhydrazide (0.26 g, 0.67 mmol) in MeOH (30 mL). The mixture was stirred at room temperature for 24 h, and the solvent was removed under reduced pressure. The residue was suspended in H_2O (10 mL), a pH of ~ 2 was adjusted (10% KHSO_4), and it was extracted with ethyl acetate ($3 \times 20\text{ mL}$). The combined organic layers were washed with H_2O (20 mL), sat. NaHCO_3 ($2 \times 20\text{ mL}$), H_2O (20 mL), and brine (20 mL). The solvent was dried (Na_2SO_4) and removed *in vacuo*. The oily residue was purified by column chromatography on silica gel using $\text{MeOH}/\text{CH}_2\text{Cl}_2$ (1:10) as eluent to obtain **62** as a white solid (0.16 g, 54% from **58**). mp $68\text{ }^{\circ}\text{C}$; $[\alpha]_{\text{D}}^{20} = +11.8$ ($c = 0.68$, CHCl_3); ^1H NMR (500 MHz, CDCl_3) δ 0.95 (d, $^3J = 6.7\text{ Hz}$, 3H, CH_3CHCH_3), 0.99 (d, $^3J = 6.3\text{ Hz}$, 3H, CH_3CHCH_3), 1.45–1.48 (m, 2H, CHCH_2), 1.73–1.79 (m, 1H, CH_3CHCH_3), 2.62 (s, 3H, $\text{CH}_3\text{C-5''}$), 3.00, 3.27 ($2 \times$ s, $2 \times$ 3H, $\text{N}(\text{CH}_3)\text{CN}$, CONCH_3), 4.29 (dd, $^2J = 15.1\text{ Hz}$, $^3J = 5.4\text{ Hz}$, 1H, CHHNH), 4.44 (dd, $^2J = 15.5\text{ Hz}$, $^3J = 6.0\text{ Hz}$, 1H, CHHNH) 4.94–4.99 (m, 1H, NHCHCO), 5.58 (t, $^3J = 5.5\text{ Hz}$, 1H, CH_2NH), 5.74 (d, $^3J = 8.8\text{ Hz}$, 1H, NHCHCO), 7.33 (d, $^3J = 8.2\text{ Hz}$, 2H, H-2', H-6'), 7.96 (d, $^3J = 8.2\text{ Hz}$, 2H, H-3', H-5'); ^{13}C NMR (125 MHz, CDCl_3) δ 12.36 ($\text{CH}_3\text{C-5''}$), 21.36,

23.29, 24.86 (CH₃CHCH₃, CH₃CHCH₃, CH₃CHCH₃), 30.49 (N(CH₃)CN, 40.86 (CONCH₃), 41.39, 44.00 (CHCH₂, CH₂NH), 48.72 (NHCHCO), 114.47 (CN), 125.73 (C-4'), 127.55, 127.78 (C-3', C-5', C-2', C-6'), 142.37 (C-1'), 158.14 (NHCONH), 168.07, 176.55, 177.05 (C-3'', NHCHCO, C-5''); FTIR (KBr, cm⁻¹) 2223 (C≡N); Anal. C₂₀H₂₇N₇O₃ (413.47 g/mol) calcd C 58.10, H 6.58, N 23.71; found C 57.62, H 6.47, N 22.97; LC-MS(ESI) (90% H₂O to 100% MeOH in 20 min, then 100% MeOH to 30 min, DAD 220.3–319.9 nm) t_r = 21.02, 99% purity, m/z = 414.1 ([M + H]⁺).

3.3.27. PREPARATION OF 63

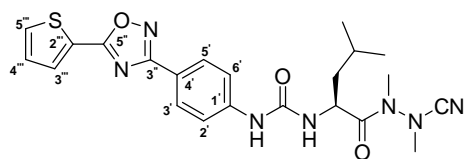
***N*-{4-[5-(2-Thienyl)-1,2,4-oxadiazol-3-yl]benzylcarbamoyl}leucyl-methylazaalanine-nitrile.** Compound **55** (2.00 g, 4.09 mmol) was dissolved in concentrated acetic acid (40 mL) and stirred at 80 °C for 5 h. After evaporation of the acetic acid, the oily product was dissolved in CH₂Cl₂ (40 mL) and treated with TFA (20 mL). The resulting solution was stirred for 3 h at room temperature. The solvent was evaporated, and the oily residue was suspended in H₂O. The aqueous suspension was extracted with ethyl acetate (3 × 20 mL). The combined organic layers were washed with H₂O (2 × 30 mL) and brine (30 mL). The solvent was dried (Na₂SO₄) and removed under reduced pressure. The solid product was recrystallized from ethyl acetate/*n*-hexane to obtain **59** as a white solid (0.59 g, 35% from **55**). Compound **59** (0.23 g, 0.55 mmol) was dissolved in dry THF (30 mL) and cooled to -25 °C. To the stirred solution, *N*-methylmorpholine (0.07 mL, 0.64 mmol) and isobutyl chloroformate (0.08 mL, 0.61 mmol) were added consecutively. 1,2-Dimethylhydrazine dihydrochloride (0.37 g, 2.78 mmol) was dissolved in H₂O (1 mL), and 5 N NaOH (2.00 mL) was added under ice-cooling. This solution was given to the reaction mixture when the precipitation of *N*-methylmorpholine hydrochloride occurred. It was allowed to warm to room temperature within 30 min, and stirred for additional 90 min. After evaporation of the solvent, the resulting aqueous residue was extracted with ethyl acetate (3 × 20 mL). The combined organic layers were washed with H₂O (20 mL), sat. NaHCO₃ (20 mL), H₂O (20 mL), and brine (20 mL). The solvent was dried (Na₂SO₄) and evaporated under reduced pressure. The crude product was purified on silica gel using ethyl acetate as eluent to obtain *N*-{4-[5-(2-thienyl)-1,2,4-oxadiazol-3-yl]benzylcarbamoyl}leucine 1,2-dimethylhydrazide as a colorless oil. Sodium acetate (0.09 g, 1.10 mmol) and cyanogen bromide (0.04 g, 0.38 mmol) were added to a suspension of *N*-{4-[5-(2-thienyl)-1,2,4-oxadiazol-3-yl]benzylcarbamoyl}leucine 1,2-dimethylhydrazide (0.17 g, 0.37 mmol) in MeOH (30 mL). The mixture was stirred at room temperature for 48 h, and the solvent was removed under reduced pressure. The residue was suspended in H₂O (10 mL), a pH of ~2 was adjusted (10% KHSO₄), and it was extracted with ethyl acetate (3 × 20 mL). The combined organic layers were washed with H₂O (20 mL), sat. NaHCO₃ (2 × 20 mL), H₂O (20 mL), and brine (20 mL). The solvent was dried (Na₂SO₄) and removed *in vacuo*. The oily residue was purified by column chromatography on silica gel

using ethyl acetate/petroleum ether (1:1) as eluent to obtain **63** as a white solid (0.12 g, 45% from **59**). mp 96–98 °C. $[\alpha]_{\text{D}}^{20} = +12.8$ ($c = 0.86$, CHCl_3); ^1H NMR (500 MHz, $\text{DMSO-}d_6$) mixture of rotamers (only the data of the major rotational isomer are noted) δ 0.91–0.94 (m, 6H, $\text{CH}(\text{CH}_3)_2$), 1.29–1.47 (m, 2H, CHCH_2), 1.70 (bs, 1H, $\text{CH}(\text{CH}_3)_2$), 3.09, 3.22 ($2 \times s$, $2 \times 3\text{H}$, $\text{N}(\text{CH}_3)\text{CN}$, CONCH_3), 4.30 (d, $^3J = 5.7$ Hz, 2H, CH_2NH), 4.74–4.77 (m, 1H, NHCHCO), 6.41 (d, $^3J = 8.2$ Hz 1H, NHCHCO), 6.55 (t, $^3J = 5.5$ Hz, 1H, CH_2NH), 7.36 (dd, $^3J = 5.1$ Hz, $^3J = 3.8$ Hz, 1H, H-4'''), 7.43 (d, $^3J = 8.2$ Hz, 2H, H-2', H-6'), 7.99 (d, $^3J = 8.6$ Hz, 2H, H-3', H-5'), 8.07, 8.10 (dd, $^3J = 3.8$ Hz, $^4J = 1.3$ Hz, 1H, dd, $^3J = 5.1$ Hz, $^4J = 1.3$ Hz, 1H, H-5'''; H-3'''); ^{13}C NMR (125 MHz, $\text{DMSO-}d_6$) δ 21.45, 23.31, 24.52 (CH_3CHCH_3 , CH_3CHCH_3 , CH_3CHCH_3), 30.50 ($\text{N}(\text{CH}_3)\text{CN}$), CONCH_3 obscured by the DMSO signal, 40.96 (CHCH_2), 42.79 (CH_2NH), 48.08 (NHCHCO), 114.30 (CN), 124.36, 124.67, 127.24, 127.79, 129.39, 132.93, 134.18, 144.85 (C-5''', C-3''', C-3', C-5', C-2', C-6', C-4''', C-4', C-2''', C-1'), 158.07 (NHCONH), 168.16, 171.19, 175.29 (C-3'', NHCHCO , C-5''); FTIR (KBr, cm^{-1}) 2222 ($\text{C}\equiv\text{N}$); Anal. $\text{C}_{23}\text{H}_{27}\text{N}_7\text{O}_3\text{S}$ (481.57 g/mol) calcd C 57.36, H 5.65, N 20.36; found C 56.63, H 5.80, N 19.43. LC-MS(ESI) (90% H_2O to 100% MeOH in 20 min, then 100% MeOH to 30 min, DAD 199.6–300.0 nm) $t_{\text{r}} = 23.00$, 95% purity, $m/z = 482.1$ ($[\text{M} + \text{H}]^+$).

3.3.28. PREPARATION OF 64***N*-[4-(5-Methyl-1,2,4-oxadiazol-3-yl)phenylcarbonyl]leucyl-methylazaalanine-nitrile.**

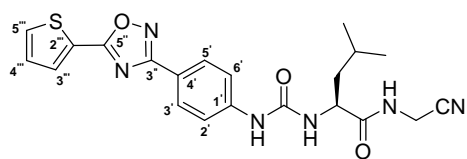
Compound **60** (1.50 g, 4.51 mmol) was dissolved in dry THF (40 mL) and cooled to $-25\text{ }^{\circ}\text{C}$. To the stirred solution, *N*-methylmorpholine (0.54 mL, 4.91 mmol) and isobutyl chloroformate (0.65 mL, 4.99 mmol) were added consecutively. 1,2-Dimethylhydrazine dihydrochloride (3.00 g, 22.6 mmol) was suspended in H_2O (3 mL), and 10 N NaOH (5.00 mL) was added under ice-cooling. This solution was given to the reaction mixture when the precipitation of *N*-methylmorpholine hydrochloride occurred. It was allowed to warm to room temperature within 30 min, and stirred for additional 90 min. After evaporation of the solvent, the resulting aqueous residue was extracted with ethyl acetate ($3 \times 30\text{ mL}$). The combined organic layers were washed with H_2O (30 mL), sat. NaHCO_3 (30 mL), H_2O (30 mL), and brine (30 mL). The solvent was dried (Na_2SO_4) and evaporated. The crude product was purified by column chromatography on silica gel using ethyl acetate to obtain *N*-[4-(5-methyl-1,2,4-oxadiazol-3-yl)phenylcarbonyl]leucine 1,2-dimethylhydrazide as a colorless oil. Sodium acetate (0.48 g, 5.85 mmol) and cyanogen bromide (0.47 g, 4.44 mmol) were added to a solution of *N*-[4-(5-methyl-1,2,4-oxadiazol-3-yl)phenylcarbonyl]leucine 1,2-dimethylhydrazide (1.10 g, 2.94 mmol) in MeOH (30 mL). The mixture was stirred at room temperature for 48 h, and the solvent was removed under reduced pressure. The residue was suspended in H_2O (10 mL), a pH of ~ 2 was adjusted (10% KHSO_4), and it was extracted with ethyl acetate ($3 \times 30\text{ mL}$). The combined organic layers were washed with H_2O (20 mL), sat. NaHCO_3 ($2 \times 30\text{ mL}$), H_2O (30 mL), and brine (30 mL). The solvent was dried (Na_2SO_4) and removed *in vacuo*. The oily residue was purified by column chromatography on silica gel using MeOH/ CH_2Cl_2 (40:1) as eluent. Additionally, the product was recrystallized from ethyl acetate/petroleum ether to obtain **64** as a white solid (0.66 g, 37% from **60**). mp $185\text{ }^{\circ}\text{C}$; $[\alpha]_{\text{D}}^{20} = +65.6$ ($c = 0.32$, CHCl_3); $^1\text{H NMR}$ (500 MHz, $\text{DMSO-}d_6$) mixture of rotamers (only the data of the major rotational isomer are noted) δ 0.93–0.97 (m, 6H, $\text{CH}(\text{CH}_3)_2$), 1.36–1.53 (m, 2H, CHCH_2), 1.73 (bs, 1H, $\text{CH}(\text{CH}_3)_2$), 2.62 (s, 3H, $\text{CH}_3\text{C-5''}$), 3.11, 3.27 ($2 \times$ s, $2 \times$ 3H, $\text{N}(\text{CH}_3)\text{CN}$, CONCH_3), 4.80–4.83 (m, 1H, NHCHCO), 6.64 (d, $^3J = 8.2\text{ Hz}$, 1H, NHCHCO), 7.53 (d, $^3J = 8.5\text{ Hz}$, 2H, H-2', H-6'), 7.85 (d, $^3J = 8.8\text{ Hz}$, 2H, H-3', H-5'), 8.89 (s, 1H, C-1'NH); $^{13}\text{C NMR}$ (125 MHz, $\text{DMSO-}d_6$) δ 12.09 ($\text{CH}_3\text{C-5''}$), 21.40, 23.29, 24.57 (CH_3CHCH_3 , CH_3CHCH_3 , CH_3CHCH_3), 30.56 ($\text{N}(\text{CH}_3)\text{CN}$), 40.46, 40.94 (CONCH_3 ,

CHCH₂), 47.91 (NHCHCO), 114.22 (CN), 117.79 (C-2', C-6'), 119.15 (C-4'), 127.92 (C-3', C-5'), 142.98 (C-1'), 154.93 (NHCONH), 167.50, 174.67, 177.07 (C-3'', NHCHCO, C-5''); FTIR (KBr, cm⁻¹) 2219 (C≡N); Anal. C₁₉H₂₅N₇O₃ (399.45 g/mol) calcd C 57.13, H 6.31, N 24.55; found C 57.05, H 6.72, N 24.06; LC-MS(ESI) (90% H₂O to 100% MeOH in 20 min, then 100% MeOH to 30 min, DAD 239.8–340.8 nm) t_r = 21.83, 98% purity, *m/z* = 400.3 ([M + H]⁺).

3.3.29. PREPARATION OF 65

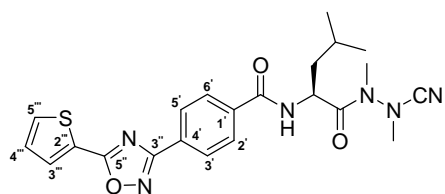
N-{4-[5-(2-Thienyl)-1,2,4-oxadiazol-3-yl]phenylcarbonyl}leucyl-methylazalanine-nitrile. Compound **61** (0.65 g, 1.62 mmol) was dissolved in dry THF (30 mL) and cooled to -25 °C. To the stirred solution, *N*-methylmorpholine (0.20 mL, 1.82 mmol) and isobutyl chloroformate (0.24 mL, 1.84 mmol) were added consecutively. 1,2-Dimethylhydrazine dihydrochloride (1.07 g, 8.04 mmol) was suspended in H₂O (1 mL), and 5 N NaOH (3.40 mL) was added under ice-cooling. This solution was given to the reaction mixture when the precipitation of *N*-methylmorpholine hydrochloride occurred. It was allowed to warm to room temperature within 30 min, and stirred for additional 90 min. After evaporation of the solvent, the resulting aqueous residue was extracted with ethyl acetate (3 × 20 mL). The combined organic layers were washed with H₂O (20 mL), sat. NaHCO₃ (20 mL), H₂O (20 mL), and brine (20 mL). The solvent was dried (Na₂SO₄) and evaporated under reduced pressure. The crude product was purified by column chromatography on silica gel using ethyl acetate as eluent to obtain *N*-{4-[5-(2-thienyl)-1,2,4-oxadiazol-3-yl]phenylcarbonyl}leucine 1,2-dimethylhydrazide as a colourless oil. Sodium acetate (0.28 g, 3.41 mmol) and cyanogen bromide (0.16 g, 1.51 mmol) were added to a solution of *N*-{4-[5-(2-thienyl)-1,2,4-oxadiazol-3-yl]phenylcarbonyl}leucine 1,2-dimethylhydrazide (0.61 g, 1.38 mmol) in MeOH (30 mL). The mixture was stirred at room temperature for 48 h, and the solvent was removed under reduced pressure. The residue was suspended in H₂O (10 mL), a pH of ~2 was adjusted (10% KHSO₄) and it was extracted with ethyl acetate (3 × 20 mL). The combined organic layers were washed with H₂O (20 mL), sat. NaHCO₃ (2 × 20 mL), H₂O (20 mL), and brine (20 mL). The solvent was dried (Na₂SO₄) and removed *in vacuo*. The oily residue was purified by column chromatography on silica gel using ethyl acetate as eluent to obtain **65** as a white solid (0.51 g, 67% from **61**). mp 92 °C; $[\alpha]_{\text{D}}^{20} = +53.0$ (c = 1.05, CHCl₃); ¹H NMR (500 MHz, DMSO-*d*₆) mixture of rotamers (only the data of the major rotational isomer are noted) δ 0.94 (d, ³*J* = 6.7 Hz, 3H, CH₃CHCH₃), 0.97 (d, ³*J* = 6.0 Hz, 3H, CH₃CHCH₃), 1.37–1.55 (m, 2H, CHCH₂), 1.74 (bs, 1H, CH₃CHCH₃), 3.12, 3.27 (2 × s, 2 × 3H, N(CH₃)CN, CONCH₃), 4.81–4.84 (m, 1H, NHCHCO), 6.65 (d, ³*J* = 7.9 Hz, 1H, NHCHCO), 7.35 (dd, ³*J* = 5.0 Hz, ³*J* = 3.8 Hz, 1H, H-4'''), 7.57 (d, ³*J* = 8.8 Hz, 2H, H-2', H-6'), 7.92 (d, ³*J* = 8.9 Hz, 2H, H-3', H-5'), 8.05, 8.09 (dd, ³*J* = 3.8 Hz, ⁴*J* = 1.0 Hz, 1H, dd, ³*J* = 4.9 Hz,

$^4J = 1.1$ Hz, 1H, H-5''', H-3'''), 8.95 (s, 1H, C-1'NH); ^{13}C NMR (125 MHz, DMSO- d_6) δ 21.39, 23.29, 24.58 (CH_3CHCH_3 , CH_3CHCH_3 , CH_3CHCH_3), 30.57 ($\text{N}(\text{CH}_3)\text{CN}$), 40.48 (CONCH_3), 40.94 (CHCH_2), 47.93 (NHCHCO), 114.21 (CN), 117.79 (C-2', C-6'), 118.64 (C-5'), 124.79 (C-4'), 128.17 (C-3', C-5'), 129.34, 132.77, 134.00 (C-3''', C-4''', C-2'''), 143.27 (C-1'), 154.89 (NHCONH), 168.03, 170.90, 174.65 (C-3'', NHCHCO , C-5''); FTIR (KBr, cm^{-1}) 2224 ($\text{C}\equiv\text{N}$). Anal. $\text{C}_{22}\text{H}_{25}\text{N}_7\text{O}_3\text{S}$ (467.54 g/mol) calcd C 56.52, H 5.39, N 20.97; found C 56.41, H 5.77, N 19.94; LC-MS(ESI) (90% H_2O to 100% MeOH in 20 min, then 100% MeOH to 30 min, DAD 220.0–400.0 nm) $t_r = 21.70$, 99% purity, $m/z = 468.5$ ($[\text{M} + \text{H}]^+$).

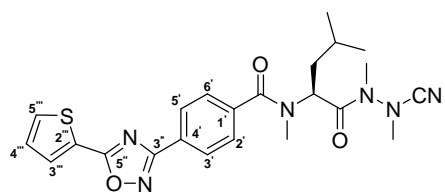
3.3.30. PREPARATION OF 66***N*-{4-[5-(2-Thienyl)-1,2,4-oxadiazol-3-yl]phenylcarbonyl}leucyl-glycine-nitrile.**

Compound **61** (1.00 g, 2.50 mmol) was dissolved in dry THF (30 mL) and cooled to -25 °C. To the stirred solution, *N*-methylmorpholine (0.30 mL, 2.73 mmol) and isobutyl chloroformate (0.36 mL, 2.76 mmol) were added consecutively. Aminoacetonitrile monosulfate (1.31 g, 8.50 mmol) was dissolved in H₂O (2 mL), and 5 N NaOH (3.00 mL) was added under ice-cooling. This solution was given to the reaction mixture when the precipitation of *N*-methylmorpholine hydrochloride occurred. It was allowed to warm to room temperature within 30 min, and stirred for additional 90 min. After evaporation of the solvent, the resulting aqueous residue was extracted with ethyl acetate (3 × 20 mL). The combined organic layers were washed with H₂O (20 mL), sat. NaHCO₃ (20 mL), H₂O (20 mL), and brine (20 mL). The solvent was dried (Na₂SO₄) and evaporated under reduced pressure. The oily crude product was purified by column chromatography on silica gel using ethyl acetate/petroleum ether as eluent to obtain **66** as a white solid (0.29 g, 26%). mp 237 °C; ¹H NMR (500 MHz, DMSO-*d*₆) δ 0.89–0.92 (m, 6H, CH(CH₃)₂), 1.42–1.52 (m, 2H, CHCH₂), 1.59–1.67 (m, 1H, CH(CH₃)₂), 4.15 (d, ³*J* = 6.3 Hz, 2H, NHCH₂CN), 4.24–4.29 (m, 1H, NHCHCO), 6.52 (d, ³*J* = 8.2 Hz, 1H, NHCHCO), 7.35 (dd, ³*J* = 5.1 Hz, ³*J* = 3.8 Hz, 1H, H-4'''), 7.58 (d, ³*J* = 8.9 Hz, 2H, H-2', H-6'), 7.92 (d, ³*J* = 8.9 Hz, 2H, H-3', H-5'), 8.05, 8.09 (dd, ³*J* = 3.6 Hz, ⁴*J* = 1.1 Hz, 1H, dd, ³*J* = 5.1 Hz, ⁴*J* = 1.3 Hz, 1H, H-5''', H-3'''), 8.83 (t, ³*J* = 5.7 Hz, 1H, NHCH₂CN), 8.93 (s, 1H, C-1'NH); ¹³C NMR (125 MHz, DMSO-*d*₆) δ 21.91, 23.06, 24.43 (CH₃CHCH₃, CH₃CHCH₃, CH₃CHCH₃), 27.21 (NHCH₂CN), 41.79 (CHCH₂), 51.29 (NHCHCO), 117.65 (CN), 117.70 (C-2', C-6'), 118.51 (C-5'''), 124.81 (C-4'), 128.19 (C-3', C-5'), 129.36, 132.77, 134.01 (C-3''', C-4''', C-2'''), 143.49 (C-1'), 154.48 (NHCONH), 168.05, 170.90, 173.44 (C-3'', NHCHCO, C-5''); FTIR (KBr, cm⁻¹) 2253 (C≡N); Anal. C₂₁H₂₂N₆O₃S (438.50 g/mol) calcd C 57.52, H 5.06, N 19.17; found C 57.50, H 5.15, N 19.02; LC-MS(ESI) (90% H₂O to 100% MeOH in 20 min, then 100% MeOH to 30 min, DAD 220.0–400.0 nm) t_r = 20.08, 100% purity, *m/z* = 439.3 ([M + H]⁺).

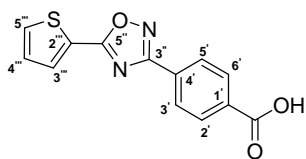
3.3.31. PREPARATION OF 67

***N*-{4-[5-(2-Thienyl)-1,2,4-oxadiazol-3-yl]benzoyl}-leucyl-methylazaalanine-nitrile.**

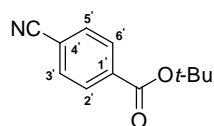
Sodium acetate (0.19 g, 2.32 mmol) and cyanogen bromide (0.19 g, 1.79 mmol) were added to a solution of **89** (0.50 g, 1.17 mmol) in MeOH (20 mL). The mixture was stirred at room temperature for 48 h, and the solvent was removed under reduced pressure. The oily residue was purified by column chromatography on silica gel using ethyl acetate/petroleum (1:1) as eluent to obtain **67** (0.28 g, 53%). mp 92–94 °C; $[\alpha]_D^{20} = +47.7$ ($c = 1.24$, CHCl_3); ^1H NMR (500 MHz, $\text{DMSO-}d_6$) mixture rotamers (only the data of the major rotational isomer are noted) δ 0.96 (d, $^3J = 6.4$ Hz, 6H, $\text{CH}(\text{CH}_3)_2$), 1.37–1.44 (m, 1H, $\text{CH}(\text{CH}_3)_2$), 1.72–1.89 (m, 2H, CHCH_2), 3.13, 3.32 ($2 \times s$, $2 \times 3\text{H}$, $\text{N}(\text{CH}_3)\text{CN}$, CONCH_3), 5.04 (bs, 1H, NHCHCO), 7.37 (dd, $^3J = 5.1$ Hz, $^3J = 3.8$ Hz, 1H, H-4'''), 8.08–8.10, 8.12 (m, 3H, dd, $^3J = 5.1$ Hz, $^4J = 1.3$ Hz, 1H, H-3''', H-3', H-5', H-5'''), 8.15 (d, $^3J = 8.2$ Hz, 2H, H-2', H-6'), 8.95 (d, $^3J = 7.0$ Hz, NHCHCO); ^{13}C NMR (125 MHz, $\text{DMSO-}d_6$) δ 21.14, 23.24, 24.73 (CH_3CHCH_3 , CH_3CHCH_3 , CH_3CHCH_3), 30.55 ($\text{N}(\text{CH}_3)\text{CN}$), CONCH_3 obscured by the DMSO, 40.89 (CHCH_2), 48.74 (NHCHCO), 114.29 (CN), 124.52 (C-5'''), 127.19, 128.63, 129.43, 133.13, 134.40, 136.41 (C-3', C-5', C-2', C-6', C-3''', C-4''', C-2''', C-4', C-1'), 166.27, 167.77, 171.50, 174.03 (C-3'', C-1'CO, NHCHCO , C-5''); FTIR (KBr, cm^{-1}) 2223 ($\text{C}\equiv\text{N}$); Anal. $\text{C}_{22}\text{H}_{24}\text{N}_6\text{O}_3\text{S}$ (452.53 g/mol) calcd C 58.39, H 5.35, N 18.57; found C 58.41, H 5.84, N 17.55; LC-MS(ESI) (90% H_2O to 100% MeOH in 20 min, then 100% MeOH to 30 min, DAD 220.0–400.0 nm) $t_r = 18.99$, 95% purity, $m/z = 453.3$ ($[\text{M} + \text{H}]^+$).

3.3.32. PREPARATION OF 68

***N*-{4-[5-(2-Thienyl)-1,2,4-oxadiazol-3-yl]benzoyl}-*N*-methylleucyl-methylazaalanine-nitrile.** Sodium acetate (0.26 g, 3.17 mmol) and cyanogen bromide (0.25 g, 2.36 mmol) were added to a solution of **90** (0.70 g, 1.59 mmol) in MeOH (30 mL). The mixture was stirred at room temperature for 31 h, and the solvent was removed under reduced pressure. The oily residue was purified by column chromatography on silica gel using ethyl acetate/petroleum ether (1:2) as eluent to obtain **68** as a white solid (0.46 g, 62%). mp 92–94 °C; $[\alpha]_D^{20} = +3.8$ ($c = 1.20$, CHCl₃); ¹H NMR (500 MHz, CDCl₃) mixture of s-cis and s-trans isomers δ 0.86_a, 1.00_b, 1.06_c, 1.09_d (bs_a, db, ³*J* = 6.0 Hz, d_c, ³*J* = 6.6 Hz, d_d, ³*J* = 6.3 Hz 6H, CH(CH₃)₂) 1.54–1.60_a, 1.67–1.77_b (2 × m, 2H, CHCH₂), 1.95–2.01 (bs, 1H, CH(CH₃)₂), 2.49, 2.81, 3.11, 3.20, 3.23, 3.36 (6 × s, 9H, CH₃NCHCO, N(CH₃)CN, CONCH₃), 5.64–5.67_a, 5.78_b (m_a, bs_b, 1H, CH₃NCHCO), 7.21 (dd, ³*J* = 4.8 Hz, ³*J* = 3.8 Hz, 1H, H-4'''), 7.52_a, 7.65–7.68_b, 7.95_c, 8.18_d (d_a, ³*J* = 8.2 Hz, m_b, 3H, dd_c, ³*J* = 3.7 Hz, ⁴*J* = 0.80 Hz, 1H, d_d, ³*J* = 8.2 Hz, 2H, H-3', H-5', H-5''', H-3''', H-2', H-6'); ¹³C NMR (125 MHz, DMSO-*d*₆) mixture of s-cis and s-trans isomers (only the data of the major rotational isomer are noted) δ 21.19, 23.23, 25.71 (CH₃CHCH₃, CH₃CHCH₃, CH₃CHCH₃), 30.28, 33.97 (N(CH₃)CN, CH₃NCHCO), 37.42 (CONCH₃), 40.73 (CHCH₂), 51.52 (CH₃NCHCO), 113.80 (CN), 125.63, 127.65, 127.70, 128.20, 128.56, 132.05, 132.19, 138.61 (C-4', C-3', C-5', C-4''', C-5''', C-2', C-6', C-3''', C-2''', C-1'), 168.15, 171.61, 172.57, 174.34 (C-3'', C-1'CO, CH₃NCHCO, C-5''); FTIR (KBr, cm⁻¹) 2219 (C≡N); Anal. C₂₃H₂₆N₆O₃S (466.56 g/mol) calcd C 59.21, H 5.62, N 18.01; found C 59.27, H 5.61, N 17.19; LC-MS(ESI) (90% H₂O to 100% MeOH in 20 min, then 100% MeOH to 30 min, DAD 220.0–400.0 nm) $t_r = 19.66$, 96% purity, $m/z = 467.6$ ([M + H]⁺).

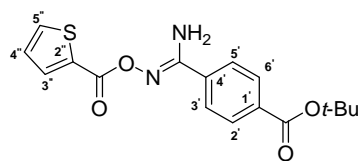
3.3.33. PREPARATION OF 69

4-[5-(2-Thienyl)-1,2,4-oxadiazol-3-yl]benzoic acid. Compound **74** (2.00 g, 5.77 mmol) was suspended in concentrated acetic acid (70 mL). The resulting reaction mixture was stirred at 80 °C overnight. Acetic acid was removed. The residue was dissolved in CH₂Cl₂ (40 mL) and treated with TFA (5 mL). The reaction mixture was stirred at room temperature for 6 h. The solvent was evaporated under reduced pressure. The crude product was recrystallized from ethyl acetate/petroleum ether to obtain **69** (1.31 g, 83% from **74**). mp 232 °C; ¹H NMR (500 MHz, DMSO-*d*₆) 7.36 (dd, ³*J* = 5.1 Hz, ³*J* = 3.8 Hz, 1H, H-4'''), 8.09, 8.11–8.13 (dd, ³*J* = 3.8 Hz, ⁴*J* = 1.3 Hz, 1H, m, 3H, H-5''', H-3', H-5', H-3'''), 8.16 (d, ³*J* = 8.9 Hz, 2H, H-2', H-6'), 13.23 (s, 1H, COOH); ¹³C NMR (125 MHz, DMSO-*d*₆) δ 124.50 (C-5'''), 127.51 (C-3', C-5'), 129.46, 129.82 (C-3''', C-4'''), 130.29 (C-2', C-6'), 133.17, 133.63, 134.46 (C-1', C-2''', C-4'), 166.75, 167.72, 171.57 (C-3'', COOH, C-5''); Anal. C₁₃H₈N₂O₃S (272.28 g/mol) calcd C 57.35, H 2.96, N 10.29; found C 57.37, H 2.88, N 10.18.

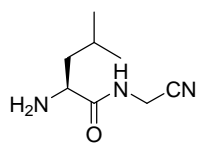
3.3.34. PREPARATION OF 73

4-Cyanobenzoic acid *tert*-butyl ester. 4-Cyanobenzoic acid **72** (4.50 g, 30.6 mmol) was dissolved in dry CH₂Cl₂ (100 mL). Oxalyl chloride (4.00 mL, 47.3 mmol) and DMF (1 mL) were added. The resulting reaction mixture was stirred at room temperature for 1 h until the gas evolution was ceased. The solvent was removed. The resulting residue was treated with 60 mL of a pyridine/*tert*-butanol mixture (1:1) and stirred for 6 h at room temperature. The solvent was evaporated under reduced pressure, and the green residue was suspended in H₂O. The aqueous suspension was extracted with ethyl acetate (3 × 50 mL). The combined organic layers were washed with 10% KHSO₄ (2 × 50 mL), H₂O (50 mL), sat. NaHCO₃ (2 × 50 mL), H₂O (50 mL), and brine (2 × 50 mL). The solvent was dried (Na₂SO₄) and evaporated. The crude product was purified by column chromatography using ethyl acetate/petroleum ether (1:4) to obtain **73** as a white solid (4.81 g, 77%). mp 78 °C; ¹H NMR (500 Hz, DMSO-*d*₆) δ 1.54 (s, 3H, C(CH₃)₃), 7.96 (d, ³J = 8.9 Hz, 2H, H-3', H-5'), 8.03 (d, ³J = 8.8 Hz, 2H, H-2', H-6'); ¹³C NMR (125 MHz, DMSO-*d*₆) δ 28.52 (C(CH₃)₃), 82.81 (C(CH₃)₃), 115.99 (C-4'), 118.98 (CN), 130.52 (C-2', C-6'), 133.54 (C-3', C-5'), 136.06 (C-1'), 164.47 (COO); Anal. C₁₂H₁₃NO₂ (203.24 g/mol) calcd C 70.92, H 6.45, N 6.89; found C 70.72, H 6.43, N 6.91.

3.3.35. PREPARATION OF 74

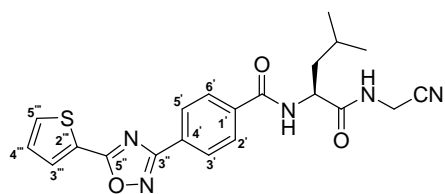


4-[(2-Thiophenecarbonyl)oxyamidino]-benzoic acid *tert*-butyl ester. Compound **73** (2.00 g, 9.84 mmol) was dissolved in EtOH (70 mL). Triethylamine (2.54 mL, 18.2 mmol) and hydroxylamine hydrochloride (1.27 g, 18.3 mmol) were added. The resulting reaction mixture was heated to reflux for 3 h. EtOH was removed, the oily residue was suspended in H₂O and extracted with ethyl acetate (3 × 50 mL). The combined organic layers were washed with 10% KHSO₄ (50 mL), H₂O (50 mL), brine (50 mL), and dried over Na₂SO₄. After evaporation of the solvent, the white solid residue was dissolved in dry MeCN (40 mL). The resulting reaction mixture was treated under ice-cooling with triethylamine (2.54 mL, 18.2 mmol) and 2-thiophenecarbonyl chloride (1.96 mL, 18.3 mmol), and stirred for 5 h at room temperature. The solvent was evaporated under reduced pressure, and the white residue was suspended in H₂O. The aqueous suspension was extracted with ethyl acetate (3 × 50 mL). The combined organic layers were washed with 10% KHSO₄ (2 × 50 mL), H₂O (50 mL), sat. NaHCO₃ (2 × 50 mL), H₂O (50 mL), and brine (2 × 50 mL). The solvent was dried (Na₂SO₄) and removed *in vacuo*. The crude product was recrystallized from ethyl acetate/petroleum ether to obtain **74** as a white solid (2.60 g, 76% from **73**). mp 170 °C; ¹H NMR (500 MHz, DMSO-*d*₆) δ 1.56 (s, 9H, C(CH₃)₃), 7.05 (s, 2H, NH₂), 7.25 (dd, ³*J* = 5.1 Hz, ³*J* = 3.8 Hz, 1H, H-4''), 7.87, 7.96–7.98 (d, ³*J* = 8.8 Hz, 2H, m, 3H, H-3', H-5', H-2', H-6', H-5''), 8.15 (dd, ³*J* = 3.8 Hz, ⁴*J* = 1.3 Hz, 1H, H-3''); ¹³C NMR (125 MHz, DMSO-*d*₆) δ 27.90 (C(CH₃)₃), 81.30 (C(CH₃)₃), 127.26 (C-3', C-5'), 128.40 (C-4''), 129.13 (C-2', C-6'), 132.64, 133.19, 133.96, 134.06 135.73 (C-1', C-4', C-5'', C-3'', C-2''), 156.39, 159.70, 164.57 (C-2''CO, N=C, C-1'CO); Anal. C₁₇H₁₈N₂O₄S (346.40 g/mol) calcd C 58.94, H 5.24, N 8.09; found C 59.04, H 5.30, N 8.07.

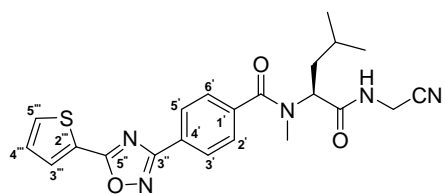
3.3.36. PREPARATION OF 77

Leucyl-glycine-nitrile. Compound **75** (5.00 g, 21.6 mmol) was dissolved in dry THF (30 mL) and cooled to $-25\text{ }^{\circ}\text{C}$. To the stirred solution, *N*-methylmorpholine (2.61 mL, 23.7 mmol) and isobutyl chloroformate (3.10 mL, 23.8 mmol) were added consecutively. Aminoacetonitrile monosulfate (6.65 g, 43.1 mmol) was suspended in H_2O (3 mL). The resulting suspension was treated with 5 N NaOH (17.0 mL) under ice-cooling and added to the reaction mixture when the precipitation of *N*-methylmorpholine hydrochloride occurred. It was allowed to warm to room temperature within 30 min, and stirred for additional 90 min. After evaporation of the solvent, the resulting aqueous residue was extracted with ethyl acetate ($3 \times 30\text{ mL}$). The combined organic layers were washed with 10% KHSO_4 (30 mL), H_2O (30 mL), sat. NaHCO_3 (30 mL), H_2O (30 mL), and brine (30 mL). The solvent was dried (Na_2SO_4) and removed *in vacuo* to obtain *N*-(*tert*-butyloxycarbonyl)leucyl-glycine-nitrile as a white solid (5.78 g, 99%). *N*-(*tert*-Butyloxycarbonyl)leucyl-glycine-nitrile (5.78 g, 21.5 mmol) was dissolved in dry THF (20 mL) and treated with methanesulfonic acid (8.40 mL, 0.13 mol). The reaction mixture was stirred at room temperature for 30 min. THF was removed under reduced pressure, and the oily residue was dissolved in H_2O (10 mL). The obtained solution was adjusted at pH ~ 12 with 2 N NaOH and extracted with ethyl acetate ($3 \times 30\text{ mL}$). The combined organic layers were washed with sat. NaHCO_3 (30 mL), H_2O (30 mL), and brine (30 mL) and dried over Na_2SO_4 . The solvent was evaporated, and the oily residue was purified by column chromatography using $\text{MeOH}/\text{CH}_2\text{Cl}_2$ (1:20) to obtain **77** as an oily product (1.20 g, 33% from *N*-(*tert*-butyloxycarbonyl)leucyl-glycine-nitrile). ^1H NMR (500 MHz, $\text{DMSO}-d_6$) δ 0.84 (d, $^3J = 6.6\text{ Hz}$, 3H, CH_3CHCH_3), 0.87 (d, $^3J = 6.6\text{ Hz}$, 3H, CH_3CHCH_3), 1.20–1.42 (m, 2H, CHCH_2), 1.66–1.74 (CH_3CHCH_3), 3.17–3.20 (NH_2CHCO), 4.09 (s, 2H, NHCH_2CN); ^{13}C NMR (125 MHz, $\text{DMSO}-d_6$) δ 21.87, 23.27, 24.17 (CH_3CHCH_3 , CH_3CHCH_3 , CH_3CHCH_3), 27.09 (NHCH_2CN), 44.26 (CHCH_2), 53.11 (NH_2CHCO), 117.83 (CN), 176.65 (NH_2CHCO).

3.3.37. PREPARATION OF 79

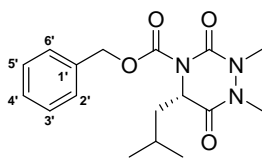


***N*-{4-[5-(2-Thienyl)-1,2,4-oxadiazol-3-yl]benzoyl}-leucyl-glycine-nitrile.** Compound **69** (1.32 g, 4.85 mmol) was dissolved in dry THF (20 mL) and cooled to $-25\text{ }^{\circ}\text{C}$. To the stirred solution, *N*-methylmorpholine (0.59 mL, 5.37 mmol) and isobutyl chloroformate (0.70 mL, 5.37 mmol) were added consecutively. Compound **77** (1.10 g, 6.50 mmol) in dry THF (10 mL) was given to the reaction mixture when the precipitation of *N*-methylmorpholine hydrochloride occurred. It was allowed to warm to room temperature within 30 min, and stirred for additional 90 min. After evaporation of the solvent, the resulting aqueous residue was extracted with ethyl acetate ($3 \times 20\text{ mL}$). The combined organic layers were washed with H_2O (20 mL), sat. NaHCO_3 (20 mL), H_2O (20 mL), and brine (20 mL). The solvent was dried (Na_2SO_4) and removed *in vacuo*. The crude product was purified by column chromatography on silica gel using ethyl acetate/petroleum ether (1:2) as eluent to obtain **79** as a white solid (1.01 g, 49% from **69**). mp $195\text{ }^{\circ}\text{C}$; $[\alpha]_{\text{D}}^{20} = -23.9$ ($c = 1.34$, CHCl_3); $^1\text{H NMR}$ (500 MHz, $\text{DMSO-}d_6$) δ 0.88 (d, $^3J = 6.3\text{ Hz}$, 3H, CH_3CHCH_3), 0.92 (d, $^3J = 6.6\text{ Hz}$, 3H, CH_3CHCH_3), 1.54–1.60 (m, 1H, CH_3CHCH_3), 1.63–1.77 (m, 2H, CHCH_2), 4.14 (d, $^3J = 5.7\text{ Hz}$, 2H, NHCH_2CN), 4.52–4.57 (m, 1H, NHCHCO), 7.37 (dd, $^3J = 5.1\text{ Hz}$, $^3J = 3.8\text{ Hz}$, 1H, H-4'''), 8.09–8.13 (m, 4H, H-3', H-5', H-3''', H-5'''), 8.15 (d, $^3J = 8.5\text{ Hz}$, 2H, H-2', H-6'), 8.73 (t, $^3J = 5.5\text{ Hz}$, 1H, NHCH_2CN), 8.76 (d, $^3J = 8.2\text{ Hz}$, 1H, NHCHCO); $^{13}\text{C NMR}$ (125 MHz, $\text{DMSO-}d_6$) δ 21.41, 23.13, 24.56 (CH_3CHCH_3 , CH_3CHCH_3 , CH_3CHCH_3), 27.30 (NHCH_2CN), CHCH_2 obscured by the DMSO signal), 51.81 (NHCHCO), 117.71 (CN), 124.53 (C-5'''), 127.12 (C-3', C-5'), 128.53 (C-3'''), 128.69 (C-2', C-6'), 129.44, 133.14, 134.41, 136.79 (C-4''', C-2''', C-4', C-1'), 165.83, 167.80, 171.51, 172.94 (C-3'', C-1'CO, NHCHCO , C-5''); FTIR (KBr, cm^{-1}) 2258 ($\text{C}\equiv\text{N}$); Anal. $\text{C}_{21}\text{H}_{21}\text{N}_5\text{O}_3\text{S}$ (423.49 g/mol) calcd C 59.56, H 5.00, N 16.54; found C 59.45, H 4.99, N 16.08. LC-MS(ESI) (90% H_2O to 100% MeOH in 20 min, then 100% MeOH to 30 min, DAD 220.0–400.0 nm) $t_{\text{r}} = 18.92$, 98% purity, $m/z = 424.3$ ($[\text{M} + \text{H}]^+$).

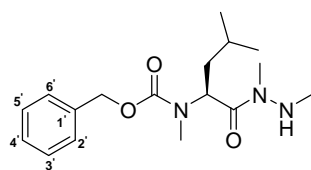
3.3.38. PREPARATION OF 80

***N*-{4-[5-(2-Thienyl)-1,2,4-oxadiazol-3-yl]benzoyl}-*N*-methylleucyl-glycine-nitrile.** Compound **76** (1.00 g, 4.08 mmol) was dissolved in dry THF (20 mL) and cooled to $-25\text{ }^{\circ}\text{C}$. To the stirred solution, *N*-methylmorpholine (0.49 mL, 4.46 mmol) and isobutyl chloroformate (0.61 mL, 4.68 mmol) were added consecutively. Aminoacetonitrile monosulfate (1.57 g, 10.2 mmol) was dissolved in H_2O (2 mL) and treated with 10 N NaOH (2 mL). This solution was given to the reaction mixture when the precipitation of *N*-methylmorpholine hydrochloride occurred. It was allowed to warm to room temperature within 30 min, and stirred for additional 90 min. After evaporation of the solvent, the resulting aqueous residue was extracted with ethyl acetate ($3 \times 20\text{ mL}$). The combined organic layers were washed with H_2O (20 mL), 10% KHSO_4 (20 mL), H_2O (20 mL), sat. NaHCO_3 (20 mL), H_2O (20 mL), and brine (20 mL). The solvent was dried (Na_2SO_4) and evaporated *in vacuo* to obtain *N*-(*tert*-butyloxycarbonyl)-*N*-methylleucyl-glycine-nitrile as a yellow oil. *N*-(*tert*-Butyloxycarbonyl)-*N*-methylleucyl-glycine-nitrile (1.17 g, 3.93 mmol) was dissolved in dry THF (20 mL) and treated with methanesulfonic acid (0.79 mL, 12.2 mmol). The resulting solution was stirred for 5 h at room temperature. The solvent was removed under reduced pressure. The oily residue was dissolved in H_2O (10 mL). The aqueous solution was adjusted at pH ~ 12 with 2 N NaOH and extracted with ethyl acetate ($3 \times 30\text{ mL}$). The combined organic layers were washed with H_2O (20 mL), sat. NaHCO_3 (20 mL), H_2O (20 mL), and brine (20 mL). The solvent was dried (Na_2SO_4) and evaporated *in vacuo* to obtain **78** as a yellow oil. Compound **69** (0.87 g, 3.20 mmol) was dissolved in dry THF (20 mL). To the stirred solution, DMAP (0.026 g, 0.21 mmol) and EDC (0.83 mL, 4.69 mmol) were added consecutively. The resulting reaction mixture was stirred for 15 min at room temperature. Compound **78** (0.86 g, 4.69 mmol) was added. It was stirred for 18 h at rt. The solvent was removed, and the oily residue was suspended in H_2O . The aqueous suspension was extracted with ethyl acetate ($3 \times 20\text{ mL}$). The combined organic layers were washed with H_2O (20 mL), 10% KHSO_4 (20 mL), H_2O (20 mL), sat. NaHCO_3 (20 mL), H_2O (20 mL), and brine (20 mL). The solvent was dried (Na_2SO_4) and evaporated. The crude product was purified by column chromatography on silica gel using ethyl acetate/petroleum ether (1:1) as eluent to obtain **80** as a yellow solid (0.60 g, 43% from **69**). mp $68\text{--}72\text{ }^{\circ}\text{C}$;

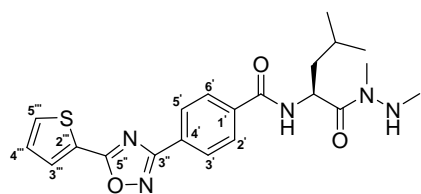
$[\alpha]_{\text{D}}^{20} = -72.1$ ($c = 1.04$, CHCl_3); $^1\text{H NMR}$ (500 MHz, $\text{DMSO-}d_6$) mixture of s-cis and s-trans isomers δ 0.60_a, 0.82_b, 0.94_c, 0.98_d (d_a , $^3J = 4.8$ Hz, b_{Sb} , d_c , $^3J = 6.3$ Hz, d_d , $^3J = 6.4$ Hz, 6H CH_3CHCH_3 , CH_3CHCH_3), 1.21_a, 1.39_b, 1.58_c, 1.70–1.76_d (b_{Sa} , b_{Sb} , b_{Sc} , m_d , 3H, CH_3CHCH_3 , CHCH_2), 2.83_a, 2.94_b ($2 \times s$, 3H, NCH_3), 4.09_a, 4.16_b (d_a , $^3J = 4.8$ Hz, d_b , $^3J = 5.4$ Hz, 2H, NHCH_2CN), 5.12–5.15 (m, 1H, CH_3NCHCO), 7.37 (dd, $^3J = 5.0$ Hz, $^3J = 3.8$ Hz, 1H, H-4'''), 7.51_a, 7.63_b (d_a , $^3J = 6.9$ Hz, d_b , $^3J = 7.9$ Hz, 2H, H-3', H-5'), 8.09–8.14 (m, 4H, H-2', H-6', H-3''', H-5'''), 8.72_a, 8.78_b ($2 \times bs$, 1H, NHCH_2CN); $^{13}\text{C NMR}$ (125 MHz, $\text{DMSO-}d_6$) mixture of s-cis and s-trans isomers δ 21.15, 21.57, 22.99, 23.28, 24.40, 24.71 (CH_3CHCH_3 , CH_3CHCH_3 , CH_3CHCH_3), 27.42, 29.35 (NHCH_2CN), 33.46, 36.78 (NCH_3), 37.72, 40.90 (CHCH_2), 54.30, 59.96 (CH_3NCHCO), 117.54, 117.67 (CN), 124.54, 126.98, 127.37, 127.46, 127.98, 129.43, 133.10, 134.37, 139.33 (C-5''', C-3', C-5', C-3''', C-2', C-6', C-4''', C-4', C-2''', C-1'), 167.79, 170.51, 170.71, 171.19, 171.46 (C-3'', C-1'CO, CH_3NCHCO , C-5''); FTIR (KBr, cm^{-1}) 2254 ($\text{C}\equiv\text{N}$); Anal. $\text{C}_{22}\text{H}_{23}\text{N}_5\text{O}_3\text{S}$ (437.51 g/mol) calcd C 60.39, H 5.30, N 16.01; found C 60.76, H 6.09, N 14.64. LC-MS(ESI) (90% H_2O to 100% MeOH in 20 min, then 100% MeOH to 30 min, DAD 220.0–400.0 nm) $t_r = 19.77$, 100% purity, $m/z = 438.4$ ($[\text{M} + \text{H}]^+$).

3.3.39. PREPARATION OF 84

4-Benzyloxycarbonyl-5-isobutyl-1,2-dimethyl-3,6-dioxo-1,2,4-triazinane. Compound **81** (5.00 g, 11.2 mmol) was cooled to $-25\text{ }^{\circ}\text{C}$. *N*-methylmorpholine (1.24 g, 12.3 mmol) and isobutyl chloroformate (1.68 g, 12.3 mmol) were added consecutively. 1,2-Dimethylhydrazine dihydrochloride (7.45 g, 56.0 mmol) was suspended in H_2O (15 mL), and 10 N NaOH (12.0 mL) was added under ice-cooling. This solution was given to the reaction mixture when the precipitation of *N*-methylmorpholine hydrochloride occurred. It was allowed to warm to room temperature within 30 min and stirred overnight at room temperature. After evaporation of the solvent, the resulting aqueous residue was extracted with ethyl acetate ($3 \times 60\text{ mL}$). The combined organic layers were washed with H_2O (30 mL), sat. NaHCO_3 ($2 \times 30\text{ mL}$), H_2O (30 mL), and brine (30 mL). The solvent was dried (Na_2SO_4) and evaporated to obtain **82** as a colourless oil without further purification (3.43 g, 100%). Compound **82** (3.43 g, 11.2 mmol) was dissolved in MeCN (20 mL). The resulting solution was treated with DMAP (0.07 g, 0.57 mmol), and $(\text{Boc})_2\text{O}$ (3.67 g, 16.8 mmol). It was stirred for 38 h at room temperature. The solvent was removed under reduced pressure. The oily residue was suspended in H_2O (30 mL), a pH of ~ 2 was adjusted (10% KHSO_4), and it was extracted with ethyl acetate ($3 \times 60\text{ mL}$). The combined organic layers were washed with 10% KHSO_4 (30 mL), H_2O (30 mL), sat. NaHCO_3 (30 mL), H_2O (30 mL), and brine (30 mL). The solvent was dried (Na_2SO_4) and removed *in vacuo*. The oily residue was purified by column chromatography on silica gel using ethyl acetate/petroleum ether (1:1) as eluent to obtain **84** as a white solid (2.43 g, 65% from **82**). mp $81\text{--}82\text{ }^{\circ}\text{C}$; $[\alpha]_{\text{D}}^{20} = -8.29$ ($c = 2.17$, CHCl_3); ^1H NMR (500 MHz, $\text{DMSO-}d_6$) δ 0.88–0.90 (m, 6H, $\text{CH}(\text{CH}_3)_2$), 1.34–1.49 (m, 2H, CHCH_2), 1.54–1.62 (m, 1H, $\text{CH}(\text{CH}_3)_2$), 3.13 (s, 3H, NCH_3), 3.21 (s, 3H, NCH_3), 4.59 (dd, $^3J = 8.8\text{ Hz}$, $^3J = 6.9\text{ Hz}$, 1H, NCHCO), 5.18 (d, 1H, $^2J = 12.6\text{ Hz}$, OCHH), 5.25 (d, 1H, $^2J = 12.6\text{ Hz}$, OCHH), 7.31–7.42 (m, 5H, H_{arom}); ^{13}C NMR (125 MHz, $\text{DMSO-}d_6$) δ 22.06, 22.34, 24.27 (CH_3CHCH_3 , CH_3CHCH_3 , CH_3CHCH_3), 32.13, 33.76, 38.85 (CHCH_2 , $2 \times \text{NCH}_3$), 55.96 (NCHCO), 68.14 (CH_2O), 127.83 ($\text{C}'\text{-2}$, $\text{C}'\text{-6}$), 128.25 ($\text{C}'\text{-4}$), 128.52 ($\text{C}'\text{-3}$, $\text{C}'\text{-5}$), 135.63 ($\text{C}'\text{-1}$), 149.15, 152.22 (OCON , NCON), 165.67 (NCHCO); Anal. $\text{C}_{17}\text{H}_{23}\text{N}_3\text{O}_4$ (333.38 g/mol) calcd C 61.25, H 6.95, N 12.60; found C 61.30, H 6.63, N 11.87. MS (ESI) m/z 334.3 ($[\text{M} + \text{H}]^+$).

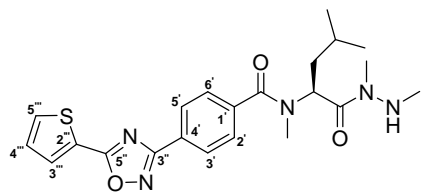
3.3.40. PREPARATION OF 86

***N*-(Benzyloxycarbonyl)-*N*-methylleucine 1,2-dimethylhydrazide.** Compound **85** (5.00 g, 17.9 mmol) was dissolved in dry THF (40 mL) and cooled to $-25\text{ }^{\circ}\text{C}$. To the stirred solution, *N*-methylmorpholine (2.17 mL, 19.7 mmol) and isobutyl chloroformate (2.57 mL, 19.7 mmol) were added consecutively. 1,2-Dimethylhydrazine dihydrochloride (11.9 g, 89.5 mmol) was suspended in H_2O (5 mL), and 10 N NaOH (18.0 mL) was added under ice-cooling. This solution was given to the reaction mixture when the precipitation of *N*-methylmorpholine hydrochloride occurred. It was allowed to warm to room temperature within 30 min, and stirred overnight at rt. After evaporation of the solvent, the resulting aqueous residue was extracted with ethyl acetate ($3 \times 30\text{ mL}$). The combined organic layers were washed with H_2O (20 mL), sat. NaHCO_3 ($2 \times 20\text{ mL}$), H_2O (20 mL), and brine (20 mL). The solvent was dried (Na_2SO_4) and evaporated. The crude product was purified by column chromatography using ethyl acetate/petroleum ether (1:1) to obtain **86** as an oily product (3.10 g, 54%). ^1H NMR (500 MHz, $\text{DMSO}-d_6$) mixture of *s*-cis and *s*-trans isomers δ 0.82_a, 0.86_b, 0.89_c (d_a, $^3J = 6.0\text{ Hz}$, d_b, $^3J = 6.0\text{ Hz}$, d_c, $^3J = 6.0\text{ Hz}$, 6H, CH_3CHCH_3 , CH_3CHCH_3), 1.39–1.47 (m, 2H, CHCH_2), 1.53–1.59 (m, 1H, CH_3CHCH_3), 2.26_a, 2.43_b (d_a, $^3J = 5.4\text{ Hz}$, d_b, $^3J = 5.7\text{ Hz}$, 3H, NHCH_3), 2.82_a, 2.86_b ($2 \times$ s, 3H, OCONCH_3), 2.89_a, 2.90_b ($2 \times$ s, 3H, CONCH_3), 4.74–4.82 (m, 1H, NHCH_3), 5.02–5.11 (m, 2H, CH_2O), 5.43_a, 5.52_b (dd_a, $^3J = 10.3\text{ Hz}$, $^3J = 4.0\text{ Hz}$, dd_b, $^3J = 10.6\text{ Hz}$, $^3J = 3.9\text{ Hz}$, 1H, CH_3NCHCO), 7.28–7.37 (m, 5H, H_{arom}); ^{13}C NMR (125 MHz, $\text{DMSO}-d_6$) mixture of *s*-cis and *s*-trans isomers δ 21.28, 21.36, 23.15, 23.21, 24.72, 24.85 (CH_3CHCH_3 , CH_3CHCH_3 , CH_3CHCH_3), 29.95, 30.19, 30.87 (OCONCH_3 , NHCH_3), 34.90, 35.03, 37.38, 37.62 (CONCH_3 , CHCH_2), 52.22, 52.32 (CH_3NCHCO), 66.24, 66.44 (CH_2O), 127.47, 127.60 (C-2', C-6'), 127.84 (C-4'), 128.38, 128.47 (C-3', C-5'), 137.00, 137.21 (C-1'), 155.83, 156.08 (OCON), 173.09, 173.52 (CH_3NCHCO).

3.3.41. PREPARATION OF 89***N*-{4-[5-(2-Thienyl)-1,2,4-oxadiazol-3-yl]benzoyl}-leucine 1,2-dimethylhydrazide.**

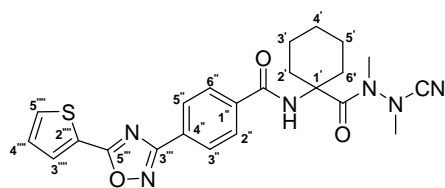
Compound **81** (10.0 g, 37.7 mmol) was dissolved in dry THF (60 mL). The resulting solution was cooled to $-25\text{ }^{\circ}\text{C}$. *N*-methylmorpholine (4.55 mL, 41.4 mmol) and isobutyl chloroformate (5.40 mL, 41.4 mmol) were added consecutively. 1,2-Dimethylhydrazine dihydrochloride (10.0 g, 75.2 mmol) was suspended in H_2O (15 mL), and 10 N NaOH (15.0 mL) was added under ice-cooling. This solution was given to the reaction mixture when the precipitation of *N*-methylmorpholine hydrochloride occurred. It was allowed to warm to room temperature within 30 min, and stirred overnight at rt. After evaporation of the solvent, the resulting aqueous residue was extracted with ethyl acetate ($3 \times 60\text{ mL}$). The combined organic layers were washed with H_2O (30 mL), sat. NaHCO_3 ($2 \times 30\text{ mL}$), H_2O (30 mL), and brine (30 mL). The solvent was dried (Na_2SO_4) and evaporated. The crude product was purified on silica gel using ethyl acetate/petroleum ether (1:1) to obtain **82** as a colourless oil (8.30 g, 72%). Compound **82** (2.00 g, 6.51 mmol) was dissolved in MeOH (10 mL). The resulting solution was treated with Pd/C (0.20 g) and hydrogenated in a hydrogen flow for 2 h (2 bar, room temperature). Pd/C was filtered off, and MeOH was removed under reduced pressure to obtain **87** without purification (1.30 g). Compound **69** (1.11 g, 4.08 mmol) was suspended in dry CH_2Cl_2 (50 mL) and treated with DMAP (0.04 g, 0.33 mmol). EDC (1.27 mL, 7.17 mmol) was added (the reaction mixture became clear), and the resulting solution was stirred for 15 min at room temperature. Compound **87** (1.30 g) in dry CH_2Cl_2 (10 mL) was added to the reaction mixture. It was stirred for 18 h at room temperature. CH_2CH_2 was removed. The resulting oily residue was suspended in H_2O and extracted with ethyl acetate ($3 \times 50\text{ mL}$). The combined organic layers were washed with sat. NaHCO_3 ($2 \times 50\text{ mL}$), H_2O (50 mL), and brine (50 mL). The solvent was dried (Na_2SO_4) and evaporated. The oily residue was purified by column chromatography on silica gel using MeOH/ CH_2Cl_2 (1:40) as eluent to obtain **89** as a white solid (0.77 g, 44% from **69**). mp $68\text{--}70\text{ }^{\circ}\text{C}$; $^1\text{H NMR}$ (500 MHz, $\text{DMSO-}d_6$) δ 0.90 (d, $^3J = 1.9\text{ Hz}$, 3H, CH_3CHCH_3), 0.92 (d, $^3J = 1.9\text{ Hz}$, 3H, CH_3CHCH_3), 1.41–1.47 (m, 1H, CH_3CHCH_3), 1.65–1.76 (m, 2H, CHCH_2), 2.55 (d, $^3J = 5.4\text{ Hz}$, 3H, NHCH_3), 2.96 (s, 3H, CONCH_3), 4.89 (q, $^3J = 5.6\text{ Hz}$, NHCH_3), 5.42–5.46 (m, 1H, NHCHCO), 7.37 (dd, $^3J = 5.0\text{ Hz}$, $^3J = 3.8\text{ Hz}$, 1H, H-4'''), 8.07 (d, $^3J = 8.5\text{ Hz}$, 2H, H-3', H-5'), 8.10, 8.12–8.13

(dd, $^3J = 3.8$ Hz, $^4J = 1.3$ Hz, 1H, m, 3H, C-3''', C-2', C-6', C-5'''), 8.48 (d, $^3J = 8.5$ Hz, 1H, NHCHCO); ^{13}C NMR (125 MHz, DMSO- d_6) δ 21.30, 23.46, 24.86 (CH₃CHCH₃, CH₃CHCH₃, CH₃CHCH₃), 31.06 (NHCH₃), 35.05 (CONCH₃), 48.28 (NHCHCO), 124.54 (C-5'''), 127.10 (C-3', C-5'), 128.28 (C-3'''), 128.52 (C-2', C-6'), 129.43, 133.11, 134.38, 137.29 (C-4''', C-2''', C-4', C-1'), 165.49, 167.83, 171.47, 174.15 (C-3'', C-1'CO, NHCHCO, C-5''); Anal. C₂₁H₂₅N₅O₃S (427.52 g/mol) calcd C 59.00, H 5.89, N 16.38; found C 58.12, H 5.90, N 16.01.

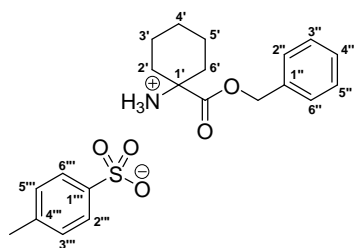
3.3.42. PREPARATION OF 90

N-{4-[5-(2-Thienyl)-1,2,4-oxadiazol-3-yl]benzoyl}-***N***-methylleucine 1,2-dimethylhydrazide. Compound **86** (2.50 g, 7.78 mmol) was dissolved in MeOH (10 mL). The resulting solution was treated with Pd/C (0.25 g) and hydrogenated in a hydrogen flow for 3 h (2 bar, room temperature). Pd/C was filtered off, and MeOH was removed under reduced pressure to obtain **88** without purification (1.61 g). Compound **69** (1.58 g, 5.80 mmol) was suspended in dry CH₂Cl₂ (50 mL) and treated with DMAP (0.05 g, 0.41 mmol). EDC (1.52 mL, 8.59 mmol) was added while the reaction mixture became clear, and it was stirred for 15 min at room temperature. Compound **88** (1.61 g) was dissolved in dry CH₂Cl₂ (10 mL) and added to the reaction mixture. It was stirred for 42 h at room temperature. CH₂CH₂ was removed, and the oily residue was extracted with ethyl acetate (3 × 50 mL). The combined organic layers were washed with sat. NaHCO₃ (2 × 50 mL), H₂O (50 mL), and brine (50 mL). The solvent was dried (Na₂SO₄) and evaporated. The oily residue was purified by column chromatography on silica gel using ethyl acetate/petroleum ether (5:1) as eluent to obtain **90** as a white solid (0.81 g, 32% from **69**). mp 58–60 °C; ¹H NMR (500 MHz, DMSO-*d*₆) mixture of *s*-cis and *s*-trans isomers δ 0.72_a, 0.75_b, (d_a, ³*J* = 6.6 Hz, d_b, ³*J* = 6.6 Hz, 3H, CH₃CHCH₃), 0.96 (app. t, ³*J* = 5.8 Hz, 3H, CH₃CHCH₃), 1.28–1.39 (m, 1H, CH₃CHCH₃), 1.50–1.76 (m, 2H, CHCH₂), 2.11_a, 2.54_b (d_a, ³*J* = 5.7 Hz, d_b, ³*J* = 5.7 Hz, 3H, NHCH₃), 2.90_a, 2.92_b (2 × s, 3H, CH₃NCHCO), 2.96_a, 2.97_b (2 × s, 3H, CONCH₃), 4.68 (q, ³*J* = 5.6 Hz, 1H, NHCH₃), 4.85–4.91 (m, 1H, CH₃NCHCO), 7.37 (dd, ³*J* = 4.7 Hz, ³*J* = 3.8 Hz, 1H, H-4'''), 7.48_a, 7.55_b (d_a, ³*J* = 8.2 Hz, d_b, ³*J* = 8.2 Hz, 2H, H-3', H-5'), 8.08–8.12 (m, 4H, H-2', H-6', H-3''', H-5'''); ¹³C NMR (125 MHz, DMSO-*d*₆) mixture of *s*-cis and *s*-trans isomers δ 21.60, 21.88, 22.34, 23.28, 24.85, 25.14 (CH₃CHCH₃, CH₃CHCH₃, CH₃CHCH₃), 29.32, 30.92, 31.05, 33.64 (CH₃NCHCO, NHCH₃), 34.75, 35.17, 37.12, 38.09 (CONCH₃, CHCH₂), 50.75, 56.03 (CH₃NCHCO), 124.55, 126.56, 126.70, 127.19, 127.42, 127.52, 127.72, 129.42, 133.08, 134.35 (C-5''', C-3', C-5', C-3''', C-2', C-6', C-4''', C-4', C-2'''), 140.09, 140.18 (C-1'), 167.80, 170.13, 170.65, 171.43, 171.86, 173.11 (C-3'', C-1'CO, CH₃NCHCO, C-5''); Anal. C₂₂H₂₇N₅O₃S (441.55 g/mol) calcd C 59.84, H 6.16, N 15.86; found C 59.59, H 6.55, N 14.72.

3.3.43. PREPARATION OF 92

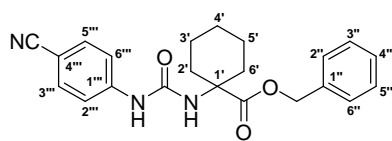


N-{4-[5-(2-Thienyl)-1,2,4-oxadiazol-3-yl]benzoyl}homocycloleucyl-methylazaalanine-nitrile. Compound **116** (0.30 g, 0.68 mmol) was suspended in MeOH (30 mL) and treated with NaOAc (0.17 g, 2.07 mmol) and BrCN (0.15 g, 1.42 mmol). The resulting mixture was stirred at room temperature for 22 h. The solvent was evaporated under reduced pressure. The residue was suspended in H₂O and extracted with ethyl acetate (3 ×30 mL), washed with 10% KHSO₄ (30 mL), H₂O (30 mL), sat. NaHCO₃ (30 mL), H₂O (30 mL), and brine (30 mL). The solvent was dried over Na₂SO₄ and removed under reduced pressure. The crude solid product was purified by column chromatography using ethyl acetate/petroleum ether 1:1 as eluent to obtain **92** as a white solid (0.12 g, 38%). mp 206 °C; ¹H NMR (500 MHz, CDCl₃) δ 1.35–1.40 (m, 1H, H_{cyclohexane}), 1.49–1.53 (m, 2H, H_{cyclohexane}), 1.68–1.79 (m, 3H, H_{cyclohexane}), 1.97–2.02 (m, 2H, H_{cyclohexane}), 2.94 (s, 3H, N(CH₃)CN), 3.22 (s, 3H, CONCH₃), 6.52 (s, 1H, C-1''CONH), 7.22 (dd, ³J = 5.1 Hz, ³J = 3.8 Hz, 1H, H-4'''), 7.67 (dd, ³J = 5.1 Hz, ⁴J = 1.3 Hz, 1H, H-3'''), 7.91 (d, ³J = 8.5 Hz, 2H, H-3'', H-5''), 7.96 (dd, ³J = 3.8 Hz, ⁴J = 1.3 Hz, 1H, H-5'''), 8.23 (d, ³J = 8.6 Hz, 2H, H-2'', H-6''); ¹³C NMR (125 MHz, CDCl₃) δ 21.75 (C-3', C-5'), 25.02 (C-4'), 31.94 (C-2', C-6'), 33.11 (NH(CH₃)CN), 41.07 (CONCH₃), 59.50 (C-1'), 114.51 (CN), 125.53 (C-5'''), 127.53 (C-3'', C-5''), 128.04 (C-2'', C-6''), 128.60, 130.13 (C-3''', C-4'''), 132.15, 132.31 (C-2''', C-4''), 136.13 (C-1''), 165.28, 167.96, 171.73, 173.10 (C-1''CONH, C-3'', NHCCO, C-5''); LC-MS(ESI) (90% H₂O to 100% MeOH in 20 min, then 100% MeOH to 30 min, DAD 220.0–400.0 nm) t_r = 15.37, 97% purity, m/z = 465.2 ([M + H]⁺).

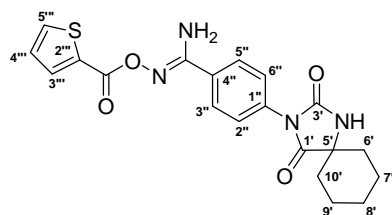
3.3.44. PREPARATION OF **94**

Homocycloleucine benzyl ester *p*-toluenesulfonate. 1-Amino-1-cyclohexanecarboxylic acid **93** (4.00 g, 27.9 mmol) and *p*-toluenesulfonic acid (6.37 g, 37.0 mmol) were suspended in a mixture of toluene and benzyl alcohol 4:1 (100 mL) and heated to reflux under Dean-Stark conditions for 8 h. Toluene was removed, and the white residue was suspended in the -25 °C cold ethyl acetate/petroleum ether (1:1) mixture. The suspension was filtered off, washed with ethyl acetate and petroleum ether, and dried to obtain **94** as a white solid (11.0 g, 97%). mp 165–167 °C; ¹H NMR (500 MHz, DMSO-*d*₆) δ 1.38–1.41 (m, 2H, H_{cyclohexane}), 1.52–1.59 (m, 4H, H_{cyclohexane}), 1.69–1.74 (m, 2H, H_{cyclohexane}), 1.94–2.00 (m, 2H, H_{cyclohexane}), 2.28 (s, 3H, C-4'''CH₃), 5.25 (s, 2H, OCH₂), 7.10–7.12 (m, 2H, H-3''', H-5'''), 7.34–7.42 (m, 5H, H_{arom}''), 7.48 (d, 2H, ³J = 7.9 Hz, H-2''', H-6'''), 8.43 (s, 3H, NH₃⁺); ¹³C NMR (125 MHz, DMSO-*d*₆) δ 20.32 (C-3', C-5'), 20.92 (C-4'''CH₃), 23.92 (C-4'), 31.39 (C-2', C-6'), 58.86 (C-1'), 67.53 (OCH₂), 125.65 (C-2'', C-6''), 128.20 (C-2''', C-6''', C-3'', C-5'''), 128.54 (C-4''), 128.69 (C-3''', C-5'''), 135.35 (C-1''), 137.80 (C-1'''), 145.81 (C-4'''), 170.87 (COO); Anal. C₂₁H₂₇NO₅S (405.51 g/mol) calcd C 62.20, H 6.71, N 3.45; found C 62.10, H 6.65, N 3.39.

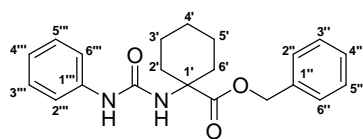
3.3.45. PREPARATION OF 95



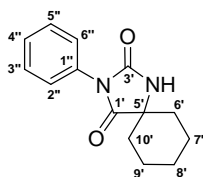
***N*-(4-Cyanophenylcarbamoyl)homocycloleucine benzyl ester.** Compound **94** (3.00 g, 7.40 mmol) and triethylamine (2.25 g, 22.2 mmol) were dissolved in a dry THF (40 mL) and treated with 4-cyanophenyl isocyanate (1.07 g, 7.42 mmol). The resulting reaction mixture was stirred at room temperature for 1 h. THF was removed, and the residue was suspended in H₂O. The aqueous suspension was extracted with ethyl acetate (3 × 30 mL). The combined organic layers were washed with saturated NaHCO₃ (2 × 30 mL), water (30 mL), 10% KHSO₄ (30 mL), H₂O (30 mL), and brine (30 mL), dried and evaporated under reduced pressure. The crude product was recrystallized from ethyl acetate to obtain **95** as a white solid (2.60 g, 93%). mp 188–190 °C; ¹H NMR (500 MHz, DMSO-*d*₆) δ 1.21–1.28 (m, 1H, H_{cyclohexane}), 1.41–1.48 (m, 2H, H_{cyclohexane}), 1.55–1.57 (m, 3H, H_{cyclohexane}), 1.70–1.76 (m, 2H, H_{cyclohexane}), 5.07 (s, 2H, OCH₂), 6.77 (s, 1H, NHC-1'), 7.22–7.31 (m, 5H, H_{arom}''), 7.52 (d, 2H, ³*J* = 9.2 Hz, H-3''', H-5'''), 7.66 (d, 2H, ³*J* = 8.9 Hz, H-2''', H-6'''), 8.95 (s, 1H, C-1''')NH; ¹³C NMR (125 MHz, DMSO-*d*₆) δ 21.04 (C-3', C-5'), 24.90 (C-4'), 32.38 (C-2', C-6'), 57.95 (C-1'), 65.84 (OCH₂), 102.81 (C-4'''), 117.63 (C-2''', C-6'''), 119.50 (CN), 127.74 (C-2'', C-6''), 127.94 (C-4''), 128.36 (C-3'', C-5''), 133.34 (C-3''', C-5'''), 136.45 (C-1'''), 144.64 (C-1''), 154.00 (NHCONH), 174.21 (COO); Anal. C₂₂H₂₃N₃O₃ (377.44 g/mol) calcd C 70.01, H 6.14, N 11.13; found C 70.04, H 6.17, N 11.12.

3.3.46. PREPARATION OF **97**

2-{4-[(2-Thiophenecarbonyl)oxyamidino]phenyl}-2,4-diazaspiro[4.5]decan-1,3-dione. Compound **95** (2.40 g, 6.36 mmol) was dissolved in EtOH (50 mL) and treated with DIPEA (1.64 g, 12.7 mmol) and hydroxylamine hydrochloride (0.88 g, 12.7 mmol). The resulting solution was refluxed for 3 h. EtOH was evaporated, the oily residue was dissolved in MeCN (30 mL) and treated with triethylamine (1.30 g, 12.8 mmol) and 2-thiophencarbonyl chloride (1.86 g, 12.7 mmol). The solution was stirred at room temperature for 1 h. The precipitated product was filtrated off and washed with 10% KHSO₄ (3 × 20 mL), H₂O (20 mL), sat. NaHCO₃ (3 × 20 mL), H₂O (20 mL), and *n*-hexane (20 mL). The dry product was recrystallised from EtOH/H₂O (10:1) to obtain **97** as a white solid (2.30 g, 88%). mp > 230 °C; ¹H NMR (500 Hz, DMSO-*d*₆) δ 1.29–1.36 (m, 1H, H_{cyclohexane}), 1.54–1.61 (m, 3H, H_{cyclohexane}), 1.68–1.78 (m, 6H, H_{cyclohexane}), 6.99 (s, 2H, NH₂), 7.25 (dd, ³*J* = 4.8 Hz, ³*J* = 3.8 Hz, 1H, H''-4), 7.49_a, 7.84_b (d_a, 2H, ³*J* = 8.8 Hz, d_b, 2H, ³*J* = 8.9 Hz, H''-3, H''-5, H''-2, H''-6), 7.97_a, 8.14_b (dd_a, ³*J* = 4.9 Hz, ⁴*J* = 1.1 Hz, 1H, dd_b, 1H, ³*J* = 3.8 Hz, ⁴*J* = 1.3 Hz, H'''-3, H'''-4), 8.99 (s, 1H, CONH); ¹³C NMR (125 MHz, DMSO-*d*₆) δ 20.93 (C-7', C-9'), 24.54 (C-8'), 33.49 (C-6', C-10'), 61.08 (C-5'), 126.58 (C''-2, C''-6), 127.39 (C-3'', C-5''), 128.39 (C-4''), 130.81 (C-4'''), 132.78, 133.87, 133.98 (C-3''', C-5''', C-2'''), 134.26 (C-1''), 154.44 (NCONH), 156.62 (COON), 159.76 (N=C), 175.75 (NHCCO); Anal. C₂₀H₂₀N₄O₄S (412.46 g/mol) calcd C 58.24, H 4.89, N 13.58; found C 58.25, H 4.89, N 13.36. MS(ESI) *m/z* = 413.3 ([M + H]⁺).

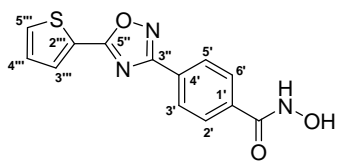
3.3.47. PREPARATION OF 98

***N*-(Phenylcarbamoyl)-homocycloleucine benzyl ester.** Compound **94** (2.00 g, 4.93 mmol) was dissolved in dry THF (50 mL) and treated with DIPEA (3.19 g, 24.7 mmol). The resulting solution was treated with phenyl isocyanate (0.59 g, 4.95 mmol) and stirred for 1 h at rt. After evaporation of the solvent, the resulting residue was suspended in H₂O and extracted with ethyl acetate (3 × 30 mL). The combined organic layers were washed with sat. NaHCO₃ (60 mL), H₂O (60 mL), 10% KHSO₄ (60 mL), H₂O (60 mL), and brine (60 mL). The solvent was dried (Na₂SO₄) and evaporated to obtain **98** as a white solid (1.36 g, 78%). mp 181–182 °C; ¹H NMR (500 MHz, DMSO-*d*₆) δ 1.20–1.28 (m, 1H, H_{cyclohexane}), 1.42–1.49 (m, 2H, H_{cyclohexane}), 1.54–1.57 (m, 3H, H_{cyclohexane}), 1.69–1.75 (m, 2H, H_{cyclohexane}), 1.95–1.98 (m, 2H, H_{cyclohexane}), 5.06 (s, 2H, OCH₂), 6.52 (s, 1H, NHCCO), 6.89–6.92 (m, 1H, H_{arom}), 7.20–7.25 (m, 5H, H_{arom}), 7.30–7.32 (m, 2H, H_{arom}), 7.34–7.36 (m, 2H, H_{arom}), 8.41 (s, 1H, C-1''''NH); ¹³C NMR (125 MHz, DMSO-*d*₆) δ 21.07 (C-3', C-5'), 24.97 (C-4'), 32.57 (C-2', C-6'), 57.71 (C-1'), 65.72 (OCH₂), 117.68 (C-2''', C-6'''), 121.33 (C-4'''), 127.68 (C-2'', C-6''), 127.85 (C-4''), 128.33, 128.79 (C-3''', C-5''', C-3'', C-5''), 136.55 (C-1'''), 140.26 (C-1''), 154.55 (NHCONH), 174.53 (COO); Anal. C₂₁H₂₄N₂O₃ (352.43 g/mol) calcd C 71.57, H 6.86, N 7.95; found C 71.55, H 7.01, N 7.99.

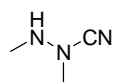
3.3.48. PREPARATION OF 100

2-(Phenyl)-2,4-diazaspiro[4.5]decan-1,3-dione. Compound **98** (0.60 g, 1.70 mmol) was dissolved in MeOH (60 mL) and treated with DIPEA (0.44 g, 3.40 mmol). The resulting reaction solution was treated with 1,2-dimethylhydrazine dihydrochloride (0.45 g, 3.38 mmol) and stirred for 2 d at rt. After evaporation of the solvent, the residue was suspended in H₂O and extracted with ethyl acetate (3 × 30 mL). The combined organic layers were washed with H₂O (60 mL) and brine (60 mL). The solvent was dried (Na₂SO₄) and evaporated. The crude product was purified by column chromatography using ethyl acetate/petroleum ether (1:2) as eluent to obtain **100** as a white solid (0.30 g, 72%). mp 215–217 °C; ¹H NMR (500 MHz, DMSO-*d*₆) δ 1.30–1.35 (m, 1H, H_{cyclohexane}), 1.53–1.61 (m, 3H, H_{cyclohexane}), 1.65–1.76 (m, 6H, H_{cyclohexane}), 7.33–7.47 (m, 5H, H_{arom}), 8.91 (s, 1H, NHCCO); ¹³C NMR (125 MHz, DMSO-*d*₆) δ 20.92 (C-7', C-9'), 24.53 (C-8'), 33.49 (C-6', C-10'), 60.99 (C-5'), 126.90 (C-2'', C-6''), 127.81 (C-4''), 128.76 (C-3'', C-5''), 132.31 (C-1''), 154.73 (NHCONH), 175.90 (COO); Anal. C₁₄H₁₆N₂O₂ (244.29 g/mol) calcd C 68.83, H 6.60, N 11.47; found C 68.72, H 6.67, N 11.47.

3.3.49. PREPARATION OF 101

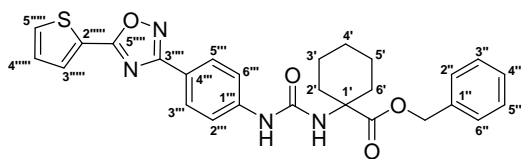


4-[5-(2-Thienyl)-1,2,4-oxadiazol-3-yl]-N-hydroxybenzamide. Compound **69** (1.20 g, 4.41 mmol) was dissolved in dry THF (40 mL). The resulting reaction mixture was cooled to $-25\text{ }^{\circ}\text{C}$, treated with *N*-methylmorpholine (0.49 g, 4.84 mmol) and isobutyl chloroformate (0.66 g, 4.83 mmol), and stirred for 10 min at $-25\text{ }^{\circ}\text{C}$. Hydroxylamine hydrochloride (1.39 g, 20.0 mmol) and sodium hydroxide (0.88 g, 22.0 mmol) were treated with MeOH (30 mL). The precipitated NaCl was filtered off, and the filtrate was added to the solution of the mixed anhydride. The resulting mixture was slowly warm to the room temperature and stirred at room temperature for 4 h. The solvent was removed under reduced pressure, and the residue was suspended in H_2O . The aqueous suspension was extracted with ethyl acetate ($3 \times 80\text{ mL}$). The combined organic layers were washed with 10% KHSO_4 (50 mL), H_2O (50 mL), brine (50 mL), and dried over Na_2SO_4 . The crude product was recrystallized from ethanol/ethyl acetate (1:8) to obtain **101** as a white solid (1.01 g, 80%). mp $190\text{ }^{\circ}\text{C}$; ^1H NMR (500 MHz, $\text{DMSO}-d_6$) 7.36 (dd, $^3J = 5.1\text{ Hz}$, $^3J = 3.8\text{ Hz}$, 1H, H-4'''), 7.94 (d, $^3J = 8.9\text{ Hz}$, H-3', H-5'), 8.09_a 8.11–8.13_b (dd_a, $^3J = 3.8\text{ Hz}$, $^4J = 1.3\text{ Hz}$, 1H, m_b, 3H, H-2', H-6', H-3''' H-5'''), 9.14 (s, 1H, NHOH), 11.39 (s, 1H, NHOH); ^{13}C NMR (125 MHz, $\text{DMSO}-d_6$) δ 124.53 (C-5'''), 127.34, 127.98, 128.35, 129.45, 133.13, 134.41, 135.73 (C-3', C-5', C-3''', C-4''', C-2', C-6', C-2''', C-4', C-1'), 163.50, 167.78, 171.49 (CONHOH, C-3'', C-5''); Anal. $\text{C}_{13}\text{H}_9\text{N}_3\text{O}_3\text{S}$ (287.29 g/mol) calcd C 54.35, H 3.16, N 14.63; found C 54.35, H 3.15, N 14.47.

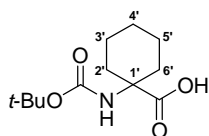
3.3.50. PREPARATION OF 102

1,2-Dimethylhydrazine-carbonitrile. 1,2-Dimethylhydrazine dihydrochloride (6.70 g, 50.4 mmol) was dissolved in H₂O (20 mL). 5 N NaOH (20.0 mL, 0.10 mol) was added under ice-cooling. Sodium acetate (8.20 g, 0.10 mol) and cyanogen bromide (3.56 g, 33.6 mmol) were added. The resulting reaction mixture was stirred for 20 h at room temperature. It was extracted with ethyl acetate (3 × 30 mL). The combined organic layers were washed with brine (50 mL) and dried over Na₂SO₄. The solvent was evaporated under reduced pressure. The product was purified by distillation to obtain **102** as a colourless fluid (0.95 g, 33%). bp 90 °C at 24 mbar. ¹H NMR (500 MHz, CDCl₃) δ 2.67 (s, 3H, NHCH₃), 2.96 (s, 3H, N(CH₃)CN), 3.78 (bs, 1H, NHCH₃); ¹³C NMR (125 MHz, CDCl₃) δ 35.38 (NHCH₃), 40.83 (N(CH₃)CN), 116.53 (CN); MS(EI) *m/z* = 85.1 (M^{•+}).

3.3.51. PREPARATION OF 103

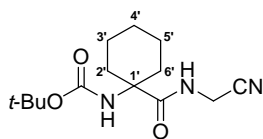


***N*-{4-[5-(2-Thienyl)-1,2,4-oxadiazol-3-yl]phenylcarbamoyl}homocycloleucine benzyl ester.** Compound **94** (1.69 g, 4.17 mmol) was dissolved in H₂O and treated with 8 mL of 5 N NaOH solution. The aqueous layer was extracted with ethyl acetate (3 × 30 mL), and the combined organic layers were washed with sat. NaHCO₃ (30 mL), H₂O (30 mL), brine (30 mL), and dried over Na₂SO₄ to obtain homocycloleucine benzyl ester without further purification. DMAP (0.034 g, 0.28 mmol) and EDC (0.44 g, 2.83 mmol) were dissolved in dry THF (30 mL) and slowly treated with compound **101** (0.80 g, 2.78 mmol) in dry THF (50 mL). The resulting reaction mixture was stirred at room temperature for 1 h. Homocycloleucine benzyl ester in dry THF (20 mL) was added, and it was stirred at room temperature for 18 h. The solvent was removed under reduced pressure, and the residue was suspended in H₂O. The aqueous suspension was extracted with ethyl acetate (3 × 50 mL). The combined organic layers were washed with 10% KHSO₄ (2 × 50 mL), H₂O (50 mL), sat. NaHCO₃ (2 × 50 mL), H₂O (50 mL), brine (50 mL) and dried over Na₂SO₄. The crude product was recrystallized from EtOH/ethyl acetate (1:1) to obtain **103** as a white solid (0.90 g, 64%). mp 216 °C; ¹H NMR (500 MHz, DMSO-*d*₆) δ 1.22–1.29 (m, 1H, H_{cyclohexane}), 1.43–1.50 (m, 2H, H_{cyclohexane}), 1.56–1.58 (m, 3H, H_{cyclohexane}), 1.71–1.77 (m, 2H, H_{cyclohexane}), 1.98–2.00 (m, 2H, H_{cyclohexane}), 5.08 (s, 2H, OCH₂), 6.68 (s, 1H, NHCCO), 7.23–7.26, 7.31–7.33 (m, 5H, H_{arom}'), 7.35 (dd, ³*J* = 4.9 Hz, ³*J* = 3.6 Hz, 1H, H-4'''''), 7.57 (d, ³*J* = 8.8 Hz, 2H, H-2''', H-6'''), 7.93 (d, ³*J* = 8.9 Hz, 2H, H-3''', H-5'''), 8.05_a, 8.09_b (dd_a, ³*J* = 3.8 Hz, ⁴*J* = 1.3 Hz, 1H, dd_b, ³*J* = 4.9 Hz, ⁴*J* = 1.1 Hz, 2H, H-3''''', H-5'''''), 8.83 (s, 1H, C-1''''NH); ¹³C NMR (125 MHz, DMSO-*d*₆) δ 21.08 (C-3', C-5'), 24.95 (C-4'), 32.49 (C-2', C-6'), 57.88 (C-1'), 65.82 (OCH₂), 117.70, 118.49, 124.82, 127.73, 127.92, 128.16, 128.37, 129.36, 132.78, 134.01, 136.51, 143.43, (C-2''', C-6''', C-5''''', C-4''', C-3''''', C-2'', C-6'', C-4'', C-3''', C-5''', C-4''''', C-3'', C-5'', C-2''''', C-1''', C-1''), 154.22 (NHCONH), 168.07, 170.90, 174.35 (C-3''''', C-5''''', NHCCO); Anal. C₂₇H₂₆N₄O₄S (502.59 g/mol) calcd C 64.52, H 5.21, N 11.15; found C 63.85, H 5.26, N 10.61. MS (ESI) *m/z* = 503.3 ([M + H]⁺).

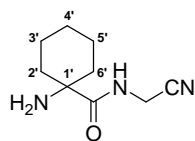
3.3.52. PREPARATION OF 107

***N*-(*tert*-Butyloxycarbonyl)homocycloleucine.** Compound **93** (2.00 g, 14.0 mmol) was dissolved in 2 N NaOH (10 mL). (Boc)₂O (6.11 g, 28.0 mmol) in dioxane (10 mL) was added. The resulting reaction mixture was stirred for 40 h at room temperature. Ethyl acetate (30 mL) was added and the layers were separated. The aqueous layer was acidified with concentrated HCl and extracted with ethyl acetate (3 × 30 mL). The combined organic layers were washed with H₂O (30 mL) and brine (30 mL), and dried over Na₂SO₄. The solvent was removed under reduced pressure to obtain **107** as a white solid (1.65 g, 48%). mp 172 °C; ¹H NMR (500 MHz, DMSO-*d*₆) δ 1.15–1.23 (m, 1H, H_{cyclohexane}), 1.36 (s, 9H, C(CH₃)₃), 1.43–1.49 (m, 5H, H_{cyclohexane}), 1.58–1.63 (m, 2H, H_{cyclohexane}), 1.88 (bs, 2H, H_{cyclohexane}), 6.82 (s, 1H, OCONH) 12.03 (s, 1H, COOH); ¹³C NMR (125 MHz, DMSO-*d*₆) δ 21.16 (C-3', C-5'), 25.16 (C-4'), 28.39 (C(CH₃)₃), 32.05 (C-2', C-6'), 58.00 (C-1'), 77.81 (C(CH₃)₃), 154.94 (OCO), 176.35 (COOH); Anal. C₁₂H₂₁NO₄ (243.30 g/mol) calcd C 59.24, H 8.70, N 5.76; found C 59.11, H 8.49, N 5.79.

3.3.53. PREPARATION OF 108

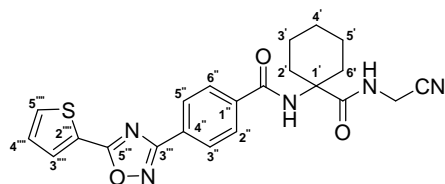


***N*-(*tert*-Butyloxycarbonyl)homocycloleucyl-glycine-nitrile.** Compound **107** (1.00 g, 4.11 mmol) was dissolved in dry THF (20 mL) and cooled to $-25\text{ }^{\circ}\text{C}$. To the stirred solution, triethylamine (1.24 g, 12.3 mmol) and isobutyl chloroformate (0.62 g, 4.54 mmol) were added consecutively. Aminoacetonitrile monosulfate (1.74 g, 11.3 mmol) was added to the reaction mixture when the precipitation of triethylamine hydrochloride occurred (ca. 5 min). It was allowed to warm to room temperature within 30 min and stirred for additional 3 h. After evaporation of the solvent, the resulting aqueous residue was extracted with ethyl acetate ($3 \times 60\text{ mL}$). The combined organic layers were washed with 10% KHSO_4 (30 mL), H_2O (30 mL), sat. NaHCO_3 (30 mL), H_2O (30 mL), and brine (30 mL). The solvent was dried (Na_2SO_4) and evaporated. The crude product was purified by column chromatography using ethyl acetate as eluent to obtain **108** (0.78 g, 67%). mp $164\text{ }^{\circ}\text{C}$; ^1H NMR (500 MHz, $\text{DMSO-}d_6$) δ 1.18–1.23 (m, 1H, $\text{H}_{\text{cyclohexane}}$), 1.36 (s, 9H, $\text{C}(\text{CH}_3)_3$), 1.45 (bs, 5H, $\text{H}_{\text{cyclohexane}}$), 1.60–1.65 (m, 2H, $\text{H}_{\text{cyclohexane}}$), 1.84 (bs, 2H, $\text{H}_{\text{cyclohexane}}$), 4.03 (d, $^3J = 5.7\text{ Hz}$, 2H, NHCH_2CN), 6.69 (bs, 1H, OCONH), 8.08 (bs, 1H, CONH); ^{13}C NMR (125 MHz, $\text{DMSO-}d_6$) δ 20.31 (C-3', C-5'), 24.35 (C-4'), 26.87 (NHCH_2CN), 27.53 ($\text{C}(\text{CH}_3)_3$), 31.12 (C-2', C-6'), 57.76 (C-1'), 77.42 ($\text{C}(\text{CH}_3)_3$), 117.02 (CN), 153.58 (OCO), 174.69 (CONH); Anal. $\text{C}_{14}\text{H}_{23}\text{N}_3\text{O}_3$ (281.35 g/mol) calcd C 59.77, H 8.24, N 14.94; found C 59.75, H 8.63, N 14.78.

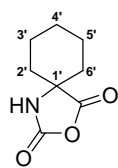
3.3.54. PREPARATION OF 109

Homocycloleucyl-glycine-nitrile. Compound **113** (0.52 g, 3.07 mmol) was dissolved in CH_2Cl_2 (20 mL) and treated with DIPEA (2.78 g, 21.5 mmol). Aminoacetonitrile monosulfate (0.57 g, 3.70 mmol) was added, and the resulting reaction mixture was refluxed for 1 h. The solvent was removed under reduced pressure. The oily residue was suspended in H_2O and extracted with ethyl acetate (3×30 mL). The combined organic layers were washed with H_2O (30 mL), sat. NaHCO_3 (30 mL), and brine (30 mL). The solvent was dried over Na_2SO_4 and removed under reduced pressure. The crude oily product was purified by column chromatography using $\text{CH}_2\text{Cl}_2/\text{MeOH}$ (9:1) as eluent to obtain **109** as a colorless oil (0.40 g, 72%). ^1H NMR (500 MHz, CDCl_3) δ 1.26–1.31 (m, 1H, $\text{H}_{\text{cyclohexane}}$), 1.35–1.40 (m, 4H, $\text{H}_{\text{cyclohexane}}$), 1.46 (s, 2H, NH_2), 1.64–1.66 (m, 3H, $\text{H}_{\text{cyclohexane}}$), 1.90–1.97 (m, 2H, $\text{H}_{\text{cyclohexane}}$), 4.14 (d, $^3J = 6.0$ Hz, 2H, NHCH_2CN), 8.34 (bs, 1H, NHCH_2CN); ^{13}C NMR (125 MHz, CDCl_3) δ 20.96 (C-3', C-5'), 25.03 (C-4'), 27.26 (NHCH_2CN), 34.35 (C-2', C-6'), 57.46 (C-1'), 116.36 (NHCH_2CN), 178.24 (CONH).

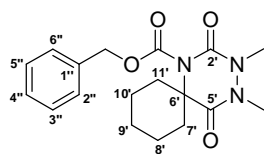
3.3.55. PREPARATION OF 111

***N*-{4-[5-(2-Thienyl)-1,2,4-oxadiazol-3-yl]benzoyl}homocycloleucyl-glycine-nitrile.**

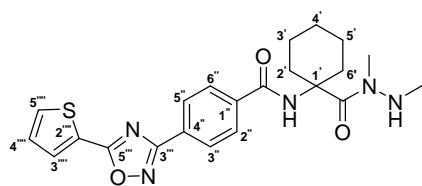
Compound **108** (0.30 g, 1.07 mmol) was dissolved in dry THF (10 mL). Dry methanesulfonic acid (0.72 g, 7.49 mmol) was added. The resulting reaction mixture was stirred for 24 h at room temperature. THF was evaporated under reduced pressure. The residue was dissolved in a small amount of H₂O. The resulting solution was adjusted with 2 N NaOH to a pH of ~12–13, extracted with ethyl acetate (3 × 30 mL), washed with brine (30 mL), and dried over Na₂SO₄. The solvent was removed under reduced pressure to obtain homocycloleucyl-glycine-nitrile (**109**, 0.20 g) as a colorless oil without purification. Compound **69** (0.29 g, 1.07 mmol) was dissolved in dry CH₂Cl₂ (20 mL) and treated with oxalyl chloride (0.19 g, 1.50 mmol) and DMF (0.5 mL). The reaction mixture was stirred at room temperature for 1 h. The solvent was removed under reduced pressure. The resulting residue was dissolved in dry THF (10 mL) and added to a mixture of homocycloleucyl-glycine-nitrile (**109**, 0.20 g) and DIPEA (0.19 g, 1.47 mmol) in dry THF (10 mL) under ice-cooling. The resulting reaction mixture was stirred for 20 h at room temperature. After evaporation of the solvent, the residue was extracted with ethyl acetate (3 × 60 mL). The combined organic layers were washed with 10% KHSO₄ (30 mL), H₂O (30 mL), sat. NaHCO₃ (30 mL), H₂O (30 mL), and brine (30 mL). The solvent was dried (Na₂SO₄) and evaporated. The crude product was purified by recrystallisation from ethyl acetate to obtain **111** (0.09 g, 19% from **108**). mp 189 °C; ¹H NMR (500 MHz, DMSO-*d*₆) δ 1.26–1.30 (m, 1H, H_{cyclohexane}), 1.55 (bs, 5H, H_{cyclohexane}), 1.75–1.81 (m, 2H, H_{cyclohexane}), 2.13–2.15 (m, 2H, H_{cyclohexane}), 4.06 (d, ³*J* = 5.7 Hz, 2H, NHCH₂CN), 7.37 (dd, ³*J* = 5.1 Hz, ³*J* = 3.8 Hz, 1H, H-4'''), 8.08 (d, ³*J* = 8.9 Hz, 2H, H-3'', H-5''), 8.10 (dd, ³*J* = 3.8 Hz, ⁴*J* = 1.3 Hz, 1H, H-3'''), 8.12–8.15 (m, 3H, H-5''', H-2'', H-6''), 8.19 (s, 1H, C-1''CONH), 8.23 (t, ³*J* = 5.7 Hz, 1H, NHCH₂CN); ¹³C NMR (125 MHz, DMSO-*d*₆) δ 21.38 (C-3', C-5'), 25.19 (C-4'), 27.76 (NHCH₂CN), 31.81 (C-2', C-6'), 59.68 (C-1'), 117.87 (CN), 124.52 (C-5'''), 126.95 (C-3'', C-5''), 128.34 (C-4'''), 128.90 (C-2'', C-6''), 129.45 (C-3'''), 133.16, 134.42 (C-2''', C-4''), 137.66 (C-1''), 165.80, 167.84, 171.52, 174.87 (C-1''CONH, C-3''', NHCCO, C-5'''); LC-ESI/MS (90% H₂O to 100% MeOH in 20 min, then 100% MeOH to 30 min, DAD 220.5–400.2 nm) *t*_r = 18.93, 97% purity, *m/z* = 436.4 ([M + H]⁺).

3.3.56. PREPARATION OF 113

Homocycloleucine-NCA. Compound **39** (4.20 g, 15.1 mmol) was dissolved in dry CH_2Cl_2 (100 mL). Oxalyl chloride (2.88 g, 22.7 mmol) and DMF (0.5 mL) were added. The resulting reaction mixture was stirred for 3 h at room temperature. CH_2Cl_2 was removed under reduced pressure. The crude product was purified by column chromatography using ethyl acetate/petroleum ether (1:1) on silica gel to obtain **113** as a white solid (2.11 g, 83%). mp 114 °C; ^1H NMR (500 MHz, $\text{DMSO}-d_6$) δ 1.29–1.37 (m, 1H, $\text{H}_{\text{cyclohexane}}$), 1.44–1.54 (m, 3H, $\text{H}_{\text{cyclohexane}}$), 1.62–1.68 (m, 2H, $\text{H}_{\text{cyclohexane}}$), 1.71–1.74 (m, 4H, $\text{H}_{\text{cyclohexane}}$), 9.43 (s, 1H, NH); ^{13}C NMR (125 MHz, $\text{DMSO}-d_6$) δ 20.81 (C-3', C-5'), 24.21 (C-4'), 33.42 (C-2', C-6'), 62.42 (C-1'), 150.96 (NHCOO), 173.82 (C-1'COO); MS (ESI) m/z = 187.2 ($[\text{M} + \text{NH}_4]^+$). Anal. $\text{C}_8\text{H}_{11}\text{NO}_3$ (169.18 g/mol) calcd C 56.80, H 6.55, N 8.28; found C 57.13, H 6.68, N 8.21.

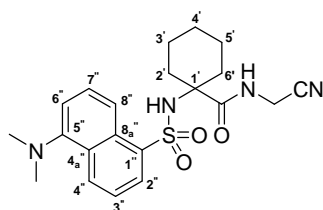
3.3.57. PREPARATION OF 115

1-(Benzyloxycarbonyl)-3,4-dimethyl-1,3,4-triazaspiro[5.5]undecan-2,5-dione. Compound **40** (0.44 g, 1.38 mmol) was dissolved in MeCN (10 mL). The resulting solution was treated with DMAP (8.4 mg, 0.069 mmol) and (Boc)₂O (0.45 g, 2.06 mmol). It was stirred for 24 h at room temperature. The solvent was removed under reduced pressure. The oily residue was purified by column chromatography on silica gel using ethyl acetate/petroleum ether (1:1) as eluent to obtain **115** (0.34 g, 71%) as a colorless oil. ¹H NMR (500 MHz, DMSO-*d*₆) δ 1.27–1.34 (m, 1H, H_{cyclohexane}), 1.46–1.51 (m, 1H, H_{cyclohexane}), 1.59–1.64 (m, 4H, H_{cyclohexane}), 1.71–1.76 (m, 2H, H_{cyclohexane}), 1.99–2.05 (m, 2H, H_{cyclohexane}), 3.12 (s, 3H, NCH₃), 3.20 (s, 3H, NCH₃), 5.16 (s, 2H, CH₂O), 7.31–7.38 (m, 5H, H_{arom}); ¹³C NMR (125 MHz, DMSO-*d*₆) δ 22.27 (C-8', C-10'), 24.52 (C-9'), 30.58 (C-7', C-11'), 32.75, 33.93 (2 × NCH₃), 61.51 (C-6'), 68.18 (CH₂O), 127.95 (C-2'', C-6''), 128.29 (C-4''), 128.53 (C-3'', C-5''), 135.51 (C-1''), 151.93, 152.75 (OCON, NCON), 167.42 (NCCO); MS (ESI) *m/z* = 346.4 ([M + H]⁺).

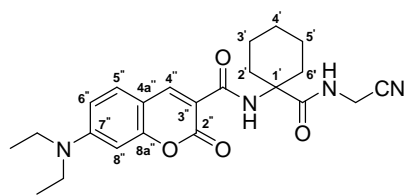
3.3.58. PREPARATION OF 116

***N*-{4-[5-(2-Thienyl)-1,2,4-oxadiazol-3-yl]benzoyl}homocycloleucine 1,2-dimethylhydrazide.** Compound **40** (0.75 g, 2.35 mmol) was dissolved in MeOH (30 mL) and treated with Pd/C (0.075 g). The resulting mixture was hydrogenated in a hydrogen flow at 2 bar and room temperature for 4 h. Pd/C was filtered off, and the solvent was removed under reduced pressure to obtain homocycloleucine 1,2-dimethylhydrazide (**106**, 0.48 g) as a colorless oil which was used without further purification. Compound **69** (0.64 g, 2.35 mmol) was suspended in dry CH₂Cl₂ (20 mL), treated with DMAP (0.015 g, 0.12 mmol) and EDC (0.36 g, 2.32 mmol), and stirred at room temperature for 10 min. Homocycloleucine 1,2-dimethylhydrazide (**106**, 0.48 g) in dry CH₂Cl₂ (10 mL) was added, and the resulting solution was stirred for 18 h at room temperature. The solvent was evaporated under reduced pressure. The residue was suspended in H₂O, extracted with ethyl acetate (3 × 30 mL), and washed with sat. NaHCO₃ (30 mL), H₂O (30 mL), and brine (30 mL). The solvent was dried over Na₂SO₄ and removed under reduced pressure. The crude oily product was purified by column chromatography using CH₂Cl₂/MeOH 20:1 as eluent to obtain **116** as a white solid (0.38 g, 37% from **40**). mp 189 °C; ¹H NMR (500 MHz, CDCl₃) δ 1.29–1.36 (m, 1H, H_{cyclohexane}), 1.49–1.57 (m, 2H, H_{cyclohexane}), 1.64–1.72 (m, 5H, H_{cyclohexane}), 1.93–1.98 (m, 2H, H_{cyclohexane}), 2.44 (s, 3H, NHCH₃), 3.10 (s, 3H, CONCH₃), 6.42 (s, 1H, C-1''CONH), 7.22 (dd, ³J = 5.1 Hz, ³J = 3.8 Hz, 1H, H-4'''), 7.66 (dd, ³J = 5.1 Hz, ⁴J = 1.3 Hz, 1H, H-3'''), 7.91 (d, ³J = 8.5 Hz, 2H, H-3'', H-5''), 7.96 (dd, ³J = 3.6 Hz, ⁴J = 1.1 Hz, 1H, H-5'''), 8.20 (d, ³J = 8.5 Hz, 2H, H-2'', H-6''); ¹³C NMR (125 MHz, CDCl₃) δ 21.84 (C-3', C-5'), 25.35 (C-4'), 32.23 (C-2'', C-6''), 33.54, 35.67 (NHCH₃, CONCH₃), 59.63 (C-1'), 125.59 (C-5'''), 127.46 (C-3'', C-5''), 127.87 (C-2'', C-6''), 128.59, 129.56 (C-3''', C-4'''), 132.10, 132.25 (C-2''', C-4''), 137.29 (C-1''), 164.98, 168.11, 171.67 (C-1''CONH, C-3''', C-5'''). Anal. C₂₂H₂₅N₅O₃S (439.53 g/mol) calcd C 60.12, H 5.73, N 15.93; found C 59.46, H 5.85, N 15.58.

3.3.59. PREPARATION OF 119

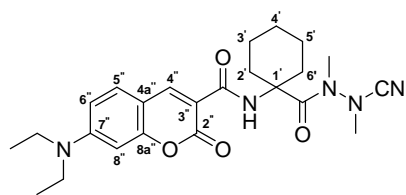
***N*-[5-(Dimethylamino)naphthalene-1-sulfonyl]homocycloleucyl-glycine-nitrile.**

Compound **109** (0.38 g, 2.10 mmol) was dissolved in dry THF (30 mL). Triethylamine (0.32 g, 3.16 mmol) and 5-(Dimethylamino)naphthalene-1-sulfonyl chloride **117** (0.62 g, 2.30 mmol) were added. The resulting reaction solution was stirred for 24 h at room temperature, and heated to reflux for additionally 24 h. The solvent was removed, and the residue was suspended in H₂O. The aqueous suspension was extracted with ethyl acetate (3 × 30 mL). The combined organic layers were washed with brine (30 mL), and dried over (Na₂SO₄). The crude product was purified by column chromatography using ethyl acetate to obtain **119** as a green solid (0.31 g, 36%). mp 79–81 °C; ¹H NMR (500 MHz, DMSO-*d*₆) δ 0.80–0.87 (m, 2H, H_{cyclohexane}), 0.97–1.07 (m, 4H, H_{cyclohexane}), 1.57–1.63 (m, 2H, H_{cyclohexane}), 1.74–1.77 (m, 2H, H_{cyclohexane}), 2.82 (s, 6H, 2 × CH₃), 3.97 (d, ³*J* = 5.7 Hz, 2H, NHCH₂CN), 7.24 (d, ³*J* = 7.3 Hz, 1H, H-6''), 7.55–7.60 (m, 2H, H-7'', H-3''), 7.97 (s, 1H, SO₂NH), 8.04 (t, ³*J* = 5.5 Hz, 1H, NHCH₂CN), 8.08 (dd, ³*J* = 7.3 Hz, ²*J* = 1.3 Hz, 1H, H-4''), 8.36_a, 8.43_b (d_a, ³*J* = 8.8 Hz, d_b, ³*J* = 8.5 Hz, 2H, H-8'', H-2''); ¹³C NMR (125 MHz, DMSO-*d*₆) δ 20.87 (C-3', C-5'), 24.59 (C-4'), 27.78 (NHCH₂CN), 32.51 (C-2', C-6'), 45.18 (N(CH₃)₂), 61.58 (C-1'), 115.05 (C-6''), 117.55 (CN), 119.35, 123.54, 127.82, 128.04, 128.95, 129.19, 129.50 (C-8'', C-2'', C-3'', C-7'', C-4'', C-8_a'', C-4_a''), 138.55, 151.38 (C-1'', C-5''), 174.54 (NHCCO); LC-MS(ESI) (90% H₂O to 100% MeOH in 20 min, then 100% MeOH to 30 min, DAD 219.7–300.7 nm) t_r = 17.67, 97% purity, *m/z* = 415.3 ([M + H]⁺).

3.3.60. PREPARATION OF 120

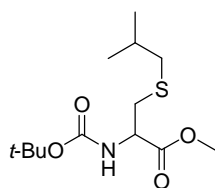
***N*-[(7-Diethylamino)-2-oxo-2*H*-chromene-3-carbonyl]homocycloleucyl-glycine nitrile.** 7-(Diethylamino)-2-oxo-2*H*-chromene-3-carboxylic acid **118** (0.22 g, 0.84 mmol) was finely suspended in dry THF (15 mL). DIPEA (0.54 g, 4.18 mmol), DMAP (0.01 g, 0.08 mmol), and EDC \times HCl (0.17 g, 0.89 mmol) were added, and the resulting reaction mixture was stirred for 20 min at room temperature. Compound **109** (0.15 g, 0.83 mmol) in dry THF (10 mL) was added. It was stirred for 22 h at room temperature, and heated additionally to reflux for 11 h. The solvent was removed under reduced pressure, and the resulting brown residue was suspended in H₂O. The aqueous suspension was further extracted with ethyl acetate (3 \times 30 mL). The combined organic layers were washed with sat. NaHCO₃ (30 mL) and brine (30 mL), and dried over (Na₂SO₄). The crude product was purified by column chromatography using ethyl acetate/petroleum ether (2:1) to obtain **120** as a green solid (70 mg, 20%). mp 248 °C; ¹H NMR (500 MHz, DMSO-*d*₆) δ 1.14 (t, ³*J* = 7.0 Hz, 6H, N(CH₂CH₃)₂), 1.21–1.26 (m, 1H, H_{cyclohexane}), 1.32–1.40 (m, 2H, H_{cyclohexane}), 1.58–1.60 (m, 3H, H_{cyclohexane}), 1.70–1.74 (m, 2H, H_{cyclohexane}), 2.02–2.05 (m, 2H, H_{cyclohexane}), 3.48 (q, ³*J* = 6.9 Hz, 4H, N(CH₂CH₃)₂), 4.01 (d, ³*J* = 5.7 Hz, 2H, NHCH₂CN), 6.64 (d, ⁴*J* = 2.2 Hz, 1H, H-8''), 6.81 (dd, ³*J* = 9.1 Hz, ⁴*J* = 2.5 Hz, 1H, H-6''), 7.67 (d, 1H, ³*J* = 9.2 Hz, H-5''), 8.38 (t, 1H, ³*J* = 5.5 Hz, NHCH₂CN), 8.62 (s, 1H, H-4''), 8.96 (s, 1H, NHCCO); ¹³C NMR (125 MHz, DMSO-*d*₆) δ 12.45 (N(CH₂CH₃)₂), 21.07 (C-3', C-5'), 24.92 (C-4'), 27.62 (NHCH₂CN), 31.69 (C-2', C-6'), 44.45 (N(CH₂CH₃)₂), 58.75 (C-1'), 95.99 (C-8''), 107.78, 109.59, 110.45 (C-6'', C-4a'', C-3''), 117.76 (CN), 131.80 (C-5''), 147.71 (C-4''), 152.74 (C-7''), 157.44 (C-8a''), 161.38, 162.51 (C-3''CO, C-2''), 174.70 (NHCCO); LC-MS(ESI) (90% H₂O to 100% MeOH in 20 min, then 100% MeOH to 30 min, DAD 220.0–480.0 nm) *t*_r = 15.56, 100% purity, *m/z* = 425.3 ([M + H]⁺).

3.3.61. PREPARATION OF 122

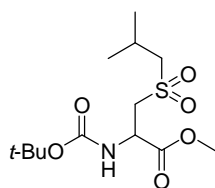


***N*-[(7-Diethylamino)-2-oxo-2*H*-chromene-3-carbonyl]homocycloleucyl-azaalanine-nitrile.** Compound **40** (0.30 g, 0.94 mmol) was dissolved in MeOH (30 mL) and treated with Pd/C (0.030 g). The resulting mixture was hydrogenated in a hydrogen flow at 2 bar and room temperature for 4 h. Pd/C was filtered off, and the solvent was removed under reduced pressure to obtain compound **106** (0.11 g) as a colorless oil without further purification. 7-(Diethylamino)-2-oxo-2*H*-chromene-3-carboxylic acid **118** (0.15 g, 0.57 mmol) was finely suspended in dry THF (15 mL). DMAP (7.0 mg, 0.06 mmol), and EDC (0.10 g, 0.64 mmol) were added, and the resulting reaction mixture was stirred for 10 min at room temperature. Compound **106** (0.11 g) was added. It was stirred for 2 d at room temperature. The solvent was removed under reduced pressure, and the resulting brown residue was suspended in H₂O. The aqueous suspension was extracted with ethyl acetate (3 × 30 mL). The combined organic layers were washed with sat. NaHCO₃ (30 mL) and brine (30 mL), and dried over (Na₂SO₄). The crude product was purified by column chromatography using CH₂Cl₂/MeOH (9:1) to obtain compound **121** as a colourless oil (0.10 mg, 25% from **40**). Compound **121** (0.10 g, 0.23 mmol) was dissolved in MeOH (20 mL) and treated with NaOAc (0.059 g, 0.72 mmol) and BrCN (0.051 g, 0.48 mmol). The resulting reaction mixture was stirred for 2 d at room temperature. The solvent was evaporated, and the residue was suspended in H₂O. The aqueous suspension was extracted with ethyl acetate (3 × 30 mL). The combined organic layers were washed with sat. NaHCO₃ (30 mL) and brine (30 mL), and dried over (Na₂SO₄). The crude product was purified by column chromatography using ethyl acetate to obtain **122** as a green solid (20 mg, 19% from **121**). ¹H NMR (500 MHz, DMSO-*d*₆) δ 1.13 (t, ³*J* = 7.1 Hz, 6H, N(CH₂CH₃)₂), 1.22 (bs, 1H, H_{cyclohexane}), 1.39–1.46 (m, 2H, H_{cyclohexane}), 1.58–1.63 (m, 3H, H_{cyclohexane}), 1.69–1.75 (m, 2H, H_{cyclohexane}), 2.15–2.18 (m, 2H, H_{cyclohexane}), 2.97 (s, 3H, NCH₃), 3.08 (s, 3H, NCH₃), 3.48 (q, ³*J* = 7.0 Hz, 4H, N(CH₂CH₃)₂), 6.63 (d, ⁴*J* = 2.2 Hz, 1H, H-8''), 6.81 (dd, ³*J* = 9.1 Hz, ⁴*J* = 2.5 Hz, 1H, H-6''), 7.66 (d, 1H, ³*J* = 9.2 Hz, H-5''), 8.60 (s, 1H, H-4''), 9.14 (s, 1H, NHCCO); ¹³C NMR (125 MHz, DMSO-*d*₆) δ 12.44 (N(CH₂CH₃)₂), 21.16 (C-3', C-5'), 24.76 (C-4'), 31.46 (C-2', C-6'), 40.61 (CONCH₃), 44.50 (N(CH₂CH₃)₂), 58.22 (C-1'), 96.07 (C-8''), 107.86, 109.34, 110.45 (C-6'', C-4a'', C-3''), 114.79 (CN), 131.79 (C-5''), 147.81 (C-4''), 152.75 (C-7''), 157.44 (C-8a'').

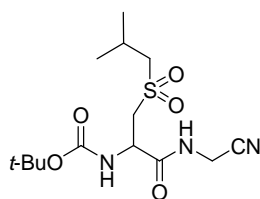
161.17, 162.54 (C-3''CO, C-2''), 172.98 (NHCCO); LC-MS(ESI) (90% H₂O to 100% MeOH in 20 min, then 100% MeOH to 30 min, DAD 220.0–450.0 nm) $t_r = 15.47$, 95% purity, $m/z = 454.3$ ($[M + H]^+$).

3.3.62. PREPARATION OF 124

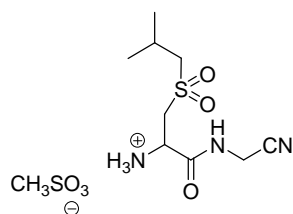
***N*-(*tert*-Butyloxycarbonyl)-*S*-(isobutyl)cysteine methyl ester.** Sodium (0.87 g, 37.8 mmol) was dissolved under ice-cooling in MeOH (30 mL) and given to *N*-(*tert*-butyloxycarbonyl)-*L*-cysteine methyl ester (**123**, 5.72 g, 24.3 mmol) in MeOH (30 mL). The resulting solution was treated with isobutyl bromide (4.01 g, 29.3 mmol), and heated to reflux for 5 h. MeOH was removed under reduced pressure, and the resulting yellow oily residue was suspended in H₂O. The aqueous suspension was extracted with ethyl acetate (3 × 30 mL). The combined organic layers were washed with 10% KHSO₄ (30 mL), H₂O (30 mL) and brine (30 mL). The solvent was dried over Na₂SO₄ and evaporated. The oily yellow crude product was purified by column chromatography using ethyl acetate/petroleum ether (1:4) to obtain **124** as a colorless oil (3.88 g, 55%); ¹H NMR (500 MHz, DMSO-*d*₆) δ 0.92 (d, ³*J* = 6.6 Hz, 6H, CH(CH₃)₂), 1.37 (s, 9H, C(CH₃)₃) 1.71 (sept, ³*J* = 6.7 Hz, 1H, CH(CH₃)₂), 2.40 (d, ³*J* = 7.0 Hz, 2H, (CH₃)₂CHCH₂S), 2.71 (dd, ²*J* = 13.6 Hz, ³*J* = 8.9 Hz, 1H, NHCHCHH), 2.82 (dd, ²*J* = 13.7 Hz, ³*J* = 5.2 Hz, 1H, NHCHCHH), 3.63 (s, 3H, OCH₃), 4.10–4.15 (m, 1H, NHCHCO), 7.22 (d, ³*J* = 8.2 Hz, 1H, NHCHCO); ¹³C NMR (125 MHz, DMSO-*d*₆) δ 21.76, 21.83, 28.10 (CH₃CHCH₃, CH₃CHCH₃, CH₃CHCH₃), 28.25 (C(CH₃)₃), 33.33 (NHCHCH₂), 40.76 ((CH₃)₂CHCH₂S), 52.03, 53.89 (OCH₃, NHCHCO), 78.49 (C(CH₃)₃), 155.38 (OCONH), 171.71 (NHCHCO); Analytical HPLC (90% H₂O to 100% MeOH in 15 min, then 100% MeOH to 30 min) *t*_r = 13.94, purity 96%.

3.3.63. PREPARATION OF 125

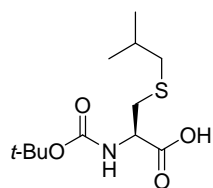
***N*-(*tert*-Butyloxycarbonyl)-*S*-(isobutyl)cysteinesulfone methyl ester.** Compound **124** (3.70 g, 12.7 mmol) was dissolved in dry CH_2Cl_2 (20 mL). MCPBA (7.84 g (70%), 31.8 mmol) in CH_2Cl_2 (20 mL) was slowly added. The resulting reaction mixture was stirred for 18 h at room temperature. The solvent was removed under reduced pressure, and the oily residue was suspended in H_2O . The aqueous suspension was extracted with ethyl acetate (3×30 mL). The combined organic layers were washed with sat. NaHCO_3 (30 mL), H_2O (30 mL) and brine (30 mL). The solvent was dried over Na_2SO_4 and evaporated. The oily crude product was purified by column chromatography using ethyl acetate/petroleum ether (1:1) to obtain **125** as a white solid (3.60 g, 88%). mp 86 °C; ^1H NMR (500 MHz, $\text{DMSO}-d_6$) δ 1.01 (d, $^3J = 2.5$ Hz, 3H, CH_3CHCH_3), 1.02 (d, $^3J = 2.6$ Hz, 3H, CH_3CHCH_3), 1.38 (s, 9H, $\text{CH}(\text{CH}_3)_3$), 2.18 (sept, $^3J = 6.7$ Hz, 1H, CH_3CHCH_3), 2.98–3.07 (m, 2H, $(\text{CH}_3)_2\text{CHCH}_2\text{S}$), 3.47–3.48 (m, 2H, NHCHCH_2S), 3.66 (s, 3H, OCH_3), 4.47–4.51 (m, 1H, NHCHCO), 7.49 (d, $^3J = 8.5$ Hz, 1H, NHCHCO); ^{13}C NMR (125 MHz, $\text{DMSO}-d_6$) δ 22.41, 22.56, 23.06 (CH_3CHCH_3 , CH_3CHCH_3 , CH_3CHCH_3), 28.21 ($\text{C}(\text{CH}_3)_3$), 48.84, 52.68, 54.08, 60.24 (NHCHCO , OCH_3 , $(\text{CH}_3)_2\text{CHCH}_2\text{S}$, NHCHCH_2S), 79.06 ($\text{C}(\text{CH}_3)_3$), 155.18 (OCONH), 170.53 (NHCHCO); Anal. $\text{C}_{13}\text{H}_{25}\text{NO}_6\text{S}$ (323.41 g/mol) calcd C 48.28, H 7.79, N 4.43; found C 48.14, H 7.56, N 4.14. MS (ESI) $m/z = 324.4$ ($[\text{M} + \text{H}]^+$).

3.3.64. PREPARATION OF 127

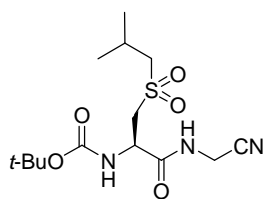
***N*-(*tert*-Butyloxycarbonyl)-*S*-(isobutyl)cysteinylsulfone-glycine-nitrile.** Compound **125** (3.50 g, 10.8 mmol) was dissolved in a THF/H₂O mixture (120 mL). Under ice-cooling, LiOH (0.65 g, 27.1 mmol) was added. When LiOH was dissolved, the reaction solution was stirred for 9 h at room temperature. The reaction solution was acidified with concentrated HCl to a pH of ~2 and extracted with ethyl acetate (3 × 80 mL). The combined organic layers were washed with H₂O (30 mL) and brine (30 mL). The solvent was dried over Na₂SO₄ and evaporated to obtain **126** as an oily product without further purification. The oily crude product was dissolved in dry THF (50 mL) and cooled to -25 °C. To the stirred solution, *N*-methylmorpholine (1.20 g, 11.9 mmol) and isobutyl chloroformate (1.63 g, 11.9 mmol) were added consecutively. Aminoacetonitrile monosulfate (4.59 g, 29.8 mmol) was dissolved in H₂O (5 mL), and 10 N NaOH (6.0 mL) was added under ice-cooling. This solution was given to the reaction mixture when the precipitation of *N*-methylmorpholine hydrochloride occurred. It was allowed to warm to room temperature within 30 min, and stirred overnight at room temperature. After evaporation of the solvent, the resulting aqueous residue was extracted with ethyl acetate (3 × 120 mL). The combined organic layers were washed with 10% KHSO₄ (30 mL), H₂O (30 mL), sat. NaHCO₃ (2 × 30 mL), H₂O (30 mL), and brine (30 mL). The solvent was dried (Na₂SO₄) and evaporated. The crude product was recrystallized from ethyl acetate to obtain **127** as a white solid (1.60 g, 43% from **125**). mp 151 °C; ¹H NMR (500 MHz, DMSO-*d*₆) δ 1.02 (d, ³*J* = 6.7 Hz, 6H, CH(CH₃)₂), 1.39 (s, 9H, C(CH₃)₃), 2.19 (sept, ³*J* = 6.7 Hz, 1H, CH(CH₃)₂), 2.97–3.07 (m, 2H, (CH₃)₂CHCH₂S), 3.38 (dd, ²*J* = 14.8 Hz, ³*J* = 9.2 Hz, 1H, NHCHCHHS), 3.48 (dd, ²*J* = 14.8 Hz, ³*J* = 3.5 Hz, 1H, NHCHCHHS), 4.06–4.16 (m, 1H, NHCH₂CN), 4.45–4.49 (m, 1H, NHCHCO), 7.33 (d, ³*J* = 8.6 Hz, 1H, NHCHCO), 8.72 (t, ³*J* = 4.4 Hz, NHCH₂CN); ¹³C NMR (125 MHz, DMSO-*d*₆) δ 22.51, 22.60, 23.01 (CH₃CHCH₃, CH₃CHCH₃, CH₃CHCH₃), 27.69 (NHCH₂CN), 28.27 (C(CH₃)₃), 49.46 (NHCHCO), 54.52 (NHCHCH₂S), 60.11 ((CH₃)₂CHCH₂S), 79.06 (C(CH₃)₃), 117.40 (CN), 155.07 (OCONH), 170.22 (NHCHCO); Anal. C₁₄H₂₅N₃O₅S (347.43 g/mol) calcd C 48.40, H 7.25, N 12.09; found C 48.19, H 7.14, N 11.88.

3.3.65. PREPARATION OF 128

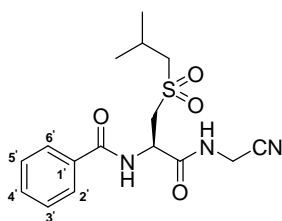
S-(Isobutyl)cysteinylsulfone-glycine-nitrile methanesulfonate. Compound **127** (1.30 g, 3.74 mmol) was dissolved in dry THF (20 mL). Dry methanesulfonic acid (1.46 mL, 22.5 mmol) was added, and the resulting reaction mixture was stirred for 24 h at room temperature. The precipitated product was filtered out, washed with cold ethyl acetate and petroleum ether, and dried to obtain **128** as a white solid (1.20 g, 93%). mp 109–111 °C; ^1H NMR (500 MHz, $\text{DMSO-}d_6$) δ 1.04 (d, $^3J = 6.7$ Hz, 6H, $\text{CH}(\text{CH}_3)_2$), 2.22 (sept, $^3J = 6.6$ Hz, 1H, $\text{CH}(\text{CH}_3)_2$), 2.40 (s, 3H, CH_3SO_3^-), 3.14–3.22 (m, 2H, $(\text{CH}_3)_2\text{CHCH}_2\text{S}$), 3.52 (dd, $^2J = 14.7$ Hz, $^3J = 7.1$ Hz, 1H, NHCHCHHS), 3.69 (dd, $^2J = 14.8$ Hz, $^3J = 5.7$ Hz, 1H, NHCHCHHS), 4.24–4.25 (m, 2H, NHCH_2CN), 4.31–4.34 (m, 1H, NHCHCO), 8.49 (s, 3H, NH_3^+), 9.37 (t, $^3J = 5.5$ Hz, 1H, NHCH_2CN); ^{13}C NMR (125 MHz, $\text{DMSO-}d_6$) δ 22.46, 23.05 ($\text{CH}(\text{CH}_3)_2$, $\text{CH}(\text{CH}_3)_2$), 27.66 (NHCH_2CN), 47.28 (NHCHCO), 53.19 (NHCHCH_2S), 59.97 ($(\text{CH}_3)_2\text{CHCH}_2\text{S}$), 116.93 (CN), 166.86 (NH_3^+CHCO).

3.3.66. PREPARATION OF 140

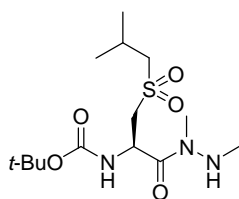
***N*-(*tert*-Butyloxycarbonyl)-*S*-(isobutyl)cysteine.** Compound **139** (5.00 g, 41.3 mmol) was dissolved in a 1:1 EtOH/2 N NaOH mixture (82 mL). 1-Bromo-2-methylpropane (6.22 g, 45.4 mmol) and tetrabutylammonium iodide (0.46 g, 1.25 mmol) were added. The resulting reaction mixture was stirred for 3 d at room temperature. (Boc)₂O (9.91 g, 45.4 mmol) was added, and it was additionally stirred for 1 d at room temperature. EtOH was evaporated under reduced pressure, the aqueous residue was acidified with conc. HCl (pH ~ 1) and extracted with ethyl acetate (3 × 30 mL). The combined organic layers were washed with 10% KHSO₄ (30 mL) and sat. NaCl (30 mL). The solvent was dried over Na₂SO₄ and evaporated to obtain **140** as an oily yellow product (10.9 g, 95%). ¹H NMR (500 MHz, DMSO-*d*₆) δ 0.92 (d, ³*J* = 6.7 Hz, 6H, CH(CH₃)₂), 1.37 (s, 9H, C(CH₃)₃), 1.72 (sept, ³*J* = 6.7 Hz, 1H, CH(CH₃)₂), 2.39–2.41 (m, 2H, (CH₃)₂CHCH₂S), 2.69 (dd, ²*J* = 13.6 Hz, ³*J* = 9.1 Hz, 1H, NHCHCHH), 2.83 (dd, ²*J* = 13.6 Hz, ³*J* = 4.8 Hz, 1H, NHCHCHH), 4.01–4.06 (m, 1H, NHCHCO), 7.01 (d, ³*J* = 8.2 Hz, 1H, NHCHCO), 12.65 (COOH); ¹³C NMR (125 MHz, DMSO-*d*₆) δ 21.81, 21.90, 28.14 (CH₃CHCH₃, CH₃CHCH₃, CH₃CHCH₃), 28.31 (C(CH₃)₃), 33.56 (NHCHCH₂), 40.79 ((CH₃)₂CHCH₂S), 53.89 (NHCHCO), 78.31 (C(CH₃)₃), 155.44 (OCONH), 172.68 (NHCHCO).

3.3.67. PREPARATION OF 142

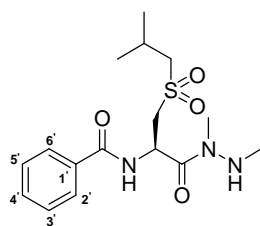
(R)-N-(tert-Butyloxycarbonyl)-S-(isobutyl)cysteinylsulfone-glycine-nitrile. Compound **140** (10.8 g, 38.9 mmol) was dissolved in AcOH (80 mL). KMnO_4 (12.3 g, 77.8 mmol) was dissolved in H_2O (130 mL) and slowly added to the reaction mixture. It was stirred for 2.5 h, followed by the addition of sat. KHSO_3 solution until the reaction mixture becomes colorless. It was concentrated under reduced pressure, and the aqueous suspension was extracted with ethyl acetate (3×100 mL). The combined organic layers were washed with H_2O (30 mL), brine (30 mL) and dried over Na_2SO_4 . The solvent was evaporated to obtain **141** as a colourless oily product (11.1 g, 92%). Compound **141** (2.00 g, 6.46 mmol) was dissolved in dry THF (40 mL), and it was cooled to -25 °C. *N*-Methylmorpholine (0.72 g, 7.12 mmol) and isobutyl chloroformate (0.97 g, 7.10 mmol) were added consecutively. Aminoacetonitrile monosulfate (1.47 g, 9.54 mmol) was dissolved in H_2O (2 mL), treated with 2 N NaOH (5 mL) and added to the reaction mixture when the precipitation of *N*-methylmorpholinium chloride occurred. It was allowed to warm to room temperature within 30 min, and stirred for additional 90 min. THF was evaporated, and the resulting aqueous suspension was extracted with ethyl acetate (3×30 mL). The combined organic layers were washed with 10 % KHSO_4 (30 mL), sat. NaHCO_3 (30 mL), H_2O (30 mL) and sat. NaCl (30 mL). The solvent was dried (Na_2SO_4) and evaporated. The product was recrystallized from ethyl acetate to obtain **142** as a white solid (0.94 g, 42% from **141**). mp 162 – 166 °C; ^1H NMR (500 MHz, $\text{DMSO}-d_6$) δ 1.02 (d, $^3J = 6.7$ Hz, 6H, $\text{CH}(\text{CH}_3)_2$), 1.39 (s, 9H, $\text{C}(\text{CH}_3)_3$), 2.56 (sept, $^3J = 6.7$ Hz, 1H, $\text{CH}(\text{CH}_3)_2$), 2.97–3.07 (m, 2H, $(\text{CH}_3)_2\text{CHCH}_2\text{S}$), 3.37 (dd, $^2J = 14.7$ Hz, $^3J = 9.3$ Hz, 1H, NHCHCHHS), 3.48 (dd, $^2J = 14.9$ Hz, $^3J = 3.5$ Hz, 1H, NHCHCHHS), 3.46–4.16 (m, 1H, NHCH_2CN), 4.45–4.49 (m, 1H, NHCHCO), 7.33 (d, $^3J = 8.5$ Hz, 1H, NHCHCO), 8.71 (bs, NHCH_2CN); ^{13}C NMR (125 MHz, $\text{DMSO}-d_6$) δ 22.50, 22.59, 23.01 (CH_3CHCH_3 , CH_3CHCH_3 , CH_3CHCH_3), 27.69 (NHCH_2CN), 28.27 ($\text{C}(\text{CH}_3)_3$), 49.44 (NHCHCO), 54.50 (CHCH_2), 60.10 (CH_2S), 79.05 ($\text{C}(\text{CH}_3)_3$), 117.40 (CN), 155.07 (OCONH), 170.21 (NHCHCO). Anal. $\text{C}_{14}\text{H}_{25}\text{N}_3\text{O}_5\text{S}$ (347.43 g/mol) calcd C 48.40, H 7.25, N 12.09; found C 48.32, H 7.18, N 11.83.

3.3.68. PREPARATION OF 144

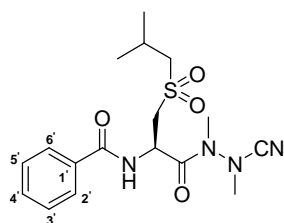
(R)-N-(Benzoyl)-S-(isobutyl)cysteinylsulfone-glycine-nitrile. Compound **142** (0.68 g, 1.96 mmol) was dissolved in dry THF (10 mL). Under ice-cooling, dry methanesulfonic acid (1.14 g, 11.9 mmol) was added, and the resulting reaction mixture was stirred for 14 h at room temperature. The precipitated product was filtered off, washed with petroleum ether, and dried to obtain compound **143** as a white solid without further purification (0.33 g). Compound **143** (0.33 g, 0.96 mmol) was dissolved in dry THF (30 mL). DIPEA (0.35 g, 2.71 mmol) and benzoyl chloride (0.19 g, 1.35 mmol) were added consecutively. The reaction solution was stirred for 24 h at room temperature. The solvent was evaporated, and the resulting white solid was extracted with ethyl acetate (3 × 30 mL). The combined organic layers were washed with 10% KHSO₄ (30 mL) and brine (30 mL). The solvent was dried (Na₂SO₄) and evaporated. The crude product was recrystallized from ethyl acetate to obtain compound **144** as a white solid (0.28 g, 83%). mp 188–192 °C; $[\alpha]_D^{20} = -54.0$ (c = 0.82, THF); ¹H NMR (500 MHz, DMSO-*d*₆) δ 0.97 (d, ³J = 6.7 Hz, 3H, CH₃CHCH₃), 0.99 (d, ³J = 6.6 Hz, 3H, CH₃CHCH₃), 2.18 (sept, ³J = 6.7 Hz, 1H, CH₃CHCH₃), 3.02–3.10 (m, 2H, (CH₃)₂CHCH₂S), 3.61 (dd, ²J = 14.7 Hz, ³J = 9.3 Hz, 1H, NHCHCHHS), 3.67 (dd, ²J = 14.5 Hz, ³J = 3.5 Hz, 1H, NHCHCHHS), 4.08–4.17 (m, 2H, NHCH₂CN), 4.97–5.01 (m, 1H, NHCHCO), 7.48–7.90 (m, 5H, H_{arom}), 8.79 (t, ³J = 5.7 Hz, 1H, NHCH₂CN), 8.94 (d, ³J = 8.2 Hz, 1H, NHCHCO); ¹³C NMR (125 MHz, DMSO-*d*₆) δ 22.44, 22.50, 23.08 (CH₃CHCH₃, CH₃CHCH₃, CH₃CHCH₃), 27.76 (NHCH₂CN), 48.33 (NHCHCO), 53.99 (NHCHCH₂S), 60.13 ((CH₃)₂CHCH₂S), 117.41 (CN), 127.75 (C-2', C-6'), 128.38 (C-3', C-5'), 131.80 (C-4'), 133.71 (C-1'), 166.45 (C-1'CONH), 169.92 (NHCHCO). LC-MS(ESI) (90% H₂O to 100% MeOH in 20 min, then 100% MeOH to 30 min, DAD 220.0–400.0 nm) t_r = 10.94, 99% purity, m/z = 352.1 ([M + H]⁺).

3.3.69. PREPARATION OF 145

***N*-(*tert*-Butyloxycarbonyl)-*S*-(isobutyl)cysteinesulfone 1,2-dimethylhydrazide.** Compound **141** (2.00 g, 6.46 mmol) was dissolved in dry THF (30 mL) and cooled to $-25\text{ }^{\circ}\text{C}$. *N*-methylmorpholine (0.72 g, 7.12 mmol) and isobutyl chloroformate (0.97 g, 7.10 mmol) were added consecutively. 1,2-Dimethylhydrazine dihydrochloride (1.72 g, 12.9 mmol) was dissolved in H_2O (2 mL), treated with 2 N NaOH (13 mL) and added to the reaction mixture when the precipitation of *N*-methylmorpholinium chloride occurred. It was allowed to warm to room temperature within 30 min, and stirred for additional 90 min. The solvent was evaporated, and the resulting white solid was extracted with ethyl acetate ($3 \times 30\text{ mL}$). The combined organic layers were washed with 10 % KHSO_4 (30 mL) and brine (30 mL). The solvent was dried (Na_2SO_4) and evaporated. The oily product was purified by column chromatography on silica gel using ethyl acetate/petroleum ether (5:1) as eluent to obtain **145** as a white solid (0.77 g, 34%). ^1H NMR (500 MHz, $\text{DMSO}-d_6$) δ 1.02 (d, $^3J = 6.6\text{ Hz}$, 6H, $\text{CH}(\text{CH}_3)_2$), 1.36 (s, 9H, $\text{C}(\text{CH}_3)_3$), 2.21 (sept, $^3J = 6.7\text{ Hz}$, 1H, $\text{CH}(\text{CH}_3)_2$), 2.48 (d, $^3J = 5.7\text{ Hz}$, 3H, NHCH_3), 2.92–2.97 (m, 4H, CONCH_3 , NHCHCHHS), 3.01 (dd, $^2J = 14.0\text{ Hz}$, $^3J = 6.5\text{ Hz}$, 1H, NHCHCHHS), 4.85 (q, $^3J = 5.6\text{ Hz}$, 1H, NHCH_3), 5.21–5.25 (m, 1H, NHCHCO), 6.98 (d, $^3J = 8.6\text{ Hz}$, 1H, NHCHCO), ^{13}C NMR (125 MHz, $\text{DMSO}-d_6$) δ 22.56, 22.67, 22.94 (CH_3CHCH_3 , CH_3CHCH_3 , CH_3CHCH_3), 28.30 ($\text{C}(\text{CH}_3)_3$), 31.29, 34.90 ($2 \times \text{NCH}_3$), 46.69 (NHCHCO), 54.97 (CHCH_2), 60.36 (CH_2S), 78.38 ($\text{C}(\text{CH}_3)_3$), 155.02 (OCONH), 170.88 (NHCHCO).

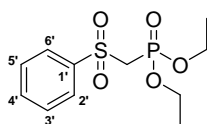
3.3.70. PREPARATION OF 147

***N*-(Benzoyl)-*S*-(isobutyl)cysteinesulfone 1,2-dimethylhydrazide.** Under ice-cooling, acetyl chloride (5 mL) was given to dry ethanol (10 mL) and stirred for 10 min at room temperature. Compound **145** (0.70 g, 1.99 mmol) was dissolved in ethyl acetate (10 mL), and the solutions were combined under ice-cooling. It was stirred for 30 min, and the solvent was evaporated. The residue was dissolved in H₂O, treated with 2 N NaOH to adjust a pH of ~12, and extracted with ethyl acetate (3 × 30 mL). The combined organic layers were washed with brine (30 mL) and dried over Na₂SO₄. The solvent was evaporated to obtain compound **146** (0.20 g, 40%). Compound **146** (0.20 g, 0.80 mmol) was dissolved in dry THF (10 mL). DIPEA (0.21 g, 1.62 mmol) and benzoyl chloride (0.12 g, 0.85 mmol) were added consecutively, and it was stirred for 18 h at room temperature. The solution was evaporated, and it was extracted with ethyl acetate (3 × 30 mL). The combined organic layers were washed with 10% NaHCO₃ (30 mL) and brine (30 mL), and dried over Na₂SO₄. The solvent was removed under reduced pressure, and the resulting crude product was purified by column chromatography on silica gel using ethyl acetate/petroleum ether (10:1) as eluent to obtain compound **147** as a colourless oil (0.05 g, 18% from **146**). ¹H NMR (500 MHz, DMSO-*d*₆) δ 1.00 (d, ³*J* = 6.6 Hz, 6H, CH(CH₃)₂), 2.23 (sept, ³*J* = 6.7 Hz, 1H, CH(CH₃)₂), 2.53 (d, ³*J* = 5.7 Hz, 3H, NHCH₃), 2.96 (s, 3H, CONCH₃), 3.01 (dd, ²*J* = 14.2 Hz, ³*J* = 6.6 Hz, 1H, NHCHCHHS), 3.08 (dd, ²*J* = 14.1 Hz, ³*J* = 6.5 Hz, 1H, NHCHCHHS), 3.46 (dd, ²*J* = 14.5 Hz, ³*J* = 3.5 Hz, 1H, (CH₃)₂CHCHHS), 3.52 (dd, ²*J* = 14.5 Hz, ³*J* = 9.2 Hz, 1H, (CH₃)₂CHCHHS), 4.93 (q, ³*J* = 5.6 Hz, 1H, NHCH₃), 5.72–5.76 (m, 1H, NHCHCO), 7.46–7.87 (m, 5H, H_{arom}), 8.64 (d, ³*J* = 8.5 Hz, 1H, NHCHCO), ¹³C NMR (125 MHz, DMSO-*d*₆) δ 22.53, 22.56, 23.00 (CH₃CHCH₃, CH₃CHCH₃, CH₃CHCH₃), 31.35, 34.91 (2 × NCH₃), 45.76 (NHCHCO), 54.37 (NHCHCH₂S), 60.26 ((CH₃)₂CHCH₂S), 127.51 (C-2', C-6'), 128.38 (C-3', C-5'), 131.55 (C-4'), 134.03 (C-1'), 166.14 (C-1'CONH), 170.55 (NHCHCO).

3.3.71. PREPARATION OF 148

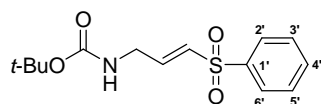
(R)-N-(Benzoyl)-S-(isobutyl)cysteinylsulfone-methylazaalanine-nitrile. Compound **147** (0.04 g, 0.11 mmol) was dissolved in MeOH (20 mL) and treated with NaOAc (0.03 g, 0.37 mmol) and BrCN (0.02 g, 0.19 mmol). The reaction mixture was stirred at room temperature for 24 h. The solvent was evaporated, and the resulting residue was extracted with ethyl acetate (3×30 mL). The combined organic layers were washed with brine (30 mL) and dried over Na_2SO_4 . The solvent was removed under reduced pressure, and the resulting crude product was purified by column chromatography on silica gel using ethyl acetate/petroleum ether (2:1) as eluent to obtain **148** as a colourless oil (0.02 g, 48%). $[\alpha]_{\text{D}}^{20} = -31.0$ ($c = 0.51$, THF); ^1H NMR (500 MHz, CDCl_3) mixture of s-cis and s-trans isomers δ 1.09–1.14 (m, 6H, $\text{CH}(\text{CH}_3)_2$), 2.30–2.43 (m, 1H, $\text{CH}(\text{CH}_3)_2$), 2.97–3.04 (m, 2H, NHCHCH_2S), 3.24, 3.31 ($2 \times$ s, 6H, $2 \times \text{NCH}_3$), 3.41–3.47 (m, 2H, $(\text{CH}_3)_2\text{CHCH}_2\text{S}$), 5.63–5.75 (m, 1H, NHCHCO), 7.40–7.80 (m, 6H, H_{arom} , NHCHCO); ^{13}C NMR (125 MHz, CDCl_3) mixture of s-cis and s-trans isomers δ 22.70, 22.73, 23.69, 23.75, 23.81 (CH_3CHCH_3 , CH_3CHCH_3 , CH_3CHCH_3), 30.77, 30.95, 40.92, 41.07, 45.43, 45.61 ($2 \times \text{NCH}_3$, NHCHCO), 53.18, 55.02 (NHCHCH_2S), 61.92, 62.18 ($(\text{CH}_3)_2\text{CHCH}_2\text{S}$), 113.49 (CN), 127.25 (C-2', C-6'), 128.73 (C-3', C-5'), 132.31 (C-4'), 132.58 (C-1'), 166.91, 167.31 (C-1'CONH), 170.26, 170.34 (NHCHCO); LC-MS(ESI) (90% H_2O to 100% MeOH in 20 min, then 100% MeOH to 30 min, DAD 220.0–400.0 nm) $t_{\text{r}} = 11.71$, 97% purity, $m/z = 381.2$ ($[\text{M} + \text{H}]^+$).

3.3.72. PREPARATION OF 151

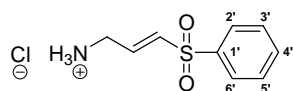


Diethyl phenylsulfonmethylphosphonate. Method A: A mixture of chloromethyl phenyl sulfide (5.00 g, 31.5 mmol) and triethyl phosphite (5.23 g, 31.5 mmol) was heated at 140°C in a sealed tube for 5 h. The resulting solution was distilled under reduced pressure to remove the starting materials. The oily residue was diethyl phenylthiomethylphosphonate **150** (6.78 g, 83%). Diethyl phenylthiomethylphosphonate **150** (3.25 g, 12.5 mmol) was dissolved in dry CH₂Cl₂ and treated with MCPBA (5.39 g, 31.2 mmol). The resulting reaction mixture was stirred at room temperature for 2 d. The precipitated solid was filtrated off, and the filtrate was evaporated under reduced pressure. The resulting residue was purified by column chromatography using ethyl acetate as eluent to obtain **151** as an oily product (1.4 g, 38%). ¹H NMR (500 MHz, DMSO-*d*₆) δ 1.13–1.16 (m, 6H, 2 × CH₂CH₃), 3.92–4.03 (m, 4H, 2 × CH₂CH₃), 4.41 (d, ²J_{PH} = 17 Hz, 2H, SO₂CH₂), 7.62–7.95 (m, 5H, H_{arom}); ¹³C NMR (125 MHz, DMSO-*d*₆) δ 16.06, 16.11 (2 × CH₂CH₃), 51.67 (d, ¹J_{PC} = 131.3 Hz), 62.44, 62.49 (2 × CH₂CH₃), 127.94 (C-2', C-6'), 129.15 (C-3', C-5'), 133.92 (C-4'), 140.65 (C-1').

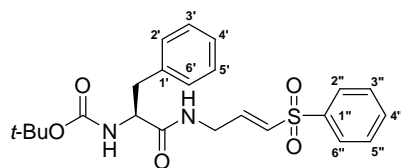
Diethyl phenylsulfonmethylphosphonate. Method B: A mixture of chloromethyl phenyl sulfide (5.00 g, 31.5 mmol) and triethyl phosphite (5.23 g, 31.5 mmol) was heated at 130°C in a sealed tube for 16 h. The resulting solution was distilled under reduced pressure to remove the starting materials. The oily residue was diethyl phenylthiomethylphosphonate **150** (7.69 g, 94%). Diethyl phenylthiomethylphosphonate **150** (7.68 g, 29.5 mmol) was dissolved in ice acetic acid (20 mL). KMnO₄ (9.34 g, 59.1 mmol) was dissolved in H₂O (50 mL) and dropped slowly to the reaction mixture. It was stirred for 1.5 h at room temperature, followed by the addition of sat. KHSO₃ solution until the reaction mixture becomes colorless. The colorless aqueous suspension was extracted with ethyl acetate (3 × 30 mL), washed with brine (30 mL), and evaporated *in vacuo* to obtain **151** as an oily colorless product (6.80 g, 79%). ¹H NMR (500 MHz, DMSO-*d*₆) δ 1.14 (t, ³J = 7.1 Hz, 6H, 2 × CH₂CH₃), 3.93–4.02 (m, 4H, 2 × CH₂CH₃), 4.41 (d, ²J_{PH} = 17 Hz, 2H, SO₂CH₂), 7.62–7.95 (m, 5H, H_{arom}); ¹³C NMR (125 MHz, DMSO-*d*₆) δ 16.07, 16.11 (2 × CH₂CH₃), 51.68 (d, ¹J_{PC} = 131.3 Hz), 62.45, 62.50 (2 × CH₂CH₃), 127.95 (C-2', C-6'), 129.16 (C-3', C-5'), 133.92 (C-4'), 140.65 (C-1').

3.3.73. PREPARATION OF 152

(E)-1-[(*tert*-Butyloxycarbonyl)amino]-3-(phenylsulfonyl)prop-2-en. Compound **151** (3.20 g, 10.9 mmol) was dissolved in dry THF (20 mL), treated with 60% NaH in mineral oil (0.52 g, 13.1 mmol), and stirred for 30 min at room temperature. *N*-Boc-glycinal (1.74 g, 10.9 mmol) was added, and the resulting reaction mixture was stirred for 2 h at rt. THF was evaporated under reduced pressure, and the oily residue was suspended in H₂O. The aqueous suspension was extracted with ethyl acetate (3 × 30 mL), washed with brine (30 mL), dried over Na₂SO₄ and evaporated *in vacuo*. The crude product was purified by column chromatography using ethyl acetate/petroleum ether (1:1) to obtain **152** as a white solid (1.68 g, 52%). ¹H NMR (500 MHz, DMSO-*d*₆) δ 1.35 (s, 9H, C(CH₃)₃), 3.78 (bs, 2H, CH₂NH), 6.65 (d, ³*J* = 15.4 Hz, 1H, CH=CHSO₂), 6.82 (dt, ³*J* = 15.1 Hz, ³*J* = 4.6 Hz, 1H, CH=CHSO₂), 7.15 (bs, 1H, NHCO), 7.62–7.85 (m, 5H, H_{arom}); ¹³C NMR (125 MHz, DMSO-*d*₆) δ 28.24 (C(CH₃)₃), 78.36 (C(CH₃)₃), 127.25 (C-2', C-6'), 129.71 (C-3', C-5'), 130.00 (CH=CHSO₂), 133.76 (C-4'), 140.47 (C-1'), 144.80 (CH=CHSO₂), 155.57 (OCONH); MS(ESI) *m/z* = 315.3 ([M + NH₄]⁺); Anal. C₁₄H₁₉NO₄S (297.37 g/mol) calcd C 56.55, H 6.44, N 4.71; found C 56.47, H 6.38, N 4.75.

3.3.74. PREPARATION OF 153

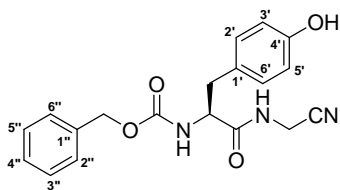
(E)-1-amino-3-(phenylsulfonyl)prop-2-en hydrochloride. Compound **152** (0.90 g, 3.03 mmol) was dissolved in ethyl acetate (10 mL). AcCl (11.0 g, 0.14 mol) was slowly dropped to MeOH (10 mL) under ice-cooling, and stirred for 10 min. The solutions were combined, and stirred for 10 min at rt. The precipitated white solid was filtered off, and the filtrate was stirred additionally for 30 min at room temperature. The precipitated white solid was again filtered off. The precipitates were combined, washed with *n*-hexane and dried *in vacuo* to obtain **153** as a white solid (0.55 g, 78%). ¹H NMR (500 MHz, DMSO-*d*₆) δ 3.71 (dd, ³*J* = 5.4 Hz, ⁴*J* = 1.6 Hz, 2H, CH₂CH=CHSO₂), 6.90 (dt, ³*J* = 15.4 Hz, ³*J* = 5.4 Hz, 1H, CH₂CH=CHSO₂), 7.10 (dt, ³*J* = 15.4 Hz, ⁴*J* = 1.6 Hz, 1H, CH₂CH=CHSO₂), 7.65–7.88 (m, 5H, H_{arom}), 8.50 (s, 3H, NH₃⁺); ¹³C NMR (125 MHz, DMSO-*d*₆) δ 38.61 (CH₂CH=CHSO₂), 127.42 (C-2', C-6'), 129.84 (C-3'; C-5'), 133.15, 134.08 (C-4', CH₂CH=CHSO₂), 138.88, 139.86 (C-1', CH₂CH=CHSO₂).

3.3.75. PREPARATION OF 155***N*-(*tert*-Butyloxycarbonyl)-phenylalanine (*E*)-3-(phenylsulfonyl)prop-2-en-1-ylamide.**

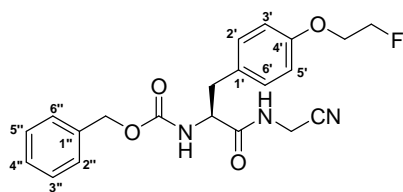
Compound **154** (1.21 g, 4.56 mmol) was dissolved in dry THF (20 mL) and cooled to $-25\text{ }^{\circ}\text{C}$. *N*-methylmorpholine (0.51 g, 5.04 mmol) and isobutyl chloroformate (0.69 g, 5.05 mmol) were added consecutively. Compound **153** (1.07 g, 4.58 mmol) was dissolved in H_2O (2 mL), treated with 2 N NaOH (3 mL) and added to the reaction mixture when the precipitation of *N*-methylmorpholinium chloride occurred. It was allowed to warm to room temperature within 30 min, and stirred for additional 90 min. The solvent was evaporated, and the resulting white solid was extracted with ethyl acetate ($3 \times 30\text{ mL}$). The combined organic layers were washed with 10 % KHSO_4 (30 mL) and brine (30 mL). The solvent was dried (Na_2SO_4) and evaporated. The oily product was purified by column chromatography on silica gel using ethyl acetate/petroleum ether (1:1) as eluent to obtain **155** as a white solid (1.05 g, 52% from **154**). ^1H NMR (500 MHz, $\text{DMSO}-d_6$) δ 1.28 (s, 9H, $\text{C}(\text{CH}_3)_3$), 2.74 (dd, $^2J = 13.6\text{ Hz}$, $^3J = 9.5\text{ Hz}$, 2H, NHCHCHH), 2.90 (dd, $^2J = 13.7\text{ Hz}$, $^3J = 5.2\text{ Hz}$, 2H, NHCHCHH) 3.82–4.02 (m, 2H, $\text{CH}_2\text{CH}=\text{CHS}$), 4.06–4.11 (m, 1H, NHCHCO), 6.59 (d, $^3J = 15.1\text{ Hz}$, 1H, $\text{CH}_2\text{CH}=\text{CHS}$), 6.85 (dt, $^3J = 15.1\text{ Hz}$, $^3J = 4.1\text{ Hz}$, 1H, $\text{CH}_2\text{CH}=\text{CHS}$), 6.99 (d, $^3J = 7.9\text{ Hz}$, 1H, NHCHCO), 7.14–7.24 (m, 5H, $\text{H}_{\text{arom}'}$), 7.62–7.83 (m, 5H, $\text{H}_{\text{arom}''}$), 8.22 (t, $^3J = 5.7\text{ Hz}$, 1H, NHCH_2CH); ^{13}C NMR (125 MHz, $\text{DMSO}-d_6$) δ 28.27 ($\text{C}(\text{CH}_3)_3$), 37.24 (NHCH_2CH), 56.15 (NHCHCO), 78.26 ($\text{C}(\text{CH}_3)_3$), 126.36, 127.19, 128.16, 129.25, 129.69, 129.72, 133.70, 138.15, 140.56, 144.65 ($\text{C}-4'$, $\text{C}-2'$, $\text{C}-6'$, $\text{C}-2''$, $\text{C}-6''$, $\text{C}-3'$, $\text{C}-5'$, $\text{C}-3''$, $\text{C}-5''$, $\text{C}-4''$, $\text{C}-1'$, $\text{C}-1''$, $\text{CH}_2\text{CH}=\text{CHS}$, $\text{CH}_2\text{CH}=\text{CHS}$), 155.48 (OCONH), 171.97 (NHCHCO).

31.97, 37.47, 39.00 (NHCHCH₂, NHCH₂CH, NCH₂CH₂CH₂CO), 54.42 (NHCHCO), 115.34, 118.68 (C-3''', C-5'''), 124.00, 125.02, 126.43, 127.19, 128.19, 129.17, 129.67, 129.79, 133.70, 134.56, 137.89, 140.50, 144.37 (C-4', C-9a'', C-5a'', C-9'', C-2', C-6', C-2'', C-6'', C-3', C-5', C-3'', C-5'', C-4'', C-10'', C-10a'', C-1', C-1'', C-7'''), 161.71, 162.93, 164.18, 171.45 (C-3''', C-1''', NCH₂CH₂CH₂CO, NHCHCO). LC-DAD (90% H₂O to 100% MeOH in 20 min, then 100% MeOH to 30 min, DAD 220.0–500.0 nm) tr = 8.59, 94% purity. MS(ESI) (pos.) m/z = 685.2 ([M + Na]⁺); MS(ESI) (neg.) 661.2 ([M - H]⁻); MS(EI) m/z = 662.4 (M^{•+}).

3.3.77. PREPARATION OF 159

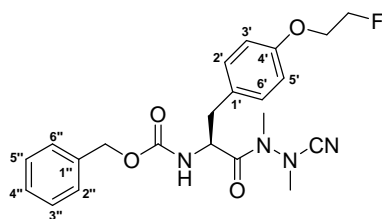


***N*-(Benzyloxycarbonyl)tyrosyl-glycine-nitrile.** Compound **26** (0.91 g, 2.89 mmol) was dissolved in dry THF (30 mL) and cooled to $-25\text{ }^{\circ}\text{C}$. To the stirred solution, *N*-methylmorpholine (0.32 g, 3.16 mmol) and isobutyl chloroformate (0.43 g, 3.15 mmol) were added consecutively. Aminoacetonitrile monosulfate (1.11 g, 7.20 mmol) was dissolved in 3 mL H_2O , treated with 3 mL of 5 N NaOH and added to the reaction mixture when the precipitation of *N*-methylmorpholinium chloride occurred. It was allowed to warm to room temperature within 30 min, and stirred for additional 2 h. The solvent was evaporated under reduced pressure, and the resulting aqueous residue was extracted with ethyl acetate ($3 \times 60\text{ mL}$). The combined organic layers were washed with 10% KHSO_4 (30 mL), H_2O (30 mL), sat. NaHCO_3 (30 mL), H_2O (30 mL), and brine (30 mL). The solvent was dried (Na_2SO_4) and evaporated. The crude product was recrystallized from ethyl acetate/petroleum to obtain **159** as a white solid (0.80 g, 78%). mp $182\text{ }^{\circ}\text{C}$; ^1H NMR (500 MHz, $\text{DMSO-}d_6$) δ 2.65 (dd, $^2J = 13.9\text{ Hz}$, $^3J = 10.1\text{ Hz}$, 1H, CHCHH), 2.87 (dd, $^2J = 13.7\text{ Hz}$, $^3J = 4.6\text{ Hz}$, 1H, CHCHH), 4.11–4.16 (m, 3H, NHCH_2CN , NHCHCO), 4.92 (d, $^2J = 12.6\text{ Hz}$, 1H, CHHO), 4.98 (d, $^2J = 13.0\text{ Hz}$, 1H, CHHO), 6.64 (d, $^3J = 8.5\text{ Hz}$, 2H, H'-3, H'-5), 7.03 (d, $^3J = 8.6\text{ Hz}$, 2H, H'-2, H'-6), 7.23–7.34 (m, 5H, H''_{arom}), 7.51 (d, $^3J = 8.5\text{ Hz}$, 1H, NHCHCO), 8.68 (t, $^3J = 5.5\text{ Hz}$, 1H NHCH_2CN), 9.16 (s, 1H, OH); ^{13}C NMR (125 MHz, $\text{DMSO-}d_6$) δ 27.24 (NHCH_2CN), 36.60 (CHCH_2), 56.50 (NHCHCO), 65.41 (CH_2O), 115.07 (C-3', C-5'), 117.59 (CN), 127.55, 127.80, 127.87, 128.41, 130.20, 137.12 (C-2', C-6', C-2'', C-6'', C-4'', C-3'', C-5'', C-1', C-1''), 156.00 (OCONH), 172.42 (CONH); FTIR (KBr, cm^{-1}) 2260 ($\text{C}\equiv\text{N}$); Anal. $\text{C}_{19}\text{H}_{19}\text{N}_3\text{O}_4$ (353.37 g/mol) calcd C 64.58, H 5.42, N 11.89; found C 64.79, H 5.69, N 11.26. LC-MS(ESI) (90% H_2O to 100% MeOH in 20 min, then 100% MeOH to 30 min, DAD 220.0–300.0 nm) $t_r = 14.65$, 97% purity, $m/z = 354.4$ ($[\text{M} + \text{H}]^+$).

3.3.78. PREPARATION OF 160

***N*-(Benzyloxycarbonyl)-*O*-(2-fluoroethyl)tyrosyl-glycine-nitrile.** Compound **159** (0.50 g, 1.41 mmol) was dissolved in dry DMF (20 mL) and cooled to -10 °C. The resulting solution was treated with sodium hydride (0.06 g (60 % in mineral oil), 1.50 mmol) and stirred at -10 °C for 30 min. 1-Bromo-2-fluoroethane (0.27 g, 2.13 mmol), which was provided by Reik Löser, was added. The reaction solution was slowly warmed to room temperature and stirred for 19 h. The solvent was evaporated under reduced pressure, the resulting residue was suspended in H₂O and extracted with ethyl acetate (3 × 30 mL). The combined organic layers were washed with H₂O (30 mL) and brine (30 mL). The solvent was dried (Na₂SO₄) and evaporated. The crude product was purified by column chromatography on silica gel using ethyl acetate/petroleum ether (1:1) to obtain **160** as a white solid (0.29 g, 51%). mp 150 °C; ¹H NMR (500 MHz, DMSO-*d*₆) δ 2.70 (dd, ²*J* = 13.9 Hz, ³*J* = 10.4 Hz, 1H, CHCHH), 2.92 (dd, ²*J* = 13.9 Hz, ³*J* = 4.4 Hz, 1H, CHCHH), 4.13–4.22 (m, 5H, NHCH₂CN, NHCHCO, OCH₂CH₂F), 4.71 (dt, ¹*J*_{H,F} = 47.7 Hz, ³*J* = 3.9 Hz, 2H, OCH₂CH₂F), 4.92 (d, ²*J* = 12.6 Hz, 1H, CHHO), 4.97 (d, ²*J* = 12.6 Hz, 1H, CHHO) 6.85 (d, ³*J* = 8.9 Hz, 2H, H-3', H-5'), 7.17 (d, ³*J* = 8.5 Hz, 2H, H-2', H-6'), 7.17–7.34 (m, 5H, H_{arom}), 7.56 (d, ³*J* = 8.5 Hz, 1H, NHCHCO), 8.71 (t, ³*J* = 5.4 Hz, 1H, NHCH₂CN); ¹³C NMR (125 MHz, DMSO-*d*₆) δ 27.23 (NHCH₂CN), 36.48 (CHCH₂), 56.38 (NHCHCO), 65.43 (CH₂O), 67.10 (d, ³*J*_{C,F} = 18.8 Hz, OCH₂CH₂F), 82.31 (d, ¹*J* = 165.6 Hz, OCH₂CH₂F), 114.31 (C-3', C-5'), 117.59 (CN), 127.58, 127.81, 128.40, 130.19, 130.37, 137.08 (C-2', C-6', C-2'', C-6'', C-4'', C-3'', C-5'', C-1', C-1''), 156.01, 156.90 (C-4', OCON), 172.32 (NHCHCO); FTIR (KBr, cm⁻¹) 2247 (C≡N); Anal. C₂₁H₂₂FN₃O₄ (399.42 g/mol) calcd C 63.15, H 5.55, N 10.52; found C 62.60, H 5.41, N 10.77. LC-MS(ESI) (90% H₂O to 100% MeOH in 20 min, then 100% MeOH to 30 min, DAD 220.1–320.7 nm) t_r = 16.48, 96% purity, *m/z* = 404.4 ([M + H]⁺).

3.3.79. PREPARATION OF 161

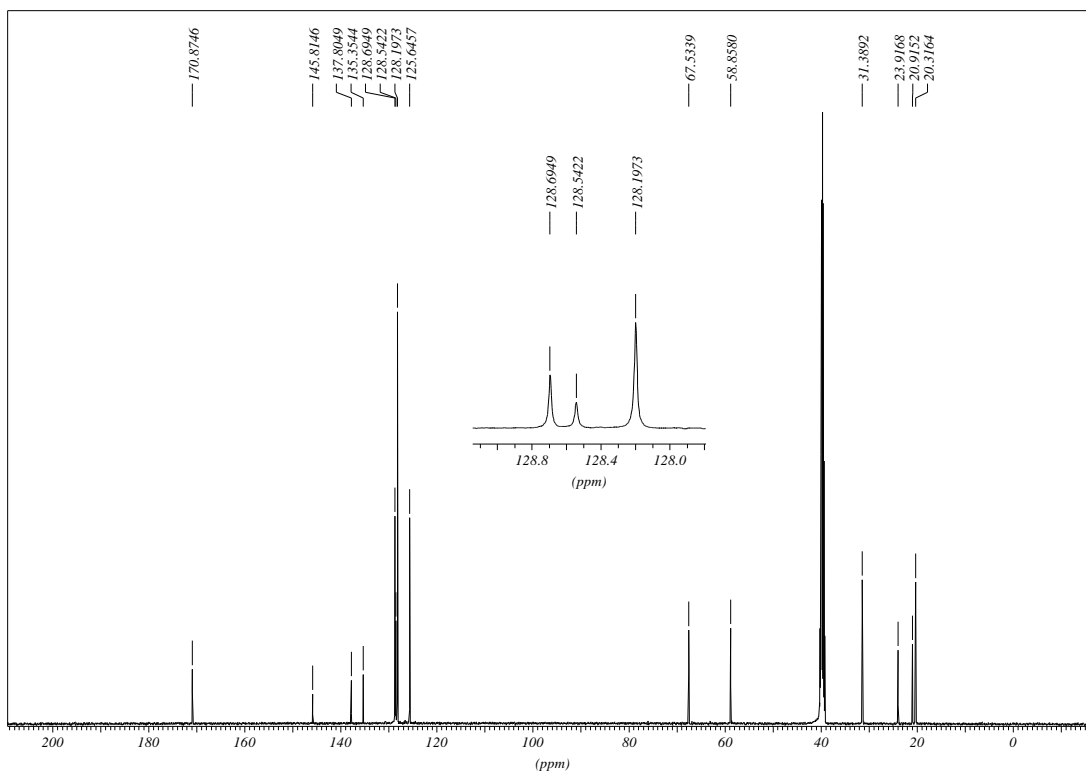
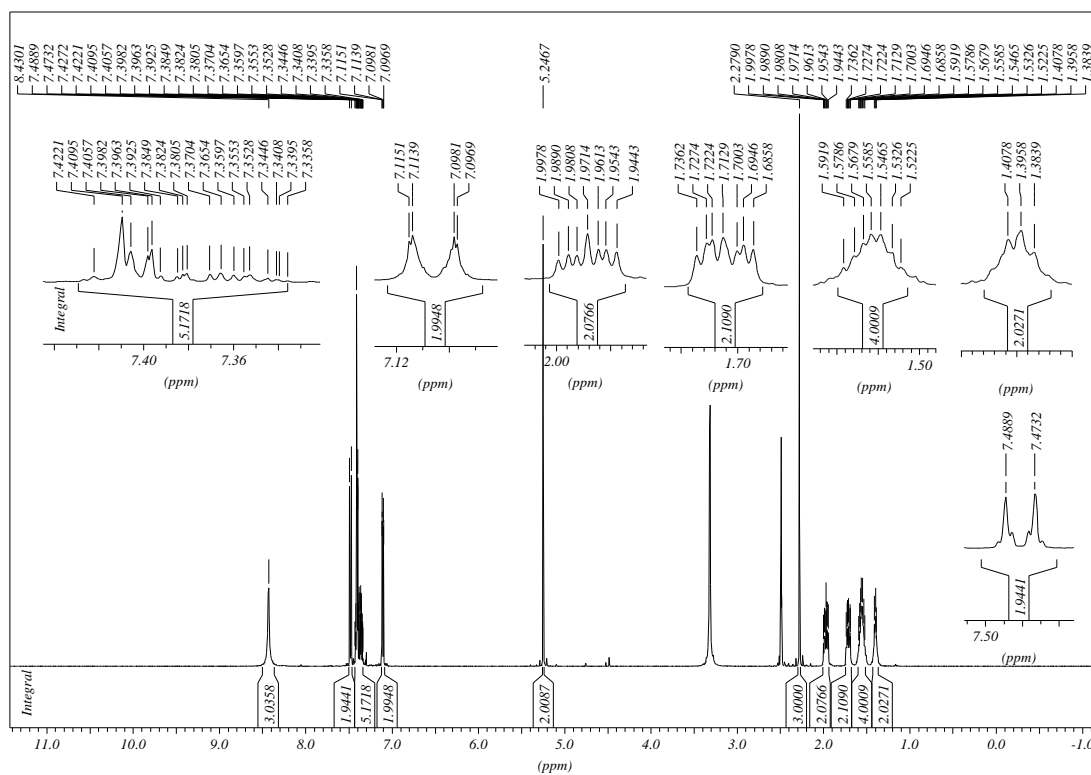


***N*-(Benzyloxycarbonyl)-*O*-(2-fluoroethyl)tyrosyl-methylazaalanine-nitrile.** Compound **38** (1.28 g, 3.35 mmol) was dissolved in dry DMF (20 mL) and cooled to $-10\text{ }^{\circ}\text{C}$. The resulting solution was treated with sodium hydride (0.14 g (60% in mineral oil), 3.50 mmol) and stirred at $-10\text{ }^{\circ}\text{C}$ for 30 min. 1-Bromo-2-fluoroethane (0.83 g, (77% purity), 5.03 mmol), which was provided by Reik Löser, was added. The reaction solution was slowly warmed to room temperature, and stirred for 19 h. The solvent was removed under reduced pressure, the resulting residue was suspended in H_2O , and extracted with ethyl acetate ($3 \times 30\text{ mL}$). The combined organic layers were washed with H_2O (30 mL) and brine (30 mL), and dried over Na_2SO_4 . The crude product was purified by column chromatography using ethyl acetate/petroleum ether (1:1) as eluent to obtain **161** as a colourless oil (0.53 g, 37%). $[\alpha]_{\text{D}}^{20} = +22.4$ ($c = 0.77$, CHCl_3); ^1H NMR (500 MHz, $\text{DMSO-}d_6$) mixture of rotamers δ 2.73–2.86 (m, 2H, CHCH_2), 2.98_a, 3.08_b, 3.12_c, 3.22_d ($4 \times s$, 6H, $2 \times \text{NCH}_3$), 4.19 (dt, $^3J_{\text{H,F}} = 30\text{ Hz}$, $^3J = 3.5\text{ Hz}$, 2H, $\text{OCH}_2\text{CH}_2\text{F}$), 4.66–4.77 (m, 3H, $\text{OCH}_2\text{CH}_2\text{F}$, NHCHCO), 4.95 (s, 2H, CH_2O), 6.88–7.34 (m, 9H, H_{arom}), 7.78_a, 7.87_b (bs_a, d_b, $^3J = 7.9\text{ Hz}$, 1H, NHCHCO); ^{13}C NMR (125 MHz, $\text{DMSO-}d_6$) mixture of rotamers δ 30.28, 30.59, 35.65, 36.04, 40.48, 40.88 ($2 \times \text{NCH}_3$, CHCH_2), 52.89, 53.34 (NHCHCO), 65.62 (CH_2O), 67.13 (d, $^2J_{\text{C,F}} = 18.8\text{ Hz}$, $\text{OCH}_2\text{CH}_2\text{F}$), 82.28 (d, $^1J_{\text{C,F}} = 165.6\text{ Hz}$, $\text{OCH}_2\text{CH}_2\text{F}$), 114.21, 114.57, 127.74, 127.91, 128.42, 129.85, 130.28, 130.50, 136.91 (CN, C_{arom}), 156.28 (OCON), 157.12 ($\text{C}_{\text{arom}}\text{O}$), 173.50 (NHCHCO); FTIR (KBr, cm^{-1}) 2222 ($\text{C}\equiv\text{N}$); LC-MS(ESI) (90% H_2O to 100% MeOH in 20 min, then 100% MeOH to 30 min, DAD 219.7–300.7 nm) $t_r = 17.23$, 96% purity, $m/z = 429.5$ ($[\text{M} + \text{H}]^+$).

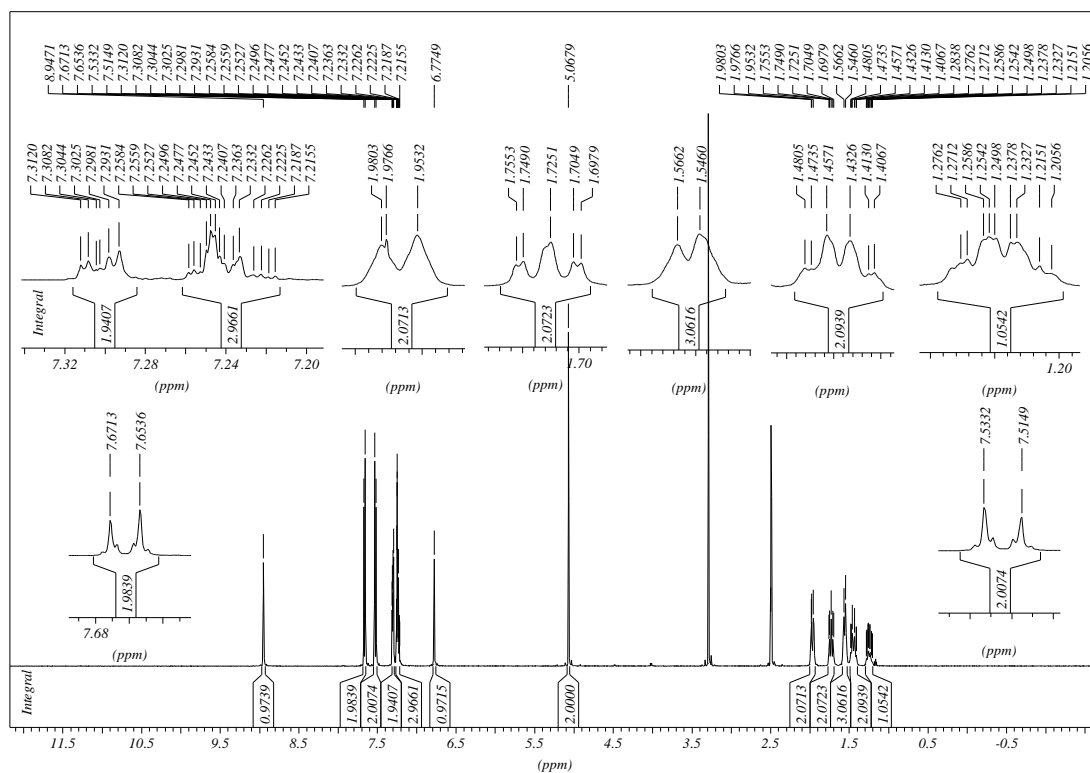
3.4. NMR SPECTRA

Only NMR spectra of not published compounds are shown. For NMR spectra of published compounds, see 'Supporting Information' of [192] and [201].

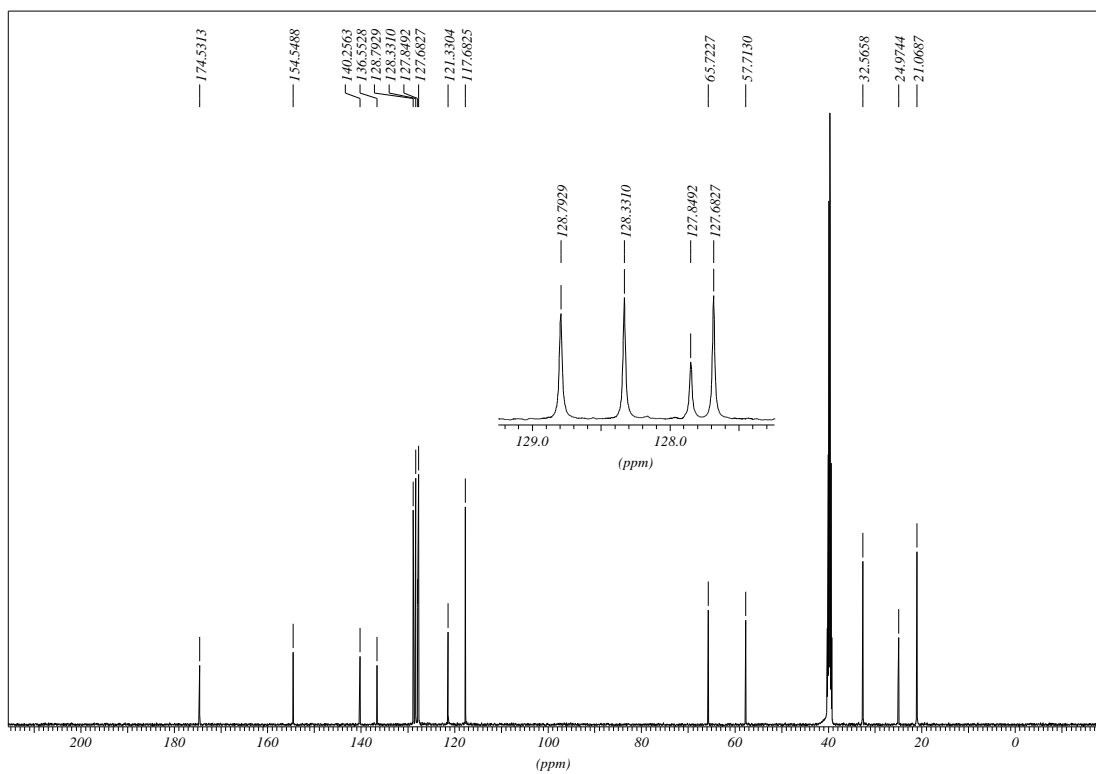
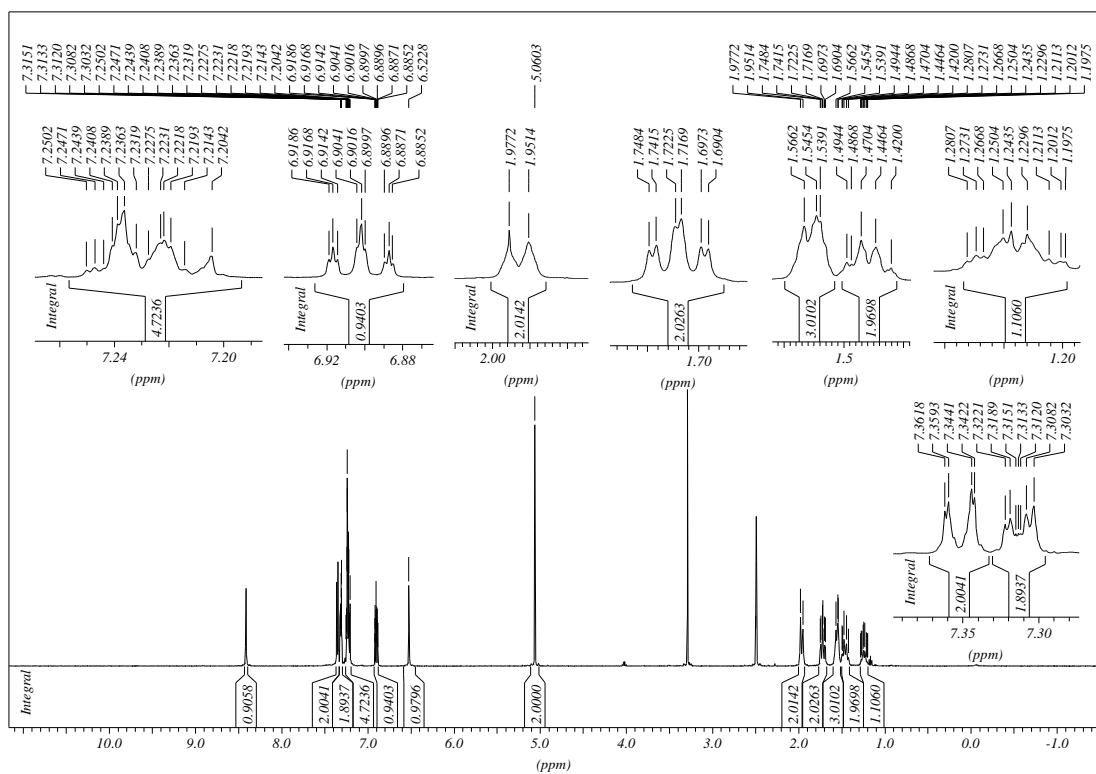
3.4.2. NMR SPECTRA OF 94



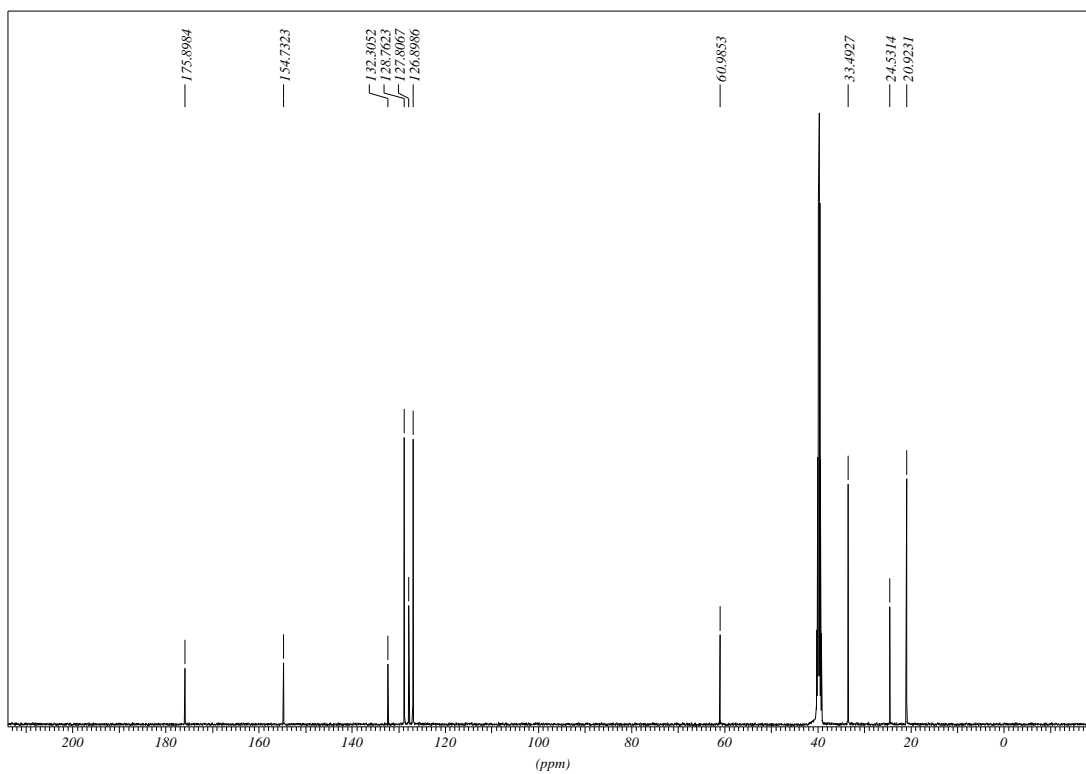
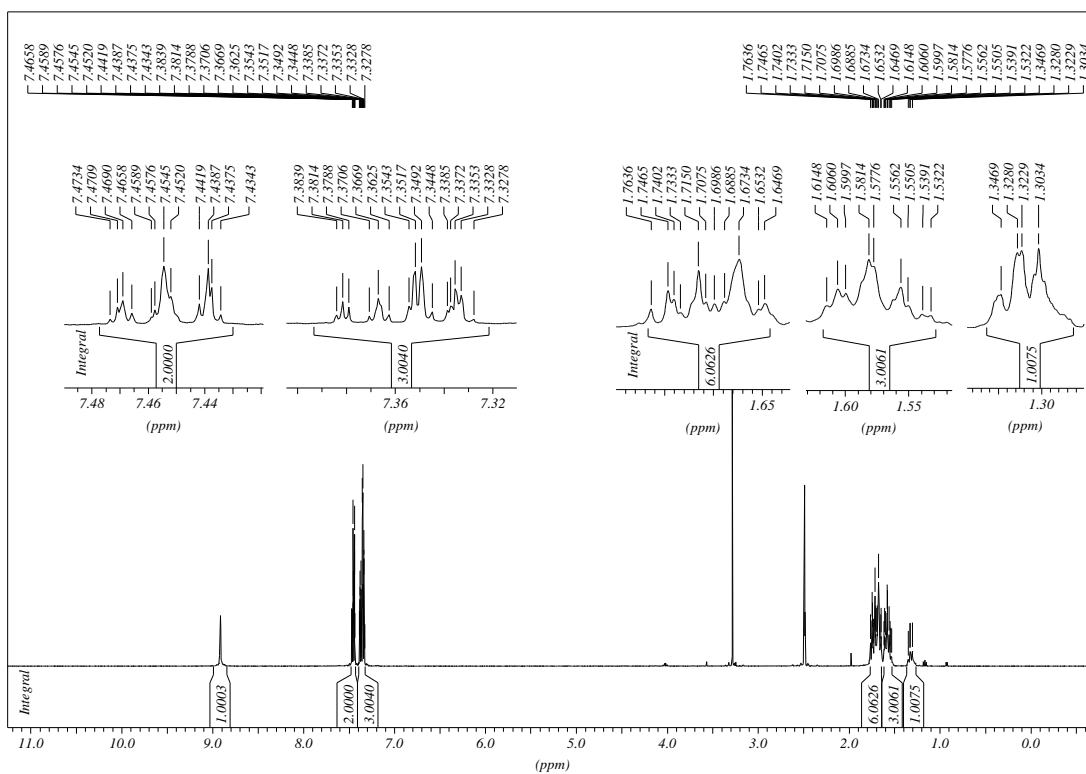
3.4.3. NMR SPECTRA OF 95



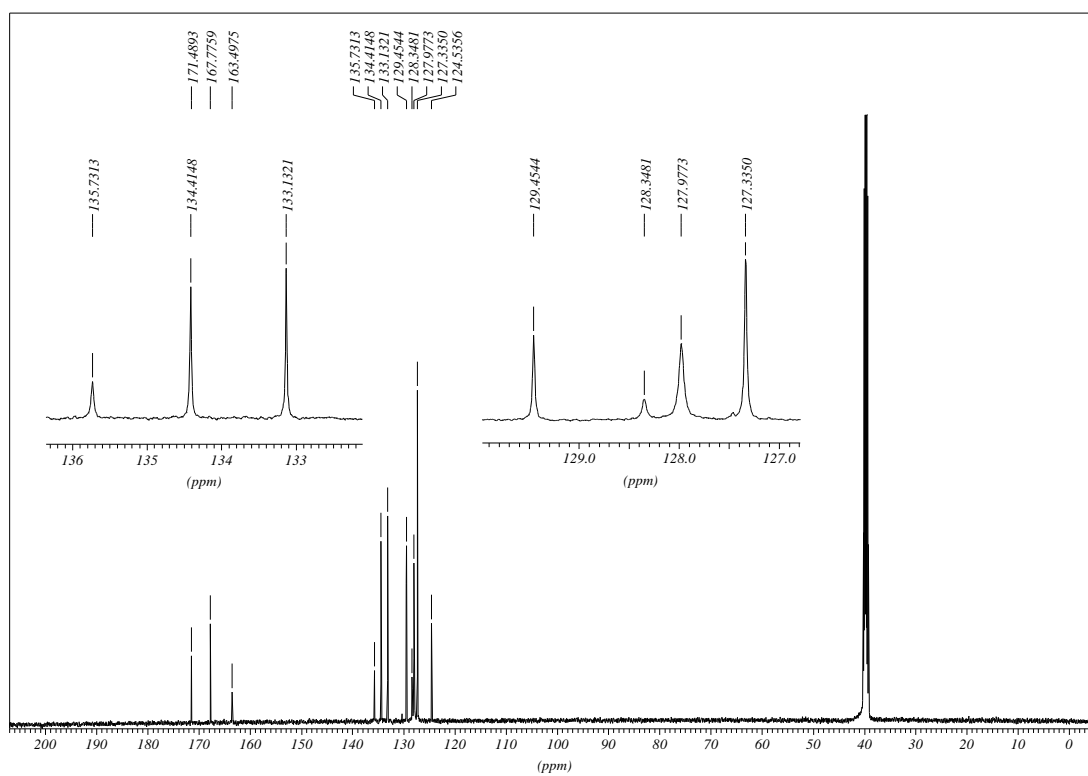
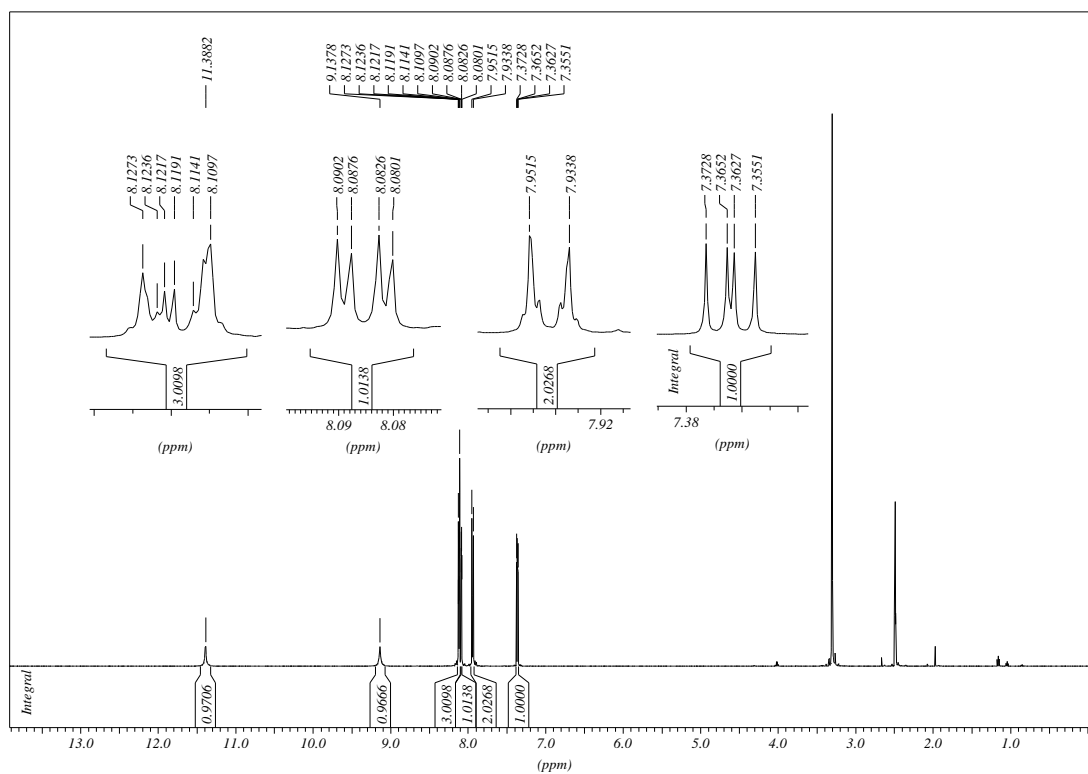
3.4.5. NMR SPECTRA OF 98



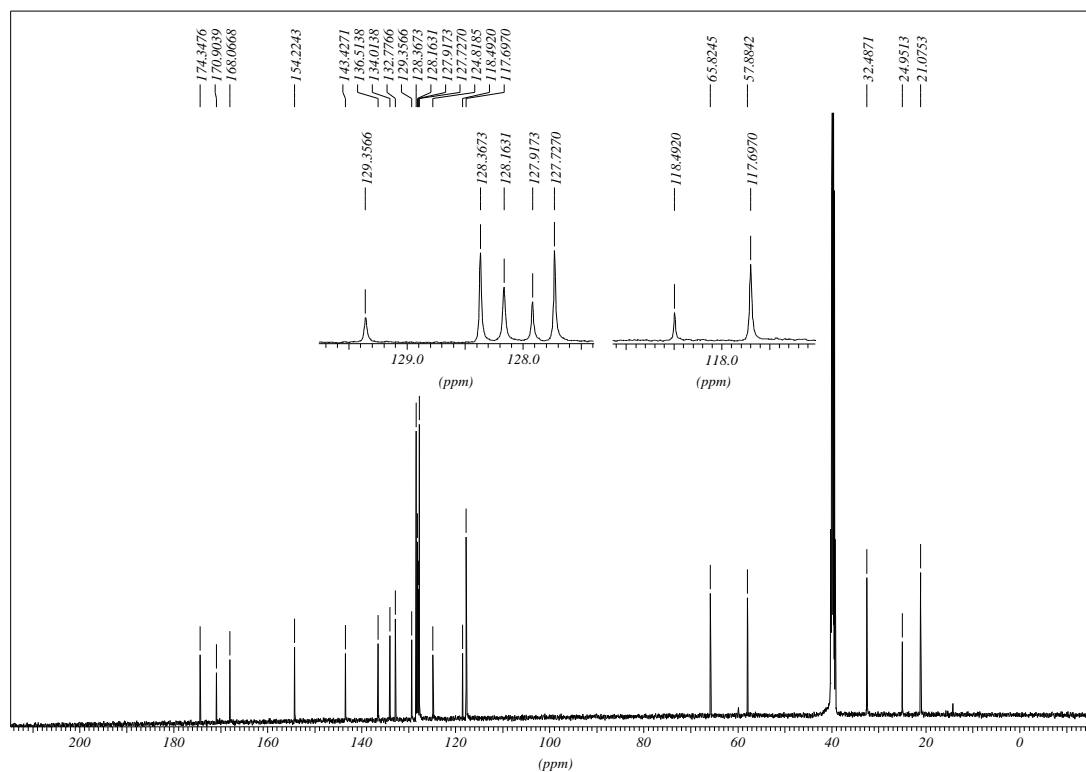
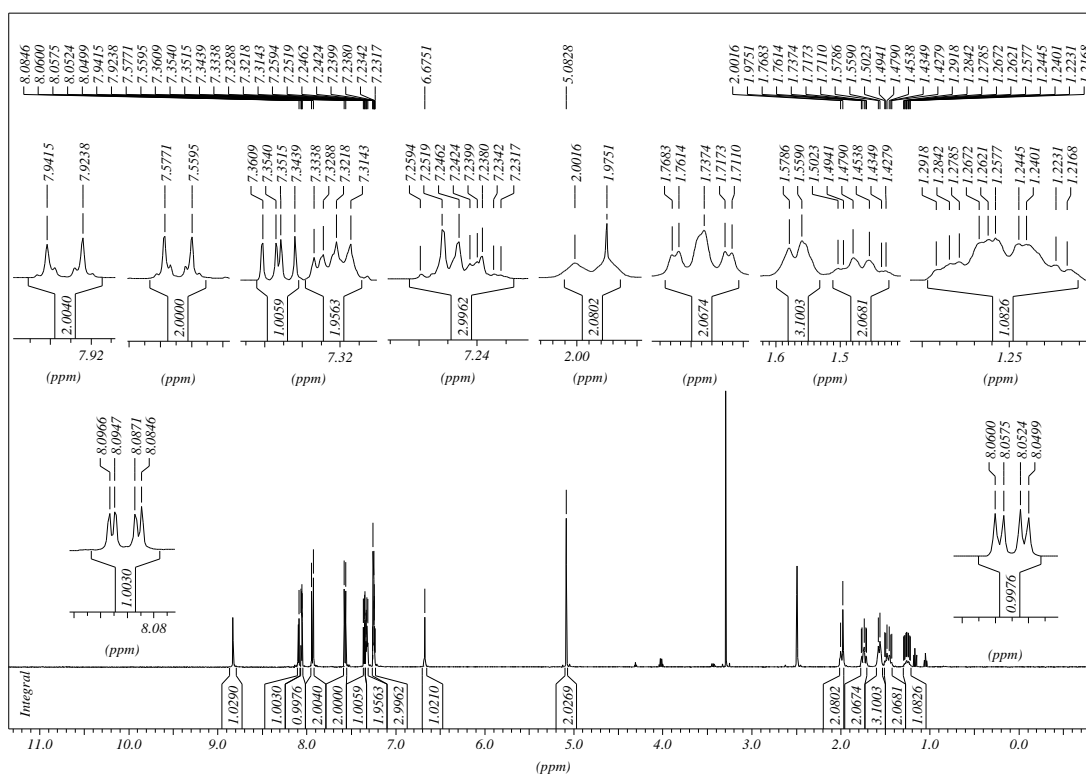
3.4.6. NMR SPECTRA OF 100



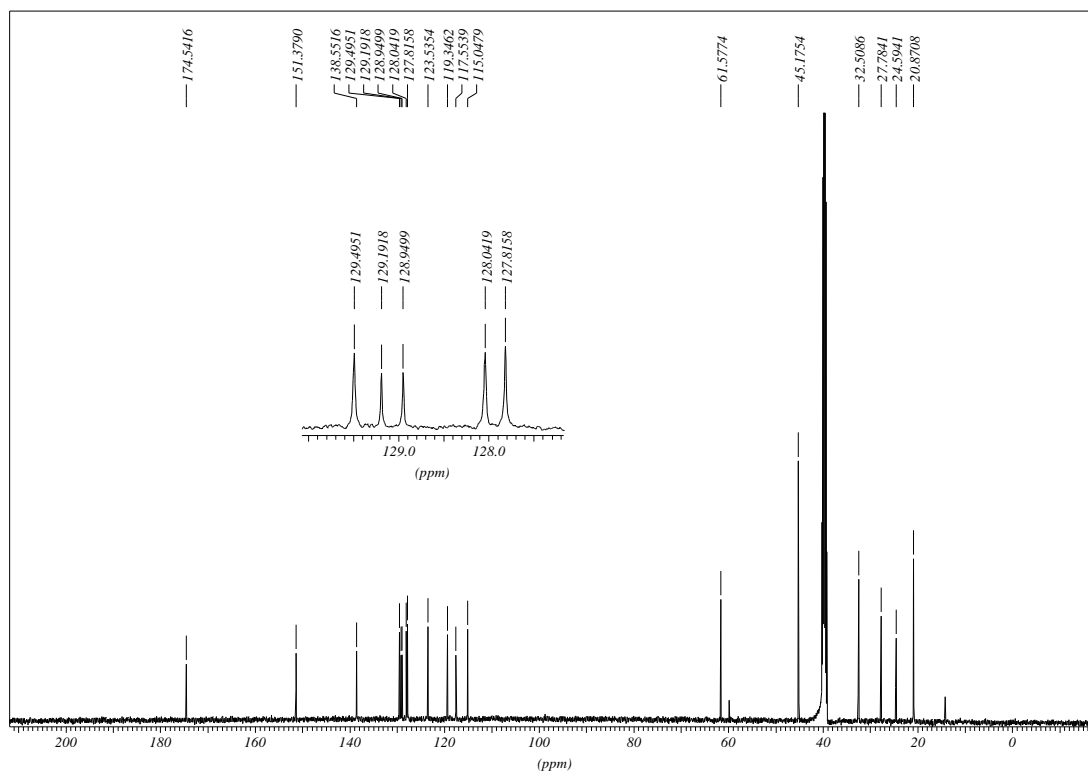
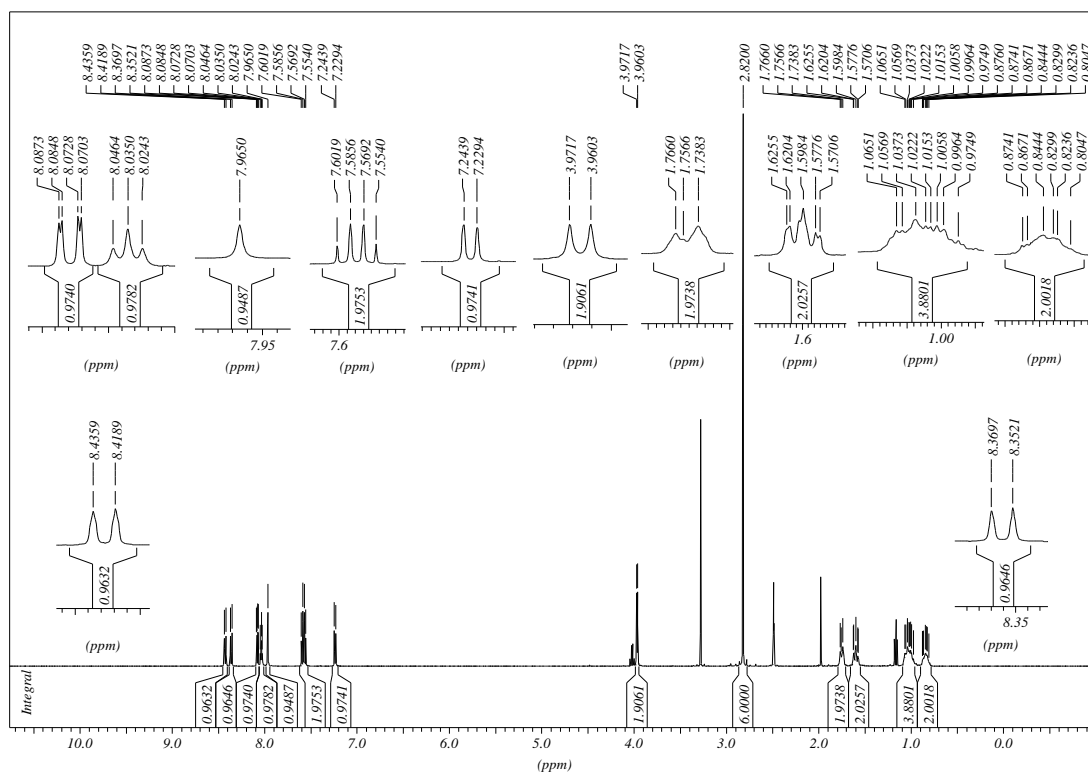
3.4.7. NMR SPECTRA OF 101



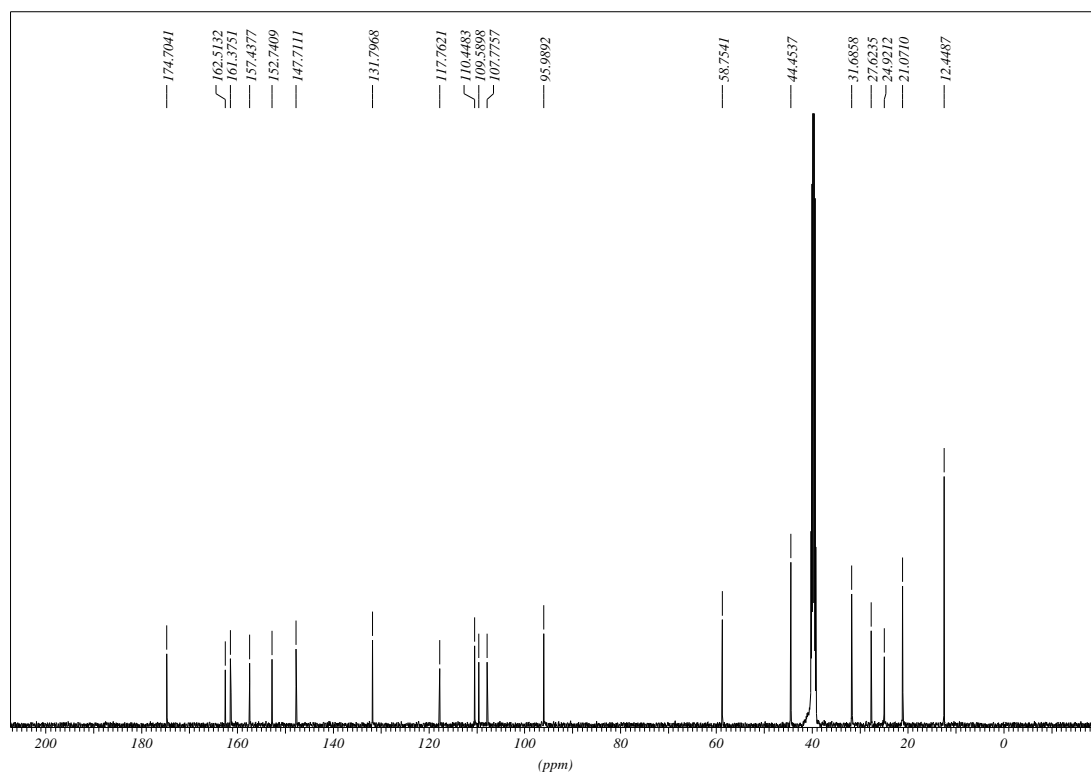
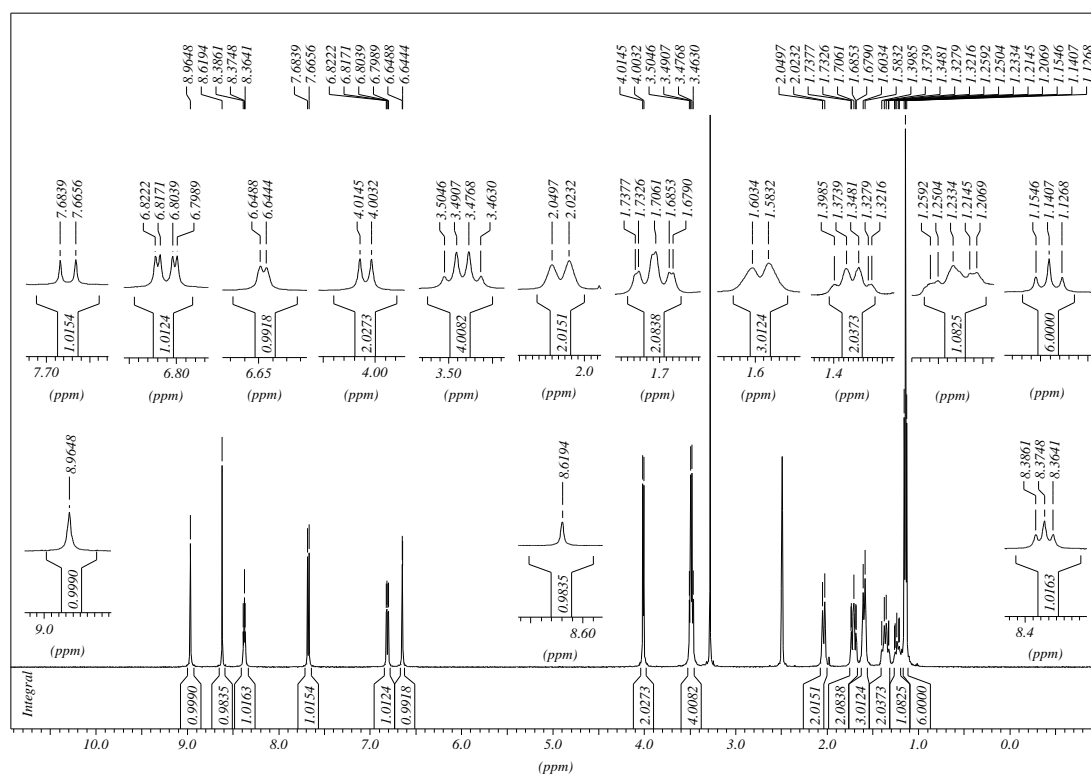
3.4.8. NMR SPECTRA OF 103



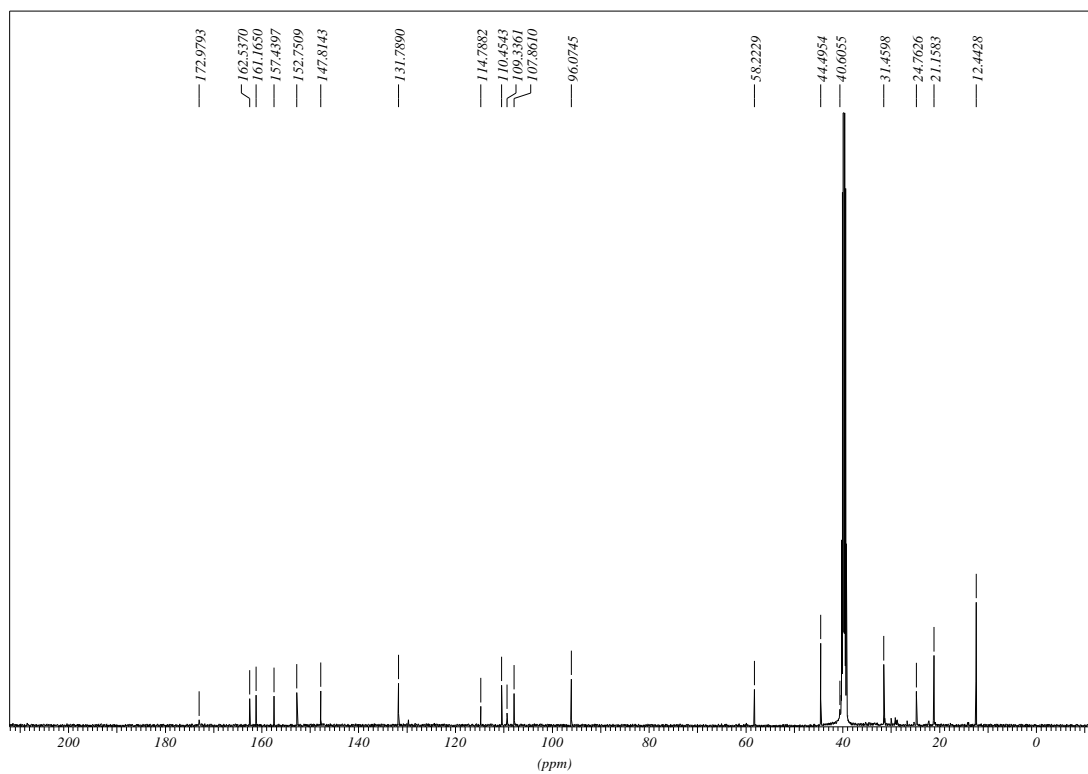
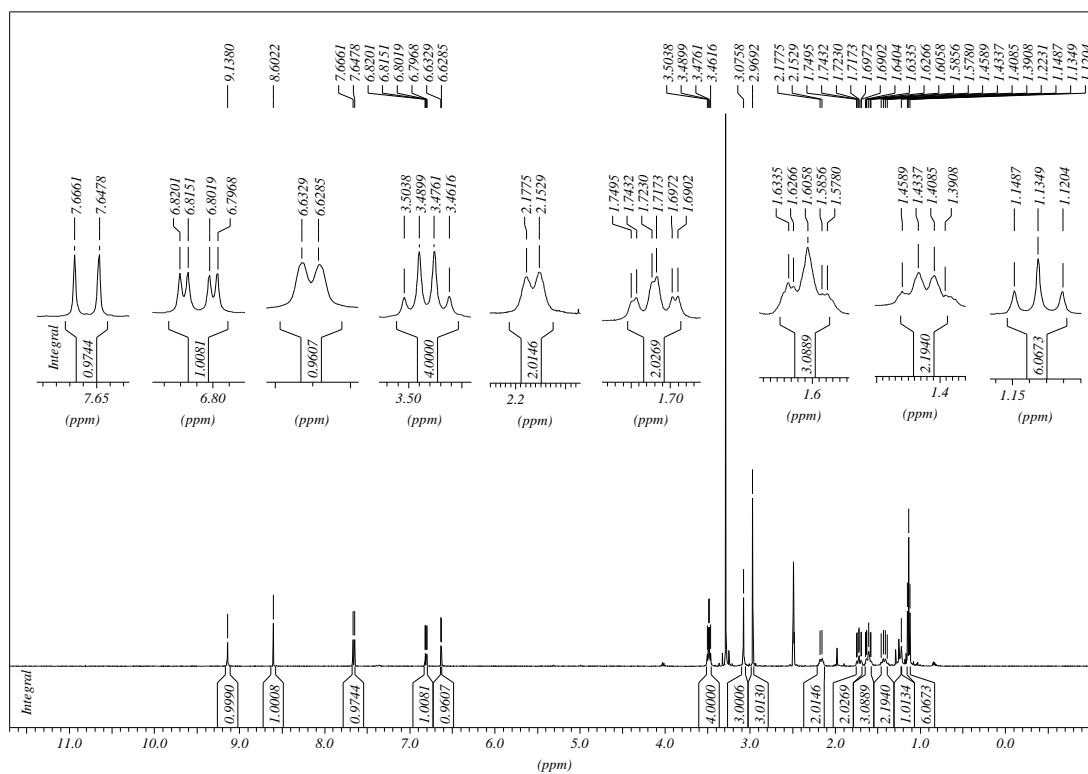
3.4.9. NMR SPECTRA OF 119



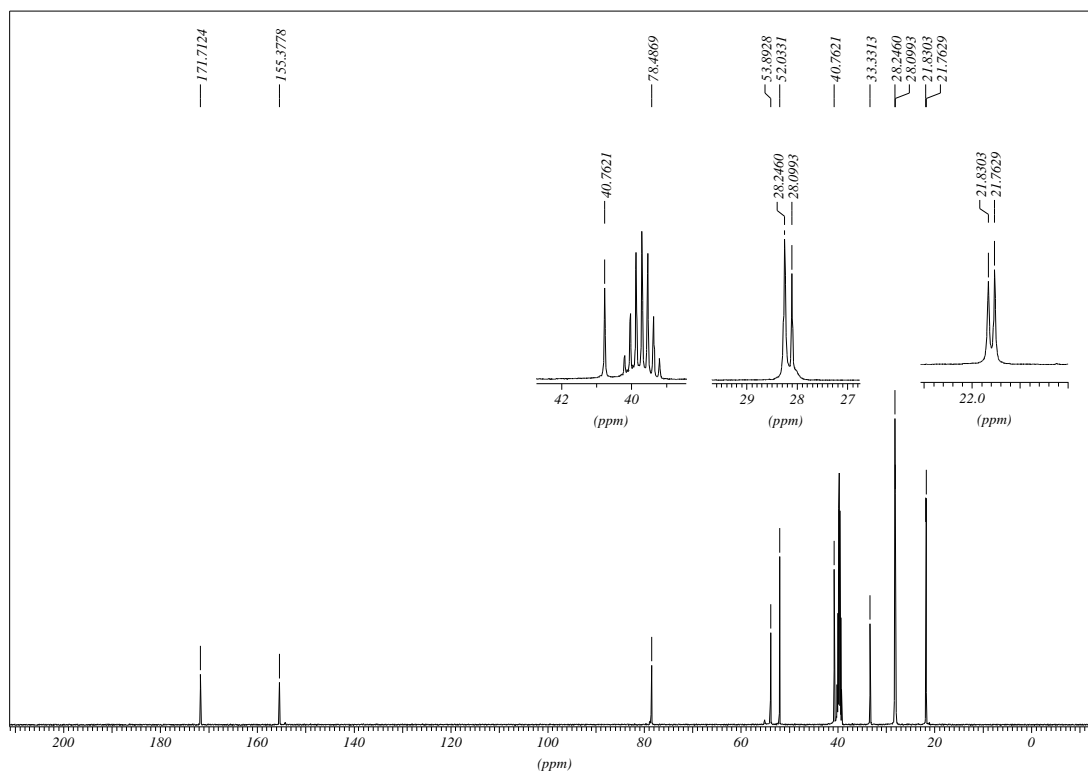
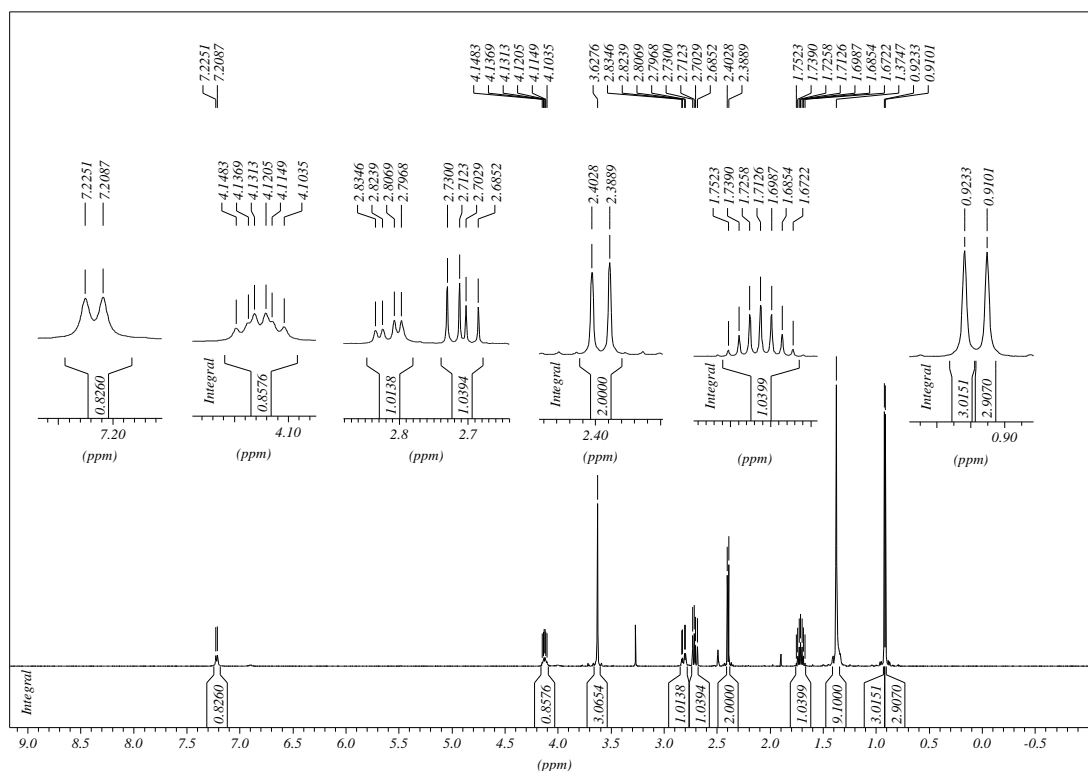
3.4.10. NMR SPECTRA OF 120



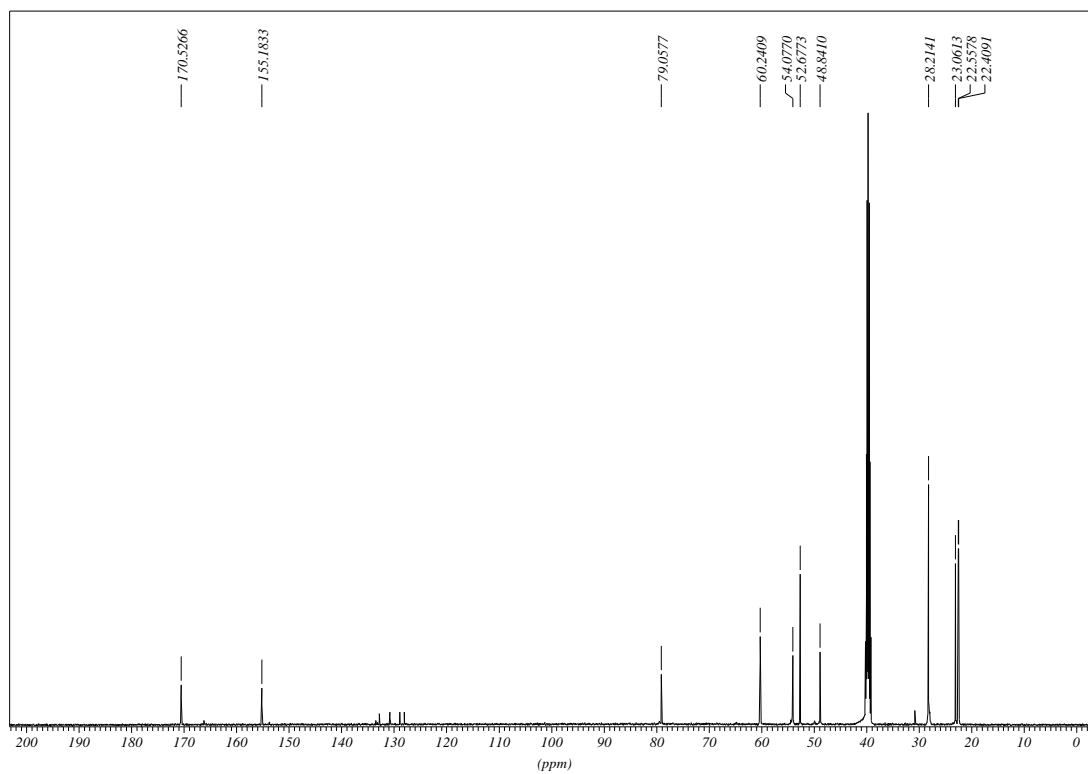
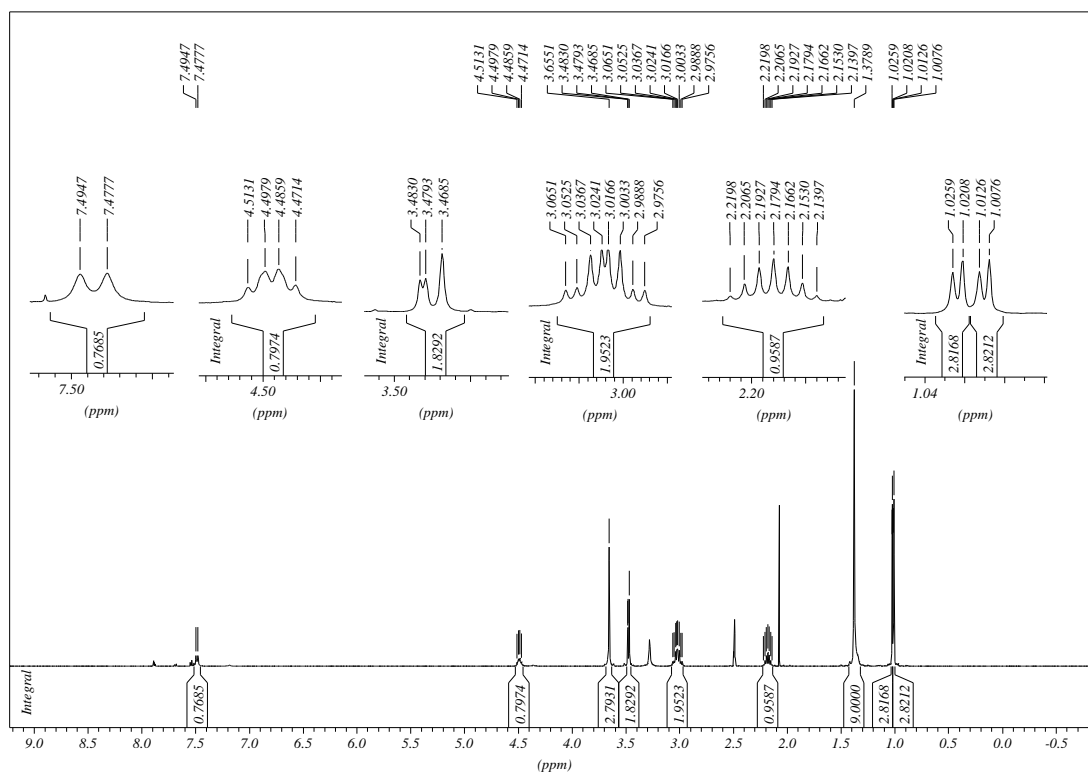
3.4.11. NMR SPECTRA OF 122



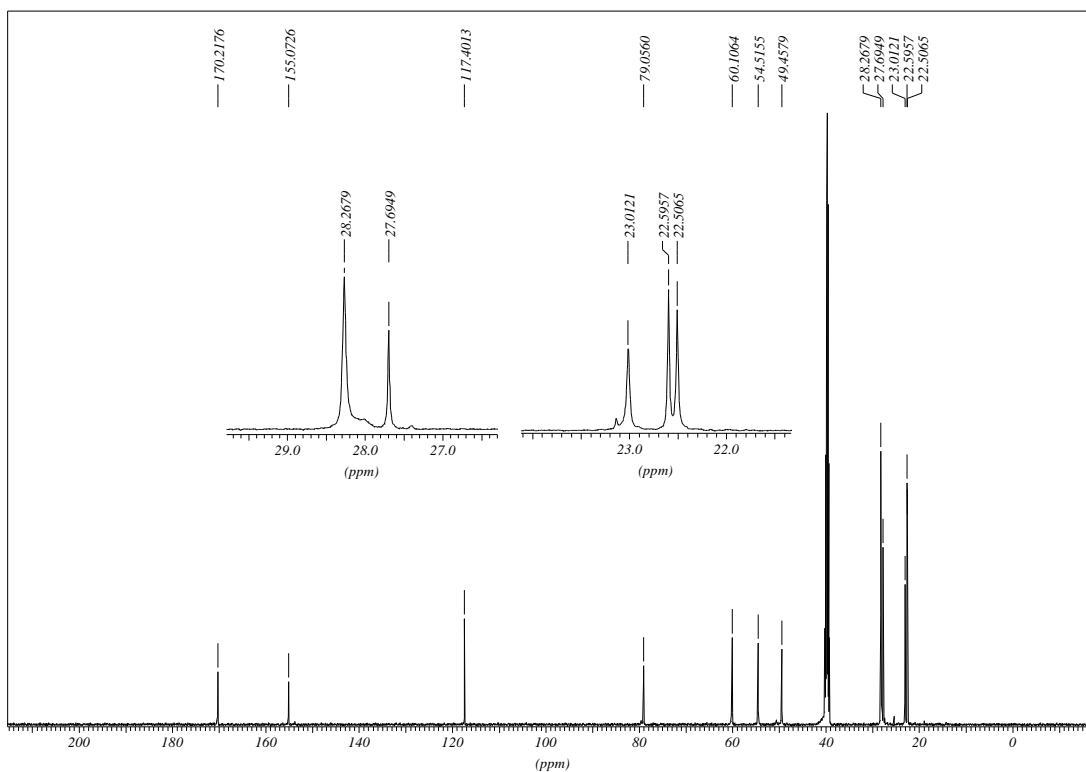
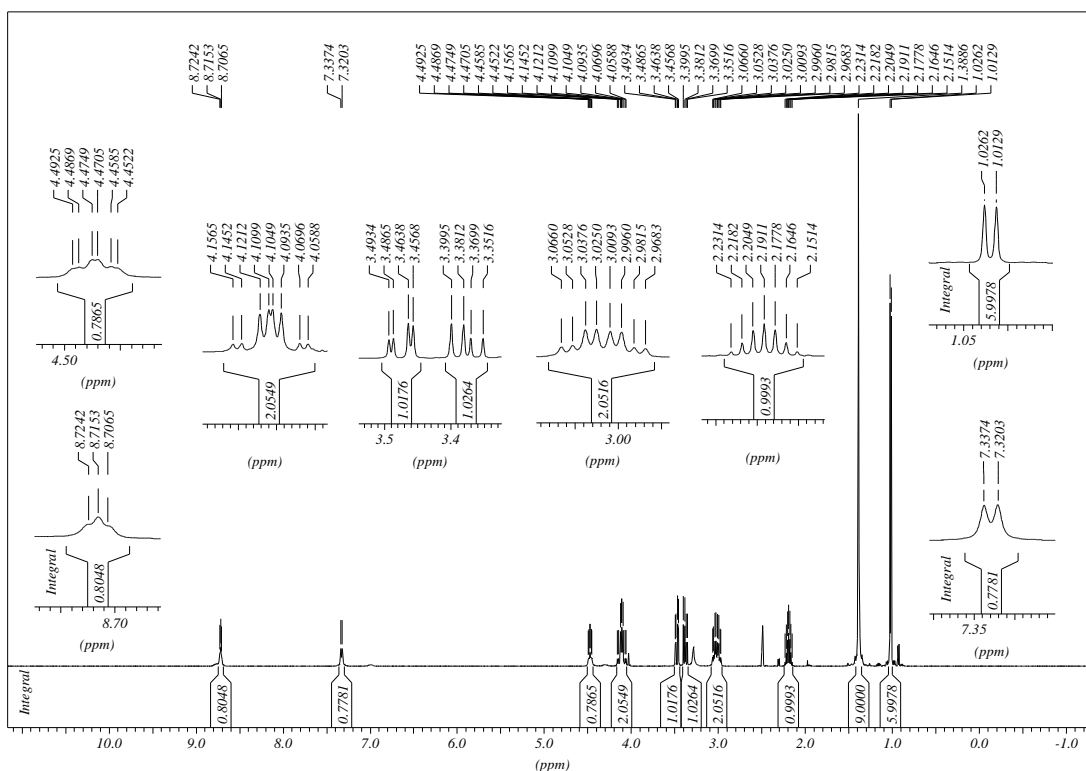
3.4.12. NMR SPECTRA OF 124



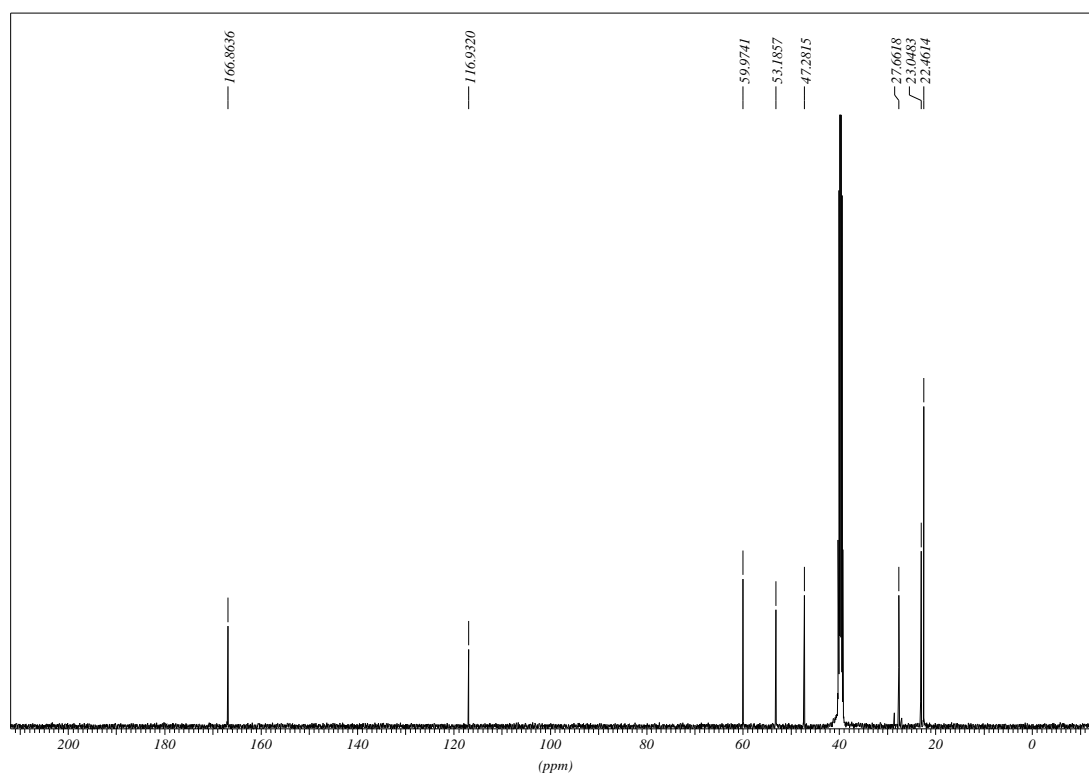
3.4.13. NMR SPECTRA OF 125



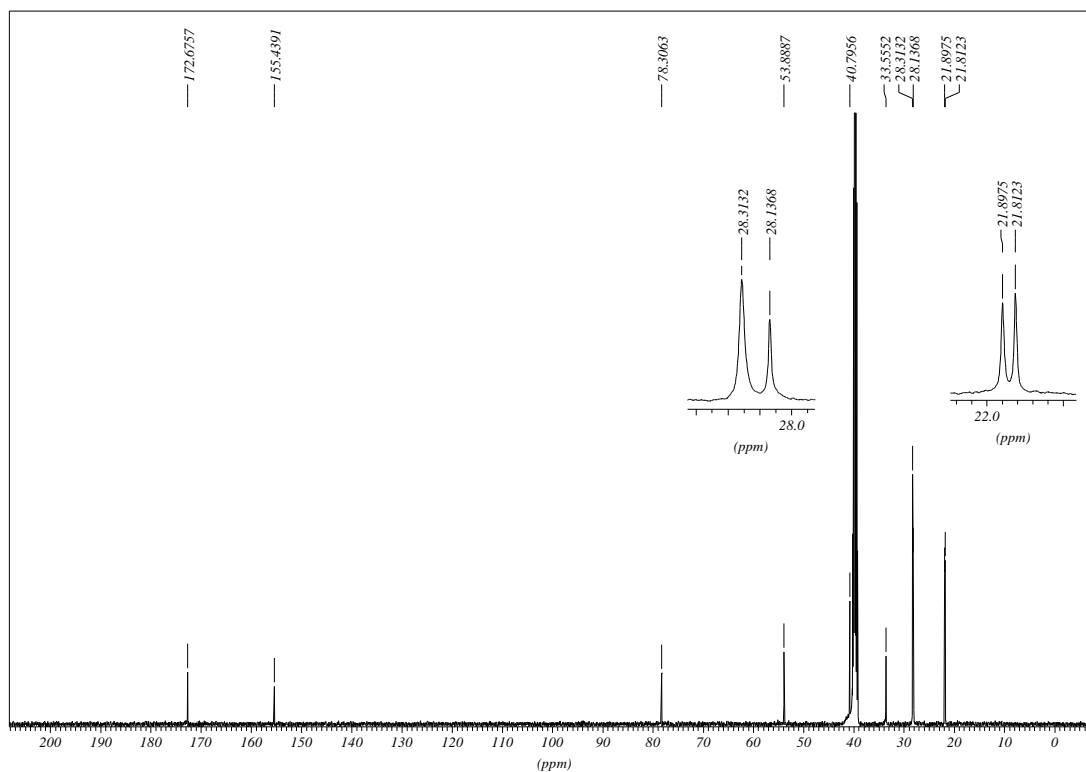
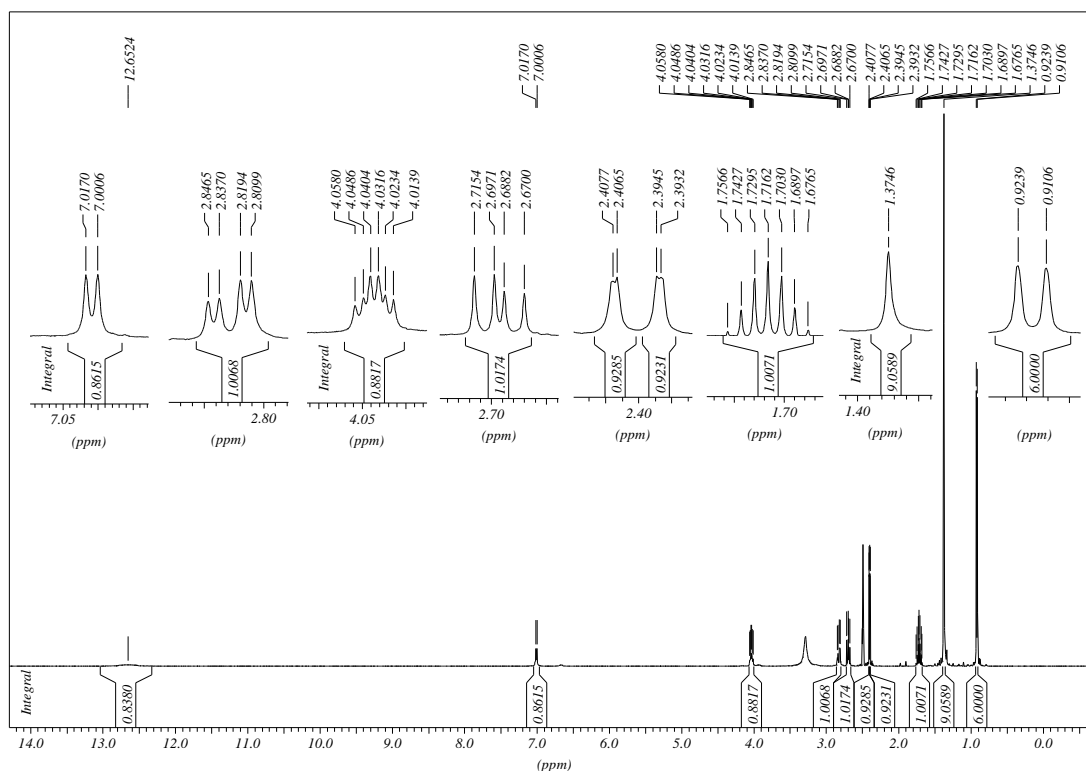
3.4.14. NMR SPECTRA OF 127



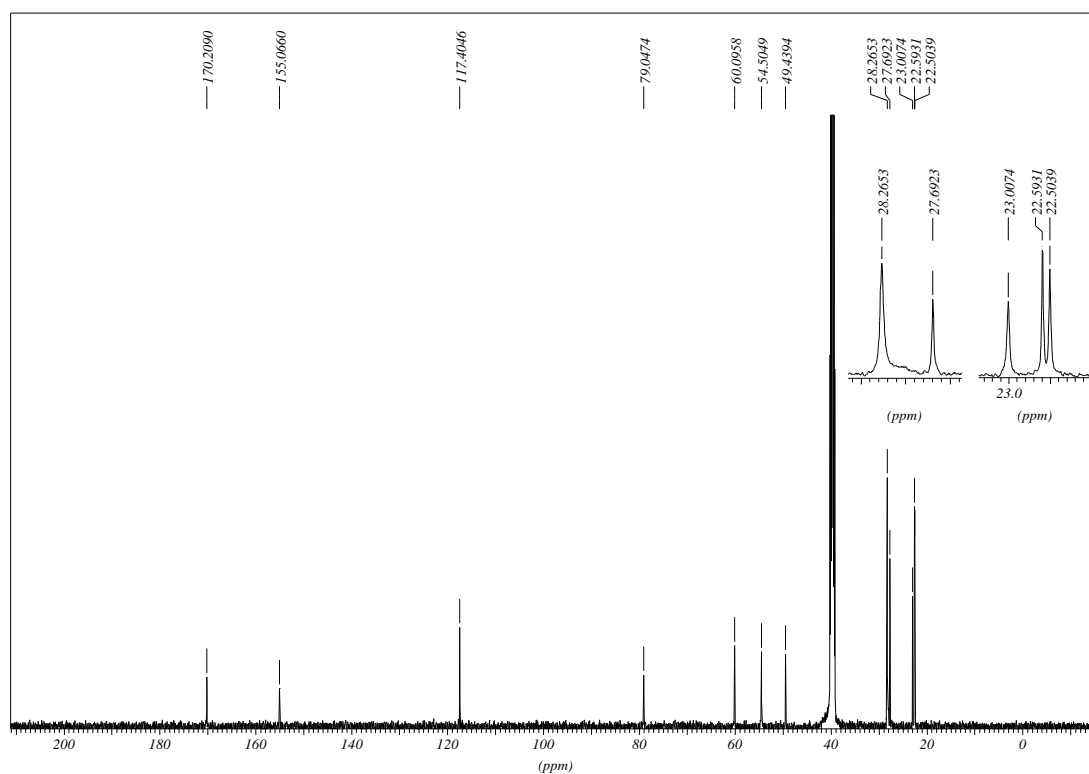
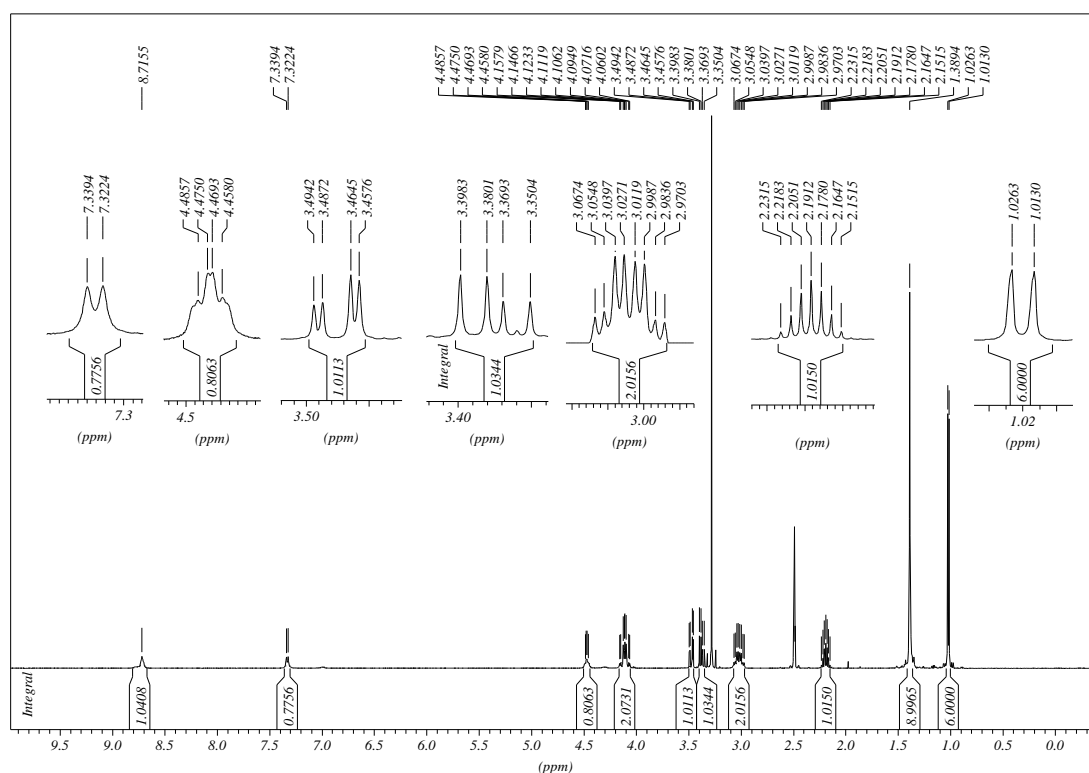
3.4.15. NMR SPECTRA OF 128



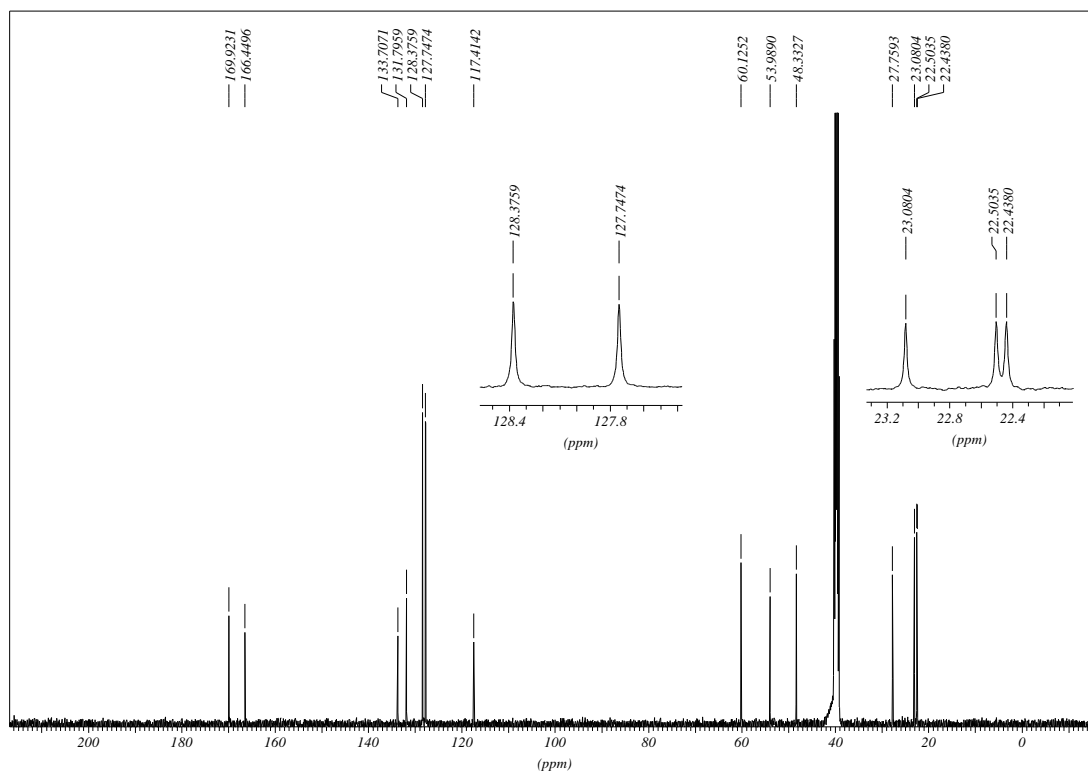
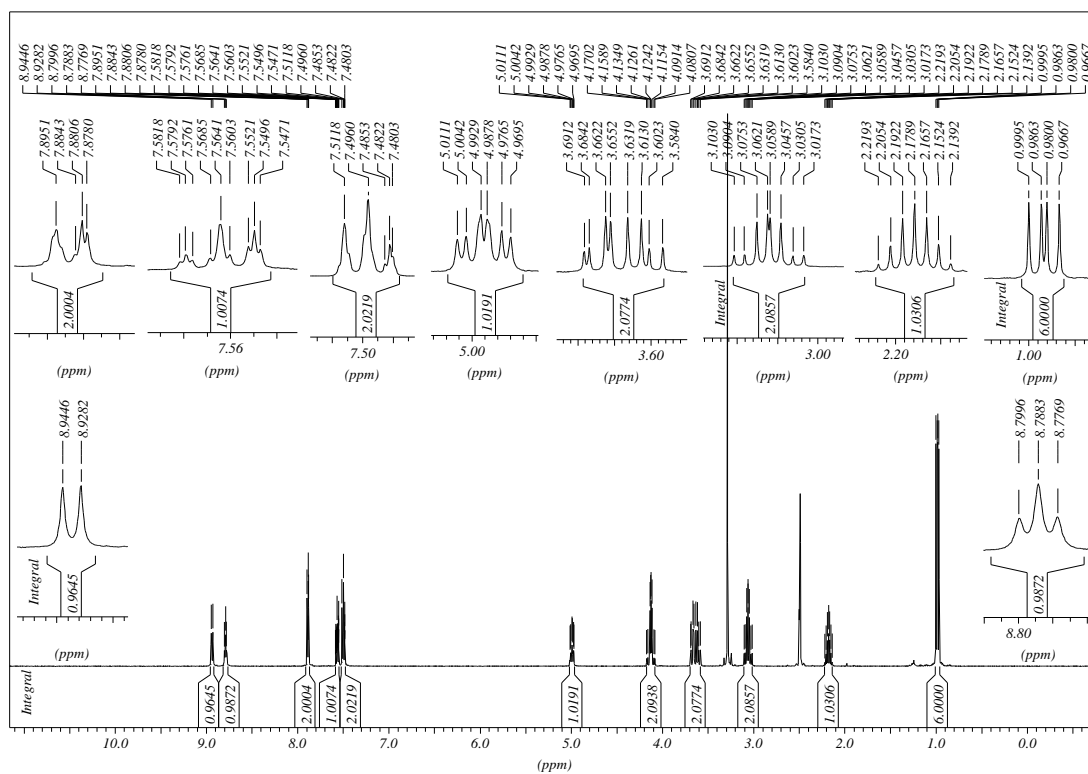
3.4.16. NMR SPECTRA OF 140



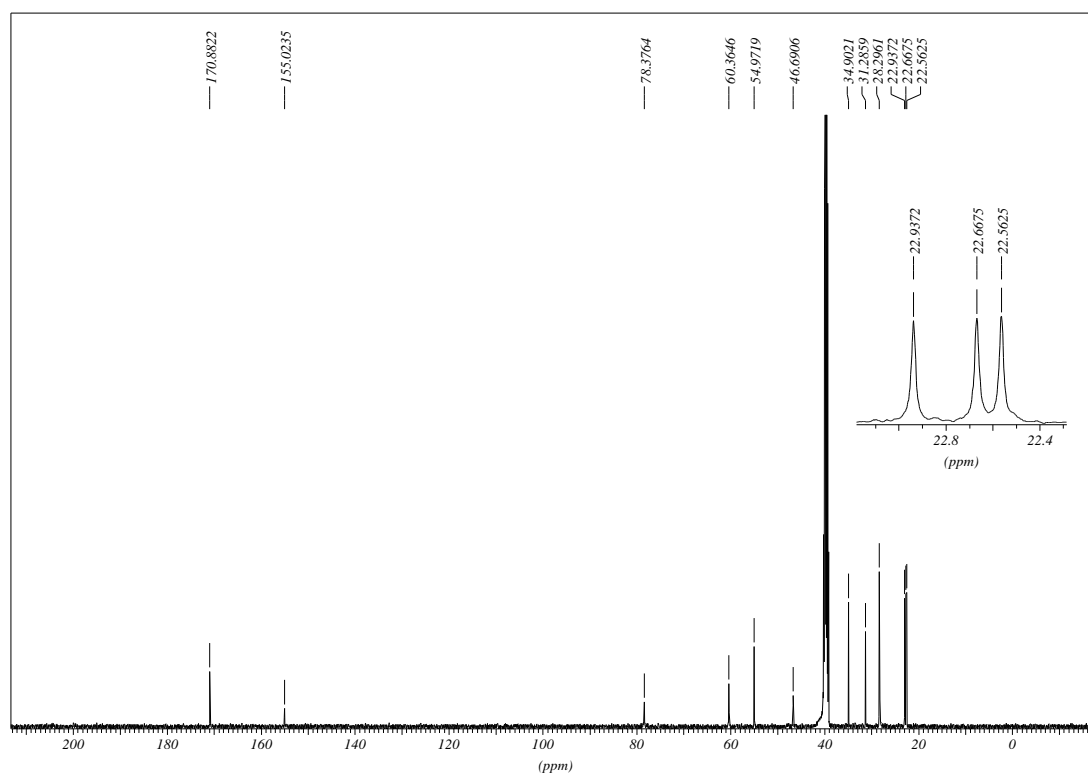
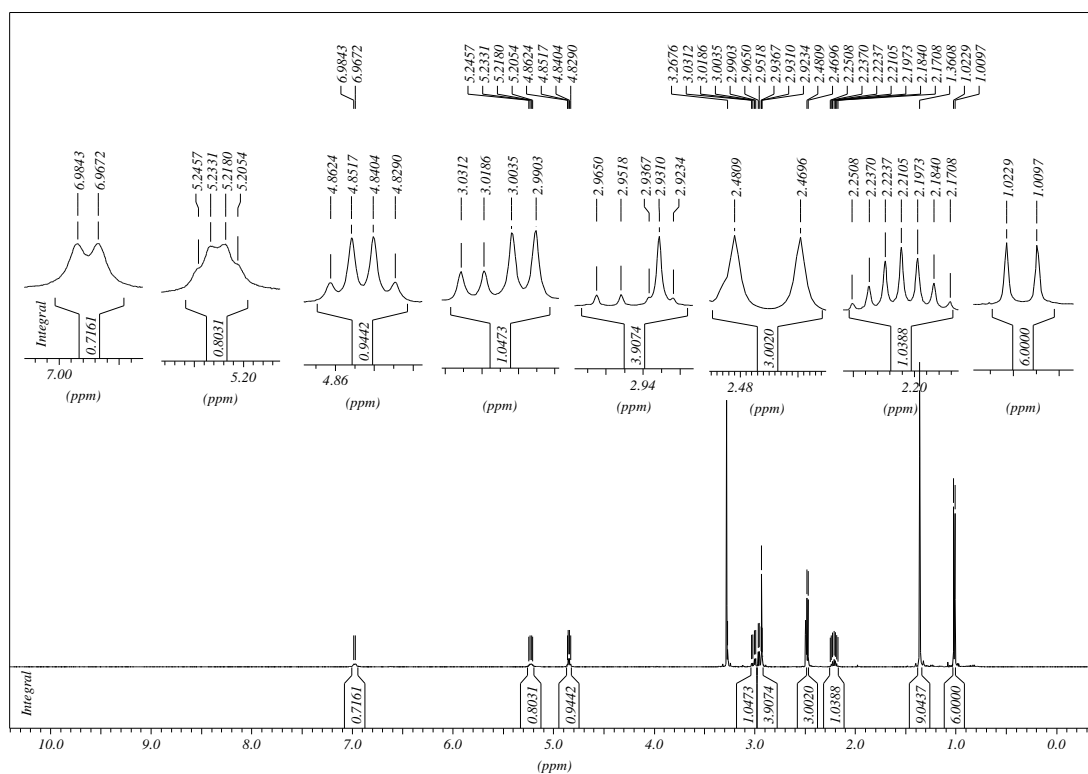
3.4.17. NMR SPECTRA OF 142



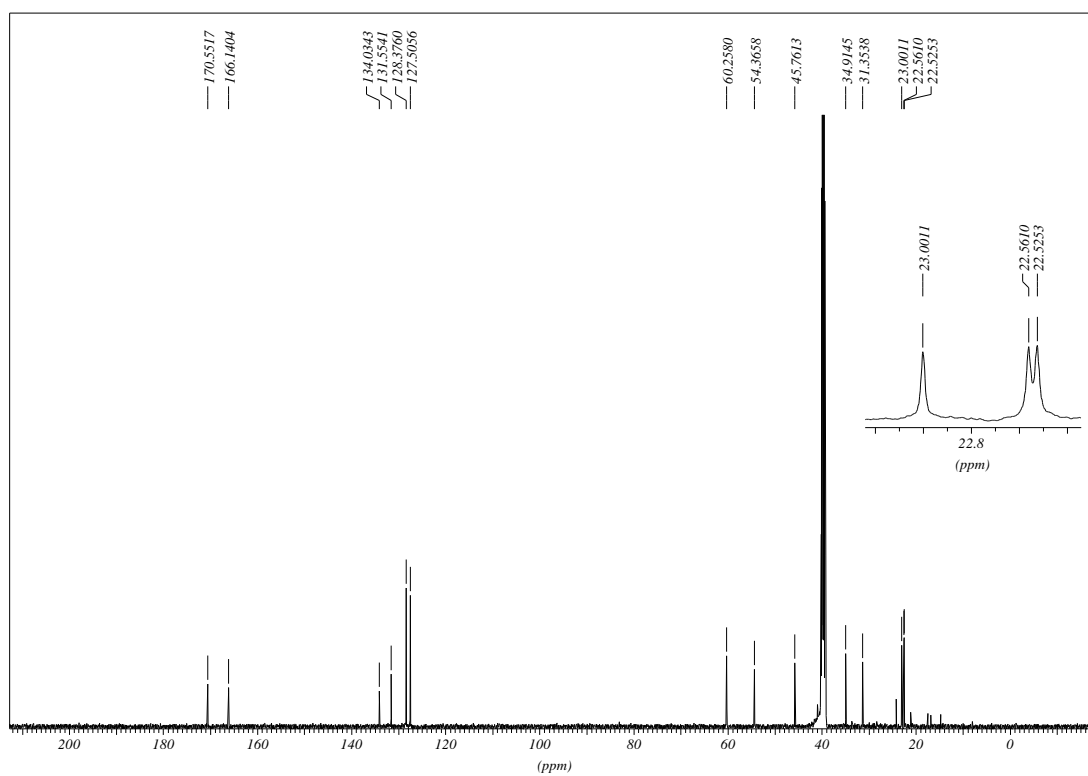
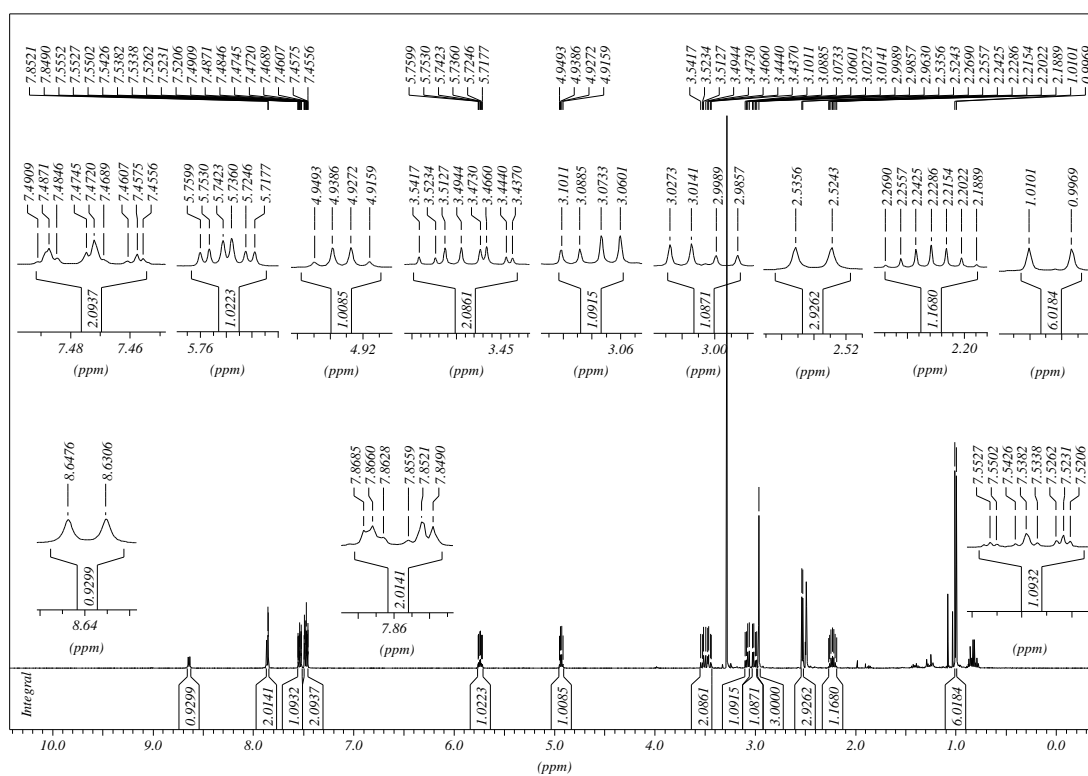
3.4.18. NMR SPECTRA OF 144



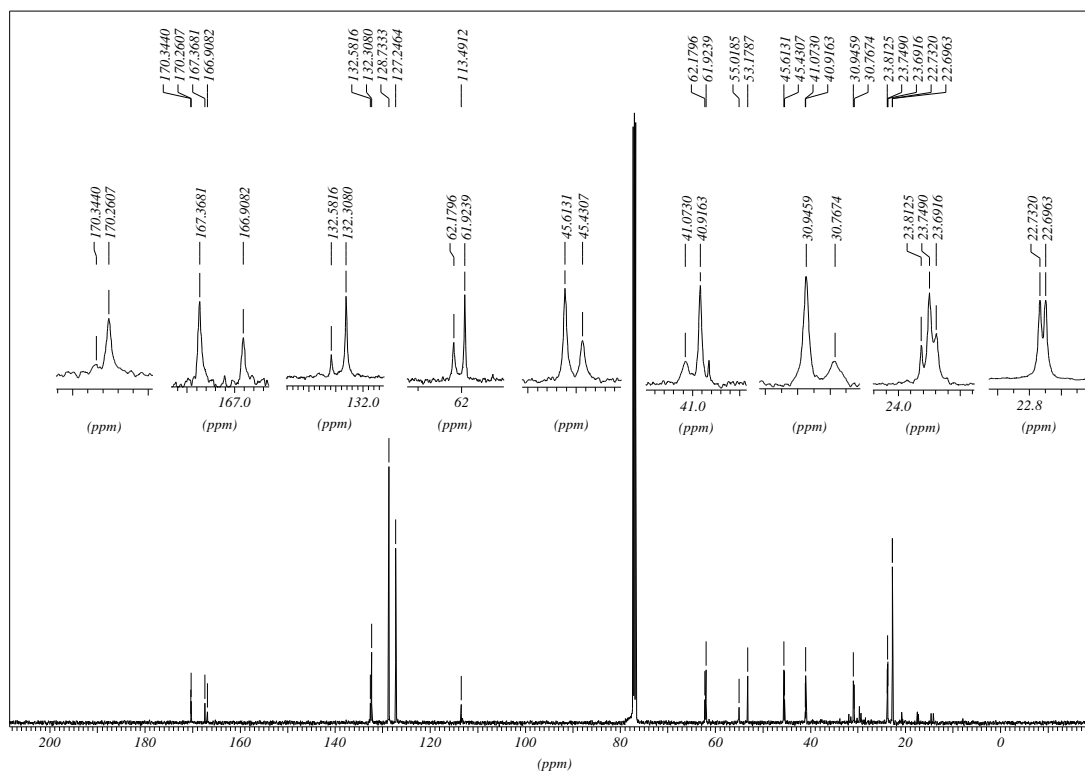
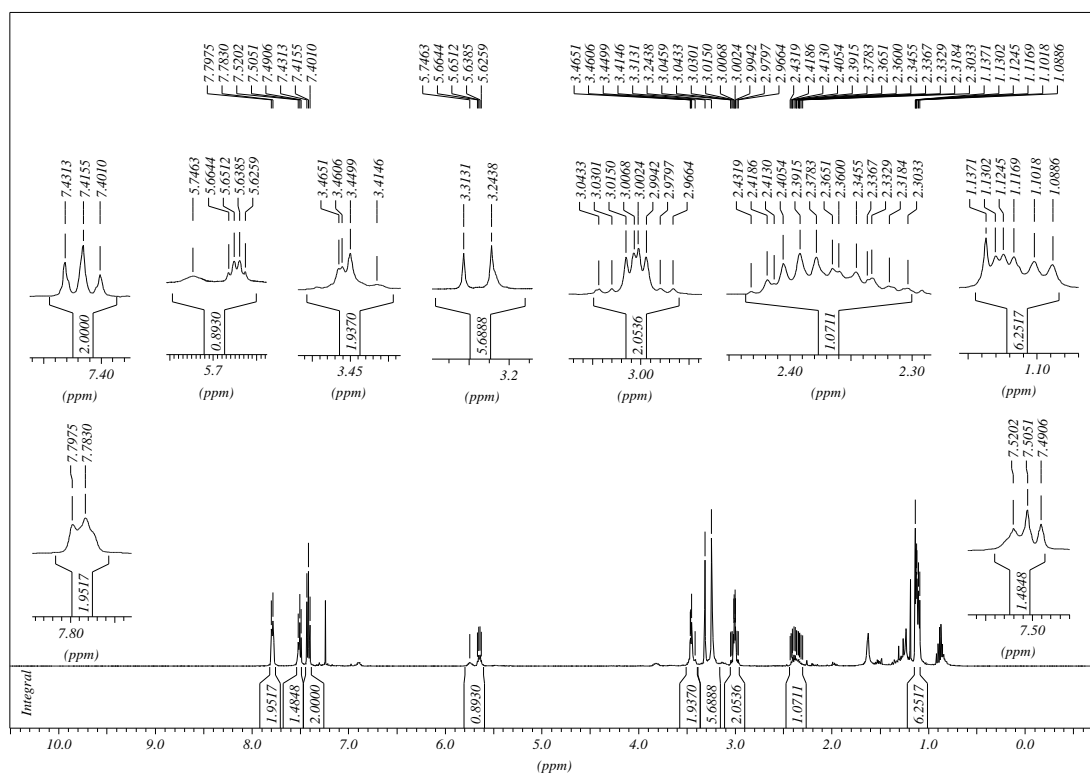
3.4.19. NMR SPECTRA OF 145



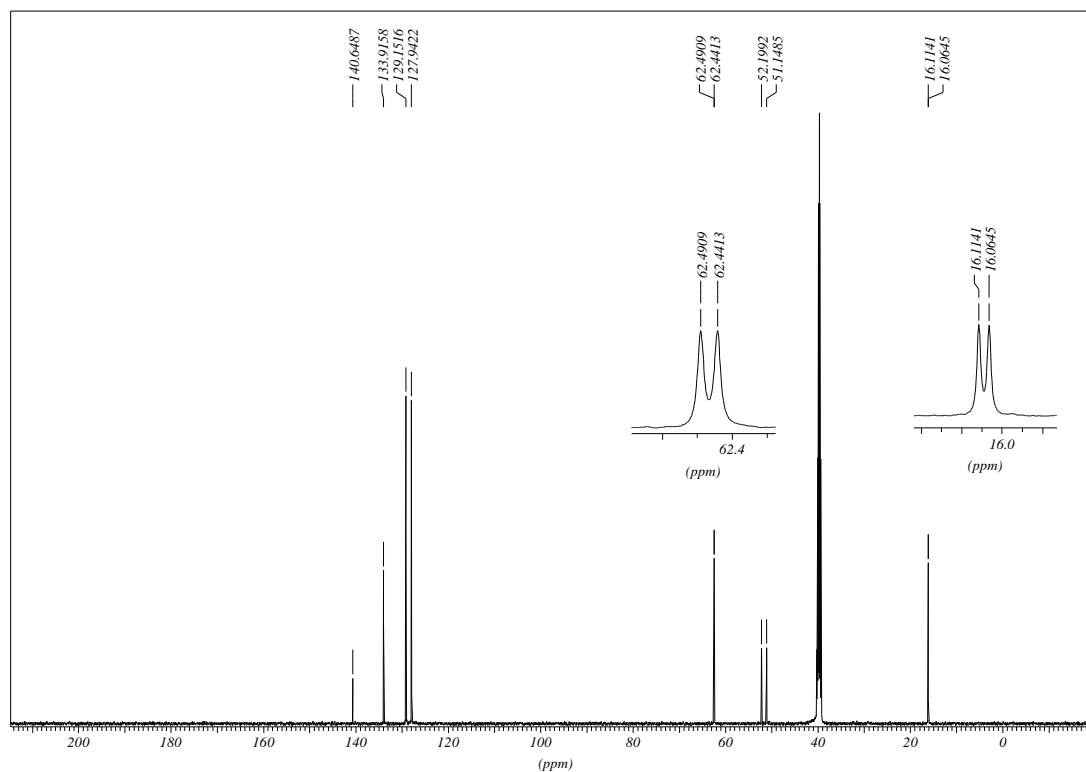
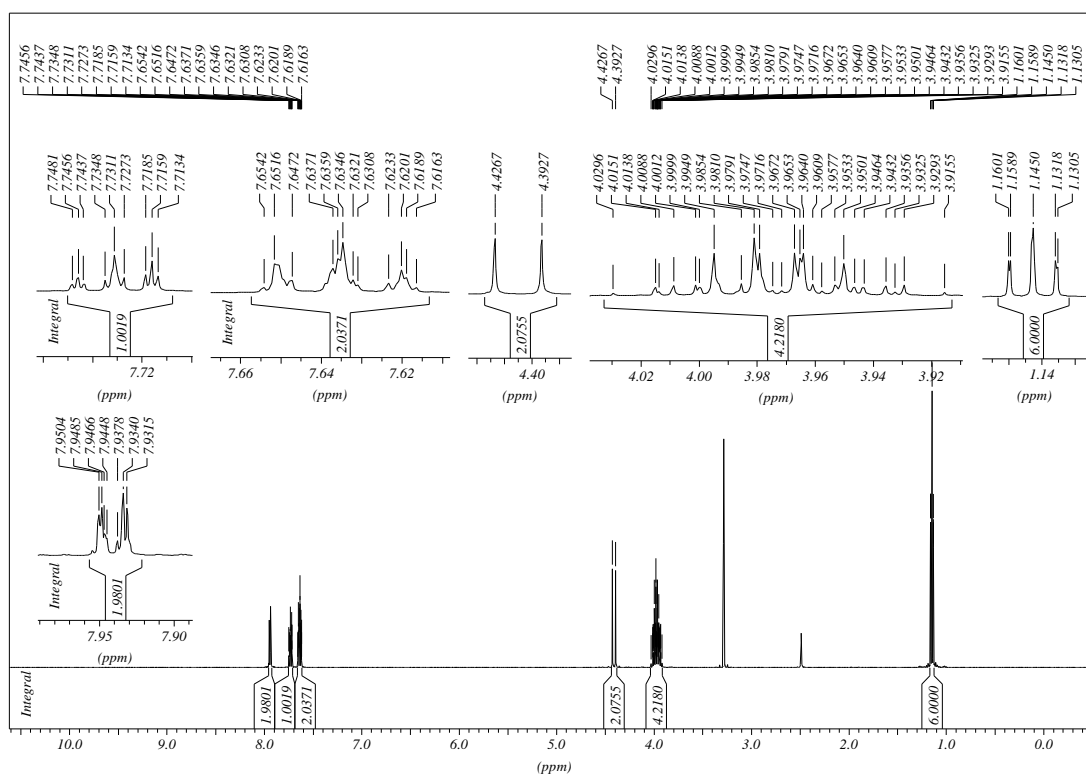
3.4.20. NMR SPECTRA OF 147



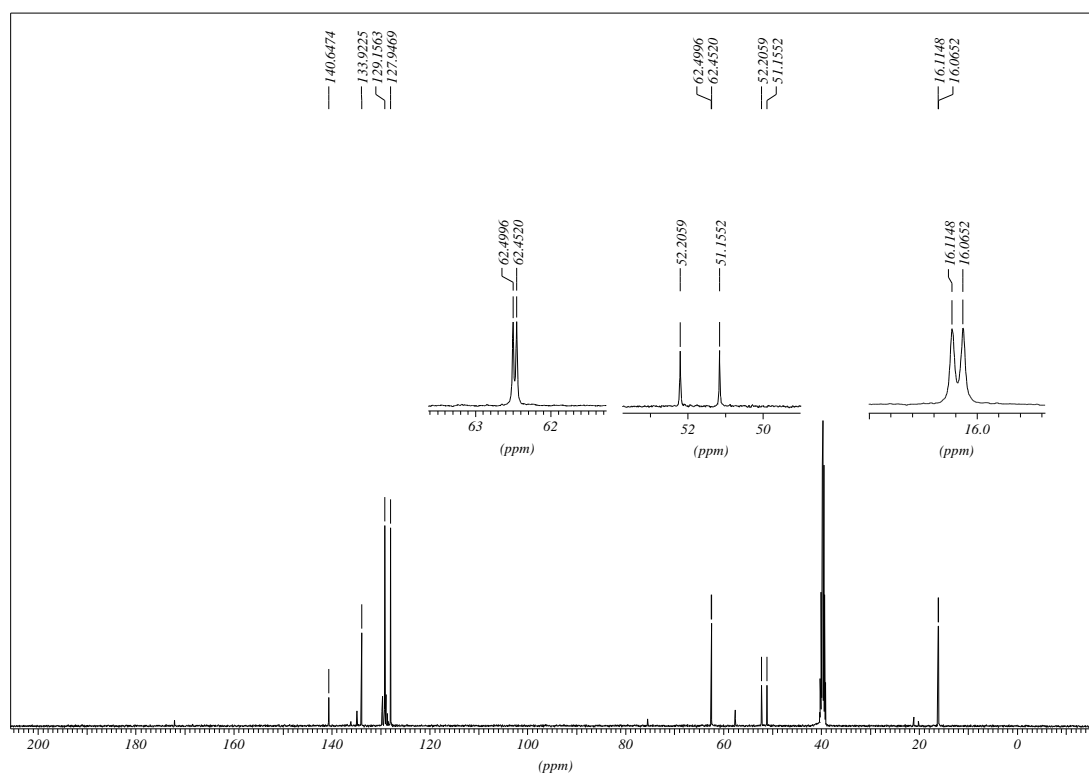
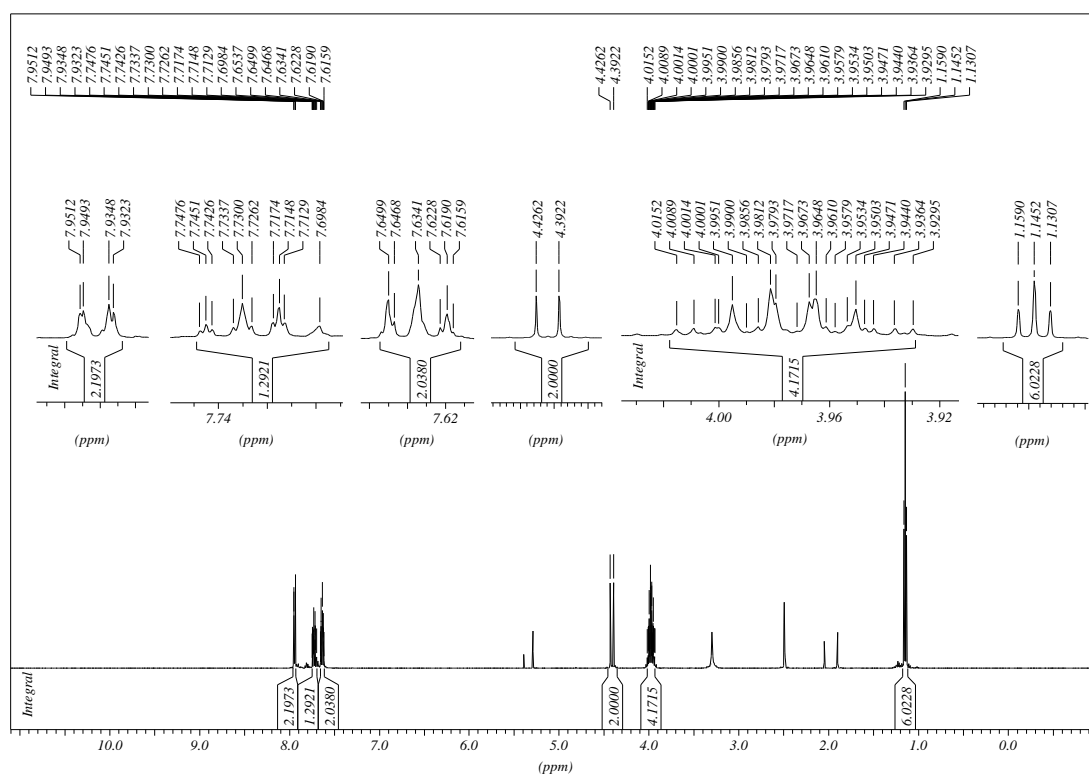
3.4.21. NMR SPECTRA OF 148



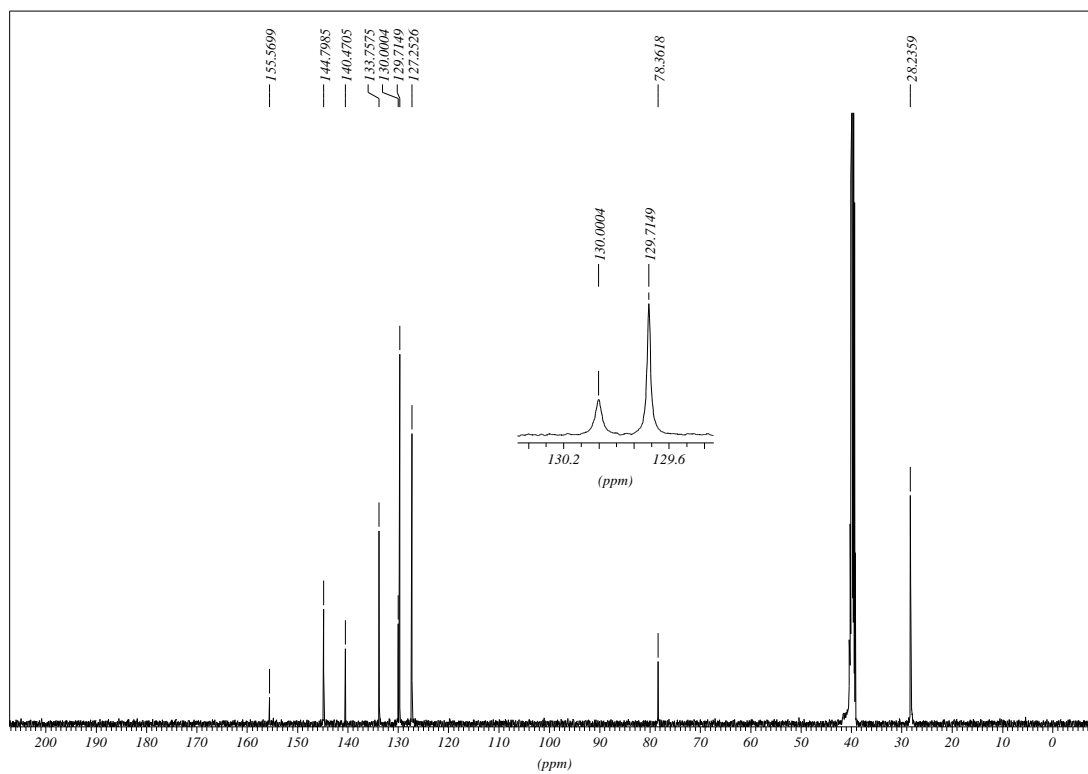
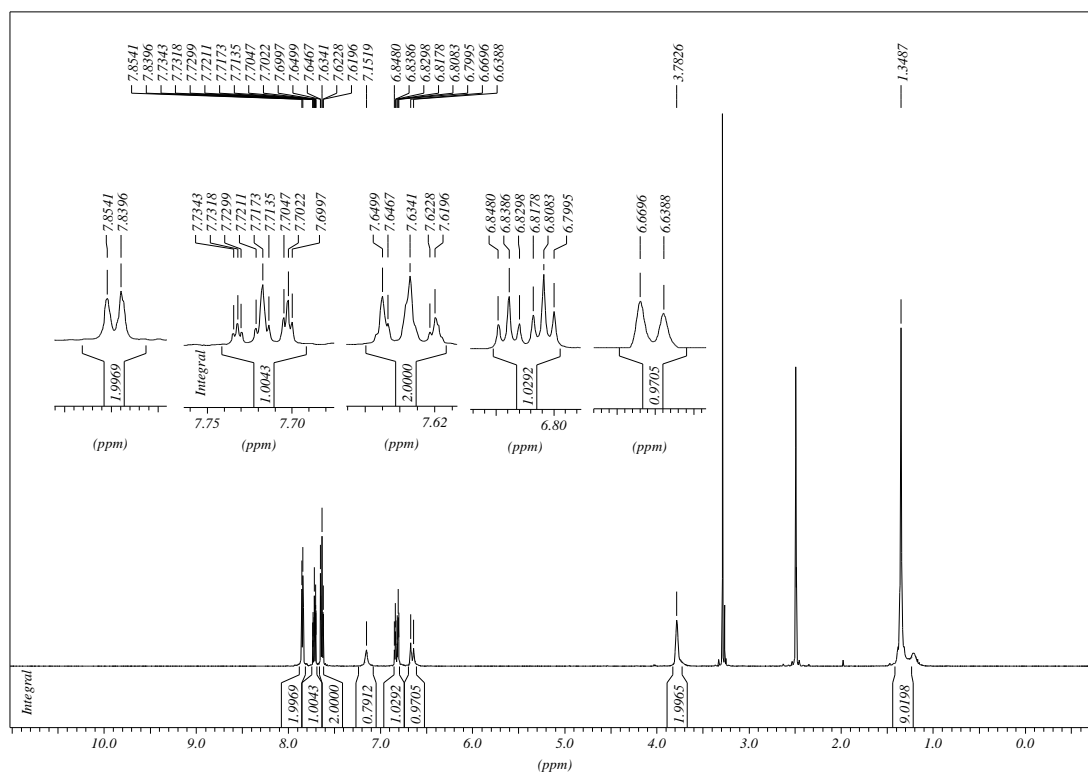
3.4.22. NMR SPECTRA OF 151 (method A)



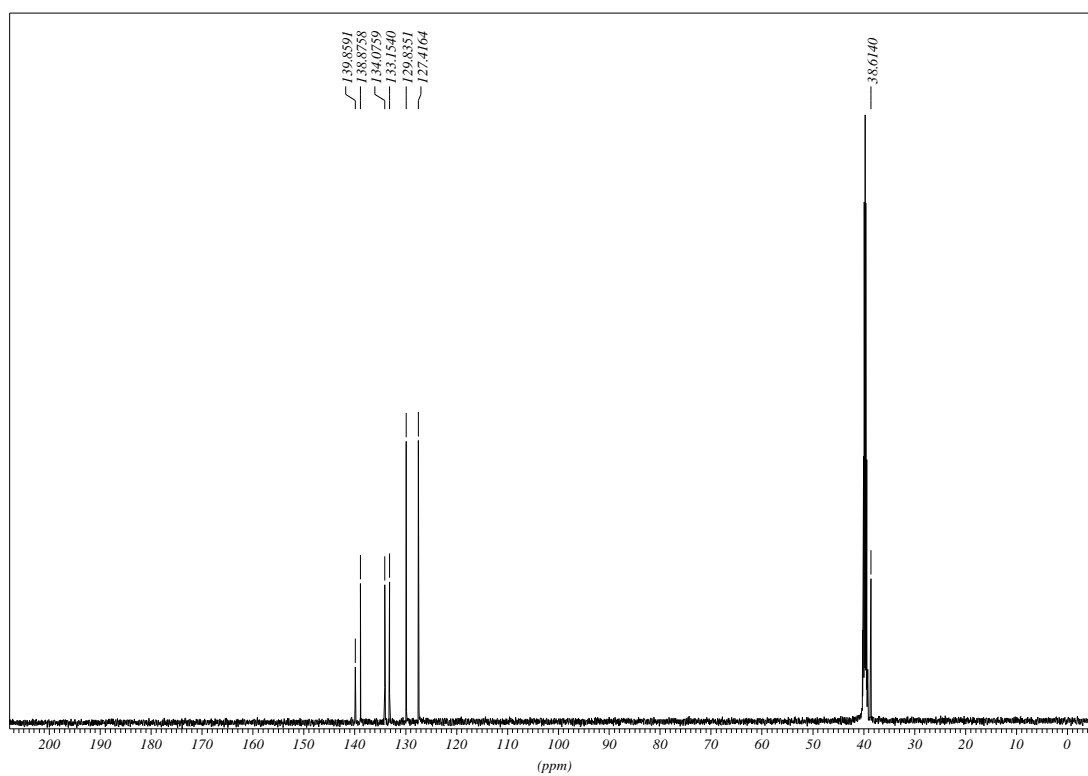
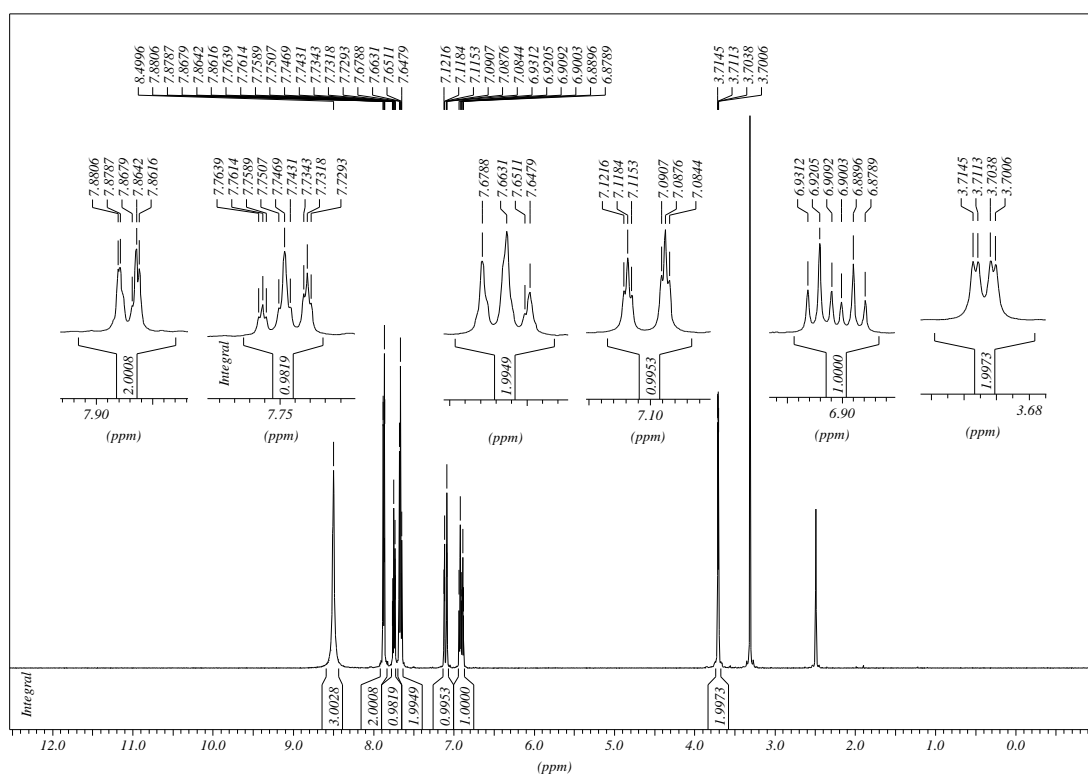
3.4.23. NMR SPECTRA OF 151 (method B)



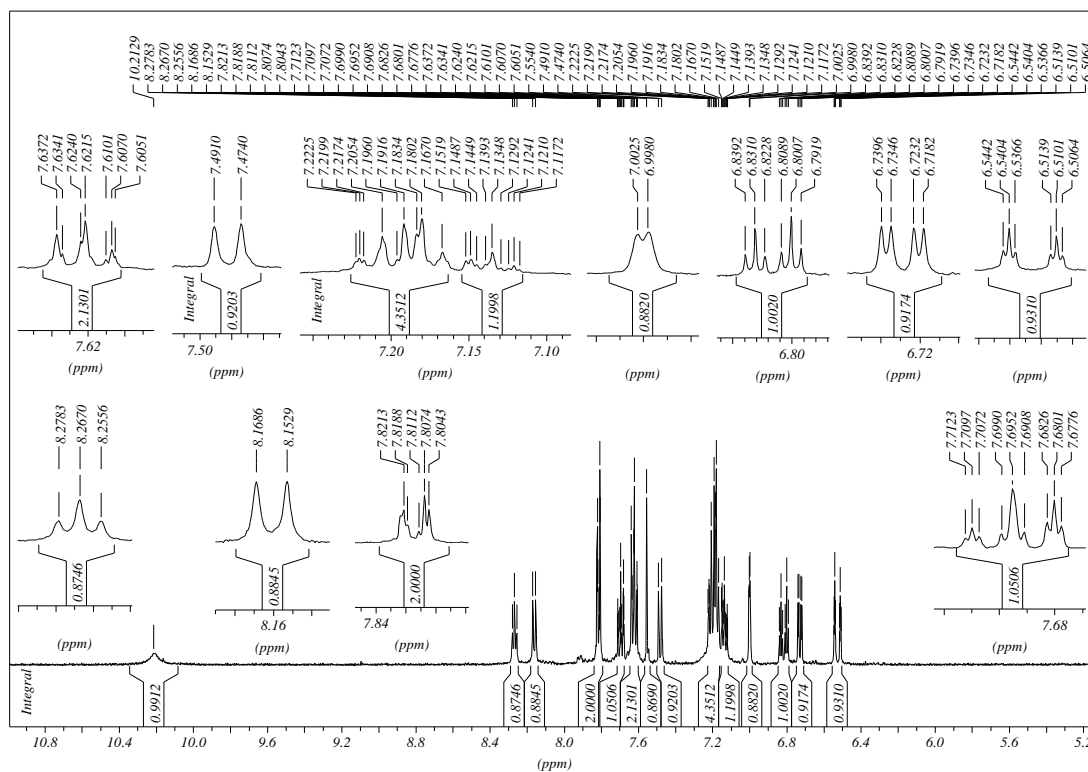
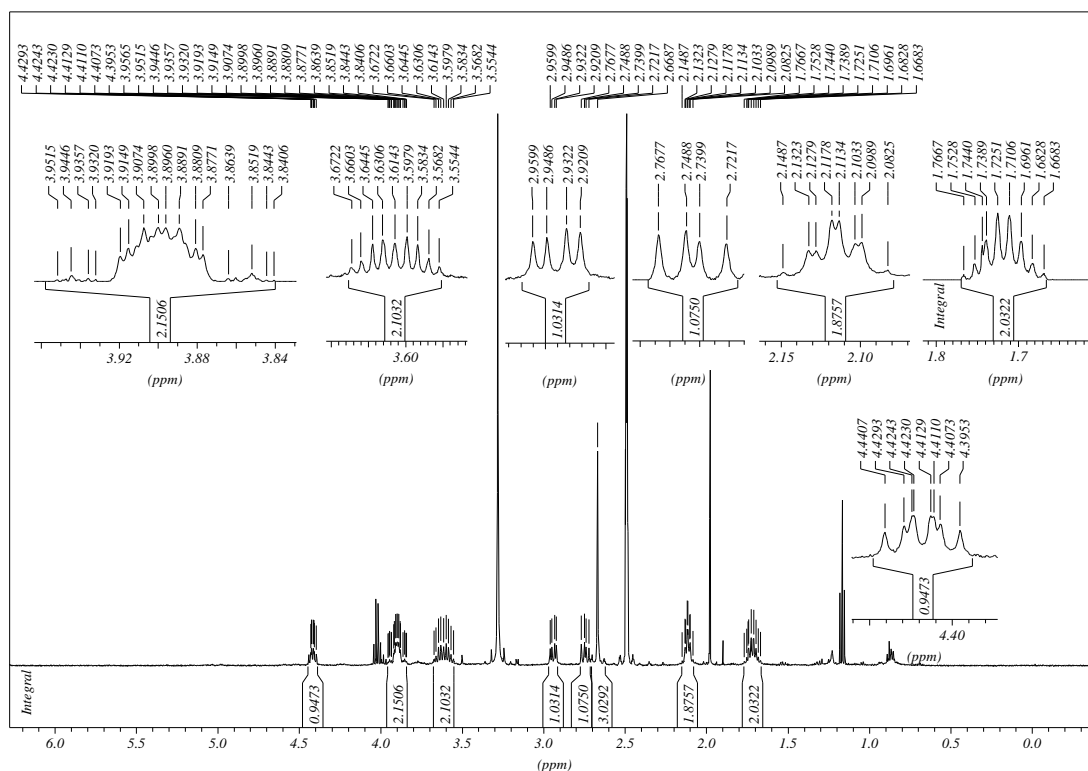
3.4.24. NMR SPECTRA OF 152

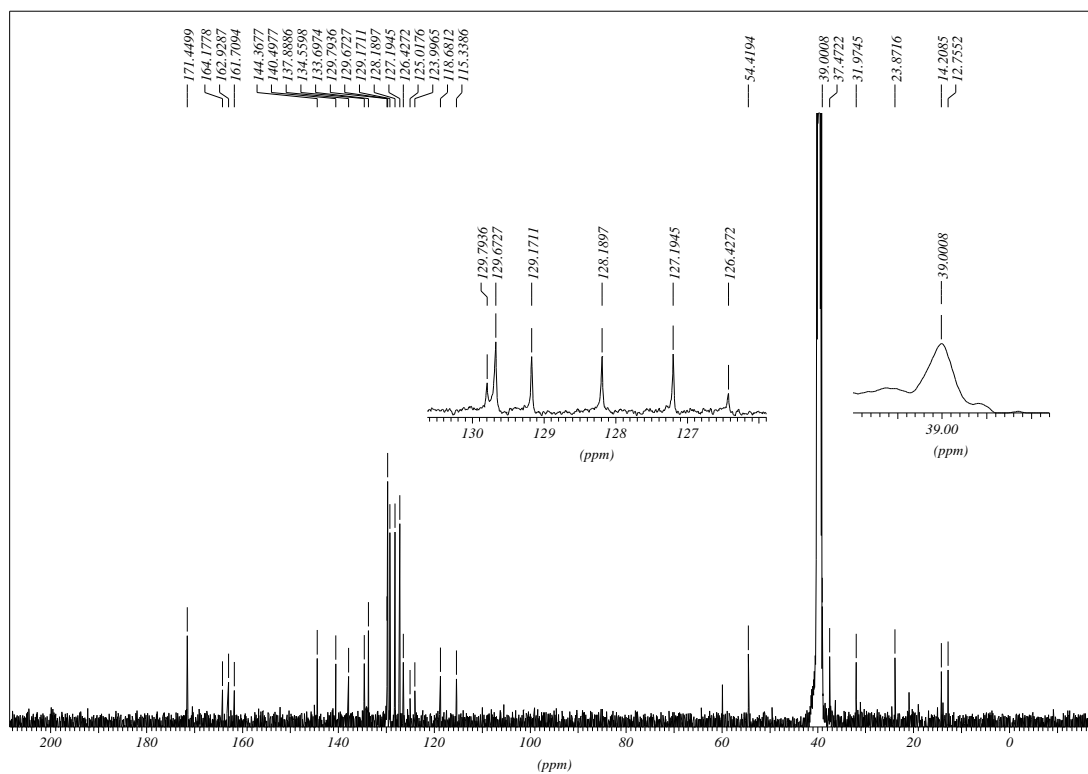


3.4.25. NMR SPECTRA OF 153

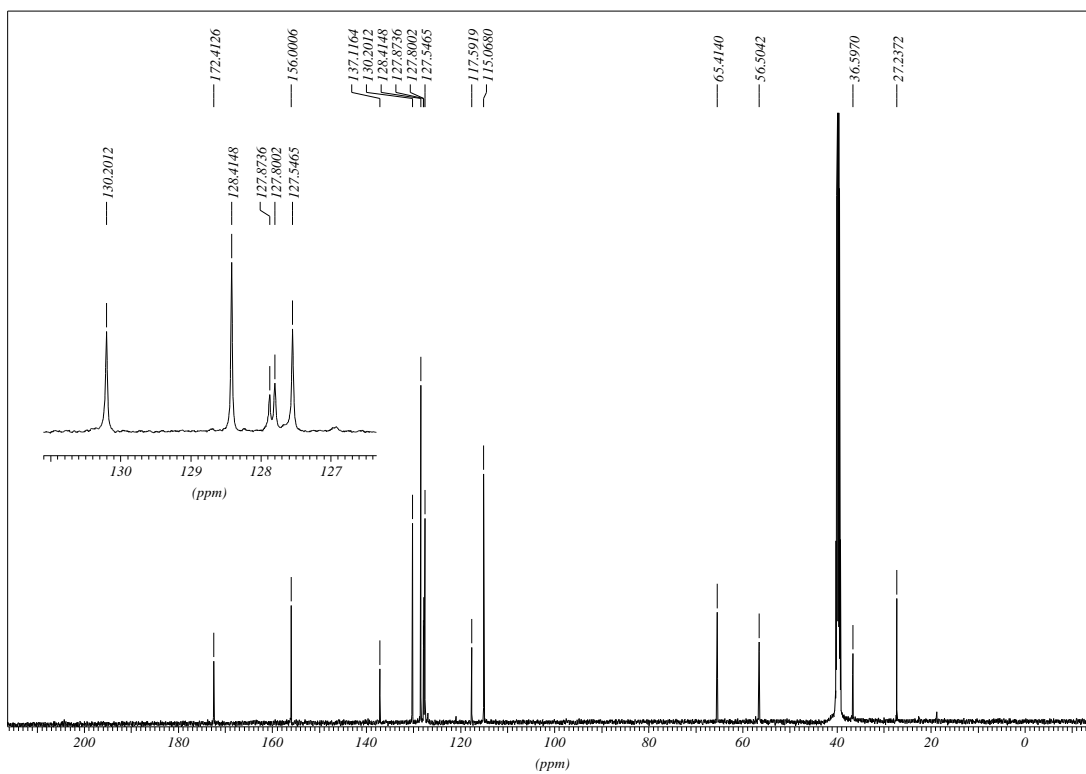
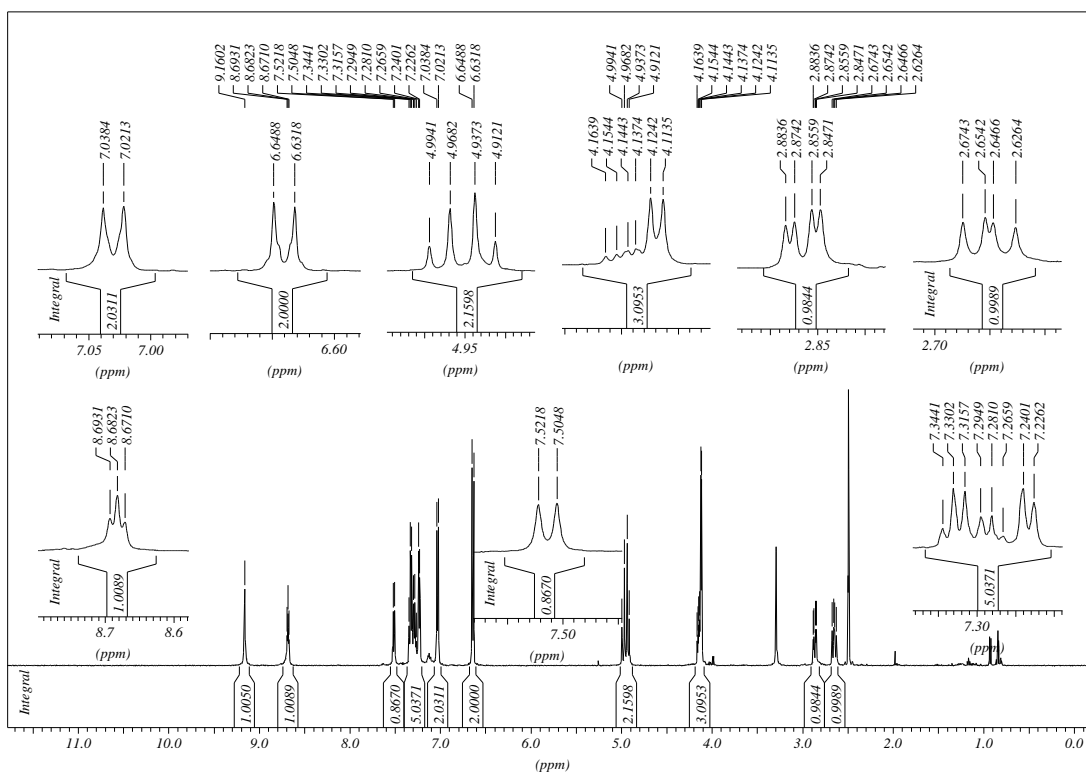


3.4.27. NMR SPECTRA OF 158

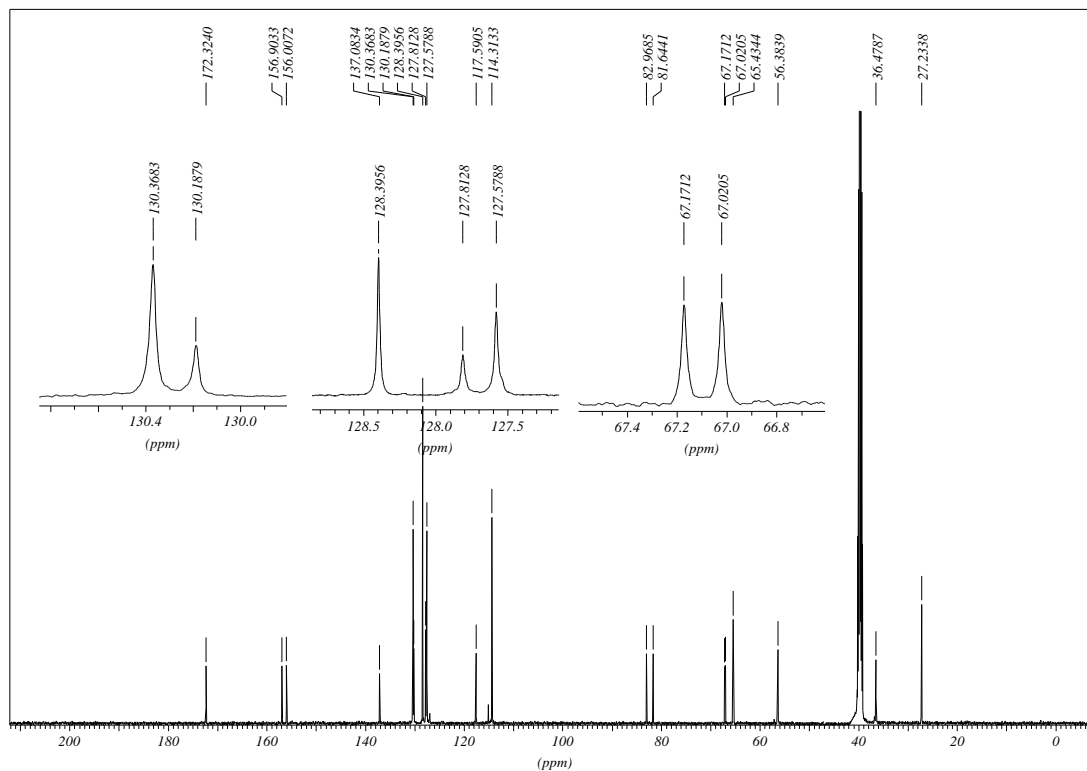
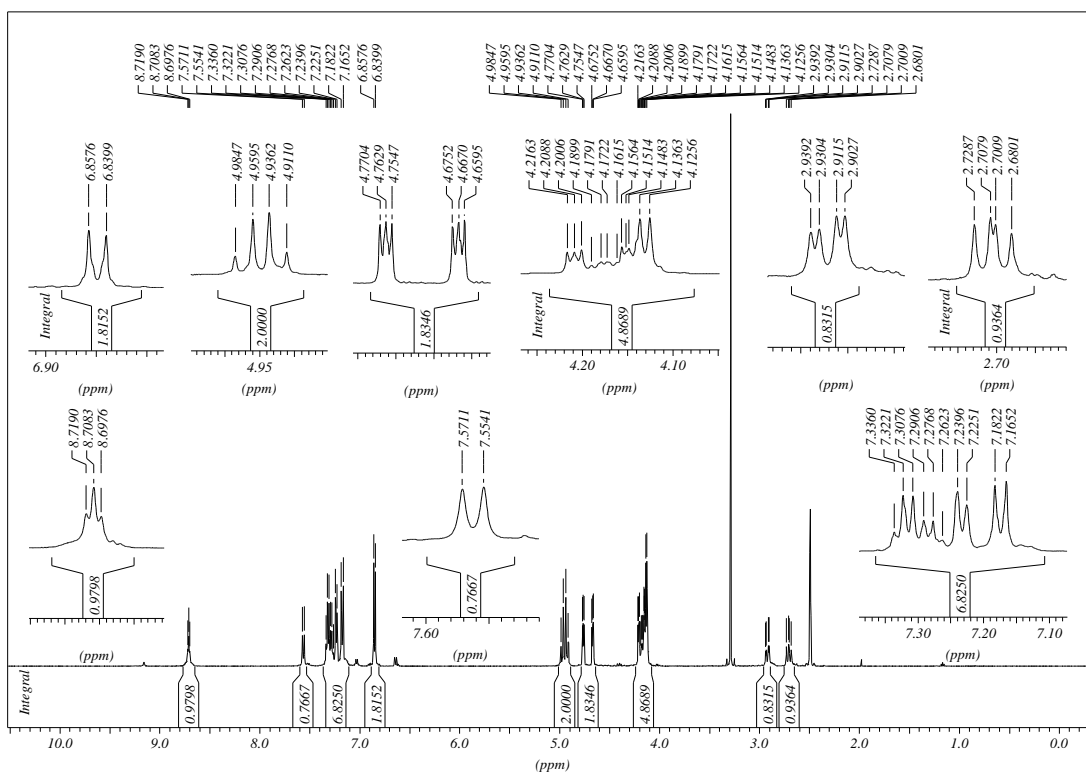




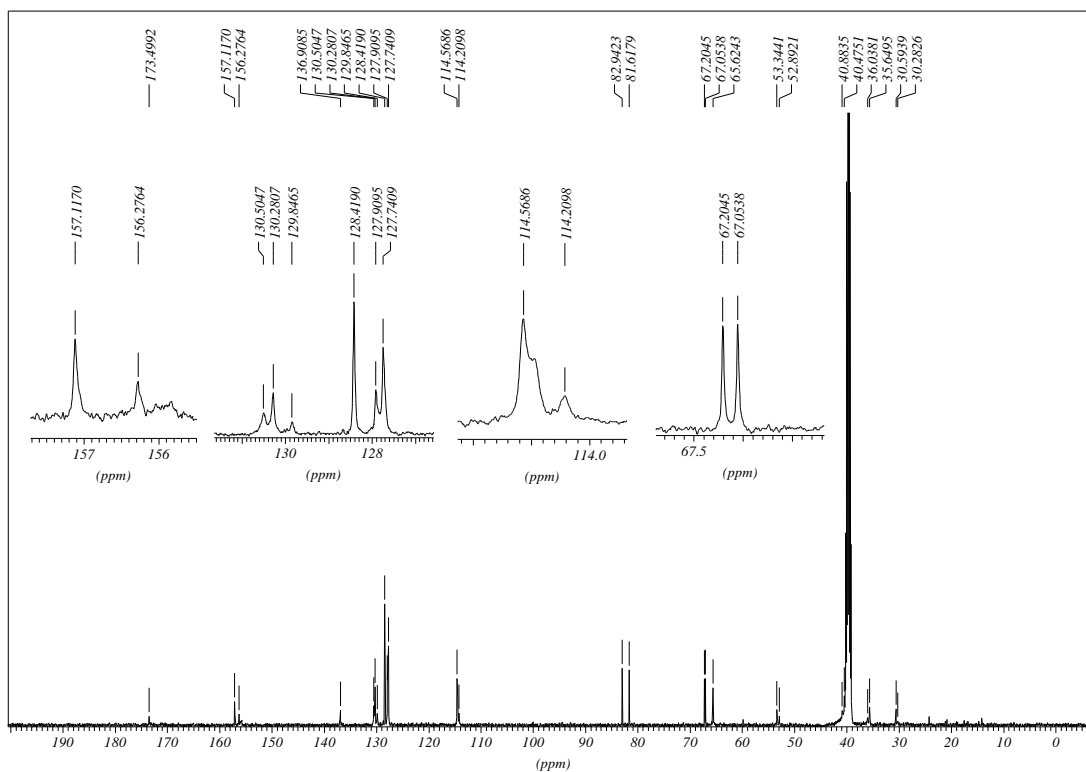
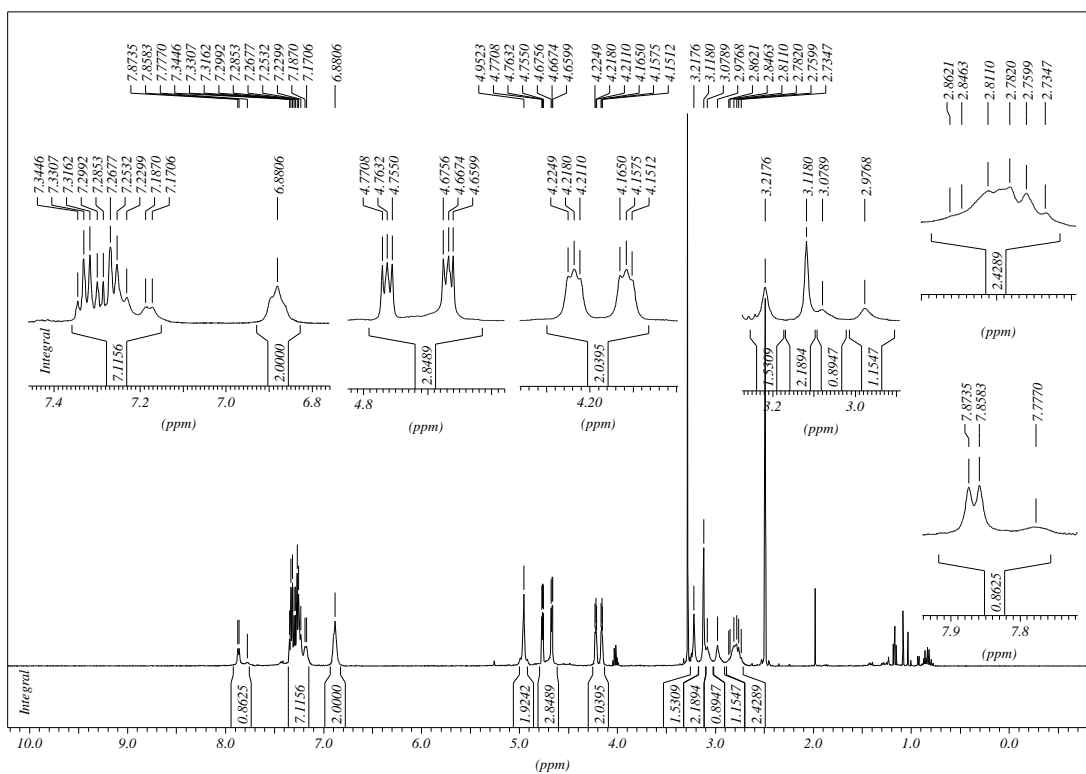
3.4.28. NMR SPECTRA OF 159



3.4.29. NMR SPECTRA OF 160



3.4.30. NMR SPECTRA OF 161



4. REFERENCES

-
- [1] López-Otín, C.; Overall, C. M. Protease degradomics: a new challenge for proteomics. *Nat. Rev. Mol. Cell Biol.*, **2002**, *3*, 509–519.
- [2] Polgar, L. *Catalytic mechanisms of cysteine peptidase*. In: Barrett, A. J.; Rawlings, N. D.; Woessner, J. F. Eds., *Handbook of Proteolytic Enzymes*, Elsevier, London, **2004**, 1072–1079.
- [3] Brix, K.; Dunkhorst, A.; Mayer, K.; Jordans, S. Cysteine cathepsins: cellular roadmap to different functions. *Biochimie.*, **2008**, *90*, 194–207.
- [4] Mort, J. S.; Buttle, D. J. Cathepsin B. *Int. J. Biochem. Cell Biol.*, **1997**, *29*, 715–720.
- [5] Ishidoh, K.; Kominami, E. Processing and activation of lysosomal proteinases. *Biol. Chem.*, **2002**, *383*, 1827–1831.
- [6] Nishimura, Y.; Kawabata, T.; Kato, K. Identification of latent procathepsins B and L in microsomal lumen: characterization of enzymatic activation and proteolytic processing *in vitro*. *Arch. Biochem. Biophys.*, **1988**, *261*, 64–71.
- [7] Kominami, E.; Tsukahara, T.; Hara, K.; Katunuma, N. Biosyntheses and processing of lysosomal cysteine proteinases in rat macrophages. *FEBS Lett.*, **1988**, *231*, 225–228.
- [8] Ménard, R.; Carmona, E.; Takebe, S.; Dufour, E.; Plouffe, C.; Mason, P.; Mort, J. S. Autocatalytic processing of recombinant human procathepsin L. Contribution of both intermolecular and unimolecular events in the processing of procathepsin L *in vitro*. *J. Biol. Chem.*, **1998**, *273*, 4478–4484.
- [9] Mach, L.; Mort, J. S.; Glössl, J. Maturation of human procathepsin B. Proenzyme activation and proteolytic processing of the precursor to the mature proteinase, *in vitro*, are primarily unimolecular processes. *J. Biol. Chem.*, **1994**, *269*, 13030–13035.
- [10] Kawabata, T.; Nishimura, Y.; Higaki, M.; Kato, K. Purification and processing of rat liver procathepsin B. *J. Biochem.*, **1993**, *113*, 389–394.
- [11] Dahl, S. W.; Halkier, T.; Lauritzen, C.; Dolenc, I.; Pedersen, J.; Turk, V.; Turk B. Human recombinant pro-dipeptidyl peptidase I (cathepsin C) can be activated by cathepsins L and S but not by autocatalytic processing. *Biochemistry*, **2001**, *40*, 1671–1678.
- [12] Dolenc, I.; Turk, B.; Pungercic, G.; Ritonja, A.; Turk, V. Oligomeric structure and substrate induced inhibition of human cathepsin C. *J. Biol. Chem.*, **1995**, *270*, 21626–21631.
- [13] Mølgaard, A.; Arnau, J.; Lauritzen, C.; Larsen, S.; Petersen, G.; Pedersen, J. The crystal structure of human dipeptidyl peptidase I (cathepsin C) in complex with the inhibitor Gly-Phe-CHN₂. *Biochem. J.*, **2007**, *401*, 645–650.

-
- [14] Drenth, J.; Jansonius, J. N.; Koekoek, R.; Swen, H. M.; Wolthers, B. G. Structure of papain. *Nature*, **1968**, *218*, 929–932.
- [15] Musil, D.; Zucić, D.; Turk, D.; Engh, R. A.; Mayr, I.; Huber, R.; Popovic, T.; Turk, V.; Towatari, T.; Katunuma, N.; Bode, W. The Refined 2.15 Å X-ray crystal structure of human liver cathepsin B: the structural basis for its specificity. *EMBO J.*, **1991**, *10*, 2321–2330.
- [16] Olsen, J. G.; Kadziola, A.; Lauritzen, C.; Pedersen, J.; Larsen, S.; Dahl, S. W. Tetrameric dipeptidyl peptidase I directs substrate specificity by use of the residual pro-part domain. *FEBS Lett.*, **2001**, *506*, 201–206.
- [17] Turk, D.; Janjić, V.; Stern, I.; Podobnik, M.; Lamba, D.; Dahl, S. W.; Lauritzen, C.; Pedersen, J.; Turk, V.; Turk, B. Structure of human dipeptidyl peptidase I (cathepsin C): exclusion domain added to an endopeptidase framework creates the machine for activation of granular serine proteases. *EMBO J.*, **2001**, *20*, 6570–6582.
- [18] Somoza, J. R.; Palmer, J. T.; Ho, J. D. The crystal structure of human cathepsin F and its implications for the development of novel immunomodulators. *J. Mol. Biol.*, **2002**, *322*, 559–568.
- [19] Gunčar, G.; Podobnik, M.; Pungercar, J.; Štrukelj, B.; Turk, V.; Turk, D. Crystal structure of porcine cathepsin H determined at 2.1 Å resolution: location of the mini-chain C-terminal carboxyl group defines cathepsin H aminopeptidase function. *Structure*, **1998**, *6*, 51–61.
- [20] Fujishima, A.; Imai, Y.; Nomura, T.; Fujisawa, Y.; Yamamoto, Y.; Sugawara, T. The crystal structure of human cathepsin L complexed with E-64. *FEBS Lett.*, **1997**, *407*, 47–50.
- [21] Gunčar, G.; Pungercar, G.; Klemenčič, I.; Turk, V.; Turk, D. Crystal structure of MHC class II-associated p41 Ii fragment bound to cathepsin L reveals the structural basis for differentiation between cathepsins L and S. *EMBO J.*, **1999**, *18*, 793–803.
- [22] McGrath, M. E.; Klaus, J. L.; Barnes, M. G.; Brömme, D. Crystal structure of human cathepsin K complexed with a potent inhibitor. *Nat. Struct. Biol.*, **1997**, *4*, 105–109.
- [23] Zhao, B.; Janson, C. A.; Amegadzie, B. Y.; D'Alessio, K.; Griffin, C.; Hanning, C. R.; Jones, C.; Kurdyla, J.; McQueney, M.; Qiu, X.; Smith, W. W.; Abdel-Meguid, S. S. Crystal structure of human osteoclast cathepsin K complex with E-64. *Nat. Struct. Biol.*, **1997**, *4*, 109–111.
- [24] McGrath, M. E.; Palmer, J. T.; Brömme, D.; Somoza, J. R. Crystal Structure of human cathepsin S. *Protein Sci.*, **1998**, *7*, 1294–1302.

- [25] Turkenburg, J. P.; Lamers, M. B.; Brzozowski, A. M.; Wright, L. M.; Hubbard, R. E.; Sturt, S. L.; Williams, D. H. Structure of a Cys25→Ser mutant of human cathepsin S. *Acta Crystallogr. D Biol. Crystallogr.*, **2002**, *58*, 451–455.
- [26] Pauly, T. A.; Sulea, T.; Ammirati, M.; Sivaraman, J.; Danley, D. E.; Griffor, M. C.; Kamath, A. V.; Wang, I. K.; Laird, E. R.; Seddon, A. P.; Ménard, R.; Cygler, M.; Rath, V. L. Specificity determinants of human cathepsin S revealed by crystal structures of complexes. *Biochemistry*, **2003**, *42*, 3203–3213.
- [27] Somoza, J. R.; Zhan, H.; Bowman, K. K.; Yu, L.; Mortara, K. D.; Palmer, J. T.; Clark, J. M.; McGrath, M. E. Crystal structure of human cathepsin V. *Biochemistry*, **2000**, *39*, 12543–12551.
- [28] Gunčar, G.; Klemenčič, I.; Turk, B.; Turk, V.; Karaoglanovic-Carmona, A.; Juliano, L.; Turk, D. Crystal structure of cathepsin X: a flip-flop of the ring of His23 allows carboxy-monopeptidase and carboxy-dipeptidase activity of the protease. *Structure*, **2000**, *8*, 305–313.
- [29] Turk, D.; Gunčar, G. Lysosomal cysteine proteases (cathepsins): promising drug targets. *Acta Crystallogr. D Biol. Crystallogr.*, **2003**, *59*, 203–213.
- [30] Cygler, M.; Sivaraman, J.; Grochulski, P.; Coulombe, R.; Storer, A. C.; Mort, J. S. Structure of procathepsin B. Model for inhibition of cysteine protease activity by the proregion. *Structure*, **1996**, *4*, 405–416.
- [31] Coulombe, R.; Grochulski, P.; Sivaraman, J.; Ménard, R.; Mort, J. S.; Cygler, M. Structure of human procathepsin L reveals the molecular basis of inhibition by the prosegment. *EMBO J.*, **1996**, *15*, 5492–5503.
- [32] Cygler, M.; Mort, J. S. Proregion structure of members of the papain superfamily. Mode of inhibition of enzymatic activity. *Biochimie*, **1997**, *79*, 645–652.
- [33] Turk, B.; Turk, D.; Turk, V. Lysosomal cysteine proteases: more than scavengers. *Biochim. Biophys. Acta*, **2000**, *1477*, 98–111.
- [34] Guay, J.; Falguyret, J. P.; Ducret, A.; Percival, M. D.; Mancini, J. A. Potency and selectivity of inhibition of cathepsin K, L and S by their respective propeptides. *Eur. J. Biochem.*, **2000**, *267*, 6311–6318.
- [35] Tyndall, J.; Nall, T.; Fairlie, D. P. Proteases Universally Recognize Beta Strands In Their Active Sites. *Chem. Rev.*, **2005**, *105*, 973–999.
- [36] Schechter, I.; Berger, A. On the Size of the Active Site in Proteases. I. Papain *Biochem. Biophys. Res. Commun.*, **1967**, *27*, 157–162.

-
- [37] Turk, D.; Gunčar, G. Lysosomal cysteine proteases (cathepsins): promising drug targets. *Acta Crystallogr. D Biol. Crystallogr.*, **2003**, *59*, 203–213.
- [38] Turk, D.; Podobnik, M.; Kuhelj, R.; Dolinar, M.; Turk, V. Crystal structures of human procathepsin B at 3.2 and 3.3 Angstroms resolution reveal an interaction motif between a papain-like cysteine protease and its propeptide. *FEBS Lett.*, **1996**, *384*, 211–214.
- [39] Turk, V.; Turk, B.; Turk, D. Lysosomal cysteine proteases: facts and opportunities. *EMBO J.*, **2001**, *20*, 4629–4633.
- [40] Sivaraman, J.; Nägler, D. K.; Zhang, R.; Ménard, R.; Cygler, M. Crystal structure of human procathepsin X: a cysteine protease with the proregion covalently linked to the active site cysteine. *J. Mol. Biol.*, **2000**, *295*, 939–951.
- [41] Nägler, D. K.; Zhang, R.; Tam, W.; Sulea, T.; Purisima, E. O.; Ménard, R. Human cathepsin X: a cysteine protease with unique carboxypeptidase activity. *Biochemistry*, **1999**, *38*, 12648–12654.
- [42] Klemenčič, I.; Carmona, A. K.; Cezari, M. H.; Juliano, M. A.; Juliano, L.; Gunčar, G.; Turk, D.; Križaj, I.; Turk, V.; Turk, B. Biochemical characterization of human cathepsin X revealed that the enzyme is an exopeptidase, acting as carboxymonopeptidase or carboxydipeptidase. *Eur. J. Biochem.*, **2000**, *267*, 5404–5412.
- [43] Chapman, H. A.; Riese, R. J.; Shi, G. P. Emerging roles for cysteine proteases in human biology. *Annu. Rev. Physiol.*, **1997**, *59*, 63–88.
- [44] Pisoni, R. L.; Acker, T. L.; Lisowski, K. M.; Lemons, R. M.; Thoene, J. G. A cysteine-specific lysosomal transport system provides a major route for the delivery of thiol to human fibroblast lysosomes: possible role in supporting lysosomal proteolysis. *J. Cell Biol.*, **1990**, *110*, 327–335.
- [45] Turk, V.; Stoka, V.; Turk, D. Cystatins: biochemical and structural properties, and medical relevance. *Front. Biosci.*, **2008**, *13*, 5406–5420.
- [46] Deussing, J.; Roth, W.; Saftig, P.; Peters, C.; Ploegh, H. L.; Villadangos, J. A. Cathepsins B and D are dispensable for major histocompatibility complex class II-mediated antigen presentation. *Proc. Natl. Acad. Sci. USA*, **1998**, *95*, 4516–4521.
- [47] Nakagawa, T.; Roth, W.; Wong, P.; Nelson, A.; Farr, A.; Deussing, J.; Villadangos, J. A.; Ploegh, H.; Peters, C.; Rudensky, A. Y. Cathepsin L: Critical role in Ii degradation and CD4 T cell selection in the thymus. *Science*, **1998**, *280*, 394–395.

-
- [48] Saftig, P.; Hunziker, E.; Wehmeyer, O.; Jones, S.; Boyde, A.; Rommerskirch, W.; Moritz, J. D.; Schu, P.; von Figura, K. Impaired osteoclastic bone resorption leads to osteopetrosis in cathepsin-K-deficient mice. *Proc. Natl. Acad. Sci. USA*, **1998**, *95*, 13453–13458.
- [49] Shi, G. P.; Villadangos, J. A.; Dranoff, G.; Small, C.; Gu, L.; Haley, K. J.; Riese, R.; Ploegh, H. L.; Chapman, H. A. Cathepsin S is required for normal MHC class II peptide loading and germinal center development. *Immunity*, **1999**, *10*, 197–206.
- [50] Pham, C. T.; Ley, T. J. Dipeptidyl peptidase I is required for the processing and activation of granzymes A and B *in vivo*. *Proc. Natl. Acad. Sci. USA*, **1999**, *96*, 8627–8632.
- [51] Roth, W.; Deussing, J.; Botchkarev, V. A.; Pauly-Evers, M.; Saftig, P.; Hafner, A.; Schmidt, P.; Schmahl, W.; Scherer, J.; Anton-Lamprecht, I.; von Figura, K.; Paus, R.; Peters, C. Cathepsin L deficiency as molecular defect of furless: hyperproliferation of keratinocytes and perturbation of hair follicle cycling. *FASEB J.* **2000**, *14*, 2075–2086.
- [52] Nägler, D. K.; Ménard, R. Family C1 cysteine proteases: biological diversity or redundancy? *Biol. Chem.*, **2003**, *384*, 837–843.
- [53] Kirschke, H.; Wiederanders, B.; Brömme, D.; Rinne, A. Cathepsin S from bovine spleen. Purification, distribution, intracellular localization and action on proteins. *Biochem. J.*, **1989**, *264*, 467–473.
- [54] Brömme, D.; Li, Z.; Barnes, M.; Mehler, E. Human cathepsin V functional expression, tissue distribution, electrostatic surface potential, enzymatic characterization, and chromosomal localization. *Biochemistry*, **1999**, *38*, 2377–2385.
- [55] Brömme, D.; Okamoto, K.; Wang, B. B.; Biroc, S. Human cathepsin O2, a matrix protein degrading cysteine protease expressed in osteoclasts. Functional expression of human cathepsin O2 in *Spodoptera frugiperda* and characterization of the enzyme. *J. Biol. Chem.*, **1996**, *271*, 2126–2132.
- [56] Brix, K.; Lemansky, P.; Herzog, V. Evidence for extracellularly acting cathepsins mediating thyroid hormone liberation in thyroid epithelial cells. *Endocrinology*, **1996**, *137*, 1963–1974.
- [57] Andrews, N. W. Regulated secretion of conventional lysosomes. *Trends Cell. Biol.*, **2000**, *10*, 316–321.
- [58] Reinheckel, T.; Deussing, J.; Roth, W.; Peters, C. Towards specific functions of lysosomal cysteine peptidases: phenotypes of mice deficient for cathepsin B or cathepsin L. *Biol. Chem.*, **2001**, *382*, 735–741.

-
- [59] Büth, H.; Buttigieg, P. L.; Ostafe, R.; Rehders, M.; Dannenmann, S. R.; Schaschke, N.; Stark, H. -J.; Boukamp, P.; Brix, K. Cathepsin B is essential for regeneration of scratch-wounded normal human epidermal keratinocytes. *Eur. J. Cell Biol.*, **2007**, *86*, 747–761.
- [60] Obermajer, N.; Jevnikar, Z.; Doljak, B.; Kos, J. Role of cysteine cathepsins in matrix degradation and cell signalling. *Connect. Tissue Res.*, **2008**, *49*, 193–196.
- [61] Guicciardi, M. E.; Deussing, J.; Miyoshi, H.; Bronk, S. F.; Svingen, P. A.; Peters, C.; Kaufmann, S. H.; Gores, G. J. Cathepsin B contributes to TNF- α -mediated hepatocyte apoptosis by promoting mitochondrial release of cytochrome c. *J. Clin. Invest.*, **2000**, *106*, 1127–1137.
- [62] Cirman, T.; Oresić, K.; Mazovec, G. D.; Turk, V.; Reed, J. C.; Myers, R. M.; Salvesen, G. S.; Turk, B. Selective disruption of lysosomes in HeLa cells triggers apoptosis mediated by cleavage of Bid by multiple papain-like lysosomal cathepsins. *J. Biol. Chem.*, **2004**, *279*, 3578–3587.
- [63] Stoka, V.; Turk, V.; Turk, B. Lysosomal cysteine cathepsins: signaling pathways in apoptosis. *Biol. Chem.*, **2007**, *388*, 555–360.
- [64] Conus, S.; Simon, H. U. Cathepsins: key modulators of cell death and inflammatory responses. *Biochem. Pharmacol.*, **2008**, *76*, 1374–1382.
- [65] Halangk, W.; Lerch, M. M.; Brandt-Nedelev, B.; Roth, W.; Ruthenbueger, M.; Reinheckel, T.; Domschke, W.; Lippert, H.; Peters, C.; Deussing, J. Role of cathepsin B in intracellular trypsinogen activation and the onset of acute pancreatitis. *J. Clin. Invest.*, **2000**, *106*, 773–781.
- [66] Friedrichs, B.; Tepel, C.; Reinheckel, T.; Deussing, J.; von Figura, K.; Herzog, V.; Peters, C.; Saftig, P.; Brix, K. Thyroid functions of mouse cathepsins B, K, and L. *J. Clin. Invest.*, **2003**, *111*, 1733–1745.
- [67] Felbor, U.; Kessler, B.; Mothes, W.; Goebel, H. H.; Ploegh, H. L.; Bronson, R. T.; Olsen, B. R. Neuronal loss and brain atrophy in mice lacking cathepsins B and L. *Proc. Natl. Acad. Sci. USA*, **2002**, *99*, 7883–7888.
- [68] Brömme, D.; Okamoto, K. Human cathepsin O2, a novel cysteine protease highly expressed in osteoclastomas and ovary. Molecular cloning, sequencing and tissue distribution. *Biol. Chem. Hoppe Seyler*, **1995**, *376*, 379–384.
- [69] Inaoka, T.; Bilbe, B.; Ishibashi, O.; Tezuka, K.; Kumegawa, M.; Kokubo, T. Molecular cloning of human cDNA for cathepsin K: novel cysteine proteinase predominantly expressed in bone. *Biochem. Biophys. Res. Comm.*, **1995**, *206*, 89–96.

- [70] Bühling, F.; Gerber, A.; Häckel, C.; Krüger, S.; Köhnlein, T.; Brömme, D.; Reinhold, D.; Ansorge, S.; Welte, T. Expression of cathepsin K in lung epithelial cells. *Am. J. Respir. Cell Mol. Biol.*, **1999**, *20*, 612–619.
- [71] Tepel, C.; Brömme, D.; Herzog, V.; Brix, K. Cathepsin K in thyroid epithelial cells: sequence, localization and possible function in extracellular proteolysis of thyroglobulin. *J. Cell Sci.*, **2000**, *113*, 4487–4498.
- [72] Quintanilla-Dieck, M. J.; Codriansky, K.; Keady, M.; Bhawan, J.; Rüniger, T. M. Expression and regulation of cathepsin K in skin fibroblasts. *Exp. Dermatol.*, **2009**, *18*, 596–602.
- [73] Dodds, R. A.; James, I. E.; Rieman, D.; Ahern, R.; Hwang, S. M.; Connor, J. R.; Thompson, S. D.; Veber, D. F.; Drake, F. H.; Holmes, S.; Lark, M. W.; Gowen, M. Human osteoclast cathepsin K is processed intracellularly prior to attachment and bone resorption. *J. Bone Miner. Res.*, **2001**, *16*, 478–486.
- [74] Zhao, Q.; Jia, Y.; Xiao, Y. Cathepsin K: a therapeutic target for bone diseases. *Biochem. Biophys. Res. Commun.*, **2009**, *380*, 721–723.
- [75] Wilson, S. R.; Peters, C.; Saftig, P.; Brömme, D. Cathepsin K activity-dependent regulation of osteoclast actin ring formation and bone resorption. *J. Biol. Chem.*, **2009**, *284*, 2584–1592.
- [76] Riese, R. J.; Wolf, P. R.; Brömme, D.; Natkin, L. R.; Villadangos, J. A.; Ploegh, H. L.; Chapman, H. A. Essential role for cathepsin S in MHC class II-associated invariant chain processing and peptide loading. *Immunity*, **1996**, *4*, 357–366.
- [77] Villadangos, J. A.; Riese, R. J.; Peters, C.; Chapman, H. A.; Ploegh, H. L. Degradation of mouse invariant chain: roles of cathepsins S and D and the influence of major histocompatibility complex polymorphism. *J. Exp. Med.*, **1997**, *186*, 549–560.
- [78] Nakagawa, T.; Brissette, W. H.; Lira, P. D.; Griffiths, R. J.; Petrushova, N.; Stock, J.; McNeish, J. D.; Eastman, S. E.; Howard, E. D.; Clarke, S. R. M.; Rosloniec, E. F.; Elliott, E. A.; Rudensky, A. Y. Impaired invariant chain degradation and antigen presentation and diminished collagen-induced arthritis in cathepsin S null mice. *Immunity*, **1999**, *10*, 207–217.
- [79] Honey, K.; Rudensky, A. Y. Lysosomal cysteine proteases regulate antigen presentation. *Nat. Rev. Immunol.*, **2003**, *3*, 472–482.
- [80] Gupta, S.; Singh, R. K.; Dastidar, S.; Ray, A. Cysteine cathepsin S as an immunomodulatory target: present and future trends. *Expert Opin. Ther. Targets*, **2008**, *12*, 291–299.

-
- [81] Palmer, J. T.; Rasnick, D.; Klaus, J. L.; Brömme, D. Vinyl sulfones as mechanism-based cysteine protease inhibitors. *J. Med. Chem.*, **1995**, *38*, 3193–3196.
- [82] Lützner, N.; Kalbacher, H. Quantifying cathepsin S activity in antigen presenting cells using a novel specific substrate. *J. Biol. Chem.*, **2008**, *283*, 36185–36194.
- [83] Shi, G. P.; Bryant, R. A.; Riese, R.; Verhelst, S.; Driessen, C.; Li, Z.; Brömme, D.; Ploegh, H. L.; Chapman, H. A. Role of cathepsin F in invariant chain processing and major histocompatibility complex class II peptide loading by macrophages. *J. Exp. Med.*, **2000**, *191*, 1177–1186.
- [84] Green, E. L. The genetics of a new hair deficiency, furless. *J. Hered.*, **1954**, *45*, 115–118.
- [85] Hook, V. Y. Protease pathways in peptide neurotransmission and neurodegenerative diseases. *Cell. Mol. Neurobiol.*, **2006**, *26*, 449–469.
- [86] Abboud-Jarrous, G.; Atzmon, R.; Peretz, T.; Palermo, C.; Gadea, B. B.; Joyce, J. A.; Vlodaysky, I. Cathepsin L is responsible for processing and activation of proheparanase through multiple cleavages of a linker segment. *J. Biol. Chem.*, **2008**, *283*, 18167–18176.
- [87] Zavašnik-Bergant, T.; Turk, B. Cysteine proteases: destruction ability *versus* immunomodulation capacity in immune cells. *Biol. Chem.*, **2007**, *388*, 1141–1149.
- [88] Adkison, A. M.; Raptis, S. Z.; Kelley, D. G.; Pham, C. T. Dipeptidyl peptidase I activates neutrophil-derived serine proteases and regulates the development of acute experimental arthritis. *J. Clin. Invest.*, **2002**, *109*, 363–371.
- [89] Méthot, N.; Rubin, J.; Guay, D.; Beaulieu, C.; Ethier, D.; Reddy, T. J.; Riendeau, D.; Percival, M. D. Inhibition of the activation of multiple serine proteases with a cathepsin C inhibitor requires sustained exposure to prevent pro-enzyme processing. *J. Biol. Chem.*, **2007**, *282*, 20836–20846.
- [90] Vasiljeva, O.; Reinheckel, T.; Peters, C.; Turk, D.; Turk, V.; Turk, B. Emerging roles of cysteine cathepsins in disease and their potential as drug targets. *Curr. Pharm. Des.*, **2007**, *13*, 387–403.
- [91] Berdowska, I. Cysteine proteases as disease markers. *Clin. Chim. Acta*, **2004**, *342*, 41–69.
- [92] Chang, W. S. W.; Wu, H. R.; Yeh, C. T.; Wu, C. W.; Chang, J. Y. Lysosomal cysteine proteinase cathepsin S as a potential target for anti-cancer therapy. *J. Cancer Mol.*, **2007**, *3*, 5–14.

-
- [93] Gocheva, V.; Joyce, J. A. Cysteine cathepsins and the cutting edge of cancer invasion. *Cell Cycle*, **2007**, *6*, 60–64.
- [94] Affara, N. I.; Andreu, P.; Coussens, L. M. Delineating protease functions during cancer development. *Methods Mol. Biol.*, **2009**, *539*, 1–32.
- [95] Kuester, D.; Lippert, H.; Roessner, A.; Krueger, S. The cathepsin family and their role in colorectal cancer. *Pathol. Res. Pract.*, **2008**, *204*, 491–500.
- [96] Palermo, C.; Joyce, J. A. Cysteine cathepsin proteases as pharmacological targets in cancer. *Trends Pharmacol. Sci.*, **2008**, *29*, 22–28.
- [97] Stoch, S. A.; Wagner, J. A. Cathepsin K inhibitors: a novel target for osteoporosis therapy. *Clin. Pharmacol. Ther.*, **2008**, *83*, 172–175.
- [98] Le Gall, C.; Bonnelye, E.; Clézardin, P. Cathepsin K inhibitors as treatment of bone metastasis. *Curr. Opin. Support. Palliat. Care*, **2008**, *2*, 218–222.
- [99] Bengtsson, E.; Nilsson, J.; Jovinge, S. Cystatin C and cathepsins in cardiovascular disease. *Front. Biosci.*, **2008**, *13*, 5780–5786.
- [100] Yasuda, Y.; Kaleta, J.; Brömme, D. The role of cathepsins in osteoporosis and arthritis: rationale for the design of new therapeutics. *Adv. Drug. Deliv. Rev.*, **2005**, *57*, 973–993.
- [101] Saegusa, K.; Ishimaru, N.; Yanagi, K.; Arakaki, R.; Ogawa, K.; Saito, I.; Katunuma, N.; Hayashi, Y. Cathepsin S inhibitor prevents autoantigen presentation and autoimmunity. *J. Clin. Invest.*, **2002**, *110*, 361–369.
- [102] Bidère, N.; Lorenzo, H. K.; Carmona, S.; Laforge, M.; Harper, F.; Dumont, C.; Senik, A. Cathepsin D triggers Bax activation, resulting in selective apoptosis-inducing factor (AIF) relocation in T lymphocytes entering the early commitment phase to apoptosis. *J. Biol. Chem.*, **2003**, *278*, 31401–31411.
- [103] Zhang, H.; Zhong, C.; Shi, L.; Guo, Y.; Fan, Z. Granulysin induces cathepsin B release from lysosomes of target tumor cells to attack mitochondria through processing of bid leading to necroptosis. *J. Immunol.*, **2009**, *182*, 6993–7000.
- [104] Grimm, J.; Kirsch, D. G.; Windsor, S. D.; Kim, C. F.; Santiago, P. M.; Ntziachristos, V.; Jacks, T.; Weissleder, R. Use of gene expression profiling to direct *in vivo* molecular imaging of lung cancer. *Proc. Natl. Acad. Sci. USA*, **2005**, *102*, 14404–14409.
- [105] Cardone, R. A.; Casavola, V.; Reshkin, S. J. The role of disturbed pH dynamics and the Na⁺/H⁺ exchanger in metastasis. *Nat. Rev. Cancer*, **2005**, *5*, 786–795.

-
- [106] Gelb, B. D.; Shi, G. P.; Chapman, H. A.; Desnick, R. J. Pycnodysostosis, a lysosomal disease caused by cathepsin K deficiency. *Science*, **1996**, *273*, 1236–1238.
- [107] Toomes, C.; James, J.; Wood, A. J.; Wu, C. L.; McCormick, D.; Lench, N.; Hewitt, C.; Moynihan, L.; Roberts, E.; Woods, C. G.; Markham, A.; Wong, M.; Widmer, R.; Ghaffar, K. A.; Pemberton, M.; Hussein, I. R.; Temtamy, S. A.; Davies, R.; Read, A. P.; Sloan, P.; Dixon, M. J.; Thakker, N. S. Loss-of-function mutations in the cathepsin C gene result in periodontal disease and palmoplantar keratosis. *Nat. Genet.*, **1999**, *23*, 421–424.
- [108] Pennacchio, L. A.; Lehesjoki, A. E.; Stone, N. E.; Willour, V. L.; Virtaneva, K.; Miao, J.; D'Amato, E.; Ramirez, L.; Faham, M.; Koskiniemi, M.; Warrington, J. A.; Norio, R.; de la Chapelle, A.; Cox, D. R.; Myers, R. M. Mutations in the gene encoding cystatin B in progressive myoclonus epilepsy. *Science*, **1996**, *271*, 1731–1734.
- [109] Selkoe, D. J. Alzheimer's disease: genes, proteins, and therapy. *Physiol. Rev.*, **2001**, *81*, 741–766.
- [110] Thinakaran, G.; Koo, E. H. Amyloid precursor protein trafficking, processing, and function. *J. Biol. Chem.*, **2008**, *283*, 29615–29619.
- [111] Hook, V.; Toneff, T.; Bogoyo, M.; Greenbaum, D.; Medzihradzsky, K. F.; Neveu, J.; Lane, W.; Hook, G.; Reisine, T. Inhibition of cathepsin B reduces beta-amyloid production in regulated secretory vesicles of neuronal chromaffin cells: evidence for cathepsin B as a candidate β -secretase of Alzheimer's disease. *Biol. Chem.*, **2005**, *386*, 931–940.
- [112] Mueller-Stainer, S.; Zhou, Y.; Arai, H.; Roberson, E. D.; Sun, B.; Chen, J.; Wang, X.; Yu, G.; Esposito, L.; Mucke, L.; Gan, L. Antiamyloidogenic and neuroprotective Functions of Cathepsin B: implications for Alzheimer's disease. *Neuron*, **2006**, *51*, 703–714.
- [113] Hook, V.; Kindy, M.; Hook, G. Cysteine protease inhibitors effectively reduce *in vivo* levels of brain beta-amyloid related to Alzheimer's disease. *Biol. Chem.*, **2007**, *388*, 247–252.
- [114] Hook, V. Y.; Kindy, M.; Hook, G. Inhibitors of cathepsin B improve memory and reduce beta-amyloid in transgenic Alzheimer disease mice expressing the wild-type, but not the Swedish mutant, β -secretase site of the amyloid precursor protein. *J. Biol. Chem.*, **2008**, *283*, 7745–7753.

-
- [115] Hook, V. Y.; Kindy, M.; Reinheckel, T.; Peters, C.; Hook, G. Genetic cathepsin B deficiency reduces β -amyloid in transgenic mice expressing human wild-type amyloid precursor protein. *Biochem. Biophys. Res. Commun.*, **2009**, *386*, 284–288.
- [116] Klein, D. M.; Felsenstein, K. M.; Brenneman, D. E. Cathepsins B and L differentially regulate amyloid precursor protein processing. *J. Pharmacol. Exp. Ther.*, **2009**, *328*, 813–821.
- [117] Hadjidakis, D. J.; Androulakis, I. I. Bone Remodeling. *Ann. N. Y. Acad. Sci.*, **2006**, *1092*, 385–396.
- [118] Cohen, M. M. Jr. The new bone biology: pathologic, molecular, and clinical correlates. *Am. J. Med. Genet. A.*, **2006**, *140*, 2646–2706.
- [119] Lecaille, F.; Kaleta, J.; Brömme, D. Human and parasitic papain-like cysteine proteases: their role in physiology and pathology and recent developments in inhibitor design. *Chem. Rev.*, **2002**, *102*, 4459–4488.
- [120] Singh, S. V.; Tripathi, A. An overview of osteoporosis for the practising prosthodontist. *Gerodontology*, **2010**, *27*, 308–314.
- [121] Kanis, J. A.; Johnell, O. Requirements for DXA for the management of osteoporosis in Europe. *Osteoporos. Int.*, **2005**, *16*, 229–238.
- [122] Yasothan, U.; Kar, S. Osteoporosis: overview and pipeline. *Nat. Rev. Drug. Discov.*, **2008**, *7*, 725–726.
- [123] European Medicines Agency. Summary of positive opinion for prolia. EMA/CHMP/776168/2009.
- [124] Pérez-Castrillón, J. L.; Pinacho, F.; De Luis, D.; Lopez-Menendez, M.; Dueñas Laita, A. Odanacatib, a new drug for the treatment of osteoporosis: review of the results in postmenopausal women. *J. Osteoporos.*, **2010**: 401581.
- [125] van den Hoorn, T.; Paul, P.; Jongsma, M. L.; Neefjes, J. Routes to manipulate MHC class II antigen presentation. *Curr. Opin. Immunol.*, **2011**, *23*, 88–95.
- [126] Honey, K.; Rudensky, A. Y. Lysosomal cysteine proteases regulate antigen presentation. *Nat. Rev. Immunol.*, **2003**, *3*, 472–482.
- [127] Shoenfeld, Y.; Isenberg, D. A. The mosaic of autoimmunity. *Immunol. Today.*, **1989**, *10*, 123–126.
- [128] Deodhar, S. D. Autoimmune diseases: overview and current concepts of pathogenesis. *Clin. Biochem.*, **1992**, *25*, 181–185.
- [129] Rioux, J. D.; Abbas, A. K. Paths to understanding the genetic basis of autoimmune disease. *Nature*, **2005**, *435*, 584–589.

-
- [130] Davidson, A.; Diamond, B. Autoimmune diseases. *N. Engl. J. Med.*, **2001**, *345*, 340–350.
- [131] Miescher, P. A.; Beris, P. Immunosuppressive therapy in the treatment of autoimmune diseases. *Springer Semin. Immunopathol.*, **1984**, *7*, 69–90.
- [132] Kazkaz, H.; Isenberg, D. Anti B cell therapy (rituximab) in the treatment of autoimmune diseases. *Curr. Opin. Pharmacol.*, **2004**, 398–402.
- [133] Maini, R. N.; Breedveld, F. C.; Kalden, J. R.; Smolen, J. S.; Davis, D.; Macfarlane, J. D.; Antoni, C.; Leeb, B.; Elliott, M. J.; Woody, J. N.; Schaible, T. F.; Feldmann, M. Therapeutic efficacy of multiple intravenous infusions of anti-tumor necrosis factor alpha monoclonal antibody combined with low-dose weekly methotrexate in heumatoid arthritis. *Arthritis Rheum.*, **1998**, *41*, 1552–1563.
- [134] Moreland, L. W.; Baumgartner, S. W.; Schiff, M. H.; Tindall, E. A.; Fleischmann, R. M.; Weaver, A. L.; Ettliger, R. E.; Cohen, S.; Koopman, W. J.; Mohler, K.; Widmer, M. B.; Bloch, C. M. Treatment of rheumatoid arthritis with a recombinant human tumor necrosis factor receptor (p75)-Fc fusion protein. *N. Engl. J. Med.*, **1997**, *337*, 141–147.
- [135] Feldmann, M.; Steinman, L. Design of effective immunotherapy for human autoimmunity. *Nature*, **2005**, *435*, 612–619.
- [136] Yang, H.; Kala, M.; Scott, B. G.; Goluszko, E.; Chapman, H. A.; Christadoss, P. Cathepsin S is required for murine autoimmune myasthenia gravis pathogenesis. *J Immunol.*, **2005**, *174*, 1729–1737.
- [137] Saegusa, K.; Ishimaru, N.; Yanagi, K.; Arakaki, R.; Ogawa, K.; Saito, I.; Katunuma, N.; Hayashi, Y. Cathepsin S inhibitor prevents autoantigen presentation and autoimmunity. *J. Clin. Invest.*, **2002**, *110*, 361–369.
- [138] Lucas, E. C.; Williams, A. The pH dependencies of individual rate constants in papain-catalyzed reactions. *Biochemistry*, **1969**, *8*, 5125–5135.
- [139] Lewis, C. A. Jr.; Wolfenden R. Thiohemiacetal formation by inhibitory aldehydes at the active site of papain. *Biochemistry*, **1977**, *16*, 4890–4895.
- [140] Thompson, S. A.; Andrews, P. R.; Hanzlik, R. P. Carboxyl-modified amino acids and peptides as protease inhibitors. *J. Med. Chem.*, **1986**, *29*, 104–111.
- [141] Moon, J. B.; Coleman, R. S.; Hanzlik, R. P. Reversible covalent inhibition of papain by a peptide nitrile. ¹³C-NMR evidence for a thioimidate ester adduct. *J. Am. Chem. Soc.*, **1986**, *108*, 1350–1351.

- [142] Liang, T. C.; Abeles, R. H.; Inhibition of papain by nitriles: mechanistic studies using NMR and kinetic measurements. *Arch. Biochem. Biophys.*, **1987**, *252*, 626–634.
- [143] Brisson, J.-R.; Carey, P. R.; Storer, A. C. Benzoylamidoacetonitrile is bound as a thioimidate in the active site of papain. *J. Biol. Chem.*, **1986**, *261*, 9087–9089.
- [144] Hanzlik, R. P.; Jacober, S. P.; Zygmunt, J. Reversible binding of peptide aldehydes to papain. Structure-activity relationships. *Biochim. Biophys. Acta*, **1991**, *1073*, 33–42.
- [145] Dufour, É.; Storer, A. C.; Ménard, R. Peptide aldehydes and nitriles as transition state analog inhibitors of cysteine proteases. *Biochemistry*, **1995**, *34*, 9136–9143.
- [146] Kim, J. B.; Kopcho, L. M.; Kirby, M. S.; Hamann, L. G.; Weigelt, C. A.; Metzler, W. J.; Marcinkeviciene, J. Mechanism of Gly-PropNA cleavage catalyzed by dipeptidyl peptidase-IV and its inhibition by saxagliptin (BMS-477118). *Arch. Biochem. Biophys.*, **2006**, *445*, 9–18.
- [147] Ho, T.-L. The hard soft acids bases (HSAB) principle and organic chemistry. *Chem. Rev.*, **1975**, *75*, 2–20.
- [148] Ho, T.-L.; Ho, H. C.; Hamilton, L. D. Biochemical significance of the hard and soft acids ad bases principle. *Chem. Biol. Interact.*, **1978**, *23*, 65–84.
- [149] Thornberry, N. A.; Weber, A. E. Discovery of JANUVIA (sitagliptin), a selective dipeptidyl peptidase IV inhibitor for the treatment of type 2 diabetes. *Curr. Top. Med. Chem.*, **2007**, *7*, 557–568.
- [150] Brandt, I.; Joossens, J.; Chen, X.; Maes, M.-B.; Scharpé, S.; De Meester, I.; Lambeir, A.-M. Inhibition of dipeptidyl-peptidase IV catalyzed peptide truncation by Vildagliptin ((2S)-{[(3-hydroxyadamantan-1-yl)amino]acetyl}-pyrrolidine-2-carbonitrile). *Biochem. Pharmacol.*, **2005**, *70*, 134–143.
- [151] Metzler, W. J.; Yanchunas, J.; Weigelt, C.; Kish, K.; Klei, H. E.; Xie, D.; Zhang, Y.; Corbett, M.; Tamura, J. K.; He, B.; Hamann, L. G.; Kirby, M. S.; Marcinkeviciene, J. Involvement of DPP-IV catalytic residues in enzyme-saxagliptin complex formation. *Protein Sci.*, **2008**, *17*, 240–250.
- [152] Hanzlik, R. P.; Zygmunt J.; Moon, J. B. Reversible covalent binding of peptide nitriles to papain. *Biochim. Biophys. Acta*, **1990**, *1035*, 62–70.
- [153] Dufour, É.; Storer, A. C.; Ménard, R. Engineering nitrile hydratase activity into a cysteine protease by a single mutation. *Biochemistry*, **1995**, *34*, 16382–16388.
- [154] Versari, A.; Ménard, R.; Lortie, R. Enzymatic hydrolysis of nitriles by an engineered nitrile hydratase (papain Gln19Glu) in aqueous-organic media. *Biotechnol. Bioeng.*, **2002**, *79*, 9–14.

- [155] Reddy, S. Y.; Kahn, K.; Zheng, Y. J.; Bruice, T. C. Protein engineering of nitrile hydratase activity of papain: molecular dynamics study of a mutant and wild-type enzyme. *J. Am. Chem. Soc.*, **2002**, *124*, 12979–12990.
- [156] Gour-Salin, B. J.; Storer, A. C.; Castelhana, A.; Krantz, A.; Robinson, V. Inhibition of papain by peptide nitriles: reactions of external nucleophiles with the thioimidate ester adduct. *Enzyme Microb. Technol.*, **1991**, *13*, 408–411.
- [157] Robichaud, J.; Oballa, R.; Prasit, P.; Falguyret, J. P.; Percival, M. D.; Wesolowski, G.; Rodan, S. B.; Kimmel, D.; Johnson, C.; Bryant, C.; Venkatraman, S.; Setti, E.; Mendonca, R.; Palmer, J. T. A novel class of nonpeptidic biaryl inhibitors of human cathepsin K. *J. Med. Chem.*, **2003**, *46*, 3709–3727.
- [158] Stoch, S. A.; Zajic, S.; Stone, J.; Miller, D. L.; Van Dyck, K.; Gutierrez, M. J.; De Decker, M.; Liu, L.; Liu, Q.; Scott, B. B.; Panebianco, D.; Jin, B.; Duong, L. T.; Gottesdiener, K.; Wagner, J. A. Effect of the cathepsin K inhibitor odanacatib on bone resorption biomarkers in healthy postmenopausal women: two double-blind, randomized, placebo-controlled phase I studies. *Clin. Pharmacol. Ther.*, **2009**, *86*, 175–182.
- [159] Palmer, J. T.; Bryant, C.; Wang, D. X.; Davis, D. E.; Setti, E. L.; Rydzewski, R. M.; Venkatraman, S.; Tian, Z. Q.; Burrill, L. C.; Mendonca, R. V.; Springman, E.; McCarter, J.; Chung, T.; Cheung, H.; Janc, J. W.; McGrath, M.; Somoza, J. R.; Enriquez, P.; Yu, Z. W.; Strickley, R. M.; Liu, L.; Venuti, M. C.; Percival, M. D.; Falguyret, J. P.; Prasit, P.; Oballa, R.; Riendeau, D.; Young, R. N.; Wesolowski, G.; Rodan, S. B.; Johnson, C.; Kimmel, D. B.; Rodan, G. Design and synthesis of tri-ring P3 benzamide-containing aminonitriles as potent, selective, orally effective inhibitors of cathepsin K. *J. Med. Chem.*, **2005**, *48*, 7520–7534.
- [160] Peroni, A.; Zini, A.; Braga, V.; Colato, C.; Adami, S.; Girolomoni G. Drug-induced morphea: report of a case induced by balicatib and review of the literature. *J. Am. Acad. Dermatol.*, **2008**, *59*, 125–129.
- [161] Falguyret, J. P.; Desmarais, S.; Oballa, R.; Black, W. C.; Cromlish, W.; Khougaz, K.; Lamontagne, S.; Massé, F.; Riendeau, D.; Toulmond, S.; Percival, M. D. Lysosomotropism of basic cathepsin K inhibitors contributes to increased cellular potencies against off-target cathepsins and reduced functional selectivity. *J. Med. Chem.*, **2005**, *48*, 7535–7543.

- [162] Gauthier, J. Y.; Chauret, N.; Cromlish, W.; Desmarais, S.; Duong le, T.; Falgueyret, J. P.; Kimmel, D. B.; Lamontagne, S.; Léger, S.; LeRiche, T.; Li, C. S.; Massé, F.; McKay, D. J.; Nicoll-Griffith, D. A.; Oballa, R. M.; Palmer, J. T.; Percival, M. D.; Riendeau, D.; Robichaud, J.; Rodan, G. A.; Rodan, S. B.; Seto, C.; Thérien, M.; Truong, V. L.; Venuti, M. C.; Wesolowski, G.; Young, R. N.; Zamboni, R.; Black, W. C. The discovery of odanacatib (MK-0822), a selective inhibitor of cathepsin K. *Bioorg. Med. Chem. Lett.*, **2008**, *18*, 923–928.
- [163] Black, W. C.; Bayly, C. I.; Davis, D. E.; Desmarais, S.; Falgueyret, J. P.; Léger, S.; Li, C. S.; Massé, F.; McKay, D. J.; Palmer, J. T.; Percival, M. D.; Robichaud, J.; Tsou, N.; Zamboni, R. Trifluoroethylamines as amide isosteres in inhibitors of cathepsin K. *Bioorg. Med. Chem. Lett.*, **2005**, *15*, 4741–4744.
- [164] Black, W. C. Peptidomimetic inhibitors of cathepsin K. *Curr. Top. Med. Chem.*, **2010**, *10*, 745–751.
- [165] Gauthier, J. Y.; Black, W. C.; Courchesne, I.; Cromlish, W.; Desmarais, S.; Houle, R.; Lamontagne, S.; Li C. S.; Massé, F.; McKay, D. J.; Ouellet, M.; Robichaud, J.; Truchon, J. F.; Truong, V. L.; Wang, Q.; Percival, M. D. The identification of potent, selective, and bioavailable cathepsin S inhibitors. *Bioorg. Med. Chem. Lett.*, **2007**, *17*, 4929–4933.
- [166] Löser, R. Cathepsin S inhibitors: WO2010070615. *Expert. Opin. Ther. Pat.*, **2011**, *21*, 585–591.
- [167] Lee-Dutra, A.; Wiener, D. K.; Sun, S. Cathepsin S inhibitors: 2004-2010. *Expert. Opin. Ther. Pat.*, **2011**, *213*, 311–337.
- [168] Löser, R.; Frizler, M.; Schilling, K.; Gütschow, M. Azadipeptide nitriles: highly potent and proteolytically stable inhibitors of papain-like cysteine proteases. *Angew. Chem. Int. Ed.*, **2008**, *47*, 4331–4334.
- [169] Löser, R.; Gut, J.; Rosenthal, P. J.; Frizler, M.; Gütschow, M.; Andrews, K. T. Antimalarial activity of azadipeptide nitriles. *Bioorg. Med. Chem. Lett.*, **2010**, *20*, 252–255.
- [170] Loh, Y.; Shi, H.; Hu, M.; Yao, S. Q. "Click" synthesis of small molecule-peptide conjugates for organelle-specific delivery and inhibition of lysosomal cysteine proteases. *Chem. Commun.*, **2010**, *46*, 8407–8409.
- [171] Heal, W. P.; Dang, T. H.; Tate, E. W. Activity-based probes: discovering new biology and new drug targets. *Chem. Soc. Rev.*, **2011**, *40*, 246–257.

- [172] Edgington, L. E.; Berger, A. B.; Blum, G.; Albrow, V. E.; Paulick, M. G.; Lineberry, N.; Bogyo, M. Noninvasive optical imaging of apoptosis by caspase-targeted activity-based probes. *Nat. Med.*, **2009**, *15*, 967–973.
- [173] Porter, A. G.; Jänicke, R. U. Emerging roles of caspase-3 in apoptosis. *Cell. Death. Differ.*, **1999**, *6*, 99–104.
- [174] Falgueyret, J. P.; Black, W. C.; Cromlish, W.; Desmarais, S.; Lamontagne, S.; Mellon, C.; Riendeau, D.; Rodan, S.; Tawa, P.; Wesolowski, G.; Bass, K. E.; Venkatraman, S.; Percival, M. D. An activity-based probe for the determination of cysteine cathepsin protease activities in whole cells. *Anal. Biochem.*, **2004**, *335*, 218–227.
- [175] Veilleux, A.; Black, W. C.; Gauthier, J. Y.; Mellon, C.; Percival, M. D.; Tawa, P.; Falgueyret, J. P. Probing cathepsin S activity in whole blood by the activity-based probe BIL-DMK: cellular distribution in human leukocyte populations and evidence of diurnal modulation. *Anal. Biochem.*, **2011**, *411*, 43–49.
- [176] Witte, M. D.; Kallemeijn, W. W.; Aten, J.; Li, K. Y.; Strijland, A.; Donker-Koopman, W. E.; van den Nieuwendijk, A. M.; Bleijlevens, B.; Kramer, G.; Florea, B. I.; Hooibrink, B.; Hollak, C. E.; Ottenhoff, R.; Boot, R. G.; van der Marel, G. A.; Overkleeft, H. S.; Aerts, J. M. Ultrasensitive in situ visualization of active glucocerebrosidase molecules. *Nat. Chem. Biol.*, **2010**, *6*, 907–913.
- [177] Paulick, M. G.; Bogyo, M. Development of Activity-Based Probes for Cathepsin X. *ACS Chem. Biol.*, **2011**, *6*, 563–572.
- [178] Frizler, M.; Stirnberg, M.; Sisay, M. T.; Gütschow, M. Development of nitrile-based peptidic inhibitors of cysteine cathepsins. *Curr. Top. Med. Chem.*, **2010**, *10*, 294–322.
- [179] Wieland, T.; Bernhard, H. Über Peptidsynthesen. 3. Die Verwendung von Anhydriden aus *N*-acylierten Aminosäuren und Derivaten anorganischer Säuren. *Liebigs Ann. Chem.*, **1951**, *572*, 190–194.
- [180] Boissonnas, R. A. Une nouvelle methode de synthese peptidique. *Helv. Chim. Acta*, **1951**, *34*, 874–879.
- [181] Vaughan, jr. V. R. Acylalkylcarbonates as Acylating Agents for the Synthesis of Peptides. *J. Am. Chem. Soc.*, **1951**, *73*, 874.
- [182] Löser, R.; Schilling, K.; Dimmig, E.; Gütschow, M. Interaction of papain-like cysteine proteases with dipeptide-derived nitriles. *J. Med. Chem.*, **2005**, *48*, 7688–7707.
- [183] Sculley, M. J.; Morrison, Wallace Cleland, W. W. Slow-binding inhibition: the general case. *Biochim. Biophys. Acta.*, **1996**, *1928*, 78–86.

- [184] Szedlacsek, S. E.; Duggleby, R. G. Kinetics of slow and tight-binding inhibitors. *Methods Enzymol.*, **1995**, *249*, 144–180.
- [185] Cha, S. Tight-binding inhibitors-I. Kinetic behavior. *Biochem. Pharmacol.*, **1975**, *24*, 2177–2185.
- [186] Cha, S.; Agarwal, R. P.; Parks, jr. R. E. Tight-binding inhibitors-II. Non-steady state nature of inhibition of milk xanthine oxidase by allopurinol and alloxanthine and of human erythrocytic adenosine deaminase by coformycin. *Biochem. Pharmacol.*, **1975**, *24*, 2187–2197.
- [187] Cha, S. Tight-binding inhibitors-III. A new approach for the determination of competition between tight-binding inhibitors and substrates--inhibition of adenosine deaminase by coformycin. *Biochem. Pharmacol.*, **1976**, *25*, 2695–2702.
- [188] Lagrille, O.; Taillades, J.; Boiteau, L.; Commeyras, A. *N*-Carbamoyl derivatives and their nitrosation by gaseous NOX; a new, promising tool in stepwise peptide synthesis. *Eur. J. Org. Chem.*, **2002**, 1026–1032.
- [189] Pace, A.; Pierro, P. The new era of 1,2,4-oxadiazoles. *Org. Biomol. Chem.*, **2009**, *7*, 4337–4348.
- [190] Dosa, S.; Daniels, J.; Gütschow, M. Biaryl Sulfonamides from O-Acetyl Amidoximes: 1,2,4-Oxadiazole Cyclization under Acidic Conditions. *J. Heterocyclic Chem.*, **2011**, *48*, 407–413.
- [191] Pinnen, F.; Luisi, G.; Calcagni, A.; Lucente, G.; Gavuzzo, E.; Cerrini, S. Approaches to pseudopeptidic ergopeptines. Part 2. Consequences of the incorporation of an α -azaproline residue into the oxacyclic system. *J. Chem. Soc. Perkin Trans.*, **1994**, *1*, 1611–1617.
- [192] Frizler, M.; Lohr, F.; Furtmann, N.; Kläs, J.; Gütschow, M. Structural optimization of azadipeptide nitriles strongly increases association rates and allows the development of selective cathepsin inhibitors. *J. Med. Chem.*, **2011**, *54*, 396–400.
- [193] Bessley, R. M.; Ingold, C. K.; Thorpe, J. F. The Formation and Stability of spiro-Compounds. Part I: *spiro*-Compounds from Cyclohexane. *J. Am. Chem. Soc.*, **1915**, *107*, 1081–1092.
- [194] Jung, M. E.; Piizzi, G. *gem*-Disubstituent effect: Theoretical basis and synthetic applications. *Chem. Rev.*, **2005**, *105*, 1735–1766.
- [195] Sammes, P. G.; Weller, D. J. Steric promotion of ring formation. *Synthesis*, **1995**, 1205–1222.

- [196] Hoffmann, E.; Faiferman, I. A peptide synthesis via hydroxamic acids. *J. Org. Chem.*, **1964**, *29*, 748–751.
- [197] Narendra, N.; Chennakrishnareddy, G.; Sureshbabu, V. V. Application of carbodiimide mediated Lossen rearrangement for the synthesis of α -ureidopeptides and peptidyl ureas employing *N*-urethane α -amino/peptidyl hydroxamic acids. *Org. Biomol. Chem.*, **2009**, *7*, 3520–3526.
- [198] When performing the cyclization of Cbz-phenylalanine with phosphorous pentoxide *in the presence of triethylamine*, the corresponding 2-benzyloxy-5(4*H*)-oxazolone was obtained, *see* Jones, J. H.; Witty, M. J. An oxazol-5(4*H*)-one derived from a benzyloxycarbonylamino-acid. *J. C. S. Chem. Comm.*, **1977**, 281–282.
- [199] For the formation of NCAs from 5(4*H*)-oxazolones, derived from Boc-protected amino acids, *see* a) Mobashery, S.; Johnston, M. J. A new approach to the preparation of *N*-carboxy- α -amino acid anhydrides. *Org. Chem.*, **1985**, *50*, 2200–2202; b) Wilder, R.; Mobashery, S., The use of triphosgene in preparation of *N*-carboxy- α -amino acid anhydrides. *J. Org. Chem.*, **1992**, *75*, 2755–2756; c) Agami, C.; Couty, F. The reactivity of the *N*-Boc protecting group: an underrated feature. *Tetrahedron*, **2002**, *58*, 2701–2724.
- [200] For a review on NCAs, *see* Kricheldorf, H. R. Polypeptides and 100 years of chemistry of α -amino acid *N*-carboxyanhydrides. *Angew. Chem. Int. Ed.*, **2006**, *45*, 5752–5784.
- [201] Frizler, M.; Lohr, F.; Lülldorff, M.; Gütschow M. Facing the *gem*-dialkyl effect in enzyme inhibitor design: preparation of homocycloleucine-based azadipeptide nitriles. *Chem. Eur. J.*, **2011**, *17*, 11419–11423.
- [202] Song, A.; Wang, X.; Lam, K. S. A convenient synthesis of coumarin-3-carboxylic acids *via* Knoevenagel condensation of Meldrum's acid with *ortho*-hydroxyaryl aldehydes or ketones. *Tetrahedron Lett.*, **2003**, *44*, 1755–1758.
- [203] Götz, M. G.; Caffrey, C. R.; Hansell, E.; McKerrow, J. H.; Powers, J. C. Peptidyl allyl sulfones: a new class of inhibitors for clan CA cysteine proteases. *Bioorg. Med. Chem.*, **2004**, *12*, 5203–5211.
- [204] Bhattacharya, A. K. The Michaelis-Arbuzov rearrangement. *Chem. Rev.*, **1981**, *81*, 415–430.

- [205] Maryanoff, B. E.; Reitz, A. A. The Wittig olefination reaction and modifications involving selected synthetic aspects phosphoryl-stabilized carbanions. stereochemistry, mechanism, and selected synthetic aspects. *Chem. Rev.*, **1989**, *89*, 863–927.
- [206] Perrey, D. A.; Uckun, F. M. An improved method for cysteine alkylation. *Tetrahedron Lett.*, **2001**, *42*, 1859–1861.
- [207] Seko, T.; Kato, M.; Kohno, H.; Shizuka, O.; Hashimura, H. T.; Nakai, K.; Maegawa, H.; Katsube, N.; Toda, M. Structure-activity Study of L-amino acid-based N-type Calcium Channel Blockers. *Bioorg. Med. Chem.*, **2003**, *11*, 1901–1913.
- [208] Holzer, G.; Noske, H.; Lang, T.; Holzer, L.; Willinger, U. Bone-turnover markers in fracture healing. *J. Lab. Clin. Med.*, **2005**, *146*, 13–17.
- [209] Muñoz-Torres, M.; Reyes-García, R.; Mezquita-Rayab, P.; Fernández-García, D.; Alonso, G.; de Dios Lunac, J.; Ruiz-Requenad, M. E.; Escobar-Jiménez, F. Serum cathepsin K as a marker of bone metabolism in postmenopausal women treated with alendronate. *Maturitas*, **2009**, *64*, 188–92.
- [210] Mohamed, M. M.; Sloane, B. F. Cysteine cathepsins: multifunctional enzymes in cancer. *Nat. Rev. Cancer.*, **2006**, *6*, 764–775.
- [211] Nouh, A. M.; Mohamed, M. M.; El-Shinawi, M.; Shaalan, M. A.; Cavallo-Medved, D.; Khaled, H. M.; Sloane, B. F. Cathepsin B: a potential prognostic marker for inflammatory breast cancer. *J. Transl. Med.*, **2011**, *9*:1.
- [212] Götz, M. G.; Caffrey, C. R.; Hansell, E.; McKerrow, J. H.; Powers, J. C. Peptidyl allyl sulfones: a new class of inhibitors for clan CA cysteine proteases. *Bioorg. Med. Chem.*, **2004**, *12*, 5203–5211.
- [213] Yampolsky, I. V.; Balashova, T. A.; Lukyanov, K. A. Synthesis and spectral and chemical properties of the yellow fluorescent protein zFP538 chromophore. *Biochemistry*, **2009**, *48*, 8077–8082.
- [214] Ivashkin, P. E.; Lukyanov, K. A.; Lukyanov, S.; Yampolsky, I. V. A synthetic GFP-like chromophore undergoes base-catalyzed autoxidation into acylimine red form. *J. Org. Chem.*, **2011**, *76*, 2782–2791.
- [215] Palmer, J. T.; Rasnik, D.; Klaus, J. L.; Brömme, D. Peptidyl vinyl sulphones : a new class of potent and selective cysteine protease inhibitors. *J. Med. Chem.*, **1995**, *38*, 3193–3196.

-
- [216] Ettari, R.; Zappalà, M.; Micale, N.; Grazioso, G.; Giofrè, S.; Schirmeister, T.; Grasso, S. Peptidomimetics containing a vinyl ketone warhead as falcipain-2 inhibitors. *Eur. J. Med. Chem.*, **2011**, *46*, 2058–2065.
- [217] Zhou, J.-M.; Liu, C.; Tsou, C.-L. Kinetics of trypsin inhibition by its specific inhibitors. *Biochemistry*, **1989**, *28*, 1070-1076.

ZUSAMMENFASSUNG

Die Papain-ähnlichen Cysteinproteasen der Unterfamilie C1A sind in vielen lebenden Organismen einschließlich der Bakterien, Viren, Pflanzen sowie der niederen und höheren Tiere verbreitet. Bis zum heutigen Tag sind beim Menschen elf verschiedene lysosomale Papain-ähnliche Cysteinproteasen bekannt, die Cathepsine B, C, H, F, K, L, O, S, V, W und X, die untereinander eine hohe Homologie aufweisen. Die meisten Cathepsine sind Endopeptidasen mit Ausnahme von Cathepsinen C und X, die als „wahre“ Exopeptidasen fungieren. Neben ihrer katabolischen Funktion im lysosomalen Proteinabbau üben die thiolabhängigen Cathepsine auch spezifische Aufgaben in einer Vielzahl von physiologischen Prozessen einschließlich der Homöostase des Knochengewebes, Immunantwort, Apoptose und des Umbaus der extrazellulären Matrix. Weiterhin wurde für einige Cathepsine die Beteiligung an pathologischen Zuständen wie Osteoporose, Autoimmunität und maligne Entartungen beschrieben. Aus diesem Grund repräsentieren die menschlichen Cathepsine wichtige Zielstrukturen für die Entwicklung neuer Arzneistoffe und Diagnostika.

Cathepsin K wird in Osteoklasten exprimiert, deren proteolytische Aktivität hauptsächlich durch diese Cysteinprotease vermittelt wird. Es wurde gezeigt, dass Cathepsin K in der Lage ist, verschiedene Komponenten der Knochenmatrix, unter anderem auch Kollagen des Typs I, zu spalten. Diesem Enzym wird deswegen eine entscheidende Rolle im Prozess der homöostatischen Knochenerneuerung zugeschrieben. Cathepsin K steht aktuell im Fokus des wissenschaftlichen Interesses als eine mögliche Zielstruktur zur Behandlung der Osteoporose.

Cathepsin S wird hauptsächlich im lymphatischen Gewebe wie Lymphknoten, Milz und Makrophagen exprimiert. Diese Cysteinprotease ist durch die Prozessierung der invarianten Kette an der MHC-II-vermittelten Antigenpräsentation beteiligt. Es wurde gezeigt, dass die Hemmung von Cathepsin S mit einer verringerten Präsentation von Autoantigenen in einem murinen Modell verbunden ist. Basierend auf dieser Tatsache wird Cathepsin S als ein mögliches Target für die Behandlung der Autoimmunität betrachtet.

Das primäre Ziel dieser Arbeit war die systematische Entwicklung von Dipeptidnitrilen und Azadipeptidnitrilen als hochpotente und selektive Inhibitoren für die therapeutisch interessanten Cathepsine K und S. Im Rahmen dieser Arbeit wurde außerdem eine fluoreszierende molekulare Sonde für die Detektion und Quantifizierung von Cathepsinen mittels SDS-PAGE etabliert.

Nitril-abgeleitete Dipeptide und Azadipeptide inhibieren Cysteinproteasen durch eine kovalente Interaktion mit dem aktiven Cysteinrest unter reversibler Ausbildung eines

enzymgebundenen Thioimidats bzw. eines enzymgebundenen Isothiosemicarbazids (Abbildung. 1).

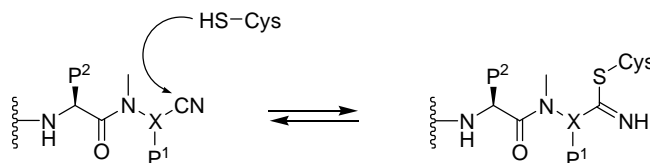
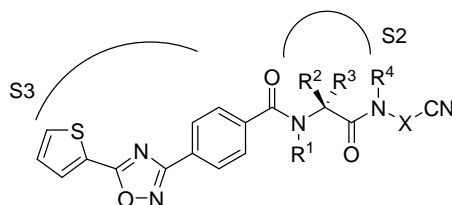


Abbildung 1. Reversible Ausbildung von kovalenten Addukten.

X = CH (im Fall von Dipeptidnitrilen); X = N (im Fall von Azadipeptidnitrilen).

Durch die stufenweise Optimierung der peptidischen Grundgerüste wurden hochpotente Cathepsin K-Inhibitoren entwickelt, die zusätzlich eine beträchtliche Selektivität für dieses Enzym zeigten. Um die Selektivität für Cathepsin K zu erreichen musste ein großer aromatischer P3-Substituent mit L-Leucin oder Homocycloleucin in der P2-Position kombiniert werden. Im Fall des L-Leucin-abgeleiteten Azadipeptidnitrils war außerdem die Methylierung des P3-P2-Linkers nötig. Generell war die inhibitorische Aktivität der Azadipeptidnitrile höher als die der entsprechenden Kohlenstoff-Analoga (Tabelle 1).

Tabelle 1. K_i -Werte von Cathepsin K-selektiven Dipeptidnitrilen und Azadipeptidnitrilen.



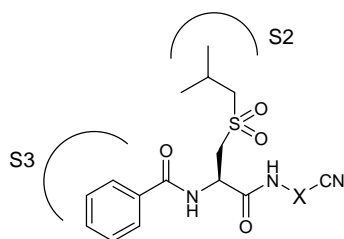
R ¹	R ²	R ³	R ⁴	X	K _i (nM)			
					Cath L	Cath S	Cath K	Cath B
H	<i>iso</i> -Butyl	H	H	CH ₂	940	140	2,9	> 22000
Me	<i>iso</i> -Butyl	H	Me	NMe	2700	140	0.63	510
H	-(CH ₂) ₅ -	H	H	CH ₂	> 5000	> 5000	13	> 5000
H	-(CH ₂) ₅ -	H	Me	NMe	280	78	0,35	150

S3, S2 – Bindungstaschen von Cathepsin K

Im zweiten Projekt dieser Arbeit wurde die Bindungstasche S3 von Cathepsin S systematisch untersucht. Dafür wurde ein großer P2-Rest mit unterschiedlichen aromatischen P3-Substituenten kombiniert. Die synthetisierten Substanzen wurden an den menschlichen Cathepsinen L, S, K und B evaluiert und zeigten alle inhibitorische Aktivitäten im

nanomolaren Bereich gegenüber Cathepsin S. Obwohl die Bindungstasche S3 von Cathepsin S auch größere aromatische P3-Substituenten akzeptierte, erreichte das Dipeptidnitril mit einem kleinen Benzoylrest in der P3-Position die höchste Hemmaktivität. Weiterhin zeigte dieser Inhibitor auch eine beachtliche Selektivität für Cathepsin S über die Antitargets, Cathepsine L, K und B. Das entsprechende Azadipeptidnitril war weniger selektiv, während seine inhibitorische Aktivität deutlich höher lag (Tabelle 2).

Tabelle 2. K_i -Werte eines Cathepsin S-selektiven Dipeptidnitrils und seines Stickstoff-Analogons



X	K_i (nM)			
	Cath L	Cath S	Cath K	Cath B
CH ₂	37000	33	> 40000	24000
NMe	15	0,55	0,66	5,8

S3, S2 – Bindungstaschen von Cathepsin S

In einem weiteren Projekt wurde eine fluoreszierende molekulare Sonde für die Visualisierung von thiolabhängigen Cathepsinen entwickelt. Diese Sonde besteht aus vier Teilen: (1) einem Vinylsulfon für eine irreversible Interaktion mit dem aktiven Cysteinrest im Sinne einer Michael Addition; (2) L-Phenylalanin in der P2-Position; (3) einem Linker und (4) einem fluoreszierenden Reporter. Die Hemmaktivität der synthetisierten Sonde wurde an Cathepsinen L, S, K and B evaluiert und die grundsätzliche Möglichkeit zur Visualisierung von Cathepsinen wurde am Beispiel von Cathepsin K gezeigt (Abbildung 2).

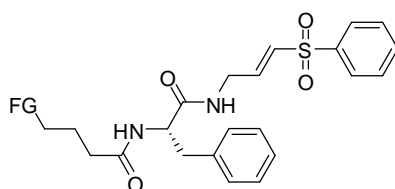


Abbildung 2. Eine fluoreszierende molekulare Sonde.

FG – fluoreszierende Gruppe.

SELBSTSTÄNDIGKEITSERKLÄRUNG

Hiermit erkläre ich, die vorliegende Dissertation selbstständig und ohne unerlaubte fremde Hilfe angefertigt zu haben. Ich habe keine anderen als die im Literaturverzeichnis angeführten Quellen benutzt und sämtliche Textstellen, die wörtlich oder sinngemäß aus veröffentlichten oder unveröffentlichten Schriften entnommen wurden, als solche kenntlich gemacht. Ebenfalls sind alle von anderen Personen bereitgestellten Materialien, Daten oder erbrachten Dienstleistungen als solche gekennzeichnet.

Bonn, Februar 2012

Maxim Frizler

DANKSAGUNG

In erster Linie möchte ich meinem Doktorvater, Herrn Professor Dr. Michael Gütschow, für die freundliche Aufnahme in seinem Arbeitskreis und für die Überlassung dieses außerordentlich interessanten Themas danken. Weiterhin danke ich ihm für die fortlaufende Unterstützung der Arbeit, die anregenden Diskussionen und seine stets konstruktiven Ratschläge.

Frau Professor Dr. Christa E. Müller danke ich sehr herzlich für die Übernahme des Koreferates und für die Betreuung im Rahmen der NRW Forschungsschule Biotech-Pharma.

Mein besonderer Dank gilt Frau Friederike Lohr und Frau Janina Schmitz für die überaus wertvolle Mitarbeit auf dem spannenden Gebiet der Cathepsine.

Weiterhin möchte ich unseren Praktikanten, Anne Cöse, Norbert Furtmann, Henriette Günther, Christoph Hauser, Judith Kinzy, Julia Kläs, Patrick Jim Küppers, Michael Lültdorff und Anna Schulz-Fincke, danken, die wir hoffentlich für die Wissenschaft begeistern konnten.

Für die erfolgreiche Zusammenarbeit danke ich auch ganz herzlich unseren Kooperationspartnern, Santos Fustero, Reik Löser, Vanessa Rodrigo und Ilia V. Yampolsky.

Außerdem möchte ich mich bei allen Kollegen des Arbeitskreises, Stefan Dosa, Hans-Georg Häcker, Stephanie Hautmann, Eva Mauer, Matthias Mertens, Philipp Aaron Ottersbach, Janina Schmitz, Marit Stirnberg, Anne Stöbel und Miheret Tekeste Sisay, für eine angenehme Arbeitsatmosphäre und für eine sehr schöne Zeit bedanken.

Mein tiefster Dank gilt meinen Eltern und meiner Schwester Julia, die mir immer unterstützend zur Seite standen.

Die Durchführung der Arbeit wurde mir durch ein Stipendium der NRW Forschungsschule Biotech-Pharma ermöglicht.